U.PORTO
FEUP FACULDADE DE ENGENHARIA
UNIVERSIDADE DO PORTO

COUPLING BIOELECTROCHEMICAL SYSTEMS AND REDOX FLOW BATTERIES FOR SUSTAINABLE ENERGY PRODUCTION AND STORAGE

Dou parecer favorável,



MÁRCIA SOFIA DA SILVA SANTOS

DISSERTATION SUBMITTED IN PARTIAL FULFILMENT OF THE REQUIREMENTS FOR THE DEGREE OF DOCTOR IN ENVIRONMENTAL ENGINEERING

BY

UNIVERSITY OF PORTO

SUPERVISORS

ADÉLIO MIGUEL MAGALHÃES MENDES
MARIA MADALENA DOS SANTOS ALVES
CÉLIA MARIA DIAS FERREIRA

FACULTY OF ENGINEERING – UNIVERSITY OF PORTO

PORTO, 2020

This work was financially supported by:

(i) Base Funding – UIDB/00511/2020 of the Laboratory for Process Engineering, Environment, Biotechnology and Energy – LEPABE – funded by national funds through the Portuguese Foundation for Science and Technology (FCT/MCTES (PIDDAC);

(ii) NORTE-01-0145-FEDER-000005–LEPABE-2-ECO-INNOVATION, co-financed by the Northern Regional Operational Program (NORTE 2020), through Portugal 2020 and the European Regional Development Fund (FEDER).

(iii) “SunStorage - Harvesting and storage of solar energy”, with reference POCI-01-0145-FEDER-016387, funded by European Regional Development Fund (ERDF), through COMPETE 2020 - Operational Programme for Competitiveness and Internationalisation (POCI), and by national funds, through FCT - Fundação para a Ciência e a Tecnologia I.P.”;

(iv) Project PTDC/EQU-EQU/30510/2017 - POCI-01-0145-FEDER-030510 – Sunflow “Solar energy storage into redox flow batteries” funded by FEDER funds through COMPETE2020 - Operational Program for Competitiveness and Internationalization (POCI) and by national funds (PIDDAC) through FCT/MCTES.

(v) FCT under the scope of the strategic funding of UIDB/04469/2020 unit and BioTecNorte operation (NORTE-01-0145-FEDER-000004) funded by the European Regional Development Fund under the scope of NORTE 2020.

(vi) Portuguese Foundation for Science and Technology (FCT), for PhD grant attributed (reference SFRH/BD/104087/2014).

Acknowledgments

I am thankful to the Portuguese Foundation for Science and Technology (FCT), for my PhD grant. I also want to thank all the remaining financial support from LEPABE, CEB and CERNAS for the development of this thesis.

My gratitude to University of Porto, FEUP and to Professor Fernando Veloso Gomes, Director of Doctoral Program in Environmental Engineering, for allowing me to attend the Doctoral Program. I would like to thank to Professor Doctor Adélio Mendes, Professor Doctor Madalena Alves and Professor Doctor Célia Dias Ferreira for proposing this thesis theme, for the encouragement, advices, teachings and support.

I would like to thank LEPABE for providing the necessary conditions to carry out my work. A special thanks to all colleagues in the department, specially to Doctor João Azevedo, Doctor André Monteiro and Ms. Kashif Mushtaq for all the help with Electrochemistry and Redox Flow Batteries.

My gratitude to Institute Polytechnic of Coimbra and CERNAS and to all the colleagues, my appreciation for the hospitably, coffee times during my time in Coimbra, and all the notes and support for finishing the thesis work.

I want to thank University of Minho and CEB for allowing me, with the supervision of Professor Doctor Madalena Alves and Doctor Luciana Peixoto, to perform an advanced scientific internship where the work of Bioelectrochemistry for my thesis was developed. Special tanks to Doctor Luciana Peixoto for the knowledge on Bioelectrochemistry, Bioelectrochemical Systems operation and to help me accomplish the aims of this work, all the support and friendship. My appreciation to Doctor Sónia Barbosa and Doctor Marta Ferreira for all the support, for all interesting suggestions and discussions. My appreciation to Doctor Pier Parpot for all the helpful notes and access to electrochemistry materials. Special thanks to all colleagues in BRIDGE group for all the good moments, teachings and support.

I want to thank my parents and family all understanding, strength, help and unconditional love. A heartfelt thanks to my grandmother, who was by my side until the end. A special thanks to Eduardo for being by my side at all times.

To all who have contributed in some way to this work, thank you very much.

Abstract

This thesis studies for the first time ever a combined system where Bioelectrochemical Systems (BESs) are used for charging electrochemical fuels used in Redox Flow Cells (RFCs); the coupled system was named Microbial Redox Flow Cell (MRFC). Using microorganisms as biocatalysts, BESs convert organic fuels (*e.g.* wastes) into electrochemical energy. RFCs use redox pairs dissolved in a supporting electrolyte that undergo reversible redox reactions during which chemical energy is either stored or released in the form of electricity. For the first time ever, a MRFC was studied using as redox pairs anthraquinone-2,6-disulfonate (2,6-AQDS) – negalyte – and ferrocyanide, ($[Fe(CN)_6]^{4-}$) – posilyte.

The reduction of 2,6-AQDS to anthrahydroquinone-2,6-disulfonate (2,6-$AQDSH_2$) in a BES was studied, where the Electrochemically Active Bacteria (EAB), *Geobacter sulfurreducens* and acetate were introduced in the anodic chamber. The anode and cathode chambers were physically separated with a Nafion™ NM 117 Proton Exchange Membrane. The reduction of 2,6-AQDS at the BES was studied first applying an external electrical bias of -0.200 V *vs.* Ag/AgCl (3 M) and then recording the electrical current history; secondly, the reduction of 2,6-AQDS was also obtained inserting an electrical resistance in the circuit, and measuring the potential difference at its ends. A BES loaded with 20 mM 2,6-AQDS aqueous solution in the cathodic chamber reached $3.3x10^{-3}$ mW cm^{-2} (0.04 mA cm^{-2}) with the BES closed with a 500 Ω resistor. In a second stage, the BES was operated with a 500 Ω resistor and reached a maximum of 0.05 mA cm^{-2} and 0.03 mW cm^{-2}, during the electrolyte charging. Studies with Ultraviolet-visible spectrophotometry (UV-Vis spectrophotometry) confirmed the presence of *ca*. 5 mM of 2,6-$AQDSH_2$ at the cathode side, highlighting that the initial 2,6-AQDS molecules were successfully reduced. Because 2,6-$AQDSH_2$ was produced following the bio-reduction that took place on the cathode side of the BES, this molecule was named as microbial electrochemical fuel. The 2,6-$AQDSH_2$ bioelectrochemically reduced was then introduced in a 16 cm^2 RFC (negalyte) with ferricyanide, ($[Fe(CN)_6]^{3-}$), (posilyte – electrically charged), and the RFC was allowed to discharge. The characteristic charge–discharge curve versus time was obtained, thus demonstrating the concept of a MRFC; a Coulombic Efficiency (CE) of *ca.* 100 % and Energy Efficiency (EE) *ca.* 85 % over 10 cycles were obtained.

The reduction of 2,6-AQDS was also evaluated using wastewater at the anode side of a BES. In this case the organic components in the wastewater were bio-oxidized, instead of the previously used acetate. This experience highlights that organic wastes can also be used in BES to generate microbial electrochemical fuels. Experiments were carried out with 2,6-AQDS in different pH conditions, pH = 7, pH = 9 and pH = 12, in the cathode chamber; pH of the anode was kept at 7. The results suggest that the pH of 2,6-AQDS does not influence its conversion during the BESs operations. The BES with the quinone in neutral conditions reached 0.108 mA cm^{-2} and CEs were greater than 50 %. In the 16 cm^2 RFC with the 2,6-AQDSH_2 bioelectrochemically reduced aqueous solution (wastewater as carbon source) as the anolyte and $[Fe(CN)_6]^{3-}$ as catholyte, the CE was *ca.* 100 % with the RFC operating at neutral pH.

Finally, a BES was used for the bioelectrochemical oxidation of $[Fe(CN)_6]^{4-}$ into $[Fe(CN)_6]^{3-}$. *G. sulfurreducens* was introduced in the BES for forming a biofilm on the electrode surfaces, with acetate as carbon source. The use of an anodic potential for *G. sulfurreducens* to operate as exoelectrogenic bacteria in bioanodes, took place along several days where $[Fe(CN)_6]^{3-}$ in the cathode chamber was used as final electron acceptor. After the biofilm formation, the applied potential was lowered to convert the bioelectrodes into biocathodes and *G. sulfurreducens* was analyzed as electrotrophic bacteria, for the conversion of $[Fe(CN)_6]^{4-}$ to $[Fe(CN)_6]^{3-}$. The microbial electrochemical fuel $[Fe(CN)_6]^{3-}$ was introduced as posilyte of a RFC while the microbial electrochemical fuel 2,6-AQDSH_2 was introduced as negalyte. The RFC with 9 cm^2 was then allowed to discharge and the potential *vs.* time response was obtained. This last experiment demonstrates the biocharge of both negalyte and posilyte redox pairs (microbial electrochemical fuels), to feed a RFC for producing electricity. The bioelectrochemical charge of redox pairs usable in RFC is far more flexible and far more efficient than the production of other bioelectrochemical fuels such as hydrogen.

Sumário

Esta tese estuda, pela primeira vez, um sistema acoplado para armazenar energia, onde Sistemas Bioeletroquímicos (BESs) são utilizados para carregar combustíveis eletroquímicos usados em Baterias Redox de Escoamento (RFCs); este sistema acoplado foi denominado Microbial Redox Flow Cell (MRFC). Usando microrganismos como biocatalizadores, os BESs convertem combustíveis orgânicos (*e.g.* resíduos) em energia eletroquímica. Por sua vez, RFCs utilizam pares redox dissolvidos num eletrólito de suporte, que executam reações redox reversíveis durante as quais a energia química é armazenada ou libertada na forma de eletricidade. Pela primeira vez, uma "Biobateria Redox de Escoamento" foi estudada usando como par redox o ácido antraquinona-2,6-dissulfónico (2,6-AQDS) – anólito – e ferricianeto, ($[Fe(CN)_6]^{4-}$) – católito.

A redução de 2,6-AQDS para ácido de antrahidroquinona-2,6-dissulfónico (2,6-$AQDSH_2$) foi estudada num BES, onde as Bactérias Electroquimicamente Ativas (EAB) *Geobacter sulfurreducens* e acetato foram introduzidas na câmara anódica. As câmaras anódica e catódica foram separadas fisicamente com uma membrana de troca iónica - Nafion™ NM 117. A redução de 2,6-AQDS no BES foi realizada, primeiro aplicando um potencial anódico de -0.200 V *vs.* Ag/AgCl (3 M), registando a evolução da corrente elétrica, e posteriormente, com BES inserindo uma resistência elétrica no circuito, medindo a diferença de potencial da célula e a evolução da corrente elétrica. BES com uma solução aquosa de 20 mM 2,6-AQDS no cátodo alcançou $3.3x10^{-3}$ mW cm^{-2} (0.04 mA cm^{-2}) quando o circuito da BES foi fechado com uma resistência de 500 Ω. Num segundo procedimento, o BES com uma resistência de 500 Ω atingiu um máximo de 0.05 mA cm^{-2} e 0.03 mW cm^{-2}, durante o carregamento do eletrólito. Estudos com Espectrofotometria Ultravioleta-Visível confirmaram a presença de *ca.* 5 mM de 2,6-$AQDSH_2$ no lado do cátodo, destacando que o 2,6-AQDS foi reduzido bioelectroquimicamente. O 2,6-$AQDSH_2$ no cátodo de BES, por ter sido bioelectroquimicamente reduzido é denominado de combustível eletroquímico microbiano. A Célula Redox de Escoamento (RFC) de 16 cm^2 foi testada com o par redox 2,6-$AQDSH_2$ (anólito) e ferricianeto, ($[Fe(CN)_6]^{3-}$), eletricamente carregado (católito). A RFC foi submetida a uma descarga e a curva característica de carga-descarga *vs.* tempo foi obtida, demonstrando

assim o conceito de MRFC. Foi alcançada uma Eficiência Coulômbica (CE) de *ca*. 100 % e uma Eficiência Energética (EE) *ca*. 85 % em 10 ciclos.

A redução de 2,6-AQDS também foi avaliada usando água residual no lado anódico da BES. Neste caso, a fração orgânica da água residual foi bioxidada, como alternativa ao acetato de sódio. Este desenho experimental destaca que os resíduos orgânicos também podem ser usados para obter combustíveis eletroquímicos de carga microbiana. As BES foram analisadas com 2,6-AQDS em diferentes condições de pH no cátodo, pH = 7, pH = 9 e pH = 12 e com água residual a pH7 no ânodo. Os resultados obtidos sugerem que o pH do 2,6-AQDS não influencia a sua conversão durante as operações da BESs. A BES com 2,6-AQDS em condições neutras alcançou 0.11 mA cm^{-2} e foram registadas CEs superiores a 50 % para as BES. Na RFC de 16 cm^2 com a solução aquosa de 2,6-AQDSH_2 bioelectroquimicamente reduzida (anólito) e $[Fe(CN)_6]^{3-}$ (católito - eletricamente carregado), a CE foi *ca*. 100 % com RFC operando em pH neutro.

Finalmente, BES foi estudado para a oxidação bioeletroquímica de $[Fe(CN)_6]^{4-}$ em $[Fe(CN)_6]^{3-}$. *G. sulfurreducens* foi introduzido no BES para formar um biofilme nas superfícies do elétrodo, com acetato como fonte de carbono. A aplicação de um potencial anódico em BES para *G. sulfurreducens* operar como bactéria exoelectrogénica (bioânodo) ocorreu ao longo de vários dias com $[Fe(CN)_6]^{3-}$ na câmara catódica, como aceitador final de eletrões. Após a formação do biofilme, o potencial aplicado foi reduzido para converter o bioânodo em biocátodo e *G. sulfurreducens* foi analisada como bactéria electrotrófica, para a conversão de $[Fe(CN)_6]^{4-}$ em $[Fe(CN)_6]^{3-}$. O $[Fe(CN)_6]^{3-}$ carregado bioelectroquimicamente foi introduzido como católito da RFC, enquanto o 2,6-AQDSH_2 carregado bioelectroquimicamente foi introduzido como anólito. Uma RFC com 9 cm^2 foi testada com os pares carregados bioelectroquimicamente, e a respetiva curva de potencial *vs.* tempo foi obtida. Este último ensaio demonstra o carregar, por via bioeletroquímica, de combustíveis eletroquímicos microbianos para uma RFC, para produzir energia elétrica; o uso de combustíveis eletroquímicos microbianos na RFC é muito mais flexível e muito mais eficiente do que a produção de outros combustíveis bioeletroquímicos, como o hidrogênio.

Table of Contents

Acknowledgments V

Abstract VII

Sumário IX

List of Figures XIII

List of Tables XVII

Acronyms XIX

Chapter 1. Introduction 21

1.1. Microbial electrochemical technologies 23

1.2. Bioelectrochemical Systems 24

1.2.1. Electrochemically Active Bacteria 25

1.2.2. Microbial Fuel Cells 28

1.2.3. Microbial Electrolysis Cells 30

1.2.4. Microbial Electrosynthesis Cells 31

1.3. BES materials and configurations 32

1.4. BES bioenergy storage advances 35

1.4.1. BES for bioenergy storage 39

1.5. Microbial Redox Flow Cell 41

1.5.1. Aqueous Redox Flow Cells 43

1.5.2. Aqueous Organic Redox Flow Cells 45

1.6. Motivation and outline 51

1.7. References 55

Chapter 2. Unravelling the Bioelectrochemical Systems capacity to promote a microbial electrochemical fuel 87

Abstract 89

2.1. Introduction 90

2.2. Material and methods 92

2.3. Results and discussion 96

2.4. Conclusion 104

2.5. Acknowledgements 104

2.6. References 105

Chapter 3. Microbial electrochemical fuel for energy storage in a Redox Flow Cell 113

Abstract 115

3.1. Introduction 116

3.2. Material and methods 119

3.3. Results and discussion 124

3.4. Conclusion 134

3.5. Acknowledgements 134

3.6. References 135

Chapter 4. Wastewater as a renewable energy source for a Microbial Redox Flow Cell 145

Abstract 147

4.1. Introduction 148

4.2. Materials and methods 150

4.3. Results and discussion 153

4.4. Conclusion 168

4.5. Acknowledgements 168

4.6. References 169

Chapter 5. Bioelectrochemical energy storage in a Microbial Redox Flow Cell **175**

Abstract 177

5.1. Introduction 178

5.2. Materials and methods 179

5.3. Results and discussion 185

5.4. Conclusions 193

5.5. Acknowledgements 194

5.6. References 195

Chapter 6. General conclusions and future perspectives 199

List of Figures

Figure 1.1. Renewable electricity consumption up to 2016, approximated estimates for 2017 and the expected European Union renewable energy action plans developments by 2020 [1]. 23

Figure 1.2. Schematic representation of a typical configuration of an MFC (A), an MEC (B) and an MES (C). 25

Figure 1.3. Schematic representation of directly or mediated Extracellular Electron Transfer (EET) processes: A) Direct Electron Transfer (DET) and B) Mediated Electron Transfer (MET) (adapted from [32, 33, 36]). 26

Figure 1.4. Power densities (kW L^{-1}) (A) and power level (mW) (B) of MFC and energy conversion devices [89]. 29

Figure 1.5. Research trends in MFCs, MECs, MESs and BESs from 1990 to 2020 (SCOPUS database access in February of 2020). 35

Figure 1.6. Schematic overview of the possible combinations of microbial and chemical catalysis in BESs. Energy is harvested in MFCs (E_{anode}<$E_{cathode}$) and energy is consumed in MECs (E_{anode}>$E_{cathode}$) [258]. 39

Figure 1.7. Simplified scheme of a Redox Flow Cell (RFC). 42

Figure 1.8. Comparison of A) power and current densities for Non-aqueous RFCs (green) and Aqueous RFCs (blue) [293] and B) acceptable chemical cost factor on an active material basis (in \$ kg^{-1}) versus Open Circuit Potential for a range of reactor costs for Non-aqueous RFCs (green) and aqueous RFCs (blue) [273]. 44

Figure 1.9. Redox potentials of different inorganic and organic redox couples seen in RFCs [254]. 46

Figure 1.10. General scheme of p-benzoquinone redox reactions in buffered aqueous solution (adapted from [320]). 47

Figure 2.1. Schematic representation of Bioelectrochemical System (BES) with anthraquinone-2,6-disulphonate (2,6-AQDS) as cathodic electron acceptors (in the left side); the anthrahydroquinone-2,6-disulphonate (2,6-$AQDSH_2$) (microbial electrochemical fuel) was tested as negalyte in a Redox Flow Cell (RFC) (in the right side). 94

Figure 2.2. Current density over time for the BESs during bioelectrochemical reduction of 2,6-AQDS with (A) bias anode potential at -0.200 V *vs.* Ag/AgCl (3 M) (replicates BES AP 1 and BES AP 2) and in (B) BES closed with an electrical resistance load (500 Ω) (replicates BES Ω 1 and BES Ω 2). 97

Figure 2.3. Polarization (black square) and power curves (triangle square) obtained for BESs with a bias anode potential at -0.200 V *vs.* Ag/AgCl (3 M) for the duplicate BES AP 1 (A) and for duplicate BES AP 2 (B). Polarization (black square) and power curves (triangle square) obtained for BESs closed with an electrical resistance (500 Ω) for BES Ω 1 (C) and for BES Ω 2 (D). The lines were added for readability. 99

Figure 2.4. Cyclic voltammograms obtained at 5 mV s^{-1} for BESs with a bias potential at -0.200 V *vs.* Ag/AgCl (3 M) (BES AP 1 and BES AP 2) (B) and closed with an external resistance load of 500 Ω (BES Ω 1 and BES Ω 2) (B). 100

Figure 2.5. Charge–discharge curves versus time (A), Coulombic (black square), Potential (white triangle) and Energy efficiencies (black diamond) versus the cycle number (B) for RFC with 2,6-AQDSH_2 from the BES AP 1 as negalyte. 102

Figure 2.6. Charge–discharge curves versus time (A), Coulombic (black square), Potential (white triangle) and Energy efficiencies (black circle) versus the cycle number (B) for RFC with 2,6-AQDSH_2 from the BES Ω 1 as negalyte. 103

Figure 3.1. Power densities reported for BES (normalized to electrode-projected surface areas) and power density of MFC for the conversion of microbially-charged electrochemical fuel (BES of the present study) (adapted from [69]). 117

Figure 3.2. Diagram of the proposed Microbial Redox Flow Cell: BES (at the left) for the direct charge of the negalyte (2,6-AQDS→2,6-AQDSH_2), coupled with a RFC (2,6-AQDS||$[Fe(CN)_6]^{4-}$). On the right side, a second BES (in grey, not reported) is set for charging the posilyte of the RFC. 119

Figure 3.3. BES with *G. Sulfurreducens* (anode) and 2,6-AQDS (cathode) at instant zero (A) and at the end of the assay (B). 125

Figure 3.4. Current density over time for the bioelectrochemical reduction of 2,6-AQDS in BES A operated in series; (------) corresponds to the removal of the exhausted 2,6-AQDS. 125

Figure 3.5. Polarization (A) and power curves (B) obtained for BES A operated in series. The lines were added for readability. 126

Figure 3.6. Current density over time for the bioelectrochemical reduction of 2,6-AQDS in BESs (BES B1 and BES B2). 128

Figure 3.7. The polarization curve (A) and power curve (B) for BESs (BES B1 and BES B2). 128

Figure 3.8. Cyclic voltammograms at 20 mV s^{-1} of the culture medium of *Geobacter sulfurreducens.* 130

Figure 4.1. Scheme of the Microbial Redox Flow Cell (MRFC) with wastewater: Bioelectrochemical Systems (BES) for the direct charge of the negalyte (2,6-AQDS -> 2,6-

$AQDSH_2$) (at the left), coupled with a Redox Flow Cell (RFC) (2,6-AQDS||$[Fe(CN)_6]^{4-}$), set for charging the posilyte of the RFC on the right hand side. 149

Figure 4.2. Current density over time for the BESs during bioelectrochemical reduction of 2,6-AQDS in cathode solution at A) pH = 7, B) pH = 9 and C) pH = 12 (BES 1 and BES 2 represent the duplicates). The black dash line represents the wastewater refresh for BES 1 and the grey dash line represents the wastewater refresh for BES 2. 154

Figure 4.3. Polarization (black line) and power curves (green line) obtained at the end of BESs bio-charged 2,6-$AQDSH_2$: A) at pH = 7 (BES 1), B) at pH = 9 (BES 1) and C) at pH = 12 (BES 1). The lines were added for readability. **ERRO! MARCADOR NÃO DEFINIDO.**

Figure 4.4. Polarization (black line) and power curves (green line) obtained at the end of BESs bio-charged 2,6-$AQDSH_2$: A) at pH = 7 (BES 2), B) at pH = 9 (BES 2) and C) at pH = 12 (BES 2). The lines were added for readability. 160

Figure 4.5. Cyclic voltammograms obtained at 1 mV s^{-1} for the bio-charged 2,6-$AQDSH_2$ at pH = 7 (red line) and for the bio-charged 2,6-$AQDSH_2$ at pH = 9 (black line) (black arrow indicates the start of scan). 162

Figure 4.6. Charge–discharge curves history for 9 cycles (A), Coulombic (black square), Potential (white triangle) and Energy efficiencies (black circle) versus the cycle number (B) and capacity data (C) at a current density of 3.75 mA cm^{-2} for the RFC loaded with $[Fe(CN)_6]^{3-}$ – posilyte – with initially bioelectrochemically-charged 2,6-$AQDSH_2$ at pH = 7 – negalyte. 165

Figure 4.7. Charge–discharge curves history for 9 cycles (A), Coulombic (black square), Potential (white triangle) and Energy efficiencies (black circle) versus the cycle number (B) and capacity data (C) at a current density of 3.75 mA cm^{-2} for the RFC loaded with $[Fe(CN)_6]^{3-}$ – posilyte – with initially bioelectrochemically-charged 2,6-$AQDSH_2$ at pH = 9 – negalyte. 166

Figure 4.8. Charge–discharge curves history for 9 cycles (A), Coulombic (black square), Potential (white triangle) and Energy efficiencies (black circle) versus the cycle number (B) and capacity data (C) at a current density of 3.75 mA cm^{-2} for the RFC loaded with $[Fe(CN)_6]^{3-}$ – posilyte – with initially bioelectrochemically-charged 2,6-$AQDSH_2$ at pH = 12 – negalyte. 167

Figure 5.1. Illustration of Microbial Redox Flow Cell (MRFC). At the left side, first BES as bioanode for the charging of the negalyte (2,6-AQDS→2,6-$AQDSH_2$). At the center, the Redox Flow Cell (2,6-AQDS||$[Fe(CN)_6]^{4-}$) having negalyte from first BES and posilyte from second BES. On the right side, the second BES as biocathode established during the oxidation of $[Fe(CN)_6]^{4-}$ to $[Fe(CN)_6]^{3-}$. 180

Figure 5.2. Scheme of the experimental plan: (A) BES 1 and BES 2 for charging of the negalyte (2,6-AQDS reduction to 2,6-$AQDSH_2$); (B) BES 3 and BES 4 operating firstly as bioanode for biofilm growth on the electrode surface and secondly as biocathode for the oxidation of $[Fe(CN)_6]^{4-}$ to $[Fe(CN)_6]^{3-}$. 182

Figure 5.3. Current density history of BES 1 (yellow line) and BES 2 (red line), during the bioelectrochemical reduction of 2,6-AQDS (negalyte of MRFC). 186

Figure 5.4. Current density over time generated in BES 3 and BES 4. Dashed lines indicated when the potential was lowered from -0.200 V *vs.* Ag/AgCl (3 M) to -0.855 V *vs.* Ag/AgCl (3 M) for BES 3 (blue line) and for BES 4 (green line). 187

Figure 5.5. Voltammograms of bioelectrodes of the BES 3 (A) and BES 4 (B), achieved at 20 mV s^{-1}, before switching the potential from -0.200 V *vs.* Ag/AgCl (3 M) to -0.855 V *vs.* Ag/AgCl (3 M) (grey line), and when assays ended (black line). 189

Figure 5.6. Redox Flow Cell assembled with negalyte 2,6-$AQDSH_2$ and with posilyte $[Fe(CN)_6]^{3-}$ both charged bioelectrochemically: (A) potential *vs.* time response at current density of 3.75 mA cm^{-2}; (B) Coulombic efficiency (CE), Potential efficiency (PE) and Energy efficiency (EE) over the charge-discharge cycle number and (C) the loss in capacity. 191

List of Tables

Table 1.1. Summary of reports with Aqueous RFCs with quinones as redox pair. 49

Table 2.1. Summary of different cathodic electron acceptors and the maximum power densities in BESs. 90

Table 4.1. Results generated from BESs with the microbial electrochemical fuels at pH = 7, pH = 9 and pH = 12 (average values of BES 1 and BES 2). 156

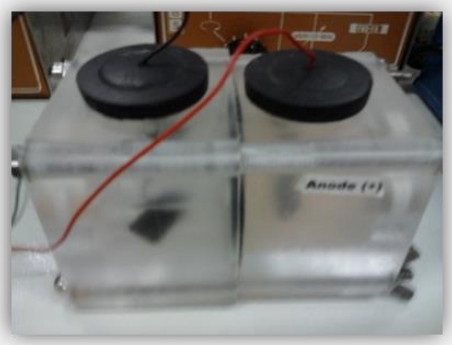
Table 4.2. Formal Redox Potential ($E_{1/2}$ / mV_{NHE}) for the BESs with the three pH-cathode conditions obtained at 1 mV s^{-1} 162

Table 5.1. Coulombic Efficiency (CE) and the concentration of the bio-charged 2,6-$AQDSH_2$ (mM) at BES 1 and BES 2. 186

Acronyms

2,6-AQDS	Anthraquinone-2,6-disulphonate
2,6-AQDSH$_2$	Anthrahydroquinone-2,6-disulphonate
AEM	Anion Exchange Membrane
BES	Bioelectrochemical System
BMFC	Benthic/Sediment Microbial Fuel Cell
CAEM	Cation Exchange Membrane
CE	Coulombic Efficiency
COD	Chemical Oxygen Demand
CNT	Carbon Nanotubes
CV	Cyclic Voltammetry
DET	Direct Electron Transfer
DIET	Direct Interspecies Electron Transfer
$E_{1/2}$	Formal Redox Potential
EAB	Electrochemically Active Bacteria
EE	Energy Efficiency
EET	Extracellular Electron Transfer
EIS	Electrochemical impedance spectroscopy
HPLC	High Pressure Liquid Chromatography
LED	Light Emitting Diodes
MDC	Microbial Desalination Cell
MEA	Membrane Electrode Assemble
MEC	Microbial Electrolysis Cell
MES	Microbial Electrosynthesis Cell
MET	Mediated Electron Transfer
MFC	Microbial Fuel Cell
MRC	Microbial Remediation Cell
MREC	Microbial Reverse Electrodialysis Cell
MRFC	Microbial Redox Flow Cell
MRFB	Microbial Redox Flow Battery
NHE	Normal Hydrogen Electrode
OCP	Open Circuit Potential
OD	Optical Density
PE	Potential Efficiency
PEM	Proton Exchange Membrane
PMFC	Photosynthetic Microbial Fuel Cell
RFB	Redox Flow Battery
RFC	Redox Flow Cell

SMFC	Sediment Microbial Fuel Cell
UV-Vis	Ultraviolet–Visible Spectroscopy
VFA	Volatile Fatty Acid





Chapter 1

Introduction

1.1. Microbial electrochemical technologies

Technologies to harvest energy from renewable sources like solar, wind and hydraulic are great opportunities for energy decarbonisation [1]. Fossil fuels are responsible for the emission of carbon dioxide and other greenhouse gases that have a strong impact in global warming [2]. The European Environment Agency in a recent report clarifies that the primary energy consumption of fossil fuels continues to dominate [1], where 80 % of the total primary energy source are mostly from fossil sources like oil, coal and natural gas [3, 4]. In the following years an increase in the energy efficiency of different sources of renewable energy is expected, with attention to solar photovoltaic, wind and biomass [5] (Figure 1.1.).

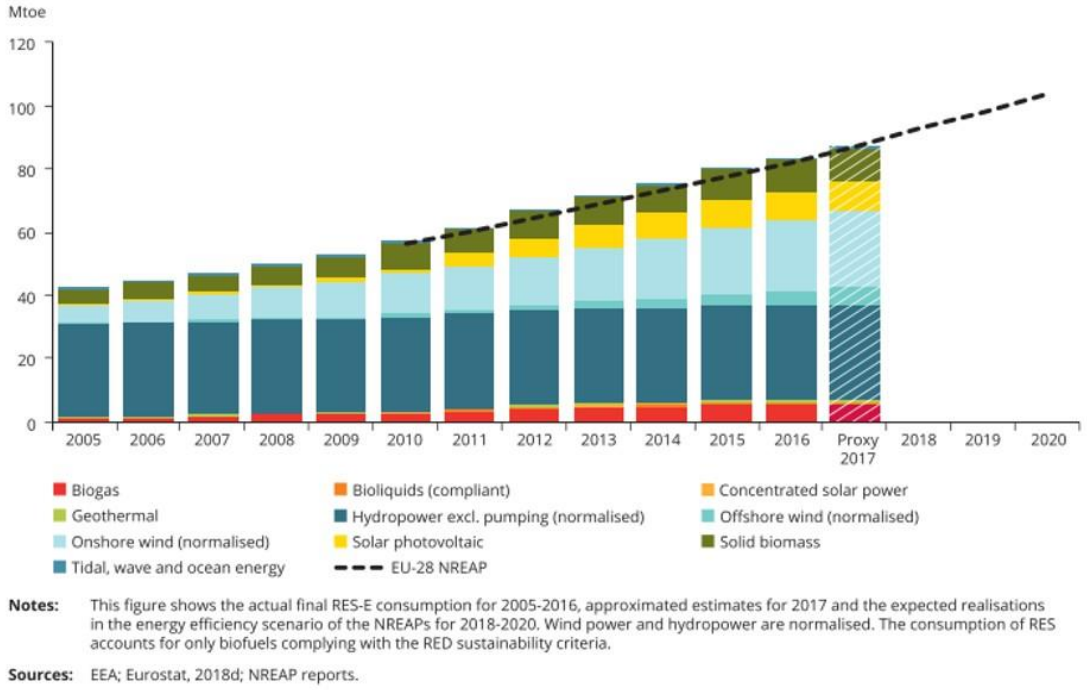


Figure 1.1. Renewable electricity consumption up to 2016, approximated estimates for 2017 and the expected European Union renewable energy action plans developments by 2020 [1].

Electrochemical technologies for energy production and storage englobe different devices that use electrochemistry as the basis of their operation technology [6–8]. Electrochemical energy and conversion methods, including Fuel Cells [7, 9] and Redox Flow Cells (RFCs) [10, 11] are highly researched for an up forward on green energy.

The research on Microbial Electrochemical Technologies with the perspective of harnessing bioenergy has expanded for multiple applications [12–14]. Waste to energy conversion

technologies such as Bioelectrochemical Systems (BESs) have emerged in the last years as a promising electrochemical device to generate bioelectricity [15, 16]. BESs are still far away from reaching the levels of power outputs and efficiencies of other electrochemical technologies [17], and the energy generated is not stored itself [18]. Efforts on the energy storage of bioenergy from BESs are being pursuit. RFCs are electrochemical devices that generate and store energy. Solar energy has already been channeled for the direct conversion of sunlight into electrochemical energy in RFCs [19]. A similar approach can be envisaged for coupling BES and RFC for energy generation and storage processes.

1.2. Bioelectrochemical Systems

Microbial electrochemistry or bioelectrochemistry is a designation attributed to the study and application of interactions between living microbial cells and electrodes (*i.e.* electron conductors or capacitive materials) [20]. BESs are electrochemical devices descendant from chemical Fuel Cells, which convert the bioelectrochemical energy of a fuel (carbon source) into electrical energy [21]. BESs englobe all systems based on bioelectrochemistry, including enzymes, microorganisms, proteins, deoxyribonucleic acid or neuro-electro-chemicals [20].

BESs technologies are divided into different types according to the bioelectrochemical process, the final product desired and the microorganisms used [22]. There are three major types: i) Microbial Fuel Cells (MFCs), where the electrical energy is generated by Electrochemically Active Bacteria (EAB) [23], through the oxidation of carbon sources [22], ii) Microbial Electrolysis Cells (MECs) for the production of chemicals such as methane [24] or hydrogen [25] and iii) Microbial Electrosynthesis Cells (MESs), where EAB drive the chemical synthesis of products with an additional energy input, such as medium chain fatty acids [26]. The general scheme of the different types of BESs is presented in Figure 1.2.

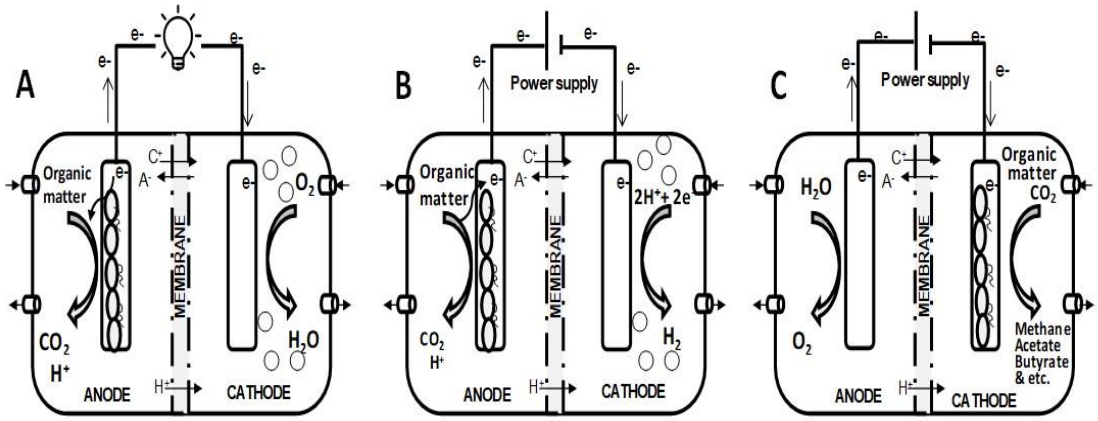


Figure 1.2. Schematic representation of a typical configuration of an MFC (A), an MEC (B) and an MES (C).

BESs' major advantages are their physical construction (low cost), fuels (highly accessible) and simple operation mode that are environmentally friendly [27–29]. Liang and coworkers [30] explained that BESs can be operated in both MFC mode in which power is delivered and in MEC mode in which power is invested to rise the kinetics of the reaction and/or to drive thermodynamically unfavorable reactions.

1.2.1. Electrochemically Active Bacteria

The Electrochemically Active Bacteria (EAB) possess electron transport proteins in the membrane that transfer electrons to the outside of the cell. The specific proteins (*e.g. c* type cytochromes) move the electrons to an external solid electron acceptor, *e.g.* metal oxides or BES electrodes [28]. The EAB have the ability to form biofilms in electrode surfaces [31].

EAB promote transfer of electrons from microorganisms to electrodes [32], directly or via mediated Extracellular Electron Transfer (EET) processes [33–36]. The EET processes for EAB are represented in Figure 1.3.

The Direct Electron Transfer (DET) is processed with a physical contact between the bacterial cell membrane (or membrane organelle) and the electrode (Figure 1.3A) [37, 38], where no diffusional redox species are involved, but *c* type cytochromes present in the cell membrane [39]. The direct long range EET can be via self-assemble of the *c* type cytochromes in the electrode surface and/or with conductive pilus-like nanowires [40].

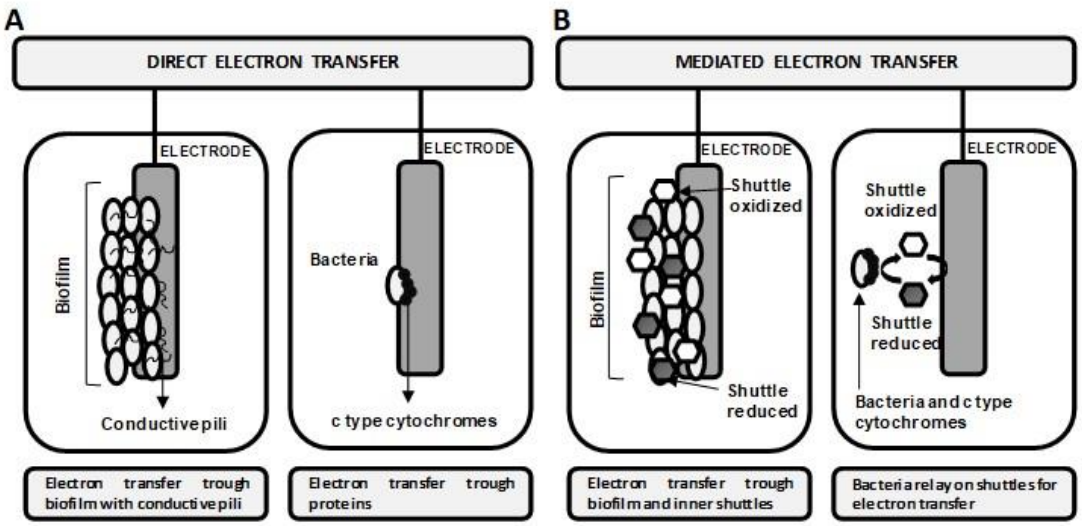


Figure 1.3. Schematic representation of directly or mediated Extracellular Electron Transfer (EET) processes: A) Direct Electron Transfer (DET) and B) Mediated Electron Transfer (MET) (adapted from [32, 33, 36]).

DET can be observed in *Geobacter sulfurreducens* and *Shewanella oneidensis* [39, 41]. *Geobacter* sp. and *Shewanella* sp. biofilms are also known to grow in solid graphite electrode [40, 42], where these catalyze electron flow from cytoplasmic oxidative reactions to electrodes [43].

In Mediated Electron Transfer (MET) the microorganisms can transfer electrons from their cells to the outside (Figure 1.3B) [37] by organic redox species of microbial origin (shuttles) stowed in the culture medium [44]. The redox mediators facilitate the electron transfer between the bacterial communities and the electrodes [33]. Ferricyanide ($[Fe(CN)_6]^{3-}$) [45] or quinones [46] are artificial mediators that can accelerate the electron transfer between the primary electron donor to a terminal electron acceptor, increasing the reaction rates [45–47]. MET is an electron transfer process seen in *Actinobacillus succinogenes, Clostridium beijerinckii, Pseudomonas* spp*, Acinetobacter calcoaceticus* and others [48].

EAB that promote microbial-assisted oxidation are seen as exoelectrogens (or electricigens or electrogens) [49] and are responsible to shuttle electrons exogenously to the electrode (electron acceptors) [50]. These microorganisms were researched in bioelectrodes for energy generation in BESs [23, 51, 52]. Exoelectrogens are the most explored EAB, as seen in the different reports published over the years. *G. sulfurreducens* [53] and *Shewanella oneidensis* [54] are well known to engender electrical current. Also gram-positive bacterium *Brevibacillus sp*. PTH1 [52], *Pseudomonas* sp. [55], *Desulfuromonas acetoxidans* [56], *Rhodoferax*

ferrireducens [57], *Escherichia coli* [58] and others [52] were identified as exoelectrogens for generation of electrical current.

EAB that promote microbial-assisted reductions are named electrotrophs [59]. Electrotrophs are microorganisms capable to draw electrons from a cathode electrode via a DET [59] or self-secreted mediators to conserve energy to grow and to provide a broad range of functions in METs [50, 59]. Electrotrophs are used in MESs as biocathodes for valuable compounds generation [60], such as chemicals [61], biofuels [62] and syngas [40] and in bioremediation of chemical pollutants [63], or metals [64]. Examples of known electrotrophs identified are *Clostridium* sp. [65], *Pseudomonas* sp. [66] and *Desulfovibrio* sp. [67].

EAB that operate as exoelectrogens and electrotrophs were researched for BESs application [59]. In the work of Gregory and coworkers [42], *Geobacter metallireducens* was shown to reduce nitrate to nitrite with the electrode as the sole electron donor, and *Geobacter sulfurreducens* reduced fumarate to succinate with the electrode as an electron donor in MFCs [42]. Also, *G. sulfurreducens* uses acetate and H_2 as electron donor and can catalyze H_2 production when the cathode potential was lowered from -0.600 V to -0.800 V in MECs [68].

The electrode potential inversion is used to research exoelectrogenic and electrotrophic bacteria capacities [69]. Research is being conducted in anode-to-cathode inversion using the same bacteria to primarily oxidize electron donors and biofilm formation in electrode surface at one potential (more positive than the electron donor) and afterwards catalyze reduction reactions at a second potential (more negative than the electron donor) [69, 70]. In the work of Saheb-Alam and coworkers [70], bioanodes with a mixture of raw municipal wastewater and effluent from an anaerobic digester were established for several days with an applied anode potential (-0.200 V) (exoelectrogenic activity) and acetate as carbon source. After the current intensity stabilization, the electrode potential was lowered and the electrode was researched as biocathode for CO_2 reduction and NH_4 generation [70]. The work of Hartline & Call [69] studied bioanodes from domestic wastewater in BESs and the polarity inversion of bioanodes. They examine the impact of bioanode substrate and electrode potentials on inverted electrotrophic activity with primarily domestic wastewater. They used two fixed bioanode potentials, −0.150 V and +0.150 V, to analyze the available energy to microbial communities and to induce different electron transfer carriers and pathways to the electrode. The polarity of the enriched bioanodes

was subsequently inverted and the ability to consume electrical current investigated. They concluded that the use of the polarity inversion of bioanodes is a possible technique to achieve different community infrastructures using specific anode pressures that result in a variety of cathodically generated products when inverted [69].

1.2.2. Microbial Fuel Cells

MFCs were the first BESs reported in the literature [32, 34]. MFCs use biodegradable substrates for electricity generation with EAB [71, 72]. MFCs present additional advantages over conventional Fuel Cells with the use of inexpensive catalysts (*e.g.* EAB) [73], simple operating conditions (*e.g.* ambient temperature) [34, 74] and several applications using different electron donors (*e.g.* acetate or glucose) [75]. Maximizing the energy and power of MFCs is one of the critical aspects of the technology, and improve the low energy transformation rates [76]. Their low power output is a consequence of the limitations of the irreversible reactions and processes that occur on the anode and cathode sides of the cell [74], such as poor cathode performance under operational restritions set by EAB [74]; inhibition of microbial ativity by the formation of pH gradients inherent to proton-coupled redox reactions that occur in poor buffered and low ionic strength electrolytes [77]; and side processes, *e.g.* oxygen reduction, scavenging susbtrate intended for prodution of electrical energy [78].

The main physic structure of an MFC is a device divided in two chambers: the anode and cathode chambers are separated by an ion exchange membrane (Figure 1.2A), with the exception of a membraneless MFC [79]. In the anode chamber the EAB, under anaerobic conditions are responsible for the oxidation reaction of the organic matter. The oxidation of the organic matter and the release of electrons occurs from respiratory process of microorganisms (electrons move through the respiratory chains of cells and are carried to electrodes). The anode is the primary electron acceptor [80]. The electrons circulate in an external circuit from the anode to the cathode chamber [81–83]. The protons from the chemical reactions are moved between chambers by migration through the membrane. In the cathode chamber the received protons and electrons react along with the reduction of an electron acceptor to a final product [13, 84, 85]. Oxygen is the most common final electron acceptor in the cathode chamber of MFCs and is mainly used due to its accessibility, oxidation potential and the formation of water

(non-toxic compound) [86]. The oxidation (1.1.) and reduction (1.2.) reactions and conditional potentials (achieved in typical conditions in MFC with an acetate oxidizing anode (acetate and bicarbonate concentration of 5.0 mM, pH7) and an oxygen reducing cathode (pO_2 = 0.2, pH = 7, using the Nernst equation $E_H = 1.229 – 0.0591pH + 0.0148 \log pO_2$) [84]:

$C_2H_4O_2 + 2H_2O \rightarrow 2CO_2 + 8H^+ + 8e^-$ E^0_{oxd}= 0.289 V *vs* NHE **1.1.**

$2O_2 + 8\ H^+ + 8e^- \rightarrow 4H_2O$ E^0_{red}= 0.805 V *vs* NHE **1.2.**

Based in these reactions, the maximum potential of an MFC is 1.09 V. The most common maximum potential applied is *ca.* 0.300-0.700 V [84]. Some studies presented higher Open Circuit Potentials (OCP) around 1.000 V for individual small-scale MFCs [84, 87]. MFCs are continuously studied to promote higher power densities to reach the values of others energy technologies, such as Fuel Cells or Batteries [87, 88] as seen in Figure 1.4.

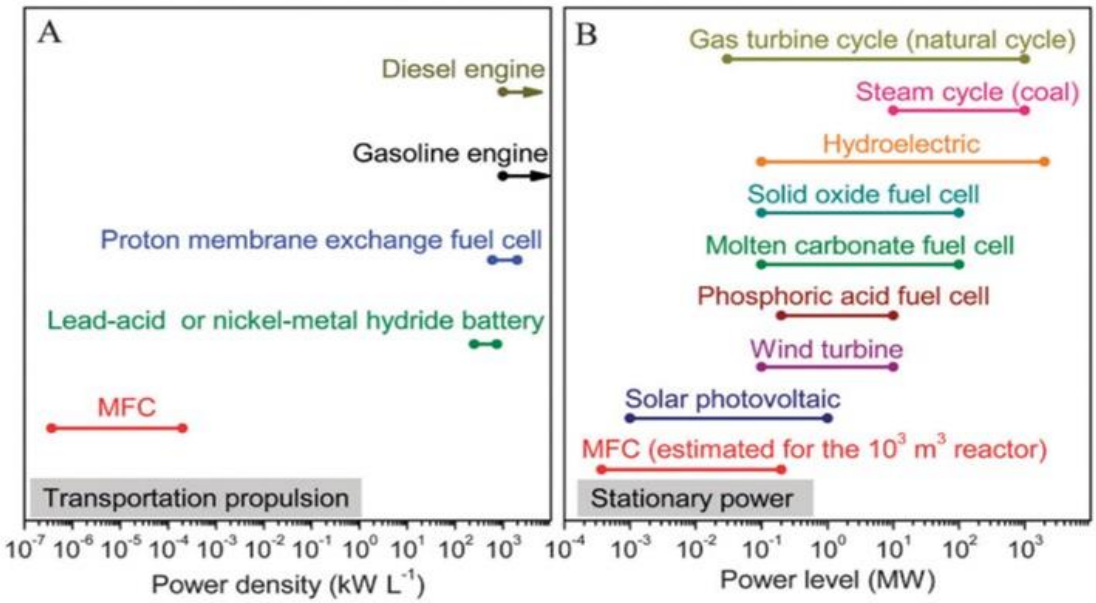


Figure 1.4. Power densities (kW L^{-1}) (A) and power level (MW) (B) of MFC and energy conversion devices [89].

MFCs aplied to recover energy from wastewater were first presented by Habermann in 1991 [90]. Wastewaters, *i.e*. domestic, agricultural and industrial wastewaters, contain organic compounds that are required to be removed prior to their discharge into the environment. The purpose of the MFCs is to lower the concentration of biodegradable compounds in wastewater resulting in the carbon removal or another biodegradable compounds (anaerobic conditions)

and electricity generation [83, 91]. When compared with the aerobic wastewater treatment, MFCs produce less biomass and do not need aeration [92]. Small on-site applications for MFCs in wastewater treatments for autonomous systems and *in situ* applications are continously researched for pratical implementations [92]. The success of stacking bench-scale MFCs has encouraged the scaling up of the MFCs modules towards a large-scale [93]. Large-scale MFCs in pilot plants are studied with different wastewaters to determine optimal configuration and operational efficiency, alongside with electrochemical energy conversion [93, 94]. Large scale MFCs face difficulties during the scale up, *e.g.* slow rates of substrate degradation [92, 95].

1.2.3. Microbial Electrolysis Cells

MECs were introduced in 2005 [96] and were reported for hydrogen gas production from acetate and present potential to be a significant contributor for CO_2 reduction strategies [97, 98]. These BES operate similarity to the MFCs. In MECs, the EAB oxidize carbon sources resulting in CO_2, electrons and protons; these are transferred to the anode by the EAB and the protons are released in the medium. Electrons travel to the cathode and protons move through the membrane to the cathode solution. Here occurs the combination of both [99]. Nevertheless, in MECs the reactions do not occur spontaneously. MECs require an external bias applied to produce hydrogen at the cathode (Figure 1.2B).

The cell reactions in MECs are depicted above (1.3. and 1.4.) and the standard potentials. The conditional potentials were determined using the Nernst equation assuming a temperature of 25 °C, a partial pressure of 1 atm of the respective gasses in the headspace, a pH of 7 at the anode and cathode, and an acetate and bicarbonate concentration of 5 mM, using the Nernst equation for calculations [84, 100]:

$C_2H_4O_2 + 2\ H_2O \rightarrow 2CO_2 + 8H^+ + 8e^-$ E^0_{oxd} = 0.289 V *vs* NHE **1.3.**

$2\ H^+ + 2e^- \rightarrow H_2$ E^0_{red}= −0.414 V *vs* NHE **1.4.**

In MECs, substrates such as acetate promote a potential difference of the cell of -0.125 V. So the acetate oxidation to hydrogen requires an additional energy potential applied (through external power supply) [100]. A minimum applied potential of -0.250 V (under pH = 7, 25 ºC and

1 atm) is needed for this practice [99, 101]. High temperature and artificially high conductivities are also used in laboratory conditions [102].

Biological hydrogen production is also well studied in dark fermentation (conversion of carbohydrates by fermentative microorganisms) [102], or in photo-fermentation (conversion of organic acids by photosynthetic microorganisms) [103]. Currently the interaction of dark fermentation and anaerobic digestion with MECs is also a viable principle being studied to enhance bio-hydrogen production [104–106].

1.2.4. Microbial Electrosynthesis Cells

The first research works with MESs were reported by Aulenta and coworkers in 2008 [107], where the biological production of CH_4 from a mixed anaerobic culture was analyzed, and in the report by Cheng and coworkers in 2009 [108], where CH_4 was directly produced using a biocathode containing methanogenic microorganisms and CO_2 reduction. This is a process called electromethanogenesis (Figure 1.2C) [109]. This process offers an alternative for biofuel production and carbon dioxide capture [110, 111], without the need for precious metal catalysts [108, 112].

Electromethanogenesis is now highly researched where methane is produced by direct biological conversion from potential applied and carbon dioxide [108, 113, 114]. Acetogenic microorganisms were shown to convert electrically generated low potential electrons and carbon dioxide into multi-carbon organic products [115]. Nevin and coworkers [116] investigated a MES with *Sporomusa ovata*, that was capable to deliver electrons using an electrode as the sole electron donor for the reduction of CO_2 to acetate. Fuels and chemicals generated in MESs using CO_2 are described as electrobiocommodities [115, 117], and are being increasingly investigated [97, 118–120]. Compared to conventional anaerobic digestion, MESs allow the physical separation of oxidized wastes from the methane production [121].

Electro-fermentation is also explored in MESs, where EAB oxidize organic or inorganic substrates, such as carbohydrates or alcohols [122], to generate electrons during respiration and production of valuable chemical products [123], using bias potential. General products generated from this process are *e.g.* acetate [124], organic acids [122] and alcohols [125, 126].

More research works in MESs are being presented in the literature and several reviews were published [98, 127–130].

1.3. BES materials and configurations

BESs are assembled with different electrodes built with carbon materials, and/or metal materials. The ideal electrodes material must present several criteria to be used in BESs such as: high electrical conductivity [131], high specific surface area and biocompatibility for biofilm formation [132] and low manufacture cost [133]. The electrode material must be stable in acid and basic environment and durable [134]. The electrical potential window applied in BESs must be adjusted to keep the electrode capacity [135]. High surface roughness is ideal to lower the fouling resultant from long-time BESs performances [13]. Carbon materials are the most used in electrodes in BESs and are normally ordered into a plane structure, a packed structure and/or a brush structure. Carbon felt electrodes are the most used because of their unleash texture that confers high surface for EAB growth, compared to carbon cloth and graphite [136, 137]. Carbon felt displays high conductivity, is inexpensive and chemically inert, and a versatile material [137, 138]. High impurities from chemical reactivity are a disadvantage for carbon felt [139]. Other carbon electrodes of different types are researched in BES: carbon paper [140], carbon mesh [141], carbon cloth [141], graphite rod [142], graphite granules [143], graphite plate [13], carbon brush [144], glassy carbon (or vitreous carbon) [145]. The diverse carbon electrode materials has been largely reviewed [13, 34, 133, 138, 142, 146–152].

Metal materials have been used in MFCs due to higher conductivity of metals over carbon materials [153, 154]. Some limitations of metals materials, *e.g.* smooth surface are responsible for weak surface adhesion of the EAB and poor biocompatibility [154–156]. But it is the cost of noble metals, such as gold, their biggest disadvantage [157]. Stainless steel is used to replace the use of catalysts because of their minor cost [13]. Other properties of metal materials used as electrode are reported in the literature [12, 34, 151, 157–159].

Nowadays a demand for novel carbon-nanotubes (CNT) based materials in bioenergy harvesting devices is denoted [160–162]. CNT are an allotrope of carbon that assumes the form of cylindrical carbon molecules. CNT consist of a hexagonal arrangement of hybridized carbon atoms, which may by molded by rolling up a single sheet of graphene (single-walled CNT) or by

multiple sheets of graphene (multiwalled carbon nanotubes) [163]. CNT present unique mechanical, thermal and electrical properties highly developed for energy harvesting devices [160, 164]. BESs explore these new CNT to expand the electrochemical activities of the EAB in the anode, and the oxygen reduction reaction at the cathode [162, 165]. CNT have been reported to enhance methane production in anaerobic digestion processes [166]. However, the cost of manufacturing these materials is still elevated. Example of electrodes adapted to be used with CNT are the carbon sponge electrodes [167]. These exhibit a three-dimensional structure for improving the anode performance in BESs, especially when carbon sponges are impregnated, which CNT that have good biocompatibility [168]. Carbon sponges are expensive due to the manufacture procedures (synthetic polymers and others), and now researches are being conducted to reduce cost [161]. CNT based materials, general properties and research advances are being reviewed [131, 142, 145, 147, 160, 162, 169–174].

Membranes are responsible for separating the chambers in BESs and their contents. Membranes allow protons/ions to migrate from the anodic chamber to the cathodic chamber [162], prevent oxygen diffusion into anode chamber; and avoid short circuit via insulation of the electrodes [175]. The electrodes have capacity to endorse sufficient turbulence so protons can be properly diffused between chambers through the membrane [12, 13]. Some BESs are exceptions and do not have membranes, *e.g.* Sediment MFCs (SMFCs), Membrane-less MFCs [79] or Single-chamber MFCs [176]. The membranes present low electrical resistance, high permeability, good mechanical, dimensional and chemical stability [12, 13]. Membrane resistance is influenced by the electrolyte composition, pH and concentration [177], and the membrane internal resistance should be as low as possible, for higher current and power densities [178]. A problem in BESs is the membrane biofouling that normally occurs on the membrane surface by attachment of bacteria and organic substrates that form a biofilm [179]. Other critical points are pH spitting, oxygen diffusion and substrate loss across the membrane [178, 180]. The cost of the membranes is also important, in particular for larger systems [181]. The membranes commonly used in BESs for energy generation are the Cation Exchange Membranes (CAEMs) [181], the Anion Exchange Membranes (AEMs) [181], the Polymer/Composite Membranes [181] and other miscellaneous types of membrane [12, 13, 182]. The CAEMs are the most used type of membranes in BESs [181]. The CAEMs include the

Proton Exchange Membranes (PEMs) [183], particularly designed to allow proton transfer and to oppose a high resistance to the transfer of all other ions [175]. Poor proton transferability is one of the most substantial deficiencies in PEMs [183]. Nafion Exchange Membranes promote high proton conductivity due to sulfonate groups fixed on an inert backbone (Polytetrafluoroethylene-like skeleton) [175, 179] and are characterized by their molecular weight cut-off and nominal thickness such as Nafion 117 or Nafion 112. Nafion Exchange Membranes are expensive and are affected by biofouling during long-term operation, which can significantly reduce their ion exchange capacity [184]. Several reports with Nafion Exchange Membranes are conducted with high power densities in MFCs [38, 179, 185, 186]. The AEMs have selective permeability for anions because they contain positively charged groups covalently bound to their polymer backbone [187]. These membranes create minimum hindrance to the pH balance by anionic species between the chambers in BESs [175]. In MFCs some reports used AEMs over others types [12, 13], because these have proved to be more subject to membrane deformation [188]. Bipolar Membranes are AEMs and CAEMs joined in series [175]. Polymer/Composite Membranes are recent membranes developed to improve the performance of anode, cathode and membrane with hybrid materials [189]. An example of hybrid material is Nafion Exchange Membranes with several composites (*e.g.* impregnation of polyaniline) to improve performances in MFCs by lowering biofouling and lower costs [190]. More information about membranes is presented and reviewed in the literature [175, 178, 181, 183, 187, 191–193].

The configurations of MFCs can also play an important role in the energy generation where the reactor designs and scale-ups were researched [13, 194]. In MFCs, the dimension and geometry of reactors, the volumes of electrolytes and electrodes area influence the power densities and the internal resistance [72, 84]. The two-chamber MFCs is the most usual MFC configuration, with H-type, Tubular up flow and Flat plate [13, 72]. Miniaturized MFCs are being researched for nano-applications [195]. The single-chamber MFCs are also highly researched [72, 196]. Examples of single-chamber MFCs are studies with air-cathodes [197] and with membraneless MFCs [198].

Works for large scale MFCs designs are conducted [74]. Logan and coworkers [194] explained that highest power densities in MFCs have all been obtained under nearly ideal conditions by

using a high concentration of a fuel (such as acetate), well-buffered and highly conductive electrolytes. MFCs that used defined substrates (most with acetate) produced more power at smaller scales than in larger scales [194]. A critical factor in power production when scaling up MFCs is the electrode spacing and electrode packing density relative to volumetric power density as the size of the reactor is increased [14, 194]. MFCs stacks and other types of designs are being researched for higher power production [196, 199]. MFCs designs and architectures are reported and reviewed in the literature [12, 14, 34, 74, 82, 196, 200–202]. Other BESs (MECs, MESs, etc.) designs and architectures that are similar to MFCs are constructed and are reported and reviewed in the literature [12, 66, 84, 99, 200, 203–205].

1.4. BES bioenergy storage advances

BESs are gathering attention from researchers and the number of reports has been growing rapidly. A bibliometric analysis of global research trends on BESs, MFCs, MECs and MESs showed an exponential growth in the number of articles from 2000 to 2020, as seen in SCOPUS database (Figure 1.5.).

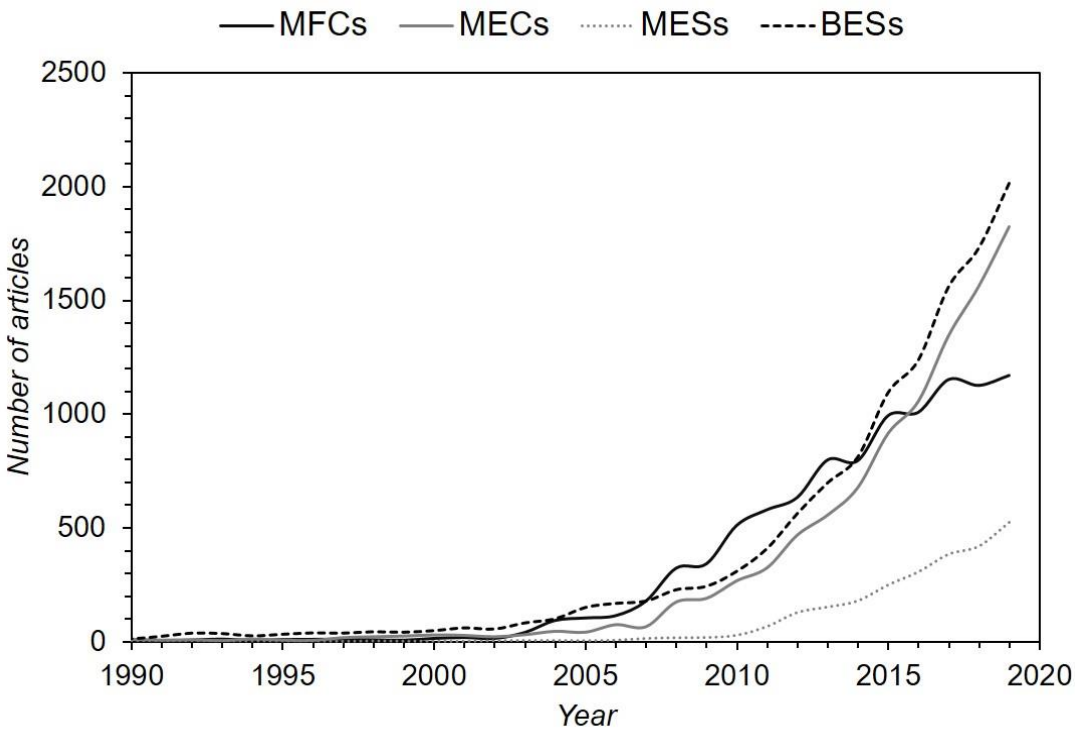


Figure 1.5. Research trends in MFCs, MECs, MESs and BESs from 1990 to 2020 (SCOPUS database access in February of 2020).

This exponential growth in the number of articles reported are related with MFCs research in electrode materials [142], mathematical modeling [204], economic assessment [206] and life cycle analysis [206]. Energy consumption and recovery in MFCs wastewater treatment is also within BESs applications focus of researchers [207]. Hydrogen-energy economy has interest for academy and industry, being an up forward for the development of MECs reports [48]. Hydrogen is a storable source of sustainable energy, as compared with other sustainable energy sources such as solar and wind [208]. Researches in MECs on scalable reactor design and configuration [99], applications in anaerobic digestion [209] and biocathodes statements [210] were studied. As for MESs, valuable chemical products generation are being researched and reviewed [116, 211–213].

BESs bioenergy is generated from the electrochemical energy conversion of fuels (*e.g.* biomass) converted into electrical energy through reduction and oxidation processes in MFCs and MECs, with EAB and chemical redox species [33].

The electrical energy generated in MFCs is captured by power sources such as resistors; MFCs cannot harvest energy in an autonomous system because the generated electricity is dissipated as heat instead of being utilized or stored [214, 215]. MECs, as equally in MFCs are based on oxidation of fuels and microbial reduction that can generate renewable hydrogen, with an external power source applied [33]. The energy is applied for the electrolysis or the synthesis of chemicals in MECs [216]. The literature shows that MFCs electrical energy have limited power output, as in Figure 1.3. For that reason, MFCs energy can be harnessed directly to power applications or implementing energy harvesting in MFCs [217]. Energy-harvesting circuits allow to chanell the MFCs energy to charge small devices [215, 218] and the power management systems are used to interface the MFC with the electronic load by collecting their energy first and then driving the load intermittently [218, 219]. The use of MFC stack devices is also presented for scaling up the technology [12, 199], as similar to the works with polymer electrolyte membrane Fuel Cell stacks [220].

Capacitors are devices with two electrodes inserted in an electrolyte solution and the electrical energy is stored in the electrical double layer at the interface between the electrolytic solution and an electronic conductor [221]. Capacitors are regularly used combined with a charge pump, a boost converter and load, establishing a power management system. One of the most

common example is MFCs connected to a capacitor, a light-emitting diode (LED) and a blinker board. The capacitor in an intermittent charging mode is initially charged by the MFC followed by a discharge [222]. The discharge of MFC results in light emission in the LED of a MFC. MFCs operation mode is a process of numerous days [223]. The supercapacitors are high-capacity capacitors capable to store 10 to 100 times more energy (per unit volume or mass) [224, 225]. Works such as the one by Hatzell and coworkers [226] employed MFC to charge MEC, where the capacitor works as a charge circuit. The goal was to increase MEC hydrogen production rates and to lower the energy expended. Their results have shown an increase of the hydrogen production rates by 38 %, MEC yields by 60 % and energy recoveries by 77 %. The report of Santoro and coworkers [227] demonstrate in-series connection of MFCs working in super capacitive mode, which are able to generate hydrogen through an additional electrode. Capacitors coupled with MFCs allowed in situ applications for powering small devices, allowing new opportunities for energy supply in remote areas, such as to power wireless sensors to monitor the environment [223], temperature sensors, LED lighting, and submersible ultrasonic receiver [228]. The use of capacitors improves the power densities of MFCs as seen in the reports reviewed in the literature [30, 219, 226, 229].

Capacitive electrodes inserted into the anodic compartment form a capacitive bioanode to enable energy storage in MFCs [230]. Capacitive electrodes are used in biosensors potentials, where energy is acquired through a dielectric layer and no electrolytes are required [231]. In the work of Deeke and coworkers [232], with the use of capacitive electrodes, 40 % more current can be gained from this capacitive electrode during intermittent operation compared to continuous operation of a noncapacitive electrode [232]. The improves of capacitive electrodes inserted in BESs are reported in several works [218, 222, 230, 232, 233]. SMFCs are being developed as potential energy sources where remote sensing and monitoring would be useful [234–236]. These are MFCs aplied for “continuous energy harvesting” [236], and for the developement of autonomous, battery-powered, low-cost devices [234]. As explained in the work of Mohamed and coworkers [234], the practical applications for the remote systems with SMFCs has two challenges that must be overcome: 1) optimizing the power output of the SMFCs and 2) predicting the performance of the SMFCs over time.

To improve BES energy storage, MFC stacks are researched to build a syngle BES, that can operate as a battery. MFC stacks are described as one simple way to improve energy generation and increase the power output of the systems [237]. In a stack, it is the number of cells that contributes to the final potential, and the surface area of each cell determines the final current [238]. MFCs have been studied in a combination of high number of MFCs connected in parallel or in series [239]. The MFCs connected in parallel are used to expand the potential and the current of the system [229] and MFCs connected in series are used for the individual potential of each MFC add-up at the output while a common current flows through the MFCs [239]. The use of MFC stacks in series promoted superior power densities than MFC stacks in parallel [240]. Works such as Aeltermann and coworkers [241] using six MFCs connected in series or parallel showed that stacks improve the potential and current generation. One of the problems of MFCs in series is the risk of potential reversal [238], that can occur as the result of substrate starvation, affecting the EAB in the biofilm and subsequent reducing performance of the stack cell. Potential reversal can be minimized by dodging low substrate concentrations, which occur in fed-batch cycling, using continuous flow and by minimizing internal resistances among cells in the stack [238]. MFC stacks can also be operated in continuous [2] or in cascade [196]. These have been investigated, since fed batch systems may not be suitable for continuous power generation [2]. Reports show MFC stacks also combined with capacitors to harvest and store energy to charge small devices [226, 242, 243]. MFC operated with different stacks connections are reported [237, 242, 244–248]. MFC stacks are also applied for treatment of different organic sources with high Chemical Oxygen Demand (COD) removal rate and energy recovery [249, 250]. MFC stacks are being pointed out in pilot scale up reports to design larger systems. An example is a 200 L modularized MFC consisting of 96 MFCs modules operated for a long period of time with wastewater [251], or the MFC stacks performed for urine treatment in a music festival [252]. The continuous energy harvesting with the use of commercially available electronics without any potential furthering components and external power supply is one of the most researched field for MFCs [253]. Now, the use of the microbial and chemical catalysis in BESs, similar to RFCs principles [254], is being used for the development of new Microbial Batteries [255] or Microbial Rechargeable Batteries for energy generation and storage [256].

1.4.1. BES for bioenergy storage

Bio-batteries were one of the first devices studied for bionergy storage. Bio-battery is an energy storing device that is powered by organic compounds (*e.g.* glucose) [257], but are less likely to retain most of their energy. MFCs can also be applied toward a concept of Bio-battery which are able to recharge devices requiring small potential. The possible combinations of microbial and chemical catalysis in BESs is important to explore for bioenergy storage [258]. With the production of electricity from organics by MFCs and the reverse conversion of electrical power to organics by MECs and MESs was settled as possible (Figure 1.9.); this paved the way for the integration of the two systems misacting as energy storage technologies; also the exploration of coupling BES with other electrochemical energy storage devices [259, 260].

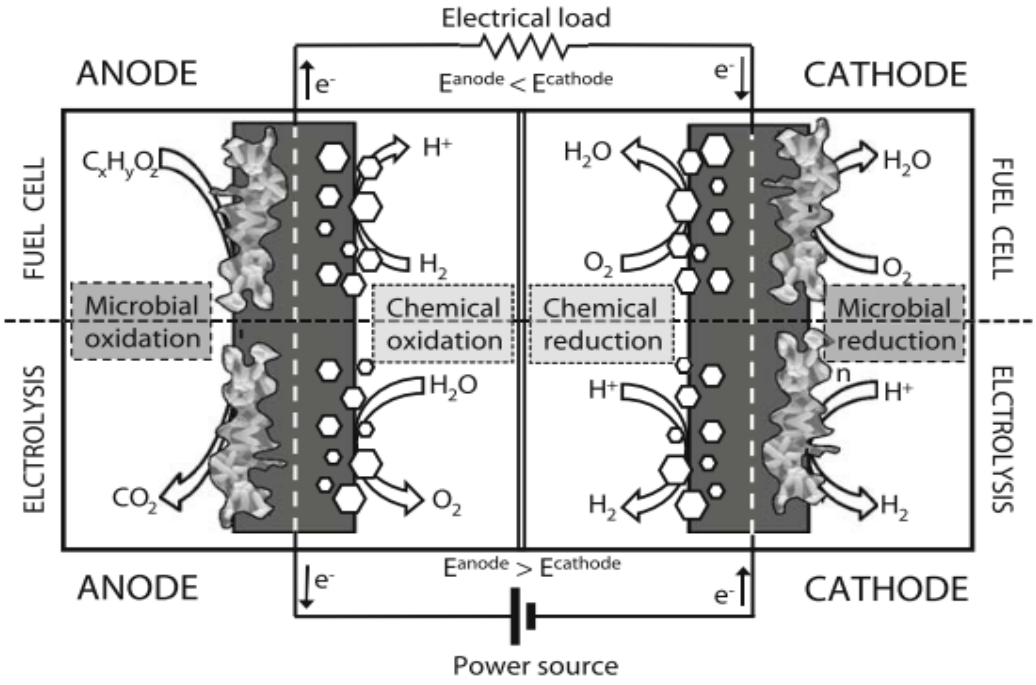


Figure 1.6. Schematic overview of the possible combinations of microbial and chemical catalysis in BESs. Energy is harvested in MFCs ($E_{anode}<E_{cathode}$) and energy is consumed in MECs ($E_{anode}>E_{cathode}$) [258].

Xie and coworkers in 2013 called “Microbial Battery” their system for energy recovery from wastewater in a two-step energy generation process [255]. This was operated in the anode side equal to an MFC anode and in the cathode side was operated similarly to a Rechargeable Battery. A solid-state cathode was introduced to replace the oxygen as the final electron acceptor. The system reached an efficiency of electrical energy conversion of 49 % from the

organic matter consumed. The authors suggested that their system can be used for treatment of complex organic mixtures, but is not suitable for large-scale applications because of the high capital cost of the silver-based electrode used [255].

A Microbial Rechargeable System was presented by Molenaar and coworkers in 2016 [256] with the coupling process between MES and a MFC to store and recover electricity. A combination of effluents from an acetate-producing biocathode and effluent from an active MES running on acetate was used. When operating the MFC, electrical energy is generated with consumption of acetate. When the system operates in the MES phase, the electrical energy of the system is consumed to form acetate. The authors studied the life cycle of the Rechargeable Battery, where ferrycianide was used as redox pair, reaching a full cycle energy efficiency of 30−40 %. One of the drawbacks that MFCs, MESs and the presented system include are sensitivity to changes in electrolyte composition and the side reactions that result from alternative metabolic pathways and bacterial growth. Molenaar and coworkers [256] concluded that their Microbial Rechargeable System could become a proper, clean, safe, and renewable alternative to existing Battery storage systems in the future, and that it could become an inexpensive local energy storage device.

BESs bioenergy generation was combined with several electrochemical devices such as Photoelectric Cells, to compete and replace the conventional fossil-fuel based energy generation approach [261]. Du and coworkers [262] developed a Hybrid Photoelectrochemical MFC for simultaneous harvesting of solar energy and bioenergy, with potential for treatment of recalcitrant compounds. They applied a titanium dioxide (TiO_2) photo-anode next to a bioanode (effluent of a glucose-fed MFC reactor) that shares the same cathode in the MFC. Power densities of 1645 mW m^{-2} were registered with the systems, being an improvement of 67 % over the MFC operating only.

BESs with enzymatic electrochemistry systems and RFCs were tested [263]. A conceptual demonstration of an enzymatic RFC where the interconversion of NAD^+/NADH as the anolyte coupled with the Fc/Fc^+ as the catholyte was demonstrated [264]. The authors developed a bioanode to create an immobilized glucose/O_2 Enzymatic Fuel Cell with a high OCP *ca.* 1.100 V.

1.5. Microbial Redox Flow Cell

Redox Flow Cells (RFCs) are electrochemical storage devices that transform electrochemical energy into electrical energy [265], with the capacity to store large amounts of electrical energy, inexpensively and efficiently. The RFC technology was described in a patent approved in 1949, and in the consequent research that followed this patent [266, 267]. Several works performed by NASA research groups in RFCs for use in remote power systems and distributed storage installations were important for the development of the technology [268, 269]. RFCs have been developed during the last decades exponentially, leading to several devices such as the Vanadium RFCs [270], Zinc/bromine RFCs [271] or Iron RFCs [272].

RFCs are derived from Fuel Cells by the replacement of traditional Chemical Fuels through reversible redox pairs (known as electrochemical fuels) [11]. The RFC consists of a main reactor, that includes two external tanks, which work as electrolyte reservoirs [11]. The chemical species that will work as redox pairs are introduced in external tanks, dissolved in aqueous or non-aqueous solutions together with the support electrolyte [273]. In the main reactor, an ion exchange membrane is placed between the electrodes, in a sandwich mode denominated as Membrane Electrode Assembly (MEA) [11]. Then redox pairs are re-circulated into the RFC where the oxidation-reduction reactions take place [11].

Figure 1.7 shows a scheme of a simple RFC. The oxidation-reduction reactions in RFCs are the following [11]:

Anode reaction (negalyte): $A^{n+} - x\, e^- \rightleftharpoons A^{(n-x)+}$ **1.5.**

Cathode reaction (posilyte): $B^{m+} + y\, e^- \rightleftharpoons B^{(m+y)+}$ **1.6.**

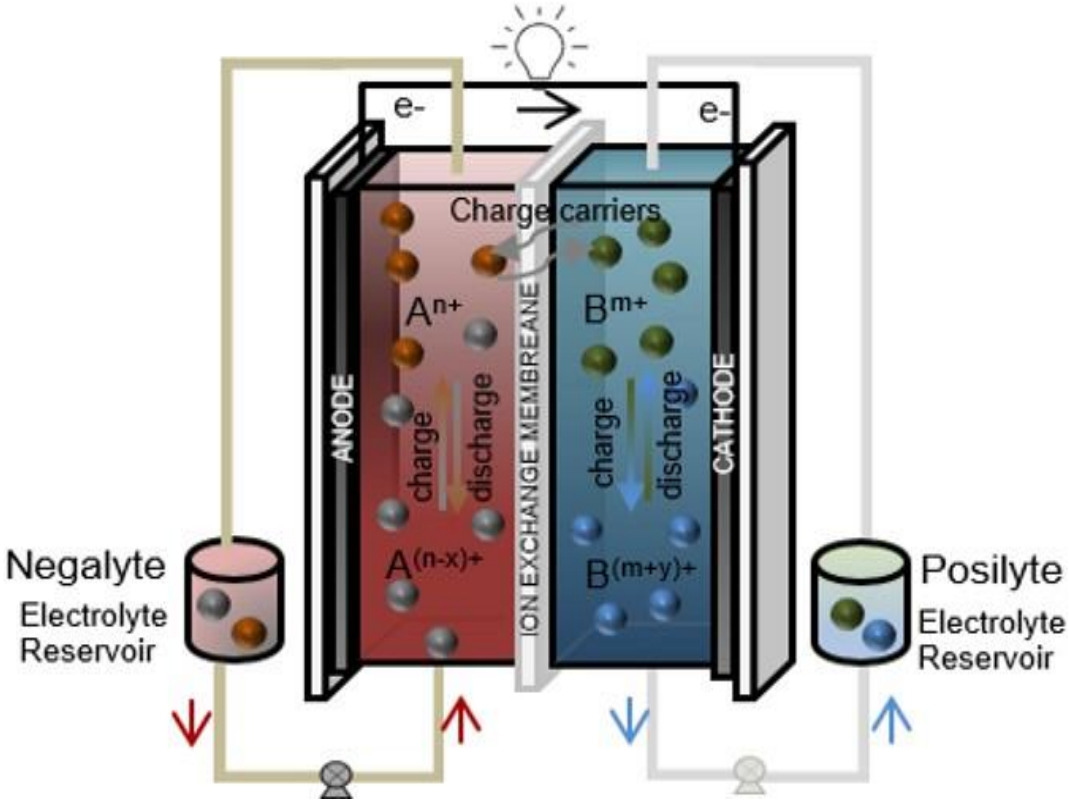


Figure 1.7. Simplified scheme of a Redox Flow Cell (RFC).

The oxidation-reduction reactions of the reversible redox pairs result in electrochemical energy that is stored/delivered according to the charge/discharge mode of the RFCs [273]. The flow plates, end plates and current collectors complete the RFCs assembly and play an important role in the chemical and physical reactions [11, 274].

RFCs have potential to be coupled with other devices for energy generation and storage with renewable energy sources, such as solar or wind. Initial works like the one by Azevedo and coworkers used a Photoelectrochemical Cell to charge a Vanadium RFC [19]. Here, the direct conversion of sunlight into electrochemical energy stored in an RFC was demonstrated. Following their work, a coupling system between a Photoelectrochemical Cell and a RFC with quinone as redox pair was demonstrated [275]. Both devices allow direct solar charging of the redox pair, developing an auspicious type of RFC and a new way to promote energy storage. More research for coupling RFCs and solar energy is being pursuit [276]. Now, biomass energy storage in a Microbial Redox Flow Cell (MRFC) is envisaged and this is the main motivation of this work.

In RFCs operation, the membranes and electrodes are decisive for the final performance. Polymeric Membranes are the most studied type of Ion Exchange Membranes, where Nafion

Exchange Membranes are included [277]. These allow the diffusion of ions between the cell [277]. Nafion Exchange Membranes in RFCs display low-permeability and let the separation of the chemicals to avoid crossover, allow good ion selectivity, high conductivity, good stability and suitable mechanical properties [278]. Carbon-based electrodes are assembled in RFCs [279]. Both present large surface area and are highly porous electrodes (*e.g.* nanostructured carbon materials). Carbon felt electrodes with chemical modifications are also used [279, 280]. Electrodes have to provide high electrochemical stability, high rate of electron transfer from/to the redox chemical species [11], support high electrical conductivity, high fluid permeability and mechanical stability [11, 279–281]. Electrodes with low cost materials, chemical and electrochemical inertness for a large window of chemicals and redox potentials are desirable [281]. The flow plate allows the mobility of the electrochemical fuels and the distribution of reactants across the main reactor [11]. Graphite flow plates are mostly used [274]. Flow plates are fabricated with diverse designs of flow channels (*e.g.* serpentine, parallel, interdigitated, spiral) responsible for the diffusion of the solutions [274]. Isolation plate offers electrical isolation [7]. The end plates close and give mechanical stability and structure [11] and the gaskets avoid leakages in the main reactor of RFCs [282].

RFCs major feature is that power and energy outputs are independent variables [11]; here power is determined by the reactor size, number of cells used and the area of the electrodes [11, 274]. The amount of energy stored depends on the reactants chosen, their concentration, electrolytes properties and the size of the reactant tanks [11, 274]. The RFCs are also built to be scalable, flexible, with long durability and high efficiency [283]. Some downsides of RFCs are the occurrence of water electrolysis (when using redox pairs in aqueous solutions [284]), cross mixing of half-cell electrolytes through the membrane (causing self-discharge and capacity loss [284]), corrosion and toxicity of some redox pairs, *e.g.* release of bromine in the form of hazardous vapors [280].

1.5.1. Aqueous Redox Flow Cells

Different RFCs technologies have been researched and published over the years using different physical structures, different solvents and different redox pairs. RFCs can be separated, in terms of the solvent used to prepare the redox couples, in Aqueous RFCs or Non-

aqueous RFCs [273]. The Aqueous RFCs where the first type of system developed [285]. The redox pairs in aqueous RFCs are water solvent-based electrolytes, prepared in acid or basic conditions (*e.g.* H_2SO_4, KOH, NaCl, HBr). Cell potential in Aqueous RFCs reaches *ca.* 1.500 V [273]. A special concern for water electrolysis is needed [284]. Aqueous RFCs present low operational costs and scalability, but low energy density is achieved (<25 Wh L^{-1} in most RFCs) [286]. Examples of aqueous RFCs are the soluble All-Iron aqueous RFCs [287] or the aqueous All-Copper RFCs [288].

The Non-aqueous RFCs were proposed in 1984 [289], and the main solvents applied are ionic liquids or organic electrolytes (liquid form or adsorbed in materials *e.g.* $TEABF_4$, $EMIPF_6$, $NaClO_4$) [290, 291]. Non-aqueous RFCs present cell potentials superior to 2 V [273]. The high cost of solvents and the potential hazardous nature of the chemicals used are disadvantages [291]. Examples are the Non-aqueous Vanadium RFCs [292] and Ruthenium Bipyridine RFCs [293]. Aqueous RFCs present higher power densities that Non-aqueous RFCs [293] and lower chemical cost (Figure 1.8).

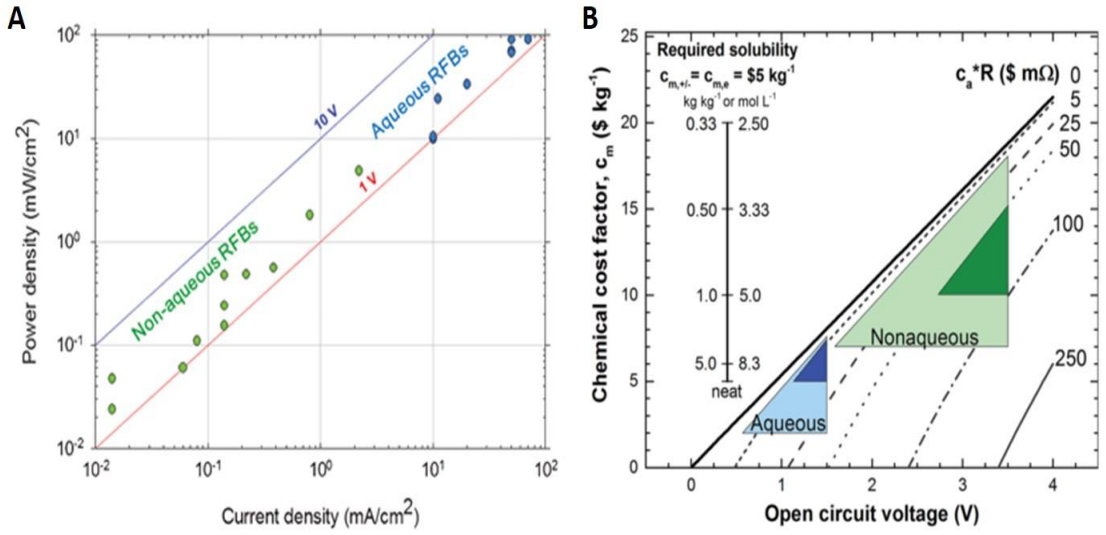


Figure 1.8. Comparison of A) power and current densities for Non-aqueous RFCs (green) and Aqueous RFCs (blue) [293] and B) acceptable chemical cost factor on an active material basis (in $ kg^{-1}) versus Open Circuit Potential for a range of reactor costs for non-aqueous RFCs (green) and aqueous RFCs (blue) [273].

The electrochemical energy storage in RFCs is based on the nature of the redox couple and the capacity to store energy depends on the energy capacity of the redox chemical species [293]. All redox species are used to increase power efficiency and create a less expensive energy

storage process [273]. The choice for metals as redox pairs in RFCs were based on the redox potentials, the states of energy and their solubility. RFCs with metals such as vanadium [294], iron [287], lead [295], copper [296] were researched over the years. All-Vanadium RFCs are highly researched, in which V^{2+}/V^{3+} and VO^{2+}/VO_2^{+} are used as redox couples, resulting in cell potential *ca.* 1 V, using 2 M H_2SO_4 solution as solvent [297]. All-Vanadium RFCs have less cross-contamination in the reactor because the same metal is used in both external tanks, generating a long life-time for the systems [297]. Concerns around toxicity of ion metals, corrosion and the low solubility of metals under specific pH and temperature values [298] promoted the replacement of metallic compounds with other redox chemical species [299]. Organic active molecules with reversible chemical reactions are used in RFCs to promote higher cell potentials [298]. Organic active molecules are presented as an advantage to be applied in RFCs because of their low cost of extraction and chemical synthesis, different redox potentials, chemical stability and solubility, structural diversity, stability, tunability and fast kinetics transfers [298, 300–304].

1.5.2. Aqueous Organic Redox Flow Cells

Aqueous organic RFCs are being studied for the goal of “green”, safe, and cost-efficient energy storage [273, 298]. Aqueous Organic RFCs are being reported with different organic compounds as redox couples. The first Aqueous Organic RFCs presented had quinones as redox pairs [305–307]. More recent reports for Aqueous Organic RFCs use as redox pairs aza-aromatic compounds like phenazine/alloxazine [308], TEMPO (2,2,6,6-Tetramethylpiperidin-1-yl)oxyl [309], viologen radicals [310] and redox-active organic materials [311]. Several redox potentials of the organic compounds applied as redox couples can be seen in the literature [301, 304, 312–317] and some are represented in the Figure 1.9.

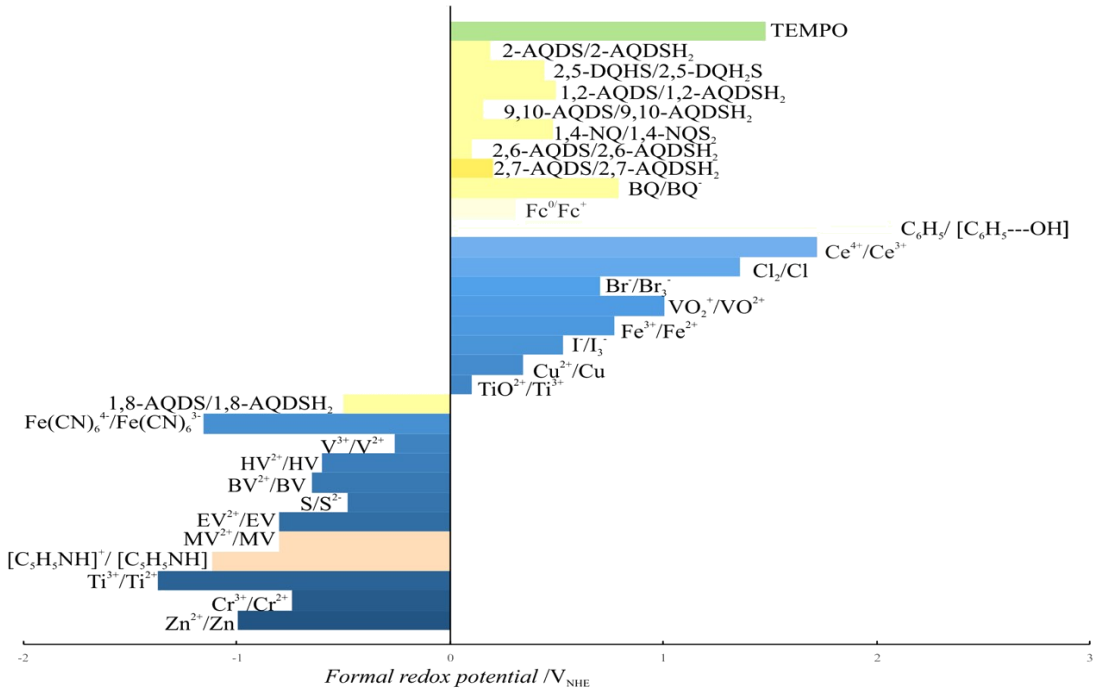


Figure 1.9. Redox potentials of different inorganic and organic redox couples seen in RFCs [254].

Quinones are the most researched type of organic compounds as redox pair in different types of Aqueous Organic RFCs tested as redox pairs with ion-metals [317] and in All-organic RFCs [303]. Quinones are small organic molecules belonging to the group of aromatic compounds. Their chemical structure is based in cyclic diketones organized in a 6-member ring structure with carbonyl groups [318]. The first research with quinones, published in 1922 [319], pointed out some chemical and physical properties of the compound. The redox potentials [320], fast kinetics [321], solubility, low cost [322], tunability and stability [301, 303, 323] are the major attractive feature for the RFCs.

The present work was focused on the develop of the Microbial Redox Flow Cell (MRFC) that explores Aqueous RFCs and quinones as redox pairs. Quinones has a large window of redox potentials, explored for quinone-based negalytes and posilytes that can provide high potential for RFCs [324, 325] (Figure 1.9. and Table 1.1.). The chemical structure of quinones presents superior energy density than ion metals, and can be reduced to hydroquinones in a well-studied reversible reaction, with fast electrochemical kinetics [321] (Figure 1.10.).

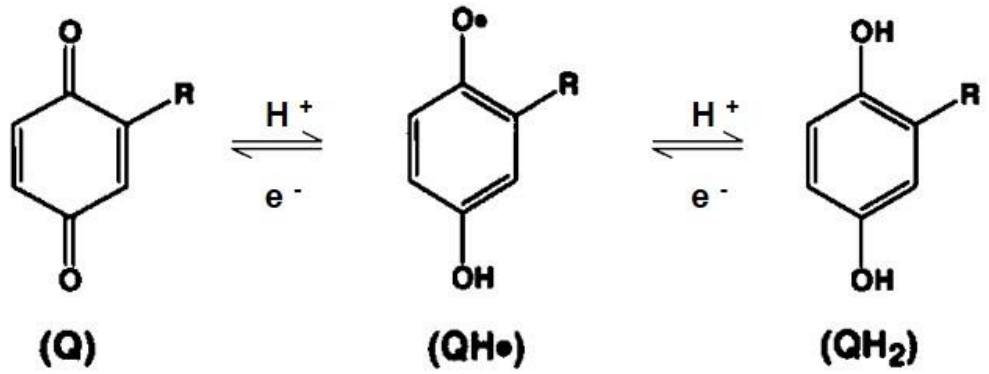


Figure 1.10. General scheme of p-benzoquinone redox reactions in buffered aqueous solution (adapted from [320]).

The fast kinetics of the redox reactions is related to good electrical conductivity due to small gaps in the energy levels of quinones [323]. Quinones allow to tune the molecules in order to achieve higher redox potentials [320], with the addition (or substitution) of functional groups (R groups) (such as halogens, nitro, carbonyl, amine, hydroxyl and methoxy groups) in the benzene ring [314, 320, 326]. Quinones solubility is superior when the R group contains hydrophilic units (*e.g.* phosphoric and sulfonic groups) [314]. The solubility and the pH values of buffered electrolyte solutions established in the RFCs operations need to reach low solvent effects and high conductivity [327]. Hydroquinone's form is stable at neutral pH due to its high pKa value (~10) [328]. However, hydroquinones in contact with oxygen are re-oxidized to the quinone form.

The classic quinone/hydroquinone couple follows an electrochemical reaction mechanism, combining a pair of electron and proton transfers, displaying two-electron Nernstian behavior [323, 327] (Figure 1.10.). Quinones present two or more C=O bonds in each quinone; each molecule has at least two units of electric charge. Such a relatively compact structure results in twice the energy storage (per unit volume) and thus in a higher energy density than other molecules with one unit of electric charge [322].

Quinones can suffer some decomposition (polymerization and oxidation of the carbon backbone) during oxidation-reduction reactions. The degradation rate will depend of the specific supporting electrolyte [301, 323]. One particularity of quinones is a change of color during their reduction-oxidation processes, that is proportional to the concentration of the respective

chemical form, allowing the identification of the redox chemical species that are present (oxidized or reduced form) [329–332].

The quinones mostly used in Aqueous Organic RFCs are benzoquinones (single benzene ring) [326], naphthoquinones (two-benzene ring) [326] and anthraquinones (three-benzene ring) [303]. RFCs with anthraquinones were studied in the work of Huskisson and coworkers, n as a Metal-Free Organic–Inorganic Aqueous RFC [333], with anthraquinone-2,7-disulfonate and bromine as redox pairs where *ca.* 99 % storage capacity retention per cycle was demonstrated. Lin and coworkers present an Alkaline Quinone Flow Battery [334], by utilizing commercially available 2,6-dihydroxyanthraquinone, where the authors explain that quinone-ferrocyanide alkaline chemistry avoids the membrane crossover, corrosivity and toxicity. An RFC with anthraquinone-2-sulfonate or anthraquinone-2,6-disulfonate on the negative side, and benzoquinone-3,5-disulfonate on the positive side was investigated [321], lowering the chemical crossover limitations. The RFC was charged and discharged multiple times at high Coulombic Efficiency without any sign of degradation [321]. In Table 1.1 are presented some of the Aqueous RFCs with quinone as redox pairs.

Table 1.1. Summary of reports with Aqueous RFCs with quinones as redox pair.

Negalyte	Posilyte	Cell potential (V)	Current density (mA cm^{-2})	Energy density / Power density	Coulombic efficiency (%)	Energy efficiency (%)	Reference
2,5-dihydroxy-1,4-benzoquinone	Anthraquinone-2,7-disulfonate	>1.0	8	N.A.	>90.0	N.A.	[301]
Anthraquinone-2,7-disulfonate	Benzoquinone-3,5-disulfonate	0.55	10	1.15 Wh L^{-1}	96.0	N.A.	[335]
Anthraquinone-2,6-disulfonate	1,2-dihydroxybenzene-3,5-disulfonate	0.70	5-200	250 mW cm^{-2}	100.0	70	[336]
Anthraquinone-2,7-disulfonate	Benzoquinone-3,5-disulfonate	0.67	100	62.4 mW cm^{-2}	98.6	45.8	[337]
1,3-cyclohexanedione	1,3-cyclohexanedione	-0.42	3.2	N.A.	99.0	N.A.	[338]
Lead sulfate	4,5-dihydroxybenzene-1,3-disulfonate	1.05	10	N.A.	98.0	75	[339]
Lead sulfate	4,5-dihydroxybenzene-1,3-disulfonate	1.10	10	2.75 mW cm^{-2}	93.0	82	[340]
Anthraquinone-2,6-disulfonate	Benzoquinone-3,5-disulfonate	0.60	5-25	N.A.	≈100.0	N.A.	[321]
Anthraquinone-2-sulfonate	benzoquinone-3,5-disulfonate	0.60	5-25	N.A.	≈100.0	N.A.	[321]
Anthraquinone-2,7-disulfonate	Hydrobromic acid	0.94	250	N.A.	99.9	98	[341]
Anthraquinone-2,7-disulfonate	Sodium iodide	0.60	10	N.A.	89.0	N.A.	[342]
Anthraquinone-2,7-disulfonate	Hydrobromic acid	0.73	250	N.A.	>90.0	>90	[343]
Anthraquinone-2,7-disulfonate	Hydrobromic acid	0.92	500	50 Wh L^{-1}	95.0	N.A.	[344]
Anthraquinone-2,7-disulfonate	Hydrobromic acid	0.87	200	N.A.	98.0	N.A.	[345]
Anthraquinone-2-sulfonate	Hydrobromic acid	1.00	250	N.A.	96.5	73.5	[303]
Anthraquinone-2,7-disulfonate / Anthraquinone-2-sulfonate	Hydrobromic acid	0.90	250	N.A:	95.7	N.A.	[346]
Potassium ferrocyanide	2,3-diaza-6-methoxy-anthracene-9,10-dione	1.00	250	N.A:	99.7	N.A.	[347]
2,6-dihydroxyanthraquinone	Potassium ferrocyanide	1.20	100	N.A.	99.0	84	[334]
Anthraquinone-2,7-disulfonate	Potassium ferrocyanide	0.70	20	N.A.	100.0	75	[275]
Anthraquinone-2,7-disulfonate	Potassium ferrocyanide	0.50	40	N.A.	98.0	98	[348]
4,40-((9,10-anthraquinone-2,6-diyl)dioxy)dibutyrate	Potassium ferrocyanide	1.05	50	17 Wh L^{-1}	100.0	100	[349]
Sulfonated derivatives of 4,4′-biphenol	1,8-dihydroxyanthraquinone	0.90	800	45 Wh L^{-1}	>95.0	90	[350]

N.A. not available

Further researches to increase the RFCs cell potential, increase the life time of the battery and synthesizing other quinones with desirable properties for use in an All-quinone RFC are being pursuit. Computational designs for quinones synthesis and prediction of redox potentials are a major support for their development [304, 314–316, 351 ,352]. More reviewed information for quinones in aqueous systems were presented [290 ,353, 354].

The RFCs and the BESs are electrochemical devices that are evaluated through the potential of the cell assessed with the Nernst potential, which is related to the concentrations of the oxidized and reduced chemical species [11]. The Coulombic Efficiency (CE) (also denominated faradaic efficiency or current efficiency) are important to estimate the efficiency of electron charge that is transferred within an electrochemical system [274]; in the case of RFCs is the ratio of cell potential between discharge and charge cycles [274]. The Potential Efficiency (PE) (also denominated voltage efficiency) indicates the ratio between the potential of the discharge and charge curves [274]. The Energy Efficiency (EE) is defined by the ratio of the energy furnished by the battery during the discharge, to the energy supplied during the charge. It represents the product of the CE and the PE [274]. In RFCs the energy input are the redox couples and the energy output is the electrical energy.

1.6. Motivation and outline

The increase in the energy demand and the concerns about the environmental impacts of fossil fuels is responsible for intensifying the research in renewable energy sources. Renewable energy, such as solar electricity, requires energy storage devices to be available. Energy storage devices such as conventional Batteries and Supercapacitors are used to generate and store accessible energy with high round-trip-efficiency. However, their energy density is low when compared with high-energy density display by fuels.

Biomass is a renewable energy source that can be transformed into solid, liquid, and gaseous fuels. Biomass is abundant, versatile, capable to generate heat, available at lower cost and is biodegradable. A safe, renewable and low–cost system using biomass as renewable energy for energy storage purposes is envisaged.

Bioelectrochemical Systems (BES) are devices capable to convert biomass as fuels (electrochemical fuels) into electrical energy or hydrogen/chemical products. BES is responsible for converting electrochemical energy into electricity by oxidizing carbon sources in Microbial Fuel Cells. It is also operated for converting electricity into chemicals in Microbial Electrosynthesis Cells.

Electrochemically Active Bacteria (EAB) are the catalysts of BES, since their capable of electric interactions with extracellularly redox-active materials, such as electrodes. Their core ability is to form biofilm in electrode surfaces. The EAB are responsible for the conversion of different types of carbon sources, and promote the transfer of electrons from microorganisms to electrodes by directly or via mediated Extracellular Electron Transfer (EET) processes. EAB can operate as exoelectrogens and electrotrophs with a large applicability as biocatalysts in BES. EAB offers the potential to generate energy and chemicals from sustainable resources, involving Electrofermentation with Electrochemistry. The development of processes that can use EAB to generate electricity denotes an innovative method of converting bioenergy, since bacteria are self-replicating and, therefore, biocatalysts for the oxidation of organic matter are self-sustainable.

BES also display a great potential to improve different types of subtracts, including wastewater. BES is responsible for the direct biotransformation of the chemical energy present in wastewater into electrical energy. These devices offer a sustainable approach for integrated

waste treatment and energy and resource recovery, because it offers a flexible device for both oxidation and reduction reactions oriented processes. BES provide means of simultaneously reducing the waste treatments costs and generate current, efficient bioremediation of the organics, toxicity reduction, gaseous pollutants treatment, synthesis of chemicals with commercial value and others. Several advances with BES materials and configurations are been achieved, with the intent to scale-up of the technology, with special focus in wastewater treatment.

One of the critical limitation of BES is the low cell potential output for practical applications. Despite the exponential increase in energy densities reported over the years, the energy density values are below the energy densities achieved by other technologies, such as Batteries. For bioenergy practical applications, BESs electrical energy was channeled for different energy harvesting and storage power systems. Energy-harvesting circuits allows to channel BESs energy to charge small devices. Power management system are used to accumulate BESs energy primarily and then conduct the load intermittently. Several reports with Capacitors, Capacitive electrodes and Stack systems were conducted and reported as a practical alternative to BES energy potentiality. Nevertheless, the power output and the costs required to scale up these systems to reach usable energy levels for real life application is still a restriction.

BES energy storage is also absent in research and few reports are described in the literature. The coupling of electrochemical devices, where renewable energy sources generate and store electrochemical energy has been vastly researched and are seen as ideal for less dependence on fossil fuels. The advantage of coupling processes of electrochemical devices is the flexibility and new energy generation processes and storage to supply energy. Coupled systems with local renewable energy generation will improve ways to decentralize storage and improve power network strength. Energy storing devices powered by organic compounds, with the use of microbial and chemical catalysis in BES, similar to Redox Flow Cells is an opportunity.

Redox Flow Cells (RFC) are electrochemical storage devices that transform electrochemical energy in electrical energy, and are considered the best stationary technology. RFC has the capacity to store large amounts of electrical energy efficiently and inexpensively. The use of reversible redox pairs as electrochemical fuels, re-circulated in a main reactor, similar to the

Fuel Cells, result in redox reactions (electrochemical energy) that is stored/delivered during the charge/discharge mode of the RFC. RFC coupling systems appear to improve power and lower the technological costs. An example is the Solar RFC, that act as a combination of Photoelectrochemical Cells and RFC. To make solar energy fully dispatchable it is necessary to store it, and RFCs storage is a technology of choice.

This thesis motivation was driven by the need to research a new approach to store bioenergy. The coupling of BES and RFC contributes for the emergence of efficient storage technologies attained through the newest approaches in converting biomass into storable energy. The energy released by the bacteria is directly converted into storable energy (electrochemical fuels) easily and efficiently convertible into electricity, making this electricity dispatchable. This makes the BES energy more attractive and cost effective.

This approach promotes the storage of bioenergy in the form of microbial electrochemical fuels. Such microbial electrochemical fuels contain redox molecules and could be applied to develop a Microbial Redox Flow Cell (MRFC). The MRFC proposes a direct transformation of chemical energy of wastes into electrochemical energy, storable and easily and efficiently convertible into electricity using a bio driven approach.

The redox pairs 2,6-AQDS and $[FeCN_6]^{4-}$ were evaluated as microbial electrochemical fuels for the MRFC. These are used as a new way to promote the recharge of an RFC, where carbon sources operate as fuel. MRFC is a new way to combine the treatment of wastes and biomass to charge a battery from biomass.

BES can be practical in energy storage processes as the catalysts in devices, using Electrochemically Active Bacteria (EAB), to generate and convert different substrates. BES capability to reduce ion metals such as vanadium and ferricyanide, that constitute redox pairs explored in RFCs, enables the conversion of different redox molecules that could be used as possible redox pairs for the MRFC. Furthermore, the EAB are not yet explored as catalysts to recharge an RFC. The use of electrochemical fuels in the RFC is much more flexible and much more efficient for the production of other bioelectrochemical fuels, such as hydrogen.

Quinones, such as 2,6-AQDS, have recently been proposed as promising redox couples in RFCs, due to their low cost, reversible redox reactions and safety. Quinones are studied in Aqueous organic RFCs, as a “green” and safe redox chemical species, where their redox

reactions, solubility, tunability, large window of redox potentials and others properties are seen as ideal for a cost-efficient energy storage. Quinones are applied as biological redox molecules in BESs. In this thesis, the quinone 2,6-AQDS, was studied as a cathodic electron acceptor in BES for the first time. Despite the advantages of using others terminal electron acceptors such as oxygen in BES, 2,6-AQDS was selected as one of the redox pairs for the charge of an RFC, and to develop a MRFC.

The present thesis is divided in main chapters as follows:

The **Chapter 2**, "Unravelling BES capacity to generate a microbial electrochemical fuel for energy storage" reports the first studies with BESs to reduce 2,6-AQDS in the cathode side, with acetate oxidation on the anode side. The study was performed with EAB *G. sulfurreducens* as biocatalysts. The BESs were operated with and without a bias potential applied to promote the reduction of 2,6-AQDS to 2,6-AQDSH_2 (microbial electrochemical fuel).

Chapter 3 presents "Microbial electrochemical fuel for energy storage in Redox Flow Cell". In this chapter the 2,6-AQDSH_2 in the BES was used as microbial electrochemical fuel in the negative side of a RFC, with $[Fe(CN)_6]^{3-}$, on the positive side. As the RFC was allowed to discharge, the charge–discharge curves versus time was obtained, thus proving the concept of a MRFC.

In **chapter 4**, wastewater was used as the organic substrate in BESs, in place of acetate. This chapter highlights that organic waste can be used in BESs to synthesize a microbial electrochemical fuel that is used in a RFC. The impact of pH values in the microbial electrochemical fuel conversion in the MFC was also researched.

Chapter 5 presents the Microbial Redox Flow Cell (MRFC), a new approach for generation and storage of bioenergy. This chapter reports the results that demonstrated the MRFC. The *G. sulfurreducens* was used for the oxidation of acetate and CO_2 reduction to reduce and oxidize the redox pairs 2,6-AQDS and $[Fe(CN)_6]^{4-}$, used as electrochemical fuels in a RFC. Finally, **chapter 6** "General Conclusions and future work" summarizes the main conclusions of this thesis. Future approaches, ideas and suggestions for research directions are presented.

1.7. References

[1] F. deLlano-Paz, A. Calvo-Silvosa, S. Iglesias Antelo, I. Soares, The European low-carbon mix for 2030: The role of renewable energy sources in an environmentally and socially efficient approach, Renew. Sustain. Energy Rev. 48 (2015) 49–61.

[2] M. Rahimnejad, A.A. Ghoreyshi, G.D. Najafpour, H. Younesi, M. Shakeri, A novel microbial fuel cell stack for continuous production of clean energy, Int. J. Hydrogen Energy. 37 (2012) 5992–6000.

[3] M.D. Leonard, E.E. Michaelides, D.N. Michaelides, Energy storage needs for the substitution of fossil fuel power plants with renewables, Renew. Energy. 145 (2020) 951–962.

[4] J. Song, S.J. Song, S.-D. Oh, Y. Yoo, Evaluation of potential fossil fuel conservation by the renewable heat obligation in Korea, Renew. Energy. 79 (2015) 140–149.

[5] F. Birol, Market report series energy efficiency 2018. Analysis and outlooks to 2040, 2018.

[6] S. Koohi-Fayegh, M.A. Rosen, A review of energy storage types, applications and recent developments, J. Energy Storage. 27 (2020) 1–23.

[7] R. O'Hayre, S.-W. Cha, W. Colella, F.B. Prinz, Fuel Cell Fundamentals, John Wiley & Sons, Inc, Hoboken, NJ, USA, 2016.

[8] S.P.S. Badwal, S.S. Giddey, C. Munnings, A.I. Bhatt, A.F. Hollenkamp, Emerging electrochemical energy conversion and storage technologies, Front. Chem. 2 (2014) 79.

[9] L. Carrette, K.A. Friedrich, U. Stimming, Fuel Cells - Fundamentals and Applications, Fuel Cells. 1 (2001) 5–39.

[10] Huamin Zhang, X. Li, J. Zhang, Redox Flow Batteries: fundamental and applications, CRC Press, 2017.

[11] A.Z. Weber, M.M. Mench, J.P. Meyers, P.N. Ross, J.T. Gostick, Q. Liu, Redox flow batteries: a review, J. Appl. Electrochem. 41 (2011) 1137–1164.

[12] K. Scott, E.H. Yu, Microbial Electrochemical and Fuel Cells: Fundamentals and applications, Elsevier, 2016.

[13] B.E. Logan, Microbial Fuel Cells, John Wiley & Sons, Inc., Hoboken, NJ, USA, 2007.

[14] S.K. Butti, G. Velvizhi, M.L.K. Sulonen, J.M. Haavisto, E. Oguz Koroglu, A. Yusuf Cetinkaya, S. Singh, D. Arya, J. Annie Modestra, K. Vamsi Krishna, A. Verma, B. Ozkaya, A.-M. Lakaniemi, J.A. Puhakka, S. Venkata Mohan, Microbial electrochemical technologies with the

perspective of harnessing bioenergy: maneuvering towards upscaling, Renew. Sustain. Energy Rev. 53 (2016) 462–476.

[15] M.D. Khan, N. Khan, S. Sultana, R. Joshi, S. Ahmed, E. Yu, K. Scott, A. Ahmad, M.Z. Khan, Bioelectrochemical conversion of waste to energy using microbial fuel cell technology, Process Biochem. 57 (2017) 141–158.

[16] H.D. Beyene, A.A. Werkneh, T.G. Ambaye, Current updates on waste to energy (WtE) technologies: a review, Renew. Energy Focus. 24 (2018) 1–11.

[17] A.J. Slate, K.A. Whitehead, D.A.C. Brownson, C.E. Banks, Microbial fuel cells: an overview of current technology, Renew. Sustain. Energy Rev. 101 (2019) 60–81.

[18] H. Beyenal, J. Babauta, Biofilms in Bioelectrochemical Systems. From laboratory practice to data interpretation, John Wiley & Sons, Inc., 2015.

[19] J. Azevedo, T. Seipp, J. Burfeind, C. Sousa, A. Bentien, J.P. Araújo, A. Mendes, Unbiased solar energy storage: Photoelectrochemical redox flow battery, Nano Energy. 22 (2016) 396–405.

[20] U. Schröder, F. Harnisch, L.T. Angenent, Microbial electrochemistry and technology: terminology and classification, Energy Environ. Sci. 8 (2015) 513–519.

[21] R.S. Berk, J.H. Canfield, Bioelectrochemical Energy Conversion., Appl. Microbiol. 12 (1964) 10–12.

[22] S. Bajracharya, M. Sharma, G. Mohanakrishna, X. Dominguez Benneton, D.P.B.T.B. Strik, P.M. Sarma, D. Pant, An overview on emerging bioelectrochemical systems (BESs): technology for sustainable electricity, waste remediation, resource recovery, chemical production and beyond, Renew. Energy. 98 (2016) 153–170.

[23] N. Chabert, O. Amin Ali, W. Achouak, All ecosystems potentially host electrogenic bacteria, Bioelectrochemistry. 106 (2015) 88–96.

[24] M.C.A.A. Van Eerten-Jansen, A. Ter Heijne, C.J.N. Buisman, H.V.M. Hamelers, Microbial electrolysis cells for production of methane from CO_2: long-term performance and perspectives, Int. J. Energy Res. 36 (2012) 809–819.

[25] H. Liu, T. Song, K. Fei, H. Wang, J. Xie, Microbial electrosynthesis of organic chemicals from CO_2 by *Clostridium scatologenes* ATCC 25775T, Bioresour. Bioprocess. 5 (2018) 1–10.

[26] A. Schievano, T. Pepé Sciarria, K. Vanbroekoven, H. De Wever, S. Puig, S.J. Andersen, K.

Rabaey, D. Pant, Electro-fermentation – merging electrochemistry with fermentation in industrial applications, Trends Biotechnol. in press (2016) 1–13.

[27] R.A. Bullen, T.C. Arnot, J.B. Lakeman, F.C. Walsh, Biofuel cells and their development, Biosens. Bioelectron. 21 (2006) 2015–2045.

[28] U. Schröder, Anodic electron transfer mechanisms in microbial fuel cells and their energy efficiency, Phys Chem Chem Phys. 9 (2007) 2619–2629.

[29] I. Ieropoulos, J. Greenman, C. Melhuish, Microbial fuel cells based on carbon veil electrodes: stack configuration and scalability, Int. J. Energy Res. 32 (2008) 1228–1240.

[30] P. Liang, W. Wu, J. Wei, L. Yuan, X. Xia, X. Huang, Alternate charging and discharging of capacitor to enhance the electron production of Bioelectrochemical Systems, Environ. Sci. Technol. 45 (2011) 6647–6653.

[31] J. Babauta, R. Renslow, Z. Lewandowski, H. Beyenal, Electrochemically active biofilms: facts and fiction. A review, Biofouling. 28 (2012) 789–812.

[32] M.C. Potter, Electrical Effects Accompanying the decomposition of organic compounds, Proc. R. Soc. B Biol. Sci. 84 (1911) 260–276.

[33] K.C. Wrighton, J.D. Coates, Microbial Fuel Cells: Plug-in and Power-on Microbiology, Microbe. 4 (2009) 281–287.

[34] C. Santoro, C. Arbizzani, B. Erable, I. Ieropoulos, Microbial fuel cells: from fundamentals to applications. A review, J. Power Sources. 356 (2017) 225–244.

[35] D.R. Lovley, Bug juice: harvesting electricity with microorganisms, Nat. Rev. Microbiol. 4 (2006) 497–508.

[36] G. Drendel, E.R. Mathews, L. Semenec, A.E. Franks, Microbial Fuel Cells, related technologies, and their applications, Appl. Sci. 8 (2018) 2384.

[37] U. Schröder, Anodic electron transfer mechanisms in microbial fuel cells and their energy efficiency, Phys Chem Chem Phys. 9 (2007) 2619–2629.

[38] D.R. Bond, D.R. Lovley, Electricity production by *Geobacter sulfurreducens* attached to electrodes, Appl. Environ. Microbiol. 69 (2003) 1548–55.

[39] S.A. Patil, C. Hägerhäll, L. Gorton, Electron transfer mechanisms between microorganisms and electrodes in bioelectrochemical systems, Bioanal. Rev. 4 (2012) 159–192.

[40] A. Kumar, L.H.H. Hsu, P. Kavanagh, F. Barrière, P.N.L. Lens, L. Lapinsonnière, J.H.

Lienhard, U. Schröder, X. Jiang, D. Leech, The ins and outs of microorganism-electrode electron transfer reactions, Nat. Rev. Chem. 1 (2017) 1–13.

[41] L. Semenec, A.E. Franks, The microbiology of microbial electrolysis cells., Microbiol. Aust. 35 (2014) A–F.

[42] K.B. Gregory, D.R. Bond, D.R. Lovley, Graphite electrodes as electron donors for anaerobic respiration, Environ. Microbiol. 6 (2004) 596–604.

[43] D.E. Ross, J.M. Flynn, D.B. Baron, J.A. Gralnick, D.R. Bond, Towards electrosynthesis in Shewanella: energetics of reversing the Mtr pathway for reductive metabolism, PLoS One. 6 (2011) 1–9.

[44] N. Uria, I. Ferrera, J. Mas, Electrochemical performance and microbial community profiles in microbial fuel cells in relation to electron transfer mechanisms, BMC Microbiol. 17 (2017) 1–12.

[45] L. Wei, H. Han, J. Shen, Effects of cathodic electron acceptors and potassium ferricyanide concentrations on the performance of microbial fuel cell, Int. J. Hydrogen Energy. 37 (2012) 12980–12986.

[46] A.B. dos Santos, F.J. Cervantes, J.B. Van Lier, Azo dye reduction by thermophilic anaerobic granular sludge, and the impact of the redox mediator anthraquinone-2,6-disulfonate (AQDS) on the reductive biochemical transformation, Appl. Microbiol. Biotechnol. 64 (2004) 62–69.

[47] Y. Wu, F. Li, T. Liu, R. Han, X. Luo, pH dependence of quinone-mediated extracellular electron transfer in a bioelectrochemical system, Electrochim. Acta. 213 (2016) 408–415.

[48] M. Zhou, H. Wang, D.J. Hassett, T. Gu, Recent advances in microbial fuel cells (MFCs) and microbial electrolysis cells (MECs) for wastewater treatment, bioenergy and bioproducts, J. Chem. Technol. Biotechnol. 88 (2013) 508–518.

[49] R. Kakarla, C. Kuppam, S. Pandit, A. Kadier, Basic principles of Microbial Fuel Cell: technical challenges and economic feasibility, in: Microb. Appl. Vol.1, 2017: pp. 165–174.

[50] L. Semenec, A. E Franks, Delving through electrogenic biofilms: from anodes to cathodes to microbes, AIMS Bioeng. 2 (2015) 222–248.

[51] O. Choi, B.-I. Sang, Extracellular electron transfer from cathode to microbes: application for biofuel production, Biotechnol. Biofuels. 9 (2016) 1–14.

[52] B.E. Logan, Exoelectrogenic bacteria that power microbial fuel cells., Nat. Rev. Microbiol. 7 (2009) 375–381.

[53] L. Mao, W.S. Verwoerd, Selection of organisms for systems biology study of microbial electricity generation: A review, Int. J. Energy Environ. Eng. 4 (2013) 1–18.

[54] V.J. Watson, B.E. Logan, Power production in MFCs inoculated with *Shewanella oneidensis* MR-1 or mixed cultures, Biotechnol. Bioeng. 105 (2010) 489–498.

[55] K. Rabaey, N. Boon, S.D. Siciliano, M. Verhaege, W. Verstraete, Biofuel Cells select for microbial consortia that self-mediate electron transfer, Appl. Environ. Microbiol. 70 (2004) 5373–5382.

[56] D.R. Bond, D.E. Holmes, L.M. Tender, D.R. Lovley, Electrode-reducing microorganisms that harvest energy from marine sediments, Science (80) 295 (2002) 483–485.

[57] S.K. Chaudhuri, D.R. Lovley, Electricity generation by direct oxidation of glucose in mediatorless microbial fuel cells, Nat. Biotechnol. 21 (2003) 1229–1232.

[58] T. Zhang, C. Cui, S. Chen, X. Ai, H. Yang, P. Shen, Z. Peng, A novel mediatorless microbial fuel cell based on direct biocatalysis of *Escherichia coli,* Chem. Commun. (2006) 2257–2259.

[59] D.R. Lovley, Powering microbes with electricity: Direct electron transfer from electrodes to microbes, Environ. Microbiol. Rep. 3 (2011) 27–35.

[60] A. Khosravanipour Mostafazadeh, P. Drogui, S.K. Brar, R.D. Tyagi, Y. Le Bihan, G. Buelna, Microbial electrosynthesis of solvents and alcoholic biofuels from nutrient waste: A review, J. Environ. Chem. Eng. 5 (2017) 940–954.

[61] L. Huang, Q. Wang, X. Quan, Y. Liu, G. Chen, Bioanodes/biocathodes formed at optimal potentials enhance subsequent pentachlorophenol degradation and power generation from microbial fuel cells, Bioelectrochemistry. 94 (2013) 13–22.

[62] K. Rabaey, R.A. Rozendal, Microbial electrosynthesis - revisiting the electrical route for microbial production., Nat. Rev. Microbiol. 8 (2010) 706–16.

[63] F. Kracke, I. Vassilev, J.O. Krömer, Microbial electron transport and energy conservation - the foundation for optimizing bioelectrochemical systems, Front. Microbiol. 6 (2015) 1–18.

[64] L. Huang, H. Xue, Q. Zhou, P. Zhou, X. Quan, Imaging and distribution of Cd (II) ions in electrotrophs and its response to current and electron transfer inhibitor in microbial electrolysis

cells, Sensors Actuators B. 255 (2018) 244–254.

[65] Z. Zaybak, J.M. Pisciotta, J.C. Tokash, B.E. Logan, Enhanced start-up of anaerobic facultatively autotrophic biocathodes in bioelectrochemical systems, J. Biotechnol. 168 (2013) 478–485.

[66] E.S. Şahin, Microbial Fuel Cell, A Bioelectrochemical System that converts waste to watts, Springer International Publishing, Cham, 2018.

[67] J.M. Pisciotta, Z. Zaybak, D.F. Call, J.Y. Nam, B.E. Logan, Enrichment of microbial electrolysis cell biocathodes from sediment microbial fuel cell bioanodes, Appl. Environ. Microbiol. 78 (2012) 5212–5219.

[68] J.S. Geelhoed, A.J.M. Stams, Electricity-assisted biological hydrogen production from acetate by *Geobacter sulfurreducens*, Environ. Sci. Technol. 45 (2011) 815–820.

[69] R.M. Hartline, D.F. Call, Substrate and electrode potential affect electrotrophic activity of inverted bioanodes, Bioelectrochemistry. 110 (2016) 13–18.

[70] S. Saheb-Alam, A. Singh, M. Hermansson, F. Persson, A. Schnürer, B.-M.M. Wilén, O. Modin, M. Hermansson, A. Singh, F. Persson, O. Modin, S. Saheb-Alam, B.-M.M. Wilén, Effect of start-up strategies and electrode materials on carbon dioxide reduction on biocathodes, Appl. Environ. Microbiol. 84 (2017) 1–14.

[71] D.R. Lovley, Bug juice: harvesting electricity with microorganisms., Nat. Rev. Microbiol. 4 (2006) 497–508.

[72] B.E. Logan, J.M. Regan, Microbial Fuel Cells—challenges and applications, Environ. Sci. Technol. 40 (2006) 5172–5180.

[73] S. Pandit, D. Das, Principles of Microbial Fuel Cell for the power generation, in: Microb. Fuel Cell, Springer International Publishing, Cham, 2018: pp. 21–41.

[74] V.B. Oliveira, M. Simões, L.F. Melo, A.M.F.R. Pinto, Overview on the developments of microbial fuel cells, Biochem. Eng. J. 73 (2013) 53–64.

[75] K. Rabaey, J. Rodríguez, L.L. Blackall, J. Keller, P. Gross, D. Batstone, W. Verstraete, K.H. Nealson, Microbial ecology meets electrochemistry: electricity-driven and driving communities, ISME J. 1 (2007) 9–18.

[76] I. Ieropoulos, J. Greenman, C. Melhuish, Microbial fuel cells based on carbon veil electrodes: stack configuration and scalability, Int. J. Energy Res. 32 (2008) 1228–1240.

[77] R.A. Rozendal, A.W. Jeremiasse, H.V.M. Hamelers, C.J.N. Buisman, Hydrogen production with a microbial biocathode hydrogen production with a microbial biocathode, Environ. Sci. Technol. 42 (2008) 629–634.

[78] B.E. Logan, D. Call, S. Cheng, H.V.M. Hamelers, T.H.J.A. Sleutels, A.W. Jeremiasse, R.A. Rozendal, Microbial Electrolysis Cells for high yield hydrogen gas production from organic matter, Environ. Sci. Technol. 42 (2008) 8630–8640.

[79] N. Bourdakos, E. Marsili, R. Mahadevan, A defined co-culture of *Geobacter sulfurreducens* and *Escherichia co*li in a membrane-less microbial fuel cell, Biotechnol. Bioeng. 111 (2014) 709–718.

[80] A.R. Schoen, Carbon fiber electrode as an electron acceptor for a Microbial Fuel Cell using Geobacter, Cantaurus. 15 (2007) 24–26.

[81] S. Venkata Mohan, G. Velvizhi, J. Annie Modestra, S. Srikanth, Microbial fuel cell: critical factors regulating bio-catalyzed electrochemical process and recent advancements, Renew. Sustain. Energy Rev. 40 (2014) 779–797.

[82] Z. Du, H. Li, T. Gu, A state of the art review on microbial fuel cells: a promising technology for wastewater treatment and bioenergy, Biotechnol. Adv. 25 (2007) 464–482.

[83] D. Pant, G. Van Bogaert, L. Diels, K. Vanbroekhoven, A review of the substrates used in microbial fuel cells (MFCs) for sustainable energy production, Bioresour. Technol. 101 (2010) 1533–1543.

[84] B.E. Logan, B. Hamelers, R. Rozendal, U. Schröder, J. Keller, S. Freguia, P. Aelterman, W. Verstraete, K. Rabaey, Microbial Fuel Cells: methodology and technology, Environ. Sci. Technol. 40 (2006) 5181–5192.

[85] B.E. Logan, C. Murano, K. Scott, N.D. Gray, I.M. Head, Electricity generation from cysteine in a microbial fuel cell, Water Res. 39 (2005) 942–952.

[86] D. Ucar, Y. Zhang, I. Angelidaki, An overview of electron acceptors in Microbial Fuel Cells, Front. Microbiol. 8 (2017) 1–14.

[87] B.C. Jong, B.H. Kim, I.S. Chang, P.W.Y. Liew, Y.F. Choo, G.S. Kang, Enrichment, performance, and microbial diversity of a thermophilic mediatorless Microbial Fuel Cell, Environ. Sci. Technol. 40 (2006) 6449–6454.

[88] N. Degrenne, F. Buret, B. Allard, P. Bevilacqua, Electrical energy generation from a large

number of microbial fuel cells operating at maximum power point electrical load, J. Power Sources. 205 (2012) 188–193.

[89] M. Sun, L.-F. Zhai, W.-W. Li, H.-Q. Yu, Harvest and utilization of chemical energy in wastes by microbial fuel cells, Chem. Soc. Rev. 45 (2016) 2847–2870.

[90] W. Habermann, E.-H. Pommer, Biological fuel cells with sulphide storage capacity, Appl. Microbiol. Biotechnol. 35 (1991) 128–133.

[91] S. Ömeroğlu, F.D. Sanin, Bioelectricity generation from wastewater sludge using Microbial Fuel Cells: a critical review, CLEAN - Soil, Air, Water. 44 (2016) 1225–1233.

[92] B.E. Logan, Simultaneous wastewater treatment and biological electricity generation, Water Sci. Technol. 52 (2005) 31–37.

[93] Z. Ge, Z. He, Long-term Performance of a 200-Liter modularized Microbial Fuel Cell system treating municipal wastewater: treatment, energy, and cost, Environ. Sci. Water Res. Technol. 2 (2016) 1–2.

[94] K. Tota-Maharaj, P. Paul, Performance of pilot-scale microbial fuel cells treating wastewater with associated bioenergy production in the Caribbean context, Int. J. Energy Environ. Eng. 6 (2015) 213–220.

[95] B.E. Logan, Scaling up microbial fuel cells and other bioelectrochemical systems, Appl. Microbiol. Biotechnol. 85 (2010) 1665–1671.

[96] H. Liu, S. Grot, B.E. Logan, Electrochemically assisted microbial production of hydrogen from acetate, Environ. Sci. Technol. 39 (2005) 4317–4320.

[97] R. Ganigué, S. Puig, P. Batlle-Vilanova, M. Dolors Balaguer, J. Colprim, Microbial electrosynthesis of butyrate from carbon dioxide, Chem. Commun. 51 (2015) 3235–3238.

[98] M. Villano, P. Paiano, E. Palma, A. Miccheli, M. Majone, Electrochemically driven fermentation of organic substrates with undefined mixed microbial cultures, ChemSusChem. 10 (2017) 3091–3097.

[99] A. Kadier, Y. Simayi, P. Abdeshahian, N. Farhana, K. Chandrasekhar, M. Sahaid, N.F. Azman, K. Chandrasekhar, M.S. Kalil, N. Farhana, K. Chandrasekhar, M. Sahaid, N.F. Azman, K. Chandrasekhar, M.S. Kalil, A comprehensive review of microbial electrolysis cells (MEC) reactor designs and configurations for sustainable hydrogen gas production, Alexandria Eng. J. 55 (2016) 427–443.

[100] P. Kuntke, T.H.J.A. Sleutels, M. Rodríguez Arredondo, S. Georg, S.G. Barbosa, A. ter Heijne, H.V.M. Hamelers, C.J.N. Buisman, (Bio)electrochemical ammonia recovery: progress and perspectives, Appl. Microbiol. Biotechnol. 102 (2018) 3865–3878.

[101] E. Croese, M.A. Pereira, G.J.W. Euverink, A.J.M. Stams, J.S. Geelhoed, Analysis of the microbial community of the biocathode of a hydrogen-producing microbial electrolysis cell, Appl. Microbiol. Biotechnol. 92 (2011) 1083–1093.

[102] S. Cotterill, E. Heidrich, T. Curtis, Microbial electrolysis cells for hydrogen production, in: Microb. Electrochem. Fuel Cells, Elsevier, 2016: pp. 287–319.

[103] M.Y. Azwar, M.A. Hussain, A.K. Abdul-Wahab, Development of biohydrogen production by photobiological, fermentation and electrochemical processes: A review, Renew. Sustain. Energy Rev. 31 (2014) 158–173.

[104] T. Chookaew, P. Prasertsan, Z.J. Ren, Two-stage conversion of crude glycerol to energy using dark fermentation linked with microbial fuel cell or microbial electrolysis cell, N. Biotechnol. 31 (2014) 179–184.

[105] A. Schievano, T. Pepè Sciarria, Y.C. Gao, B. Scaglia, S. Salati, M. Zanardo, W. Quiao, R. Dong, F. Adani, Dark fermentation, anaerobic digestion and microbial fuel cells: An integrated system to valorize swine manure and rice bran, Waste Manag. 56 (2016) 519–529.

[106] A. Marone, O.R. Ayala-Campos, E. Trably, A.A. Carmona-Martïnez, R. Moscoviz, E. Latrille, J.P. Steyer, V. Alcaraz-Gonzalez, N. Bernet, Coupling dark fermentation and microbial electrolysis to enhance bio-hydrogen production from agro-industrial wastewaters and by-products in a bio-refinery framework, Int. J. Hydrogen Energy. 42 (2017) 1609–1621.

[107] F. Aulenta, P. Reale, A. Catervi, S. Panero, M. Majone, Kinetics of trichloroethene dechlorination and methane formation by a mixed anaerobic culture in a bio-electrochemical system, Electrochim. Acta. 53 (2008) 5300–5305.

[108] S. Cheng, D. Xing, D.F. Call, B.E. Logan, Direct biological conversion of electrical current into methane by electromethanogenesis, Environ. Sci. Technol. 43 (2009) 3953–3958.

[109] R. Blasco-Gómez, P. Batlle-Vilanova, M. Villano, M. Balaguer, J. Colprim, S. Puig, On the edge of research and technological application: a critical review of Electromethanogenesis, Int. J. Mol. Sci. 18 (2017) 1–32.

[110] A. Schievano, A. Goglio, C. Erckert, S. Marzorati, L. Rago, P. Cristiani, Organic waste and

bioelectrochemical systems: a future interface between electricity and methane distribution grids, Detritus. 1 (2018) 57–63.

[111] G. Zhen, X. Lu, T. Kobayashi, G. Kumar, K. Xu, Promoted electromethanosynthesis in a two-chamber microbial electrolysis cells (MECs) containing a hybrid biocathode covered with graphite felt (GF), Chem. Eng. J. 284 (2016) 1146–1155.

[112] K. Scott, Carbon dioxide reduction and electro-organic synthesis, in: Sustain. Green Electrochem. Sci. Technol., John Wiley & Sons, Ltd, Chichester, UK, 2017: pp. 125–158.

[113] S. Bajracharya, A. Ter Heijne, X. Dominguez Benetton, K. Vanbroekhoven, C.J.N. Buisman, D.P.B.T.B. Strik, D. Pant, Carbon dioxide reduction by mixed and pure cultures in microbial electrosynthesis using an assembly of graphite felt and stainless steel as a cathode, Bioresour. Technol. 195 (2015) 14–24.

[114] A. ter Heijne, F. Geppert, T.H.J.A. Sleutels, P. Batlle-Vilanova, D. Liu, S. Puig, Mixed culture biocathodes for production of hydrogen, methane, and carboxylates, in: Educ. Technol. Soc., 2017: pp. 237–247.

[115] D.R. Lovley, K.P. Nevin, Electrobiocommodities: powering microbial production of fuels and commodity chemicals from carbon dioxide with electricity, Curr. Opin. Biotechnol. 24 (2013) 385–390.

[116] K.P. Nevin, T.L. Woodard, A.E. Franks, Microbial electrosynthesis: feeding microbes electricity to convert carbon dioxide and water to multicarbon extracellular organic, Am. Soc. Microbiol. 1 (2010) 1–4.

[117] C.S. Butler, D.R. Lovley, How to sustainably feed a microbe: strategies for biological production of carbon-based commodities with renewable electricity, Front. Microbiol. 7 (2016) 1–6.

[118] X. Christodoulou, T. Okoroafor, S. Parry, S.B. Velasquez-Orta, The use of carbon dioxide in microbial electrosynthesis: Advancements, sustainability and economic feasibility, J. CO_2 Util. 18 (2017) 390–399.

[119] P. Batlle-Vilanova, S. Puig, R. Gonzalez-Olmos, M.D. Balaguer, J. Colprim, Continuous acetate production through microbial electrosynthesis from CO_2 with microbial mixed culture, J. Chem. Technol. Biotechnol. 91 (2016) 921–927.

[120] F. Geppert, D. Liu, M. van Eerten-Jansen, E. Weidner, C. Buisman, A. ter Heijne,

Bioelectrochemical power-to-gas: state of the art and future perspectives, Trends Biotechnol. 34 (2016) 879–894.

[121] M. Villano, F. Aulenta, C. Ciucci, T. Ferri, A. Giuliano, M. Majone, Bioelectrochemical reduction of CO_2 to CH_4 via direct and indirect extracellular electron transfer by a hydrogenophilic methanogenic culture, Bioresour. Technol. 101 (2010) 3085–3090.

[122] L. Peixoto, S.G. Barbosa, M.M. Alves, M.A. Pereira, Bioelectrochemical Systems for production of valuable compounds, in: Bioelectrochemical Interface Eng., Wiley, 2019: pp. 311–323.

[123] G. Mohanakrishna, K. Vanbroekhoven, D. Pant, Imperative role of applied potential and inorganic carbon source on acetate production through microbial electrosynthesis, J. CO_2 Util. 15 (2016) 57–64.

[124] P. Kumar, K. Chandrasekhar, A. Kumari, E. Sathiyamoorthi, B. Kim, Electro-fermentation in aid of bioenergy and biopolymers, Energies. 11 (2018) 1–20.

[125] C. Kim, M.Y. Kim, I. Michie, B.H. Jeon, G.C. Premier, S. Park, J.R. Kim, Anodic electro-fermentation of 3-hydroxypropionic acid from glycerol by recombinant *Klebsiella pneumoniae* L17 in a bioelectrochemical system, Biotechnol. Biofuels. 10 (2017) 1–11.

[126] O. Choi, T. Kim, H.M. Woo, Y. Um, Electricity-driven metabolic shift through direct electron uptake by electroactive heterotroph *Clostridium pasteurianum*, Sci. Rep. 4 (2015) 6961.

[127] A. Schievano, T. Pepé Sciarria, K. Vanbroekoven, H. De Wever, S. Puig, S.J. Andersen, K. Rabaey, D. Pant, Electro-fermentation – merging electrochemistry with fermentation in industrial applications, Trends Biotechnol. 34 (2016) 1–13.

[128] Y. Jiang, H.D. May, L. Lu, P. Liang, X. Huang, Z. Jason, Z.J. Ren, Carbon dioxide and organic waste valorization by microbial electrosynthesis and electro-fermentation, Water Res. 149 (2019) 42–55.

[129] R. Moscoviz, J. Toledo-Alarcón, E. Trably, N. Bernet, Electro-Fermentation: How to drive fermentation using Electrochemical Systems, Trends Biotechnol. 34 (2016) 856–865.

[130] L. Lin, L. Tam, X. Xia, X. Li, Electro-fermentation of iron-enhanced primary sedimentation sludge in a two-chamber bioreactor for product separation and resource recovery, Water Res. 157 (2019) 145–154.

[131] Mustakeem, R. Paper, Electrode materials for microbial fuel cells : nanomaterial approach, Mater. Renew. Sustain. Energy. 4 (2015) 1–11.

[132] D.F. Call, M.D. Merrill, B.E. Logan, High surface area stainless steel brushes as cathodes in Microbial Electrolysis Cells, Environ. Sci. Technol. 43 (2009) 2179–2183.

[133] J. Wei, P. Liang, X. Huang, Recent progress in electrodes for microbial fuel cells, Bioresour. Technol. 102 (2011) 9335–9344.

[134] R. Jain, D.C. Tiwari, S. Sharma, P. Mishra, Efficiency and stability of carbon cloth electrodes for electricity production from different types of waste water using duel chamber microbial fuel cell, J. Sci. Ind. Res. (India). 74 (2015) 308–314.

[135] F. Zhao, R.C.T.T. Slade, J.R. Varcoe, Techniques for the study and development of microbial fuel cells: an electrochemical perspective, Chem. Soc. Rev. 38 (2009) 1926–1939.

[136] Y. Liu, F. Harnisch, K. Fricke, U. Schröder, V. Climent, J.M. Feliu, The study of electrochemically active microbial biofilms on different carbon-based anode materials in microbial fuel cells, Biosens. Bioelectron. 25 (2010) 2167–2171.

[137] E. Baranitharan, M.R. Khan, D.M.R.R. Prasad, W.F.A. Teo, G.Y.A. Tan, R. Jose, Effect of biofilm formation on the performance of microbial fuel cell for the treatment of palm oil mill effluent, Bioprocess Biosyst. Eng. 38 (2015) 15–24.

[138] T.X. Huong Le, M. Bechelany, M. Cretin, Carbon felt based-electrodes for energy and environmental applications: A review, Carbon N. Y. 122 (2017) 564–591.

[139] J. González-García, P. Bonete, E. Expósito, V. Montiel, A. Aldaz, R. Torregrosa-Maciá, Characterization of a carbon felt electrode: structural and physical properties, J. Mater. Chem. 9 (1999) 419–426.

[140] H. Liu, R. Ramnarayanan, B.E. Logan, Production of electricity during wastewater treatment using a single chamber microbial fuel cell, Environ.Sci.Technol. 38 (2004) 2281–2285.

[141] X. Wang, S. Cheng, Y. Feng, M.D. Merrill, T. Saito, B.E. Logan, Use of carbon mesh anodes and the effect of different pretreatment methods on power production in microbial fuel cells, Environ. Sci. Technol. 43 (2009) 6870–6874.

[142] A. Pareek, S.V. Mohan, Progress in development of electrode materials in Microbial Fuel Cells, in: Bioelectrochemical Interface Eng., Wiley, 2019: pp. 165–186.

[143] S. Freguia, K. Rabaey, Z. Yuan, J. Keller, Non-catalyzed cathodic oxygen reduction at graphite granules in microbial fuel cells, Electrochim. Acta. 53 (2007) 598–603.

[144] V. Lanas, Y. Ahn, B.E. Logan, Effects of carbon brush anode size and loading on microbial fuel cell performance in batch and continuous mode, J. Power Sources. 247 (2014) 228–234.

[145] X. Xie, C. Criddle, Y. Cui, Design and fabrication of bioelectrodes for microbial bioelectrochemical systems, Energy Environ. Sci. 8 (2015) 3418–3441.

[146] S. Sharma, Glassy Carbon: A promising material for micro- and nanomanufacturing, Materials (Basel). 11 (2018) 1–21.

[147] Y. Feng, D. Li, J. Liu, W. He, Carbon-based materials in Microbial Fuel Cells, Microb. Electrochem. Technol. (2018) 49–74.

[148] H. Yuan, Y. Hou, I.M. Abu-Reesh, J. Chen, Z. He, Oxygen reduction reaction catalysts used in microbial fuel cells for energy-efficient wastewater treatment: a review, Mater. Horiz. 3 (2016) 382–401.

[149] P. Choudhury, U.S. Prasad Uday, T.K. Bandyopadhyay, R.N. Ray, B. Bhunia, Performance improvement of microbial fuel cell (MFC) using suitable electrode and Bioengineered organisms: A review, Bioengineered. 8 (2017) 471–487.

[150] L.F. Castañeda, F.C. Walsh, J.L. Nava, C. Ponce de León, Graphite felt as a versatile electrode material: properties, reaction environment, performance and applications, Electrochim. Acta. 258 (2017) 1115–1139.

[151] S. Kalathil, S.A. Patil, D. Pant, Microbial Fuel Cells: electrode materials, in: Encycl. Interfacial Chem., Elsevier, 2018: pp. 309–318.

[152] R. Mohammadzadeh Kakhki, A review to recent developments in modification of carbon fiber electrodes, Arab. J. Chem. 12 (2019) 1783–1794.

[153] M. Shestakova, M. Sillanpää, Electrode materials used for electrochemical oxidation of organic compounds in wastewater, Rev. Environ. Sci. Biotechnol. 16 (2017) 223–238. doi:10.1007/s11157-017-9426-1.

[154] A. Dumitru, K. Scott, Anode materials for microbial fuel cells, in: Microb. Electrochem. Fuel Cells, Elsevier, 2016: pp. 117–152.

[155] H. Richter, K. McCarthy, K.P. Nevin, J.P. Johnson, V.M. Rotello, D.R. Lovley, Electricity

generation by *Geobacter sulfurreducens* attached to gold electrodes, Langmuir. 24 (2008) 4376–4379.

[156] X. Zhu, B.E. Logan, Copper anode corrosion affects power generation in microbial fuel cells, J. Chem. Technol. Biotechnol. 89 (2014) 471–474.

[157] A. Baudler, I. Schmidt, M. Langner, A. Greiner, U. Schröder, Does it have to be carbon? Metal anodes in microbial fuel cells and related bioelectrochemical systems, Energy Environ. Sci. 8 (2015) 2048–2055.

[158] Y. Hindatu, M.S.M. Annuar, A.M. Gumel, Mini-review : anode modification for improved performance of microbial fuel cell, Renew. Sustain. Energy Rev. 73 (2017) 236–248.

[159] C. Dumas, A. Mollica, D. Féron, R. Basséguy, L. Etcheverry, A. Bergel, Marine microbial fuel cell : Use of stainless steel electrodes as anode and cathode materials, Electrochim. Acta. 53 (2007) 468–473.

[160] Y. Zhang, L. Liu, B. Van der Bruggen, F. Yang, Nanocarbon based composite electrodes and their application in microbial fuel cells, J. Mater. Chem. A. 5 (2017) 12673–12698.

[161] X. Xie, M. Ye, L. Hu, N. Liu, J.R. McDonough, W. Chen, H.N. Alshareef, C.S. Criddle, Y. Cui, Carbon nanotube-coated macroporous sponge for microbial fuel cell electrodes, Energy Environ. Sci. 5 (2012) 5265–5270.

[162] A.A. Yazdi, L. D'Angelo, N. Omer, G. Windiasti, X. Lu, J. Xu, Carbon nanotube modification of microbial fuel cell electrodes, Biosens. Bioelectron. 85 (2016) 536–552.

[163] A.M. Holban, E. Andronescu, A.M. Grumezescu, E. Andronescu, Inorganic nanoarchitectonics designed for drug delivery and anti-infective surfaces, in: Surf. Chem. Nanobiomaterials, Elsevier, 2016: pp. 301–327.

[164] J.J. Gooding, Nanostructuring electrodes with carbon nanotubes: a review on electrochemistry and applications for sensing, Electrochim. Acta. 50 (2005) 3049–3060.

[165] R.H. Mahmoud, F.A. Samhan, G.H. Ali, M.K. Ibrahim, R.Y.A. Hassan, Assisting the biofilm formation of exoelectrogens using nanostructured microbial fuel cells, J. Electroanal. Chem. 824 (2018) 128–135.

[166] G. Martins, A.F. Salvador, L. Pereira, M.M. Alves, Methane production and conductive materials: a critical review, Environ. Sci. Technol. 52 (2018) 10241–10253.

[167] Y. Yuan, S. Zhou, Y. Liu, J. Tang, Nanostructured macroporous bioanode based on

polyaniline-modified natural loofah sponge for high-performance microbial fuel cells, Environ. Sci. Technol. 47 (2013) 14525–14532.

[168] Y. Zhou, J. Hou, W. Chen, Z. Liu, Carbon nanotube sponge 3D anodes for urine-powered microbial fuel cell, Energy Sources, Part A Recover. Util. Environ. Eff. 39 (2017) 1543–1547.

[169] W. Tang, Y. Zhang, Y. Zhong, T. Shen, X. Wang, X. Xia, J. Tu, Natural biomass-derived carbons for electrochemical energy storage, Mater. Res. Bull. 88 (2017) 234–241.

[170] M. Zhou, M. Chi, J. Luo, H. He, T. Jin, An overview of electrode materials in microbial fuel cells, J. Power Sources. 196 (2011) 4427–4435.

[171] A. ElMekawy, H.M. Hegab, D. Losic, C.P. Saint, D. Pant, Applications of graphene in microbial fuel cells: The gap between promise and reality, Renew. Sustain. Energy Rev. 72 (2017) 1389–1403.

[172] R. Ramachandran, S.-M. Chen, G. Peter Gnana Kumar, Enhancement of different fabricated electrode materials for Microbial Fuel cell applications: an overview, Int. J. Electrochem. Sci. 10 (2015) 7111–7137.

[173] L. Zhang, Z. Liu, G. Cui, L. Chen, Biomass-derived materials for electrochemical energy storages, Prog. Polym. Sci. 43 (2014) 136–164.

[174] F.C. Walsh, L.F. Arenas, C. Ponce de León, Developments in electrode design: structure, decoration and applications of electrodes for electrochemical technology, J. Chem. Technol. Biotechnol. 93 (2018) 3073–3090.

[175] M. Oliot, S. Galier, H.H. Roux de Balmann, A. Bergel, Ion transport in microbial fuel cells: key roles, theory and critical review, Appl. Energy. 183 (2016) 1682–1704.

[176] H. Liu, S. Cheng, B.E. Logan, Production of electricity from acetate or butyrate using a single-chamber microbial fuel cell, Environ. Sci. Technol. 39 (2005) 658–662.

[177] F. Scholz, The suitability of monopolar and bipolar Ion Exchange Membranes as separators for Biological Fuel Cells, Env. Sci Technol. 42 (2008) 1740–1746.

[178] J.X. Leong, W.R.W. Daud, M. Ghasemi, K. Ben Liew, M. Ismail, Ion exchange membranes as separators in microbial fuel cells for bioenergy conversion: a comprehensive review, Renew. Sustain. Energy Rev. 28 (2013) 575–587.

[179] K.J. Chae, M. Choi, F.F. Ajayi, W. Park, I.S. Chang, I.S. Kim, Mass Transport through a Proton Exchange Membrane (Nafion) in Microbial Fuel Cells, Energy & Fuels. 22 (2008) 169–

176.

[180] B.R. Dhar, H.-S. Lee, Membranes for bioelectrochemical systems: challenges and research advances, Environ. Technol. 34 (2013) 1751–1764.

[181] B. Christgen, K. Scott, J. Dolfing, I.M. Head, T.P. Curtis, An evaluation of the performance and economics of membranes and separators in single chamber microbial fuel cells treating domestic wastewater, PLoS One. 10 (2015) 1–13.

[182] Z. Ghassemi, G. Slaughter, Biological fuel cells and membranes, Membranes (Basel). 7 (2017) 1–12.

[183] M. Rahimnejad, G. Bakeri, M. Ghasemi, A. Zirepour, G. Najafpour, M. Ghasemi, S. Oh, A review on the role of proton exchange membrane on the performance of microbial fuel cell, Polym. Adv. Technol. 25 (2014) 1426–1432.

[184] J. Xu, G.-P.P. Sheng, H.-W.W. Luo, W.-W.W. Li, L.-F.F. Wang, H.-Q.Q. Yu, Fouling of proton exchange membrane (PEM) deteriorates the performance of microbial fuel cell, Water Res. 46 (2012) 1817–1824.

[185] B. Min, S. Cheng, B.E. Logan, Electricity generation using membrane and salt bridge microbial fuel cells, Water Res. 39 (2005) 1675–1686.

[186] R. A. Rozendal, H.V.M. Hamelers, C.J.N. Buisman, Effects of membrane cation transport on pH and Microbial Fuel Cell performance, Environ. Sci. Technol. 40 (2006) 5206–5211.

[187] J.R. Varcoe, P. Atanassov, D.R. Dekel, A.M. Herring, M.A. Hickner, P.A. Kohl, A.R. Kucernak, W.E. Mustain, K. Ninjmeijer, K. Scott, T. Xu, L. Zhuang, Anion-exchange membranes in electrochemical energy systems, Energy Environ. Sci. 7 (2014) 3135–3191.

[188] X. Zhang, S. Cheng, X. Huang, B.E. Logan, Improved performance of single-chamber microbial fuel cells through control of membrane deformation, Biosens. Bioelectron. 25 (2010) 1825–1828.

[189] E. Antolini, Composite materials for polymer electrolyte membrane microbial fuel cells, Biosens. Bioelectron. 69 (2015) 54–70.

[190] J. Chouler, I. Bentley, F. Vaz, A. O'Fee, P.J. Cameron, M. Di Lorenzo, Exploring the use of cost-effective membrane materials for Microbial Fuel Cell based sensors, Electrochim. Acta. 231 (2017) 319–326.

[191] M. Rahimnejad, A. Adhami, S. Darvari, A. Zirepour, S.-E. Oh, Microbial fuel cell as new

technology for bioelectricity generation: A review, Alexandria Eng. J. 54 (2015) 745–756.

[192] S.J. Peighambardoust, S. Rowshanzamir, M. Amjadi, Review of the proton exchange membranes for fuel cell applications, Int. J. Hydrogen Energy. 35 (2010) 9349–9384.

[193] J. Ran, L. Wu, Y. He, Z. Yang, Y. Wang, C. Jiang, L. Ge, E. Bakangura, T. Xu, Ion exchange membranes: New developments and applications, J. Memb. Sci. 522 (2017) 267–291.

[194] B.E. Logan, M.J. Wallack, K.Y. Kim, W. He, Y. Feng, P.E. Saikaly, Assessment of Microbial Fuel Cell configurations and power densities, Environ. Sci. Technol. Lett. 2 (2015) 206–214.

[195] J. Yang, S. Ghobadian, P.J. Goodrich, R. Montazami, N. Hashemi, Miniaturized biological and electrochemical fuel cells: challenges and applications, Phys. Chem. Chem. Phys. 15 (2013) 14147–14161.

[196] X. Alexis, S. Forbes, J. Greenman, I.A. Ieropoulos, From single MFC to cascade configuration : the relationship between size, hydraulic retention time and power density, Sustain. Energy Technol. Assessments. 14 (2016) 74–79.

[197] H. Liu, B.E. Logan, Electricity generation using an air-cathode single chamber microbial fuel cell in the presence and absence of a proton exchange membrane, Environ. Sci. Technol. 38 (2004) 4040–4046.

[198] C. Santoro, I. Ieropoulos, J. Greenman, P. Cristiani, T. Vadas, A. Mackay, B. Li, Current generation in membraneless single chamber microbial fuel cells (MFCs) treating urine, J. Power Sources. 238 (2013) 190–196.

[199] I. Gajda, J. Greenman, I.A. Ieropoulos, Recent advancements in real-world microbial fuel cell applications, Curr. Opin. Electrochem. 11 (2018) 78–83.

[200] A.S. Mathuriya, D.A. Jadhav, M.M. Ghangrekar, Architectural adaptations of microbial fuel cells, Appl. Microbiol. Biotechnol. 102 (2018) 9419–9432.

[201] A. Rinaldi, B. Mecheri, V. Garavaglia, S. Licoccia, P. Di Nardo, E. Traversa, Engineering materials and biology to boost performance of microbial fuel cells: a critical review, Energy Environ. Sci. 1 (2008) 417–429.

[202] Y. Zhang, M. Liu, M. Zhou, H. Yang, L. Liang, T. Gu, Microbial fuel cell hybrid systems for wastewater treatment and bioenergy production : synergistic effects, mechanisms and

challenges, Renew. Sustain. Energy Rev. 103 (2019) 13–29.

[203] E. Yang, K. Chae, M. Choi, Z. He, I.S. Kim, Critical review of bioelectrochemical systems integrated with membrane- based technologies for desalination, energy self-sufficiency, and high-efficiency water and wastewater treatment, Desalination. 452 (2019) 40–67.

[204] S. Gadkari, S. Gu, J. Sadhukhan, Towards automated design of bioelectrochemical systems: a comprehensive review of mathematical models, Chem. Eng. J. 343 (2018) 303–316.

[205] K. Rabaey, W. Verstraete, Microbial fuel cells: novel biotechnology for energy generation, Trends Biotechnol. 23 (2005) 291–298.

[206] M. Shemfe, S. Gadkari, E. Yu, S. Rasul, K. Scott, I.M. Head, S. Gu, J. Sadhukhan, Life cycle, techno-economic and dynamic simulation assessment of bioelectrochemical systems: A case of formic acid synthesis, Bioresour. Technol. 255 (2018) 39–49.

[207] W.-W. Li, H.-Q. Yu, Z. He, Towards sustainable wastewater treatment by using microbial fuel cells-centered technologies, Energy Environ. Sci. 7 (2013) 911–924.

[208] D.C. Aiken, T.P. Curtis, E.S. Heidrich, Avenues to the financial viability of microbial electrolysis cells [MEC] for domestic wastewater treatment and hydrogen production, Int. J. Hydrogen Energy. 44 (2019) 2426–2434.

[209] Z. Yu, X. Leng, S. Zhao, J. Ji, T. Zhou, A. Khan, A. Kakde, P. Liu, X. Li, A review on the applications of microbial electrolysis cells in anaerobic digestion, Bioresour. Technol. 255 (2018) 340–348.

[210] T. Jafary, W.R.W. Daud, M. Ghasemi, B.H. Kim, J. Md Jahim, M. Ismail, S.S. Lim, Biocathode in microbial electrolysis cell; present status and future prospects, Renew. Sustain. Energy Rev. 47 (2015) 23–33.

[211] A.A. Abreu, F. Tavares, M.M. Alves, M.A. Pereira, Boosting dark fermentation with co-cultures of extreme thermophiles for biohythane production from garden waste, Bioresour. Technol. 219 (2016) 132–138.

[212] S. Cheng, D. Xing, D.F. Call, B.E. Logan, Direct biological conversion of electrical current into methane by Electromethanogenesis, Environ. Sci. Technol. 43 (2009) 3953–3958.

[213] R. Muñoz-Aguilar, D. Molognoni, P. Bosch-Jimenez, E. Borràs, M. Della Pirriera, Á. Luna, Design, operation, modeling and grid integration of power-to-gas Bioelectrochemical Systems, Energies. 11 (2018) 1–15.

[214] W.-F. Liu, S.-A. Cheng, Microbial fuel cells for energy production from wastewaters: the way toward practical application, J. Zhejiang Univ. Sci. A. 15 (2014) 841–861.

[215] H. Wang, J. Park, Z. Ren, Active Energy Harvesting from Microbial Fuel Cells at the maximum power point without using resistors, Environ. Sci. Technol. 46 (2012) 5247–5252.

[216] L. Su, C.M. Ajo-Franklin, Reaching full potential: bioelectrochemical systems for storing renewable energy in chemical bonds, Curr. Opin. Biotechnol. 57 (2019) 66–72.

[217] T. Kim, J. Yeo, Y. Yang, S. Kang, Y. Paek, J.K. Kwon, J.K. Jang, Boosting voltage without electrochemical degradation using energy-harvesting circuits and power management system-coupled multiple microbial fuel cells, J. Power Sources. 410–411 (2019) 171–178.

[218] D. Zhang, F. Yang, T. Shimotori, K.C. Wang, Y. Huang, Performance evaluation of power management systems in microbial fuel cell-based energy harvesting applications for driving small electronic devices, J. Power Sources. 217 (2012) 65–71.

[219] F. Yang, D. Zhang, T. Shimotori, K.C. Wang, Y. Huang, Study of transformer-based power management system and its performance optimization for microbial fuel cells, J. Power Sources. 205 (2012) 86–92.

[220] I.-S. Han, B.-K. Kho, S. Cho, Development of a polymer electrolyte membrane fuel cell stack for an underwater vehicle, J. Power Sources. 304 (2016) 244–254.

[221] M. Winter, R.J. Brodd, What are batteries, fuel cells, and supercapacitors?, Chem. Rev. 104 (2004) 4245–4269.

[222] S. Ren, X. Xia, L. Yuan, P. Liang, X. Huang, Enhancing charge harvest from microbial fuel cells by controlling the charging and discharging frequency of capacitors, Bioresour. Technol. 146 (2013) 812–815.

[223] A. Dewan, C. Donovan, D. Heo, H. Beyenal, Evaluating the performance of microbial fuel cells powering electronic devices, J. Power Sources. 195 (2010) 90–96.

[224] C. Santoro, F. Soavi, A. Serov, C. Arbizzani, P. Atanassov, Self-powered supercapacitive microbial fuel cell: The ultimate way of boosting and harvesting power, Biosens. Bioelectron. 78 (2016) 229–235.

[225] J. Houghton, C. Santoro, F. Soavi, A. Serov, I. Ieropoulos, C. Arbizzani, P. Atanassov, Supercapacitive microbial fuel cell: characterization and analysis for improved charge storage/delivery performance, Bioresour. Technol. 218 (2016) 552–560.

[226] M.C. Hatzell, Y. Kim, B.E. Logan, Powering microbial electrolysis cells by capacitor circuits charged using microbial fuel cell, J. Power Sources. 229 (2013) 198–202.

[227] C. Santoro, F. Soavi, C. Arbizzani, A. Serov, S. Kabir, K. Carpenter, O. Bretschger, P. Atanassov, Co-generation of hydrogen and power/current pulses from supercapacitive MFCs using novel HER iron-based catalysts, Electrochim. Acta. 220 (2016) 672–682.

[228] L.M. Tender, P. Kauffman, J. Melhado, D. Flynn, S.A. Gray, J. Dobarro, E. Groveman, R.C. Tyce, D.A. Lowy, R. Petrecca, The first demonstration of a microbial fuel cell as a viable power supply: powering a meteorological buoy, J. Power Sources. 179 (2008) 571–575.

[229] Y. Kim, M.C. Hatzell, A.J. Hutchinson, B.E. Logan, Capturing power at higher voltages from arrays of microbial fuel cells without voltage reversal, Energy Environ. Sci. 4 (2011) 4662–4667.

[230] A. Deeke, T.H.J.A. Sleutels, H.V.M. Hamelers, C.J.N. Buisman, Capacitive bioanodes enable renewable energy storage in Microbial Fuel Cells, Environ. Sci. Technol. 46 (2012) 3554–3560.

[231] E. Spinelli, F. Guerrero, P. García, M. Haberman, A simple and reproducible capacitive electrode, Med. Eng. Phys. 38 (2016) 286–289.

[232] A. Deeke, T.H.J.A. Sleutels, A. Ter Heijne, H.V.M. Hamelers, C.J.N. Buisman, Influence of the thickness of the capacitive layer on the performance of bioanodes in Microbial Fuel Cells, J. Power Sources. 243 (2013) 611–616.

[233] A.N. Reshetilov, A.E. Kitova, A. Dyakov, P.M. Gotovtsev, R.G. Vasilov, M.A. Gutorov, Converter-based accumulation of electric energy generated by microbial biofuel cell, IOP Conf. Ser. Earth Environ. Sci. 52 (2017) 1–8.

[234] A. Mohamed, T. Ewing, S.R. Lindemann, J.K. Fredrickson, H. Beyenal, Autonomous device for evaluating the field performance of Microbial Fuel Cells in remote areas, J. Electrochem. Soc. 164 (2017) H3030–H3036.

[235] I. Lee, G. Kim, S. Bang, A. Wolfe, R. Bell, S. Jeong, Y. Kim, J. Kagan, M. Arias-Thode, B. Chadwick, D. Sylvester, D. Blaauw, Y. Lee, System-On-Mud: Ultra-low power oceanic sensing platform powered by small-scale Benthic Microbial Fuel Cells, IEEE Trans. Circuits Syst. I Regul. Pap. 62 (2015) 1126–1135.

[236] L. Hsu, A. Mohamed, P.T. Ha, J. Bloom, T. Ewing, M. Arias-Thode, B. Chadwick, H.

Beyenal, The influence of energy harvesting strategies on Performance and Microbial Community for sediment Microbial Fuel Cells, J. Electrochem. Soc. 164 (2017) H3109–H3114.

[237] C. Santoro, C. Flores-Cadengo, F. Soavi, M. Kodali, I. Merino-Jimenez, I. Gajda, J. Greenman, I. Ieropoulos, P. Atanassov, Ceramic Microbial Fuel Cells stack: power generation in standard and supercapacitive mode, Sci. Rep. 8 (2018) 1–12.

[238] S.E. Oh, B.E. Logan, Voltage reversal during microbial fuel cell stack operation, J. Power Sources. 167 (2007) 11–17.

[239] A. Gurung, S.E. Oh, The performance of serially and parallelly connected microbial fuel cells, Energy Sources, Part A Recover. Util. Environ. Eff. 34 (2012) 1591–1598.

[240] P. Ledezma, J. Greenman, I. Ieropoulos, MFC-cascade stacks maximise COD reduction and avoid voltage reversal under adverse conditions, Bioresour. Technol. 134 (2013) 158–165.

[241] P. Aelterman, K. Rabaey, H.T. Pham, N. Boon, W. Verstraete, Continuous electricity generation at high voltages and currents using stacked Microbial Fuel Cells, Environ. Sci. Technol. 40 (2006) 3388–3394.

[242] F. Khaled, O. Ondel, B. Allard, Optimal energy harvesting from serially connected microbial fuel cells, IEEE Trans. Ind. Electron. 62 (2015) 3508–3515.

[243] G. Papaharalabos, J. Greenman, A. Stinchcombe, I. Horsfield, C. Melhuish, I. Ieropoulos, Dynamic electrical reconfiguration for improved capacitor charging in microbial fuel cell stacks, J. Power Sources. 272 (2014) 34–38.

[244] J. Winfield, I. Ieropoulos, J. Greenman, Investigating a cascade of seven hydraulically connected microbial fuel cells, Bioresour. Technol. 110 (2012) 245–250.

[245] Y. Zhang, I. Angelidaki, Self-stacked submersible microbial fuel cell (SSMFC) for improved remote power generation from lake sediments, Biosens. Bioelectron. 35 (2012) 265–270.

[246] I.A. Ieropoulos, P. Ledezma, A. Stinchcombe, G. Papaharalabos, C. Melhuish, J. Greenman, Waste to real energy: The first MFC powered mobile phone, Phys. Chem. Chem. Phys. 15 (2013) 15312–15316.

[247] M.A. Garita-Meza, L.A. Ramírez-Balderas, R. Contreras-Bustos, A.U. Chávez-Ramírez, B. Cercado, Blocking oscillator-based electronic circuit to harvest and boost the voltage produced by a compost-based microbial fuel cell stack, Sustain. Energy Technol. Assessments. 29 (2018)

164–170.

[248] N. Zhao, I. Angelidaki, Y. Zhang, Electricity generation and microbial community in response to short-term changes in stack connection of self-stacked submersible microbial fuel cell powered by glycerol, Water Res. 109 (2017) 367–374.

[249] I. Ieropoulos, J. Greenman, C. Melhuish, Urine utilisation by microbial fuel cells; Energy fuel for the future, Phys. Chem. Chem. Phys. 14 (2012) 94–98.

[250] T. Kim, S. Kang, H.W. Kim, Y. Paek, J.H. Sung, Y.H. Kim, J.K. Jang, Assessment of organic removal in series- and parallel-connected microbial fuel cell stacks, Biotechnol. Bioprocess Eng. 22 (2017) 739–747.

[251] Z. Ge, Z. He, Long-term Performance of a 200-Liter modularized Microbial Fuel Cell system treating Municipal Wastewater: treatment, energy, and cost, Environ. Sci. Water Res. Technol. 2 (2016) 1–2.

[252] X.A. Walter, I. Merino-Jiménez, J. Greenman, I. Ieropoulos, PEE POWER®urinal II – Urinal scale-up with microbial fuel cell scale-down for improved lighting, J. Power Sources. 392 (2018) 150–158.

[253] G. Papaharalabos, A. Stinchcombe, I. Horsfield, C. Melhuish, J. Greenman, I. Ieropoulos, Autonomous energy harvesting and prevention of cell reversal in MFC Stacks, J. Electrochem. Soc. 164 (2017) H3047–H3051.

[254] M.S.S. Santos, L. Peixoto, C. Dias-Ferreira, A. Mendes, M.M. Alves, Microbially charged Redox Flow Batteries for bioenergy storage, in: R.N. Krishnaraj, R.K. Sani (Eds.), Bioelectrochemical Interface Eng., Wiley, 2019: pp. 251–269.

[255] X. Xie, M. Ye, P.-C. Hsu, N. Liu, C.S. Criddle, Y. Cui, Microbial battery for efficient energy recovery, Proc. Natl. Acad. Sci. 110 (2013) 15925–15930.

[256] S.D. Molenaar, A.R. Mol, T.H.J.A. Sleutels, A. ter Heijne, C.J.N. Buisman, Microbial Rechargeable Battery: energy storage and recovery through acetate, Environ. Sci. Technol. Lett. 3 (2016) 144–149.

[257] A M. Kannan, V. Renugopalakrishnan, S. Filipek, P. Li, G.F. Audette, L. Munukutla, Bio-batteries and bio-fuel cells: leveraging on electronic charge transfer proteins., J. Nanosci. Nanotechnol. 9 (2009) 1665–1678.

[258] P. Clauwaert, P. Aelterman, T.H. Pham, L. De Schamphelaire, M. Carballa, K. Rabaey,

W. Verstraete, L. De Schamphelaire, M. Carballa, K. Rabay, W. Verstraete, Minimizing losses in bio-electrochemical systems: The road to applications, Appl. Microbiol. Biotechnol. 79 (2008) 901–913.

[259] H. Wang, F. Qian, Y. Li, Solar-assisted microbial fuel cells for bioelectricity and chemical fuel generation, Nano Energy. 8 (2014) 264–273.

[260] W. Liu, H. Jia, J. Wang, H. Zhang, C. Xin, Y. Zhang, Microbial fuel cell and membrane bioreactor coupling system: recent trends, Environ. Sci. Pollut. Res. 25 (2018) 23631–23644.

[261] F. Fischer, Photoelectrode, photovoltaic and photosynthetic microbial fuel cells, Renew. Sustain. Energy Rev. 90 (2018) 16–27.

[262] Y. Du, X. Zhou, Y. Qu, J. Liu, Y. Feng, N. Ren, Enhanced electricity generation and pollutant degradation by hybrid Photoelectrochemical and Microbial Fuel Cells, Energy Technol. 5 (2017) 402–405.

[263] R.A. Rincón, C. Lau, H.R. Luckarift, K.E. Garcia, E. Adkins, G.R. Johnson, P. Atanassov, Enzymatic fuel cells: integrating flow-through anode and air-breathing cathode into a membrane-less biofuel cell design, Biosens. Bioelectron. 27 (2011) 132–136.

[264] T. Quah, R.D. Milton, S. Abdellaoui, S.D. Minteer, Bioelectrocatalytic NAD^+/NADH inter-conversion: transformation of an enzymatic fuel cell into an enzymatic redox flow battery, Chem. Commun. 53 (2017) 8411–8414.

[265] M.L. Perry, A.Z. Weber, Advanced Redox-Flow Batteries: a perspective, J. Electrochem. Soc. 163 (2016) A5064–A5067.

[266] A.C. Bibliography, NASA Patent Abstracts Bibliography: a continuing bibliography, 7039 (2008).

[267] W. Kangro, Verfahren zur Speicherung von elektrischer, 1962.

[268] T. Shibata, T. Kumamoto, Y. Nagaoka, K. Kawase, K. Yano, Redox flow batteries for the stable supply of renewable energy, SEI Tech. Rev. (2013) 14–22.

[269] N. Tokuda, T. Kumamoto, T. Shigematsu, H. Deguchi, T. Ito, N. Yoshikawa, T. Hara, Development of a redox flow battery system, SEI Tech Rev. 50 (1998) 88–94.

[270] T. Shigematru, Redox Flow Battery for Energy Storage, Sei Thecnical Rev. 73 (2011) 7–13.

[271] Q. Lai, H. Zhang, X. Li, L. Zhang, Y. Cheng, A novel single flow zinc-bromine battery with

improved energy density, J. Power Sources. 235 (2013) 1–4.

[272] Y.K. Zeng, T.S. Zhao, L. An, X.L. Zhou, L. Wei, A comparative study of all-vanadium and iron-chromium redox flow batteries for large-scale energy storage, J. Power Sources. 300 (2015) 438–443.

[273] R.M. Darling, K.G. Gallagher, J.A. Kowalski, S. Ha, F.R. Brushett, Pathways to low-cost electrochemical energy storage: a comparison of aqueous and nonaqueous flow batteries, Energy Environ. Sci. 7 (2014) 3459–3477.

[274] C. Ponce de León, A. Frías-Ferrer, J. González-García, D.A. Szánto, F.C. Walsh, Redox flow cells for energy conversion, J. Power Sources. 160 (2006) 716–732.

[275] K. Wedege, J. Azevedo, A. Khataee, A. Bentien, A. Mendes, Direct solar charging of an organic-inorganic, stable, and aqueous alkaline Redox Flow Battery with a hematite photoanode, Angew. Chemie Int. Ed. 55 (2016) 7142–7147.

[276] K. Wedege, P.C.K.K. Vesborg, D. Bae, E. Dražević, A. Mendes, P.C.K.K. Vesborg, A. Bentien, Unbiased, complete solar charging of a neutral flow battery by a single Si photocathode, RSC Adv. 8 (2018) 6331–6340.

[277] R. Ye, D. Henkensmeier, S.J. Yoon, Z. Huang, D.K. Kim, Z. Chang, S. Kim, R. Chen, Redox Flow Batteries for energy storage: a technology review, J. Electrochem. Energy Convers. Storage. 15 (2017) 325–335.

[278] H. Prifti, A. Parasuraman, S. Winardi, T.M. Lim, M. Skyllas-Kazacos, Membranes for redox flow battery applications, Membranes (Basel). 2 (2012) 275–306.

[279] M.H. Chakrabarti, N.P. Brandon, S.A. Hajimolana, F. Tariq, V. Yufit, M.A. Hashim, M.A. Hussain, C.T.J. Low, P. V. Aravind, Application of carbon materials in redox flow batteries, J. Power Sources. 253 (2014) 150–166.

[280] P. Leung, X. Li, C. Ponce de León, L. Berlouis, C.T.J.J. Low, F.C. Walsh, Progress in redox flow batteries, remaining challenges and their applications in energy storage, RSC Adv. 2 (2012) 10125–10156.

[281] X.L. Zhou, T.S. Zhao, L. An, Y.K. Zeng, L. Wei, Critical transport issues for improving the performance of aqueous redox flow batteries, J. Power Sources. 339 (2017) 1–12.

[282] S. Weber, J.F. Peters, M. Baumann, M. Weil, Life cycle assessment of a Vanadium Redox Flow Battery, Environ. Sci. Technol. 52 (2018) 10864–10873.

[283] H. Chen, T.N. Cong, W. Yang, C. Tan, Y. Li, Y. Ding, Progress in electrical energy storage system: a critical review, Prog. Nat. Sci. 19 (2009) 291–312.

[284] W. Wang, Q. Luo, B. Li, X. Wei, L. Li, Z. Yang, Recent progress in redox flow battery research and development, Adv. Funct. Mater. 23 (2013) 970–986.

[285] M. Müller, Regenerative Fuel Cells, in: Fuel Cell Sci. Eng. Mater. Process. Syst. Technol., Wiley-VCH, 2012: pp. 219–245.

[286] W. Wang, W. Xu, L. Cosimbescu, D. Choi, L. Li, Z. Yang, Anthraquinone with tailored structure for a nonaqueous metal–organic redox flow battery, Chem. Commun. 48 (2012) 6669–6671.

[287] K. Gong, F. Xu, J.B. Grunewald, X. Ma, Y. Zhao, S. Gu, Y. Yan, All-soluble All-Iron Aqueous Redox-Flow Battery, ACS Energy Lett. 1 (2016) 89–93.

[288] L. Sanz, D. Lloyd, E. Magdalena, J.J.J. Palma, K.K.K. Kontturi, Description and performance of a novel aqueous all-copper redox flow battery, J. Power Sources. 268 (2014) 121–128.

[289] P. Singh, Application of non-aqueous solvents to batteries, J. Power Sources. 11 (1984) 135–142.

[290] B. Li, J. Liu, Progress and directions in low-cost redox-flow batteries for large-scale energy storage, Natl. Sci. Rev. 4 (2017) 91–105.

[291] Y. Huang, S. Gu, Y. Yan, S.F.Y. Li, Nonaqueous redox-flow batteries: features, challenges, and prospects, Curr. Opin. Chem. Eng. 8 (2015) 105–113.

[292] A.A. Shinkle, T.J. Pomaville, A.E.S. Sleightholme, L.T. Thompson, C.W. Monroe, Solvents and supporting electrolytes for vanadium acetylacetonate flow batteries, J. Power Sources. 248 (2014) 1299–1305.

[293] S.H. Shin, S.H. Yun, S.H. Moon, A review of current developments in non-aqueous redox flow batteries: Characterization of their membranes for design perspective, RSC Adv. 3 (2013) 9095–9116.

[294] R. Monteiro, J. Leirós, M. Boaventura, A. Mendes, Insights into all-vanadium redox flow battery: a case study on components and operational conditions, Electrochim. Acta. 267 (2018) 80–93.

[295] Z. Na, S. Xu, D. Yin, L. Wang, A cerium–lead redox flow battery system employing

supporting electrolyte of methanesulfonic acid, J. Power Sources. 295 (2015) 28–32.

[296] G.L. Soloveichik, Flow batteries: current status and trends, Chem. Rev. 115 (2015) 11533–11558.

[297] C. Choi, S.S. Kim, R. Kim, Y. Choi, S.S. Kim, H. young Jung, J.H. Yang, H.T. Kim, A review of vanadium electrolytes for vanadium redox flow batteries, Renew. Sustain. Energy Rev. 69 (2017) 263–274.

[298] J. Winsberg, T. Hagemann, T. Janoschka, M.D. Hager, U.S. Schubert, Redox-Flow Batteries: from metals to organic redox-active materials, Angew. Chemie Int. Ed. 55 (2017) 2–28.

[299] W. Wang, V. Sprenkle, Energy storage: redox flow batteries go organic, Nat. Chem. 8 (2016) 204–206.

[300] C. Han, H. Li, R. Shi, T. Zhang, J. Tong, J. Li, B. Li, Organic quinones towards advanced electrochemical energy storage: recent advances and challenges, J. Mater. Chem. A. 7 (2019) 23378–23415.

[301] K. Wedege, E. Dražević, D. Konya, A. Bentien, Organic Redox Species in aqueous flow batteries: redox potentials, chemical stability and solubility, Sci. Rep. 6 (2016) 1–14.

[302] T.B. Schon, B.T. McAllister, P.-F. Li, D.S. Seferos, The rise of organic electrode materials for energy storage, Chem. Soc. Rev. 45 (2016) 6345–6404.

[303] M.R. Gerhardt, L. Tong, R. Gómez-Bombarelli, Q. Chen, M.P. Marshak, C.J. Galvin, A. Aspuru-Guzik, R.G. Gordon, M.J. Aziz, Anthraquinone derivatives in aqueous flow batteries, Adv. Energy Mater. 7 (2017) 1–9.

[304] Y. Moon, Y.-K. Han, Computational screening of organic molecules as redox active species in redox flow batteries, Curr. Appl. Phys. 16 (2016) 939–943.

[305] B. Huskinson, M.P. Marshak, M.R. Gerhardt, M.J. Aziz, A Quinone-Based Flow Battery for large-scale electrochemical energy storage, 224th ECS Meet. (2013) 2138–2139.

[306] M.P. Marshak, B. Huskinson, M.R. Gerhardt, M.J. Aziz, Applications of quinone redox chemistry for flow batteries, in: 224th ECS Meet., 2013.

[307] B. Huskinson, M.P. Marshak, C. Suh, S. Er, R. Michael, C.J. Galvin, X. Chen, A. Aspuru-guzik, R.G. Gordon, J. Aziz, A metal - free organic – inorganic aqueous flow battery, Nature. 505 (2014) 195–198.

[308] K. Lin, R. Gómez-Bombarelli, E.S. Beh, L. Tong, Q. Chen, A. Valle, A. Aspuru-Guzik, M.J. Aziz, R.G. Gordon, A redox-flow battery with an alloxazine-based organic electrolyte, Nat. Energy. 1 (2016) 1–8.

[309] E.S. Beh, D. De Porcellinis, R.L. Gracia, K.T. Xia, R.G. Gordon, M.J. Aziz, A neutral pH aqueous organic − organometallic Redox Flow Battery with extremely high capacity retention, ACS Energy Lett. 2 (2017) 639–644.

[310] C. DeBruler, B. Hu, J. Moss, X. Liu, J. Luo, Y. Sun, T.L. Liu, Designer two-electron storage viologen anolyte materials for Neutral Aqueous Organic Redox Flow Batteries, Chem. 3 (2017) 961–978.

[311] X. Wei, W. Pan, W. Dnan, A. Hollas, Z. Hang, B. Li, Z. Nie, J. Lin, D. Reed, W.Wang, V. Sprenkle, Materials and systems for Organic Redox Flow Batteries: status and challenges, ACS Energy Lett. 2017, 2, 9, 2187–2204.

[312] Y. Zhao, Y. Ding, Y. Li, L. Peng, H.R. Byon, J.B. Goodenough, G. Yu, A chemistry and material perspective on lithium redox flow batteries towards high-density electrical energy storage, Chem. Soc. Rev. 44 (2015) 7968–7996.

[313] O.R. Luca, J.L. Gustafson, S.M. Maddox, A.Q. Fenwick, D.C. Smith, Catalysis by electrons and holes: formal potential scales and preparative organic electrochemistry, Org. Chem. Front. 2 (2015) 823–848.

[314] U. Er, C. Suh, M.P. Marshak, A. An Aspuru-Guzik, Computational design of molecules for an all-quinone redox flow battery, Chem. Sci. 6 (2015) 845–1592.

[315] Y.-K. Han, C.-S. Jin, Computational screening of electroactive indolequinone derivatives as high-performance active materials for aqueous redox flow batteries, Curr. Appl. Phys. 18 (2018) 1507–1512.

[316] Y. Ding, Y. Li, G. Yu, Exploring bio-inspired Quinone-based Organic Redox Flow Batteries: a combined experimental and computational study, Chem. 1 (2016) 790–801.

[317] Y. Ding, C. Zhang, L. Zhang, Y. Zhou, G. Yu, Pathways to widespread applications: development of Redox Flow Batteries based on new chemistries, Chem. 5 (2019) 1964–1987.

[318] W.M. Owton, The synthesis of quinones, J. Chem. Soc. Perkin Trans. 1. 3 (1999) 2409–2420.

[319] J.B. Conant, H.M. Kahn, L.F. Fieser, S.S. Kurtz, An electrochemical study of the

reversible reduction of organic compounds, J. Am. Chem. Soc. 44 (1922) 1382–1396.

[320] M. Uchimiya, A.T. Stone, Reversible redox chemistry of quinones: Impact on biogeochemical cycles, Chemosphere. 77 (2009) 451–458.

[321] B. Yang, L. Hoober-Burkhardt, F. Wang, G.K. Surya Prakash, S.R. Narayanan, An inexpensive aqueous flow battery for large-scale electrical energy storage based on water-soluble organic redox couples, J. Electrochem. Soc. 161 (2014) A1371–A1380.

[322] V. Singh, S. Kim, J. Kang, H.R. Byon, Aqueous organic redox flow batteries, Nano Res. 12 (2019) 1–14.

[323] E.J. Son, J.H. Kim, K. Kim, C.B. Park, Quinone and its derivatives for energy harvesting and storage materials, J. Mater. Chem. A. 4 (2016) 11179–11202.

[324] M. Martínez-Cifuentes, R. Salazar, O. Ramírez-Rodríguez, B. Weiss-López, R. Araya-Maturana, Experimental and theoretical reduction potentials of some biologically active ortho-carbonyl para-quinones, Molecules. 22 (2017) 1–10.

[325] M.T. Huynh, C.W. Anson, A.C. Cavell, S.S. Stahl, S. Hammes-Schiffer, Quinone $1e^-$ and $2e^-$ /$2H^+$ reduction potentials: identification and analysis of deviations from systematic scaling relationships, J. Am. Chem. Soc. 138 (2016) 15903–15910.

[326] D.P. Tabor, R. Gómez-Bombarelli, L. Tong, R.G. Gordon, M.J. Aziz, A. Aspuru-Guzik, Mapping the frontiers of quinone stability in aqueous media: Implications for organic aqueous redox flow batteries, J. Mater. Chem. A. 7 (2019) 12833–12841.

[327] R.S. Kim, T.D. Chung, The electrochemical reaction mechanism and applications of quinones, Bull. Korean Chem. Soc. 35 (2014) 3143–3155.

[328] E. Laviron, Electrochemical reactions with protonations at equilibrium Part X. The kinetics of the p-benzoquinone/hydroquinone couple on a platinum electrode, J. Electroanal. Chem. 164 (1984) 213–227.

[329] C. Marín-Hernández, L.E. Santos-Figueroa, M.E.M.E. Moragues, M.M.M. Raposo, R.M.F. Batista, S.P.G. Costa, T. Pardo, R. Martínez-Máñez, F. Sancenón, Imidazoanthraquinone derivatives for the chromofluorogenic sensing of basic anions and trivalent metal cations, J. Org. Chem. 79 (2014) 10752–10761.

[330] L. Tong, Q. Chen, A.A. Wong, R. Gómez-Bombarelli, A. Aspuru-Guzik, R.G. Gordon, M.J. Aziz, UV-Vis spectrophotometry of quinone flow battery electrolyte for: In situ monitoring and

improved electrochemical modeling of potential and quinhydrone formation, Phys. Chem. Chem. Phys. 19 (2017) 31684–31691.

[331] S. Orsetti, C. Laskov, S.B. Haderlein, Electron transfer between iron minerals and quinones estimating the reduction potential of the Fe(II)-goethite surface from AQDS Speciation, Environ. Sci. Technol. 47 (2013) 1–6.

[332] Z. MacHatova, Z. Barbieriková, P. Poliak, V. Jancovicová, V. Lukes, V. Brezová, Study of natural anthraquinone colorants by EPR and UV/vis spectroscopy, Dye. Pigment. 132 (2016) 79–93.

[333] B. Huskinson, M.P. Marshak, C. Suh, S. Er, M.R. Gerhardt, C.J. Galvin, X. Chen, A. Aspuru-guzik, R.G. Gordon, M.J. Aziz, R. Michael, C.J. Galvin, X. Chen, A. Aspuru-guzik, R.G. Gordon, J. Aziz, A metal-free organic-inorganic aqueous flow battery., Nature. 505 (2014) 195–198.

[334] K. Lin, Q. Chen, M.R. Gerhardt, L. Tong, S.B. Kim, L. Eisenach, A.W. Valle, D. Hardee, R.G. Gordon, M.J. Aziz, M.P. Marshak, Alkaline quinone flow battery, Science (80). 349 (2015) 1529–1532.

[335] W. Li, H.-C. Fu, L. Li, M. Cabán-Acevedo, J.-H. He, S. Jin, Integrated Photoelectrochemical solar energy conversion and organic Redox Flow Battery devices, Angew. Chemie Int. Ed. 55 (2016) 13104–13108.

[336] B. Yang, L. Hoober-Burkhardt, S. Krishnamoorthy, A. Murali, G.K.S. Prakash, S.R. Narayanan, High-Performance aqueous organic flow battery with quinone-based redox couples at both electrodes, J. Electrochem. Soc. 163 (2016) 1442–1449.

[337] J. Cao, Z. Zhu, J. Xu, M. Tao, Z. Chen, Nitrogen-doped porous graphene as a highly efficient cathodic electrocatalyst for aqueous organic redox flow battery application, J. Mater. Chem. A. 5 (2017) 7944–7951.

[338] P. Leung, T. Martin, M. Liras, A.M. Berenguer, R. Marcilla, A. Shah, L. An, M.A. Anderson, J. Palma, Cyclohexanedione as the negative electrode reaction for aqueous organic redox flow batteries, Appl. Energy. 197 (2017) 318–326.

[339] Y. Xu, Y. Wen, J. Cheng, Y. Yanga, Z. Xie, G. Cao, Novel organic redox flow batteries using soluble quinonoid compounds as positive materials, in: 2009 World Non-Grid-Connected Wind Power Energy Conf., IEEE, Nanjing, China, 2009: pp. 475–478.

[340] Y. Xu, Y.-H. Wen, J. Cheng, G.-P. Cao, Y.-S. Yang, A study of tiron in aqueous solutions for redox flow battery application, Electrochim. Acta. 55 (2010) 715–720.

[341] B. Huskinson, M.P. Marshak, M.R. Gerhardt, M.J. Aziz, Cycling of a Quinone-Bromide Flow Battery for large-scale electrochemical energy storage, ECS Trans. 61 (2014) 27–30.

[342] W.D. McCulloch, M. Yu, Y. Wu, PH-Tuning a Solar Redox Flow Battery for integrated energy conversion and storage, ACS Energy Lett. 1 (2016) 578–582.

[343] Q. Chen, L. Eisenach, M.J. Aziz, Cycling analysis of a Quinone-Bromide Redox Flow Battery, J. Electrochem. Soc. 163 (2016) A5057–A5063.

[344] B. Huskinson, M.P. Marshak, C. Suh, S. Er, M.R. Gerhardt, C.J. Galvin, X. Chen, A. Aspuru-Guzik, R.G. Gordon, M.J. Aziz, R. Michael, C.J. Galvin, X. Chen, A. Aspuru-Guzik, R.G. Gordon, J. Aziz, A metal-free organic–inorganic aqueous flow battery, Nature. 505 (2014) 195–198.

[345] D.G. Kwabi, A.A. Wong, M.J. Aziz, Rational evaluation and cycle life improvement of Quinone-Based Aqueous Flow Batteries guided by In-Line Optical Spectrophotometry, J. Electrochem. Soc. 165 (2018) A1770–A1776.

[346] M.R. Gerhardt, E.S. Beh, L. Tong, R.G. Gordon, M.J. Aziz, Comparison of capacity retention rates during cycling of Quinone-Bromide Flow Batteries, MRS Adv. (2016) 1–8.

[347] J.D. Hofmann, F.L. Pfanschilling, N. Krawczyk, P. Geigle, L. Hong, S. Schmalisch, H.A. Wegner, D. Mollenhauer, J. Janek, D. Schröder, Quest for organic active materials for Redox Flow Batteries: 2,3-Diaza-anthraquinones and their electrochemical properties, Chem. Mater. 30 (2018) 762–774.

[348] W. Lee, A. Permatasari, Y. Kwon, Neutral pH aqueous redox flow batteries using an anthraquinone-ferrocyanide redox couple, J. Mater. Chem. C. 8 (2020) 5727–5731.

[349] D.G. Kwabi, K. Lin, Y. Ji, E.F. Kerr, M. Goulet, D. De Porcellinis, D.P. Tabor, D.A. Pollack, A. Aspuru-Guzik, R.G. Gordon, M.J. Aziz, Alkaline Quinone Flow Battery with long lifetime at pH 12, Joule. 2 (2018) 1894–1906.

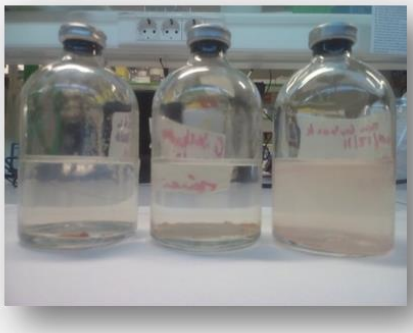
[350] A.W. Lantz, S.A. Shavalier, W. Schroeder, P.G. Rasmussen, Evaluation of an aqueous Biphenol- and Anthraquinone-Based Electrolyte Redox Flow Battery, ACS Appl. Energy Mater. (2019) 7893–7902.

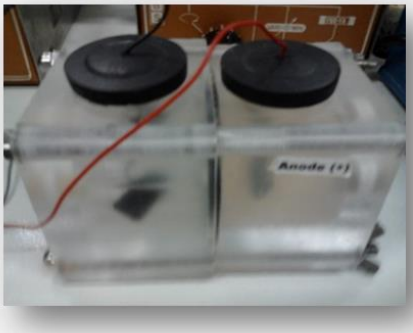
[351] K. Arumugam, U. Becker, Computational redox potential predictions: applications to inorganic and organic aqueous complexes, and complexes adsorbed to mineral surfaces, Minerals. 4 (2014) 345–387.

[352] A.H. Shah, W. Zaid, A. Shah, U.A. Rana, H. Hussain, M.N. Ashiq, R. Qureshi, A. Badshah, M.A. Zia, H.-B. Kraatz, pH dependent electrochemical characterization, computational studies and evaluation of thermodynamic, kinetic and analytical parameters of two phenazines, J. Electrochem. Soc. 162 (2014) H115–H123.

[353] H. Chen, G. Cong, Y.C. Lu, Recent progress in organic redox flow batteries: active materials, electrolytes and membranes, J. Energy Chem. 0 (2018) 1–22.

[354] Y. Ding, C. Zhang, L. Zhang, Y. Zhou, G. Yu, Molecular engineering of organic electroactive materials for redox flow batteries, Chem. Soc. Rev. 47 (2018) 69–103.





Chapter 2

Unravelling the Bioelectrochemical Systems capacity to promote a microbial electrochemical fuel

Abstract[1]

Bioelectrochemical Systems (BESs) capacity to convert biodegradable substrates (fuels) in electrical energy are prominently researched. Slight advances in store BESs bioelectrochemical energy are being pursuit. In this report the conversion of a redox chemical specie in BES, to be explored as microbial electrochemical fuel was researched. This report presents the first studies of the reduction of anthraquinone-2,6-disulphonate (2,6-AQDS) as a cathodic electron acceptor in BESs. *Geobacter sulfurreducens* and acetate as simple electron donor for substrate conversion in anode side of BESs were selected. The reduction of 2,6-AQDS was tested with BESs controlled with an anode potential at -0.200 V *vs.* Ag/AgCl (3 M) and with BESs closed with an external resistance load of 500 Ω. The reduction of 2,6-AQDS was confirmed by visual color change, as it gets charged, and studied with Cyclic Voltammetry in the end of the assays. The microbial electrochemical fuels anthrahydroquinone-2,6-disulphonate (2,6-AQDSH_2) (negalyte) and ferricyanide ($[Fe(CN)_6]^{3-}$) (posilyte) were used as redox pair in a RFC. The substrate conversion energy into microbial electrochemical fuels, without bias potential is presented. An unbiased energy storage device, using microbial electrochemical fuels in a RFC is a future research approach.

[1] The work presented in this chapter is adapted from: **M.S.S. Santos**, L. Peixoto, C. Dias-Ferreira, A. Mendes, M.M. Alves. Microbial Redox Flow Battery: coupling a Bioelectrochemical Cell with a Redox Flow Battery. ISMET 6 - Meeting of the International Society for Microbial Electrochemistry and Technology, Lisbon 2017, Oral communications – Session VII, OCVIV-2, 95.

2.1. Introduction

Bioelectrochemical Systems (BESs) are innovative electrochemical energy technologies applied for bioenergy conversion [1–3]. BESs convert organic sources (*e.g.* wastewaters) to generate electrical energy in a simple basic configuration - Microbial Fuel Cells (MFCs) [4–7]. BESs power densities are *ca.* $10x10^6$ mW cm^{-2} [8, 9, 18–21, 10–17], which are inferior to other electrochemical devices *e.g.* Redox Flow Cells (RFCs), with *ca.* $1x10^8$ mW cm^{-2} [22–24]. Unravelling more practical bioelectrochemical conversions processes to improve the power and the energy yields generated in BESs is of high interest, *i.e.* different types of Electrochemically Active Bacteria (EAB), materials and physical designs [25,26].

The use of alternative cathodic electron acceptors may expand BESs applications [27], and will allow the integration with other electrochemical energy devices. Most of the cathodic electron acceptors used in BESs are oxygen or ferricyanide; other cathodic electron acceptors are summarized in the Table 2.1.

Table 2.1.Summary of different cathodic electron acceptors and the maximum power densities in BESs.

Type of cathodic electron acceptor	Formal standard potential (V)	Maximum power density (mW cm^{-2})	Reference
Oxygen	1.230	$7.88x10^6$	[30,31]
Ferricyanide	0.430	$2.10x10^4$	[32,33]
Nitrate	0.740	$9.40x10^4$	[27,34]
Persulfate	2.120	$2.45x10^5$	[27,33]
Permanganate	1.700 /0.590	$1.16\ x10^6$	[35]
Manganese Dioxide	+0.360	$1.27\ x10^6$	[36]
Mercury	−0.320 (Hg^{2+})	$4.33\ x10^6$	[37,38]
Ferrous iron	+0.770	$8.60\ x10^6$	[39]
Copper	+0.286	$8.00\ x10^6$	[40]
Chromium	1.330	$1.50\ x10^6$	[41]
Carbon Dioxide	−0.420	$7.50\ x10^6$	[37,42]
Vanadium	0.810	$5.72\ x10^6$	[43]
2,6-AQDS	-0.184	$3.27\ x10^5$	This study

Oxygen is one of the most explored cathodic electron acceptor in MFCs, because oxygen has a high oxidation potential and is highly available [28]. Another is ferricyanide ($[Fe(CN)_6]^{3-}$), that is not limited by solubility and has low overpotential, being one of the most usual cathodic electron acceptor [29]. Different approaches for cathodic reduction reactions in BESs are being researched. The use of biocathodes in Microbial Electrosynthesis Cells (MESs) for chemical

synthesis are applied [46]. The cathodic side of BESs promote reduction reactions that allow to remove ion metals, such as vanadium [44, 45]. After complete reduction of the catholytes, these need to be replaced, because some contain toxic elements and are not environmentally sustainable.

The potential of cathodic reduction reactions was studied in a Microbial Battery [47], where a microbial anode and a solid-state oxidant cathode were analyzed. Molenaar and coworkers [48] present a Microbial Rechargeable Battery that combines MES and MFC in a single system. When the Microbial Rechargeable Battery is operating in MFC phase, electrical energy is generated with consumption of acetate. When the system operates in the MES phase, the electrical energy of the system is consumed to form acetate.

An auspicious approach to couple BESs and RFCs was inspired by the research with Solar Redox Flow Cell [49, 50], where this device convert solar energy in storable electrochemical energy, easily converted in electrical energy. RFCs are electrochemical devices that transform electrochemical energy into electrical energy, and are capable to store the energy generated. RFCs are similar to Fuel Cells, but operate with a flow-through configuration; the redox conversion of electroactive species is responsible for the release of electricity [51]. The redox species in RFCs reported in aqueous solutions are ion metals (such as vanadium) and organic redox molecules (*e.g.* quinones), from biological origin [52].

BESs reduction of a redox chemical specie in BES, to be explored as microbial electrochemical fuel was researched. Furthermore, anthraquinone-2,6-disulphonate (2,6-AQDS) is studied for the first time as a cathodic electron acceptor in this report work. The bioelectrochemical reduction of 2,6-AQDS was carried out and analyzed in BES. The reduction of 2,6-AQDS to anthrahydroquinone-2,6-disulphonate (2,6-AQDSH_2) in BESs was analyzed with a bias anode potential and an external resistance load. The aim was to evaluate the EAB capacity to promote the conversion of 2,6-AQDS, in an biased and unbiased process. The bio-charged 2,6-AQDSH_2 was designated as microbial electrochemical fuel; this microbial electrochemical fuel was tested as negalyte in a RFC. An unbiased energy storage device, coupling BES and RFC is intended to be pursuit as a follow-up of this research.

2.2. Material and methods

Chemicals and materials

The 2,6-AQDS was used as purchased (anthraquinone-2,6-disulfonic acid disodium salt (97 %), $C_{14}H_6Na_2O_8S_2$). The conducting carbon cement (Leit-C) and chemical reagents used were of analytical grade from Sigma Aldrich. The Nafion™ NM 117 Proton Exchange Membrane (PEM) was acquired from Quintech. Milli-Q® water was used in the preparation of solutions (Milli-Q® Integral Water Purification system).

G. sulfurreducens culture conditions

Medium preparation

The medium was composed of 1.50 g L^{-1} NH_4Cl, 0.60 g L^{-1} Na_2HPO_4, 0.10 g L^{-1} KCl, 10 mL L^{-1} of the trace element solution and 1 mL L^{-1} selenite-tungstate solution. The trace element and the selenite-tungstate solutions introduced were from stock solutions prepared, filtered (0.22 µm) and reserved in sterile glass bottles at 4 °C. The trace element solution was prepared with: 1.50 g L^{-1} nitrilotriacetic acid, 3.00 g L^{-1} $MgSO_4 \cdot 7H_2O$, 0.50 g L^{-1} $MnSO_4 \cdot 7H_2O$, 1.00 g L^{-1} NaCl, 0.10 g L^{-1} $FeSO_4 \cdot 7H_2O$, 0.18 g L^{-1} $CoSO_4 \cdot 7H_2O$, 0.10 g L^{-1} $CaCl \cdot 2H_2O$, 0.18 g L^{-1} $ZnSO_4 \cdot 7H_2O$, 0.01 g L^{-1} $CuSO_4 \cdot 5H_2O$, 0.02 g L^{-1} $KAl(SO_4)_2 \cdot 12H_2O$, 0.01 g L^{-1} H_3BO_3, 0.01 g L^{-1} $Na_2MoO_4 \cdot 2H_2O$, 0.03 g L^{-1} $NiCl_2 \cdot 6H_2O$, 0.0003 g L^{-1} $Na_2SeO_3 \cdot 5H_2O$. The selenite-tungstate solution contained 0.50 g L^{-1} NaOH, 0.003 g L^{-1} $Na_2SeO_3 \cdot 5H_2O$ and 0.004 g L^{-1} $Na_2WO_4 \cdot 2H_2O$. The medium prepared was boiled and cooled down in an ice bath, until reach room temperature and simultaneously deoxygenated with a stream of N_2:CO_2 (80 %:20 %). After the medium cooled down, 2.50 g L^{-1} of $NaHCO_3$ was dissolved, with the gas mixture flowing, to buffering it at pH = 6.8. The medium was disposed in serum bottles (50 mL each). To ensure the anaerobic conditions, the vials were flushed with N_2:CO_2 (80 %:20 %) gas mixture, controlling the pressure with a manifold connected to a vacuum and compressor systems. Finally, the serum bottles were sterilized in autoclave (121 ºC, 21 min).

Electroactive bacteria cultivation

Before inoculation of bacteria, 5 mL L^{-1} of the trace vitamin solution was added to the serum bottles. The vitamin solution was prepared and stored as a stock solution and contains 4.00 mg L^{-1} biotin, 4.00 mg L^{-1} folic acid, 20.00 mg L^{-1} pyridoxine-HCl, 10.00 mg L^{-1} thiamine-HCl·H_2O, 10.00 mg L^{-1} riboflavin, 10.00 mg L^{-1} nicotinic acid, 10.00 mg L^{-1} D-Ca-pantothenate, 0.20 mg L^{-1} vitamin B12, 10.00 mg L^{-1} p-aminobenzoic acid, 10.00 mg L^{-1} lipoic acid. The 1.64 g L^{-1} Na-acetate and 8.00 g L^{-1} Na_2-fumarate were also added to the serum bottles, as carbon source and electron acceptor [14, 15]. The Na-acetate and Na_2-fumarate were previously prepared, filtered with a sterilized filter (0.22 µm) and stored at 4 °C in sterile conditions. Finally, 10 % of *Geobacter sulfurreducens* from previous stock culture, was used to inoculate the medium, and growth at 30 ºC and 100 rpm in an incubator.

BESs setup and experimental conditions

BESs were assembled inside a laminar flow chamber to prevent external sources of contamination. The BESs were assembled with a 50 cm^3 chambers separated by a Nafion™ NM 117 PEM (Figure 2.1.). The membrane was previously treated during 3 h at 40 ºC with 10 % H_2SO_4 solution and rinsed several times with Milli-Q® water. The electrodes were made of carbon felt (0.1 x 4 cm^2), and were connected to electrical wires using conducting carbon cement. The electrodes were introduced in the respective chamber and sustained with rubber gaskets to close the BESs chambers.

The anode chamber of BESs was filled with *Geobacter sulfurreducens* from the serum bottles (pH = 6.8). In the anode chamber 1.64 g L^{-1} Na-acetate solution was added as electron donor and the electrode was the electron receptor. The cathode side was filled with 20 mM 2,6-AQDS prepared in 0.10 M phosphate buffer solution, at pH = 7 (Figure 2.1).

BESs were flushed with N_2:CO_2 (80 %:20 %) gas mixture using sterile filters (0.2 µm) to promote anaerobic conditions. BESs were operated in batch conditions, in a stirring plate and monitored at room temperature (20 °C) [53]. BESs were sheltered from light to avoid oxidation during the bioelectrochemical reduction of 2,6-AQDS [54].

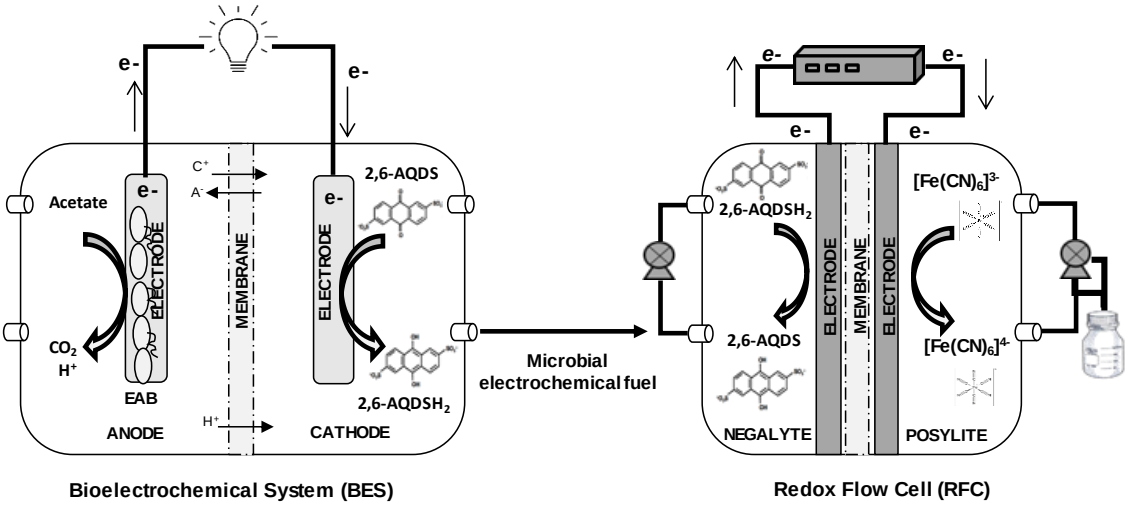


Figure 2.1. Schematic representation of Bioelectrochemical System (BES) with anthraquinone-2,6-disulphonate (2,6-AQDS) as cathodic electron acceptors (in the left side); the anthrahydroquinone-2,6-disulphonate (2,6-AQDSH_2) (microbial electrochemical fuel) was tested as negalyte in a Redox Flow Cell (RFC) (in the right side).

The reduction of 2,6-AQDS in BES was researched with a bias anode potential at -0.200 V *vs.* Ag/AgCl (3 M) and with BES closed with an external resistance load of 500 Ω.

A bias anode potential at -0.200 V *vs.* Ag/AgCl (3 M) was applied in two BESs, aiming the biofilm formation and acetate consumption [55]. This experimental setup was named BES AP. The two BESs were run in these conditions, in parallel as duplicates (identified as BES AP 1 and BES AP 2). All electrodes were connected with a potentiostat (Potentiostat / Galvanostat VSP, BioLogic Science Instruments, France). The respective data acquisition software (EC-Lab software) was used to record the current density (j, mA cm^{-2}) over time (t, h) [55].

Additionally, two BESs were closed with an external resistance load of 500 Ω. This experimental setup was designated BES Ω. BESs were run in parallel as duplicates (identified as BES Ω 1 and BES Ω 2). The electric circuits of BESs were closed with an external resistance load of 500 Ω and the potential difference was registered with an Ecograph T data logger (RSG 30 Endress+Hauser B.V., Naarden). The current density over time was calculated [11].

BESs electrochemical characterization

The bioelectrochemical reduction of 2,6-AQDS in all BESs was evaluated through color change. The 2,6-AQDS exhibit a yellow color; and as it gets charged, in the cathode chamber of BESs, 2,6-AQDS changed to a dark red (almost brown) color, characteristic of the 2,6-AQDSH_2. This

color change was observed as referred in previous literature [56, 57]. All BESs assays were ended when the dark red color was seen for more than 24 h. The bio-charged 2,6-AQDSH_2 is designated as microbial electrochemical fuel, that will be further used as negalyte.

When all BESs experiments finished, a polarization and power curves were performed. The Open Circuit Potential (OCP) of BESs and the Potential (*E*, mV) were measured using a multimeter (HP Hewlett Packard 34401A multimeter). The curves were performed using a series of resistances ranging between 31 kΩ to 10 Ω [58]. The Power density (*P*, mW cm^{-2}) was calculated. BESs internal resistances were estimated from the slope of polarization curve results [11].

Cyclic Voltammetry of microbial electrochemical fuels

At the end of the experiments, Cyclic Voltammetry (CV) of the microbial electrochemical fuels were performed in the BESs. The BESs were previously deoxygenated with N_2 (100 %). The working electrode was the electrode in the cathode side, the Ag/AgCl (3 M) reference electrode was positioned in the cathode side, and the counter electrode in the anode side. All electrodes were connected with a potentiostat (Potentiostat / Galvanostat VSP, BioLogic Science Instruments, France) and with the respective potentiostat software [55]. All the results were converted and presented as Normal Hydrogen Electrode (NHE). The CVs were performed in a reductive direction [59], between +1.000 V *vs.* NHE to −0.600 V *vs.* NHE, at a scan rate of 5 mV s^{-1} [55]. The microbial electrochemical fuels were finally collected and introduced in serum bottles, previously deoxygenated with N_2 (100 %) to safeguard [60].

Redox Flow Cell characterization

Microbial electrochemical fuels from BESs were tested for the coupling purpose. For this, a RFC was assembled with a Nafion™ NM 117 PEM and 25 cm^2 carbon felt electrodes (Figure 2.1). The cell was loaded with negalyte 2,6-AQDSH_2 (microbial electrochemical fuels) and with posilyte $[Fe(CN)_6]^{3-}$. The RFC was tested with microbial electrochemical fuels of BES AP and BES Ω as negalyte, respectively. The posilyte was chemically prepared (40 mM of $[Fe(CN)_6]^{3-}$ pH = 7 in 0.10 M phosphate buffer aqueous solution). The aqueous solutions were introduced in

the respective external flasks. Argon (100 %) was flushed continuously to diminish oxidation of species on both reservoirs.

The charge-discharge curves studies were carried out using a Ec-Lab Potentiostat, BioLogic Scientific Instruments electrochemical workstation, and respective software, in a two-electrode galvanostatic configuration. The cycling measurements were conducted at default current densities of 20 mA cm^{-2} using the electrochemical station, between 0.1 V to 1 V [61]. Watson Marlow 101 U/R pumps to keep the electrolyte flow rate at 20 mL min^{-1} through the cycling measurements. The Coulombic Efficiency (CE, %), Potential Efficiency (PE) and Energy Efficiency (EE) were computed as described elsewhere [39].

2.3. Results and discussion

BES current density over time

The current densities over time for experimental setups BES AP and for BES Ω were calculated and the results are represented in Figure 2.2. [56]. BESs reactions (2.1. and 2.2.) and conditional potentials (an acetate oxidizing anode (acetate and bicarbonate concentration of 5 mM) and 20 mM AQDS in basal medium at 25 ºC and at pH = 7, achieved with the Nernst Equation) ([56, 62, 63]) are described below:

$C_2H_4O_2 + 2H_2O \rightarrow 2CO_2 + 8H^+ + 8e^-$ E^0_{oxd} = 0.289 V *vs.* NHE **2.1.**

$C_{14}H_6Na_2O_8S_2 + 2e^- + 2H^+ \rightarrow C_{14}H_8Na_2O_8S_2$ E^0_{red} =-0.184 V *vs.* NHE **2.2.**

The potential of -0.200 V *vs.* Ag/AgCl (3 M) is pointed in the literature as the ideal anode potential *for G. sulfurreducens* growth, regulating the activity and growth of bacteria to sustain a higher current and power generation [55]. In Figure 2.2A, the BES promoted maximum current density of 0.21 mA cm^{-2} at 88 h for BES AP 1. At this time, the BES AP 1 was ended, because the red dark color (2,6-$AQDSH_2$) was observed for more than 24 h. As for BES AP 2, the experiment promoted maximum current density of 0.19 mA cm^{-2} at 126 h, and the experiment was ended at 140 h.

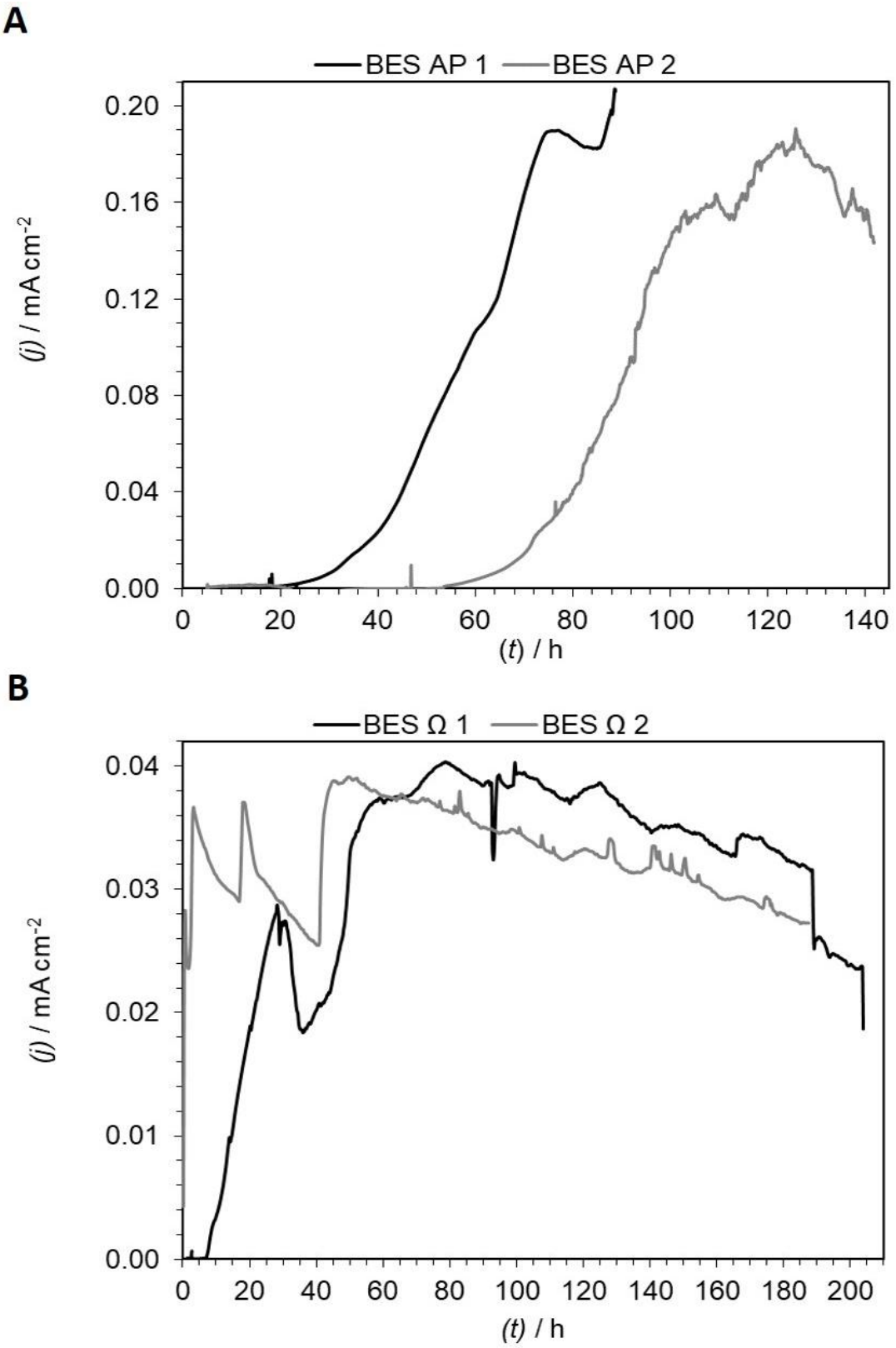


Figure 2.2. Current density over time for the BESs during bioelectrochemical reduction of 2,6-AQDS with (A) bias anode potential at -0.200 V *vs.* Ag/AgCl (3 M) (replicates BES AP 1 and BES AP 2) and in (B) BES closed with an electrical resistance load (500 Ω) (replicates BES Ω 1 and BES Ω 2).

The microbial lag phase in the BES AP 1 presented a smaller period of time, likened to the microbial lag phase of BES AP 2. The current generation is directly proportional to the anode biofilm growth [13]. This explains the differences in the total period of time between the two replicates. An applied potential enhances the growth rate of biofilms, resulting in a higher biocatalyst density, in faster starting up of the electricity generated and higher current generation [65]. The current densities reached in BES AP setup are similar to reported BESs with *G. sulfurreducens* as bioanode, when the same potential was applied [55, 64].

In Figure 2.2B are stated the results for BES Ω 1 and BES Ω 2; these were inferior to the results with the bias anode potential at - 0.200 V *vs.* Ag/AgCl (3 M). The maximum current density for the BES Ω 1 was 0.40 mA cm^{-2} at 59 h, as for BES Ω 2 was 0.39 mA cm^{-2} at 89 h. The experiments ended at *ca.* 210 h for BES Ω 1 and at *ca.* 185 h for BES Ω 2. The results were similar to reported values with *G. sulfurreducens* bioanodes using a 500 Ω [66, 67]. The use of electrical resistance to close the circuits in BES are responsible to modulate the anode availability as an electron donor. The electron flux through the closed circuit and the ratio between the cell potential and the current is measured [25, 26].

The results achieved indicate the reduction of 2,6-AQDS was reached using *G. sulfurreducens* as bioanode. Higher current densities were reached with an applied anode potential, due to the biofilm adaptation conditions promoted [55, 64]. Nevertheless, it was settled that 2,6-AQDS reduction to 2,6-AQDSH_2 was possible in BESs with an electrical resistance load (500 Ω), with color change as it gets charged. The experimental setup BES Ω conditions can be used for an unbiased energy storage device.

BES polarization and power curves

BESs performances with 2,6-AQDS as cathodic electron acceptor were analyzed with polarization and power curves determined at the end of each BES (Figure 2.3.).

The experimental setup BES AP, at stable phase of power generation, exhibit an OCP of 230 mV for BES AP 1 and 23 mV for BES AP 2 was measured. Maximum power densities for BES AP 1 were $1.0x10^{-4}$ mW cm^{-2} ($1.0x10^{-3}$ mA cm^{-2}) (Figure 2.3A), and for BES AP 2 was recorded 11.80 mW cm^{-2} ($5.4x10^{-4}$ mA cm^{-2}) (Figure 2.3B).

The results achieved were inferior to reported maximum power densities [32, 33], such as works with an applied potential and $[Fe(CN)_6]^{3-}$ as cathodic electron acceptor ($21x10^4$ mW cm^{-2}), as summarized in Table 2.1. The internal resistance was estimated for BES AP 1 (41.0 kΩ) and for BES AP 2 (4.6 kΩ). Lower internal resistances are responsible for the higher power densities [11].

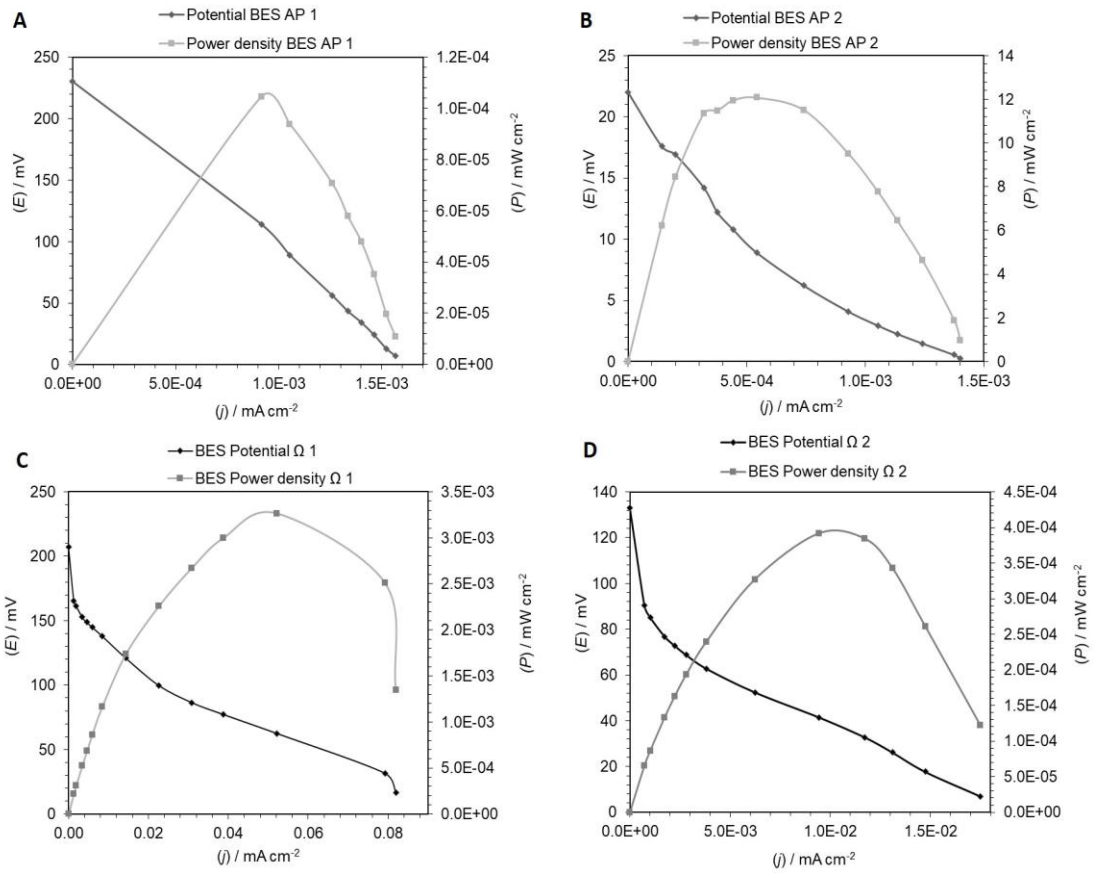


Figure 2.3. Polarization (black square) and power curves (triangle square) obtained for BESs with a bias anode potential at -0.200 V *vs.* Ag/AgCl (3 M) for the duplicate BES AP 1 (A) and for duplicate BES AP 2 (B). Polarization (black square) and power curves (triangle square) obtained for BESs closed with an electrical resistance (500 Ω) for BES Ω 1 (C) and for BES Ω 2 (D). The lines were added for readability.

For BES Ω experimental setup, at stable phase of power generation, an OCP of 207 mV for BES Ω 1 and 133 mV for BES Ω 2 were recorded. The maximum power density recorded for BES Ω 1 was $3.3x10^{-3}$ mW cm^{-2} (0.05 mA cm^{-2}) (Figure 2.3C) and for BES Ω 2 was $3.9x10^{-4}$ mW cm^{-2} (0.01 mA cm^{-2}) (Figure 2.3D). These values are related to the reported in the Table 2.1. [37], where works with an electrical resistance in the circuits promoted power densities in the same order of magnitude. Internal resistance was estimated for BES Ω 1 (3 MΩ) and for

BES AP 2 (1 MΩ). Polarization losses associated with bacterial metabolic losses are seen in BESs [68].

Cyclic Voltammetry of microbial electrochemical fuels

The cyclic voltamograms obtained at 5 mV s^{-1} for the microbial electrochemical fuels from BESs are observed in Figure 2.4.

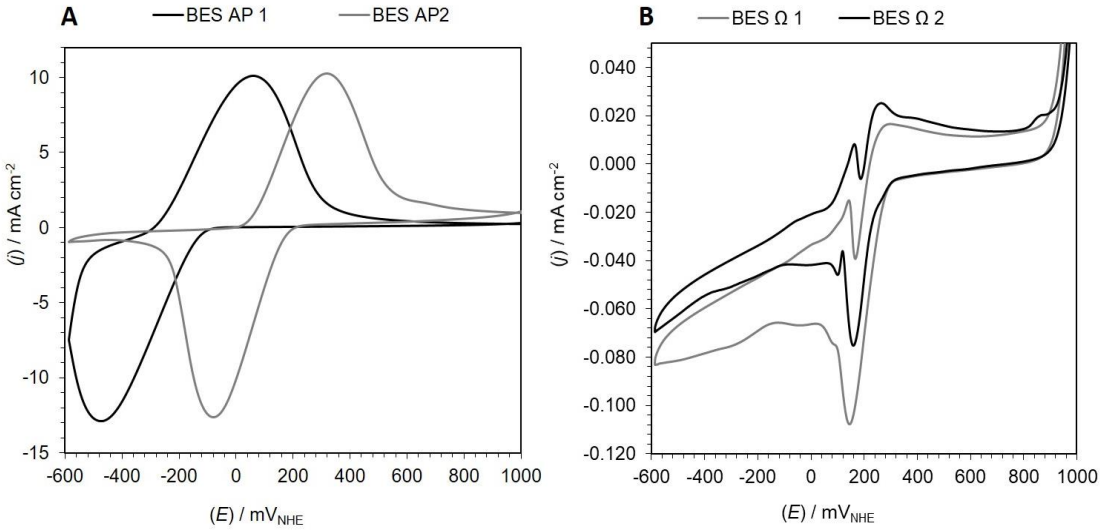


Figure 2.4. Cyclic voltammograms obtained at 5 mV s^{-1} for BESs with a bias potential at -0.200 V *vs.* Ag/AgCl (3 M) (BES AP 1 and BES AP 2) (A) and closed with an external resistance load of 500 Ω (BES Ω 1 and BES Ω 2) (B).

The CVs obtained for the microbial electrochemical fuels with bias potential at -0.200 V *vs.* Ag/AgCl (3 M) (Figure 2.4A) were similar to CVs previously reported [56, 69]. The quasi-reversible voltamograms were depicted for BES AP 1 and BES AP 2. The Formal Redox Potential ($E_{1/2}$) estimated in the CV of BES AP 1 was -188 mV and for BES AP 2 was 137 mV. The $E_{1/2}$ is specific to the experimental conditions employed, and the pH (pH = 7) of the microbial electrochemical fuels did not change during the reduction, and were similar to previous CVs reported by Cadena and coworkers (2007) [56].

The voltamograms obtained at 5 mV s^{-1} for the BESs with an electrical resistance (500 Ω) are similar to CV previously reported [59]. The $E_{1/2}$ in BES Ω 1 is 119 mV and the $E_{1/2}$ in BES Ω 2 is 166 mV. In Figure 2.4.B, separated redox waves were observed. As explained by Kim & Chung

(2014) [70], this occurs when quinones are reduced to Q^{2-} at a more negative potential, giving rise to two peaks [70].

Redox Flow Cell characterization

A cell was tested with negalyte 2,6-AQDSH_2 (microbial electrochemical fuels) and with posilyte $[Fe(CN)_6]^{3-}$. A nominal cell potential of 0.620 V was expected. The results were achieved by starting the RFC at the discharged mode. The charge–discharge curves over time for the RFC with 2,6-AQDSH_2 from the BES AP 1 as negalyte is presented in Figure 2.5A. The plotted results in Figure 2.5B indicated for 10 cycles were estimated at *ca.* 100 % CE, *ca.* 25 % EE and *ca.* 25 % PE. The OCP is directly related with the energy density it can provide [50].

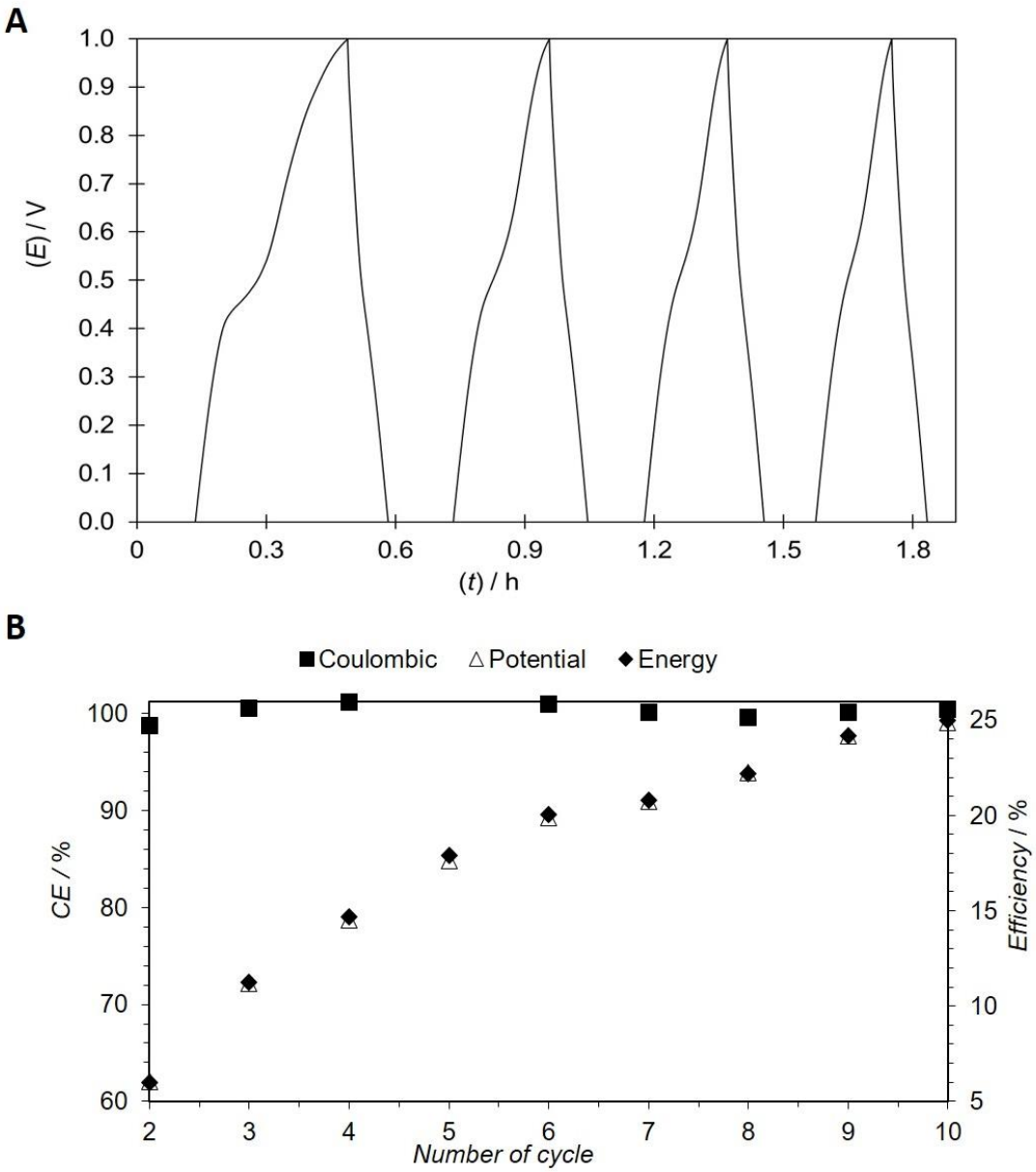


Figure 2.5. Charge–discharge curves versus time (A), Coulombic (black square), Potential (white triangle) and Energy efficiencies (black diamond) versus the cycle number (B) for RFC with 2,6-AQDSH$_2$ from the BES AP 1 as negalyte.

Figure 2.6A represents the charge–discharge curves over time of the RFC with 2,6-AQDSH$_2$ from the BES Ω 1 as negalyte. The OCP of RFC assembled was *ca.* 0.7 V. The plotted results in Figure 2.6B show 10 cycles estimated with *ca.* 100 % CE, *ca.* 76 % EE and *ca*. 73 % PE.

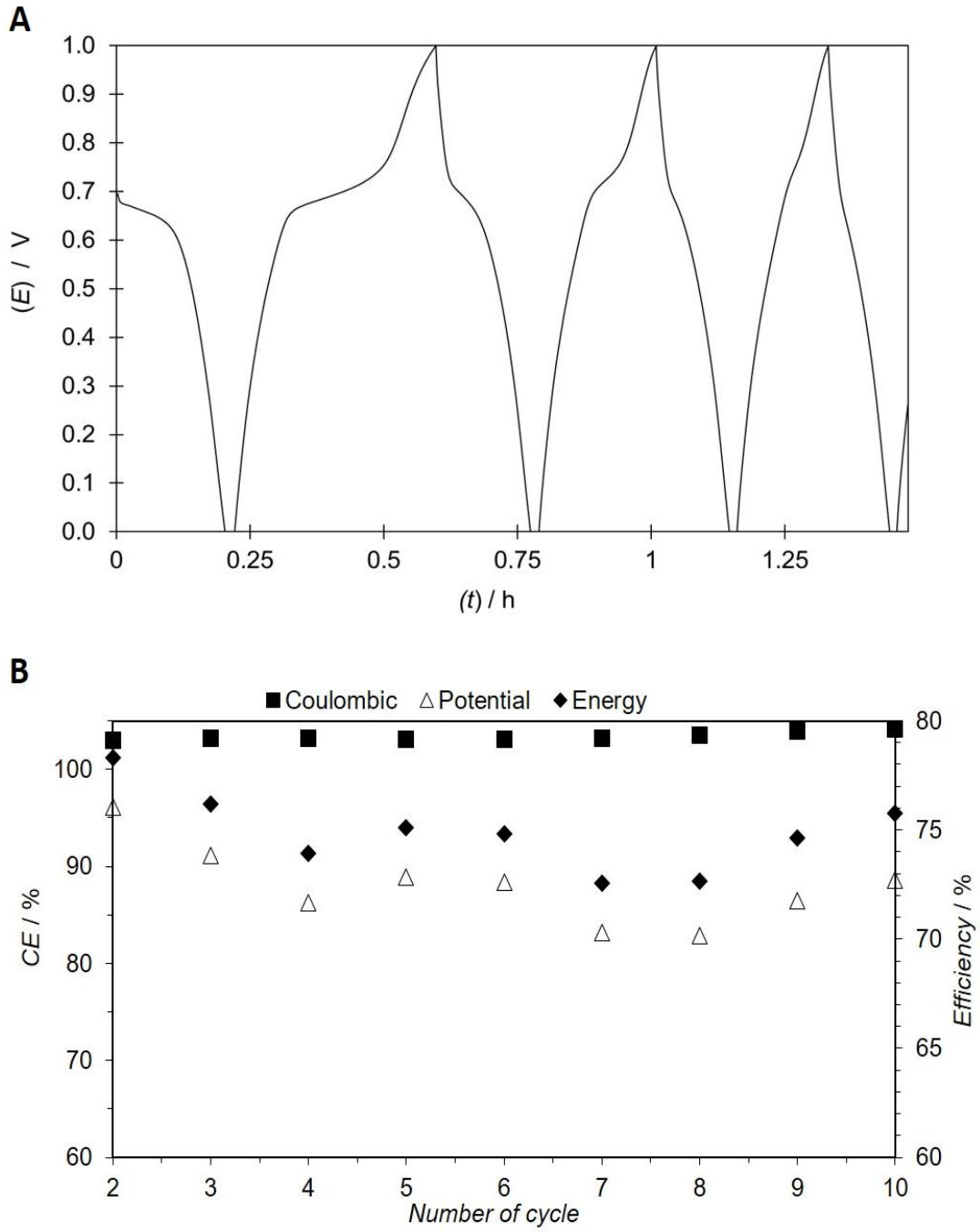


Figure 2.6. Charge–discharge curves versus time (A), Coulombic (black square), Potential (white triangle) and Energy efficiencies (black circle) versus the cycle number (B) for RFC with 2,6-AQDSH$_2$ from the BES Ω 1 as negalyte.

RFCs efficiencies results reached with bioelectrochemically charged 2,6-AQDSH$_2$ as negalyte were inferior to the efficiencies reported for anthraquinone/ferrocyanide Battery [71]. The results presented were the first results tested with microbial electrochemical fuels, that were discharged in the cell.

2.4. Conclusion

The bioelectrochemical conversion of 2,6-AQDS into 2,6-AQDSH_2 (microbial electrochemical fuel) in BESs was researched, and its role as negalyte was reported. The maximum current densities were reached in the BESs with an applied potential of -0.200 V *vs.* Ag/AgCl (3 M)) (BES AP experimental setup). A maximum current density of 0.21 mA cm^{-2} at 88 h for BES AP 1 was recorded. The maximum power densities were reached in the BESs closed with an external resistance load of 500 Ω (BES Ω 1 was $3.3x10^{-3}$ mW m^{-2} (0.05 mA cm^{-2}). The CVs of microbial electrochemical fuels were electrochemically reversible and were similar to CVs reported in the literature.

The BES Ω experimental setup results indicate that BESs closed with an external resistance load of 500 Ω was a viable choice for the bioelectrochemical conversion of 2,6-AQDS. The *G. sulfurreducens* was a capable biocatalyst for the promotion of microbial electrochemical fuels, with acetate consumption, with no bias potential applied.

The RFC assembled with the microbial electrochemical fuel 2,6-AQDSH_2 as negalyte and $[Fe(CN)_6]^{3-}$ as posilyte demonstrated that microbial electrochemical fuels are a viable redox pair for RFC operations.

2.5. Acknowledgements

M.S.S. Santos is grateful to Portuguese Foundation for Science and Technology (FCT) for her PhD grant (reference: SFRH/BD/104087/2014). J. Azevedo is grateful to the FCT for is Postdoctoral Grant (Reference: SFRH/BPD/116648/2016). The authors would like to acknowledge to the FCT under the scope of the strategic funding of UID/BIO/04469 unit and COMPETE 2020 (POCI-01-0145-FEDER-006684) and BioTecNorte operation (NORTE-01-0145-FEDER-000004) funded by the European Regional Development Fund (ERDF), under the scope of Norte2020 - Programa Operacional Regional do Norte. The authors also acknowledge the Projects: i) POCI-01-0145-FEDER-006939 (LEPABE - Laboratory for Process Engineering, Environment, Biotechnology and Energy – UID/EQU/00511/2013), funded by the ERDF, through COMPETE2020 – Programa Operacional Competitividade e Internacionalização (POCI) and by nationals funds through FCT, ii) by the Project SunStorage - Harvesting and

storage of solar energy", with reference POCI-01-0145-FEDER-016387, funded by ERDF, through COMPETE 2020-POCI), and by national funds, through FCT and iii) NORTE-01-0145-FEDER-000005 – LEPABE-2-ECO-INNOVATION, supported by North Portugal Regional Operational Programme (Norte 2020), under the Portugal 2020 Partnership Agreement, through the ERDF.

2.6. References

[1] D. Pant, A. Singh, G. Van Bogaert, S. Irving Olsen, P. Singh Nigam, L. Diels, K. Vanbroekhoven, Bio-Electrochemical Systems (BES) for sustainable energy production and product recovery from organic wastes and industrial wastewaters, RSC Adv. 2 (2012) 1248–1263.

[2] U. Schröder, F. Harnisch, Life electric—nature as a blueprint for the development of Microbial Electrochemical Technologies, Joule. 1 (2017) 244–252.

[3] S.K. Butti, G. Velvizhi, M.L.K. Sulonen, J.M. Haavisto, E. Oguz Koroglu, A. Yusuf Cetinkaya, S. Singh, D. Arya, J. Annie Modestra, K. Vamsi Krishna, A. Verma, B. Ozkaya, A.-M. Lakaniemi, J.A. Puhakka, S. Venkata Mohan, Microbial electrochemical technologies with the perspective of harnessing bioenergy: maneuvering towards upscaling, Renew. Sustain. Energy Rev. 53 (2016) 462–476.

[4] A. Nordin, Chemical elemental characteristics of biomass fuels, Biomass and Bioenergy. 6 (1994) 339–347.

[5] R. Karthikeyan, J. Xuan, M.K.H. Leung, Microbial Fuel Cell for Biomass Energy Conversion, in: Handb. Clean Energy Syst., John Wiley & Sons, Ltd, Chichester, UK (2015) 1–21.

[6] S.A. Patil, F. Harnisch, C. Koch, T. Hübschmann, I. Fetzer, A.A. Carmona-Martínez, S. Müller, U. Schröder, Electroactive mixed culture derived biofilms in Microbial Bio-Electrochemical Systems: The role of pH on biofilm formation, performance and composition, Bioresour. Technol. 102 (2011) 9683–9690.

[7] K. Rabaey, W. Verstraete, Microbial Fuel Cells: novel biotechnology for energy generation, Trends Biotechnol. 23 (2005) 291–298.

[8] T.C. Pannell, R.K. Goud, D.J. Schell, A.P. Borole, Effect of fed-batch *vs.* continuous mode of operation on Microbial Fuel Cell performance treating biorefinery wastewater, Biochem. Eng. J.

116 (2016) 85–94.

[9] S.G. Barbosa, L. Peixoto, A. ter Heijne, P. Kuntke, M.M. Alves, M.A. Pereira, Investigating bacterial community changes and organic substrate degradation in Microbial Fuel Cell operating on real human urine, Environ. Sci. Water Res. Technol. 3 (2017) 897–904.

[10] S.G. Barbosa, L. Peixoto, O.S.G.P. Soares, M.F.R. Pereira, A. ter Heijne, P. Kuntke, M.M. Alves, M.A. Pereira, Influence of carbon anode properties on performance and microbiome of Microbial Electrolysis Cells operated on urine, Electrochim. Acta. 267 (2018) 122–132.

[11] L. Peixoto, R. Nogueira, A. Brito, C. Póvoa, P. Kroff, P. Parpot, Electroactivity of *Geobacter sulfurreducens* evaluated by cyclic voltammetry, in: II Int. Conf. Environ. Ind. Appl. Microbiol. (BioMicroWorld 2007), 176.

[12] C. Koch, A. Kuchenbuch, J. Kretzschmar, H. Wedwitschka, J. Liebetrau, S. Müller, F. Harnisch, Coupling electric energy and biogas production in anaerobic digesters – impacts on the microbiome, RSC Adv. 5 (2015) 31329–31340.

[13] G. Reguera, K.P. Nevin, J.S. Nicoll, S.F. Covalla, T.L. Woodard, D.R. Lovley, Biofilm and nanowire production leads to increased current in *Geobacter sulfurreducens* Fuel Cells, Appl. Environ. Microbiol. 72 (2006) 7345–7348.

[14] K.P. Nevin, H. Richter, S.F. Covalla, J.P. Johnson, T.L. Woodard, A.L. Orloff, H. Jia, M. Zhang, D.R. Lovley, Power output and columbic efficiencies from biofilms of *Geobacter sulfurreducens* comparable to mixed community Microbial Fuel Cells, Environ. Microbiol. 10 (2008) 2505–2514.

[15] M.S. Kim, Y.J. Lee, Optimization of culture conditions and electricity generation using *Geobacter sulfurreducens* in a dual-chambered Microbial Fuel Cells, Int. J. Hydrogen Energy. 35 (2010) 13028–13034.

[16] A.M. Speers, G. Reguera, Electron donors supporting growth and electroactivity of *Geobacter sulfurreducens* anode biofilms, Appl. Environ. Microbiol. 78 (2012) 437–444.

[17] M.-S. Kim, J. Cha, D.-H. Kim, Enhancing factors of electricity generation in Microbial Fuel Cell using *Geobacter sulfurreducens*., J. Microbiol. Biotechnol. 22 (2012) 1395–400.

[18] G. Martins, L. Peixoto, D.C. Ribeiro, P. Parpot, A.G. Brito, R. Nogueira, Towards implementation of a Benthic Microbial Fuel Cell in lake Furnas (Azores): phylogenetic affiliation and electrochemical activity of sediment bacteria, Bioelectrochemistry. 78 (2010) 67–71.

[19] B.E. Logan, Microbial Fuel Cells, John Wiley & Sons, Inc., Hoboken, NJ, USA, 2007.

[20] G. Nöll, G. Hauska, P. Hegemann, K. Lanzl, T. Nöll, M. Von Sanden-flohe, B. Dick, C.W.V. Gmbh, C. Kgaa, T. Nöll, M. von Sanden-Flohe, B. Dick, Redox properties of LOV domains : chemical versus photochemical reduction, and influence on the photocycle, ChemBioChem. 8 (2007) 2256–2264.

[21] B.R. Ringeisen, E. Henderson, P.K. Wu, J. Pietron, R. Ray, B. Little, J.C. Biffinger, J.M. Jones-Meehan, High power density from a miniature Microbial Fuel Cell using *Shewanella oneidensis* DSP10, Environ. Sci. Technol. 40 (2006) 2629–2634.

[22] A. Orita, M.G. Verde, M. Sakai, Y.S. Meng, A biomimetic Redox Fow Battery based on flavin mononucleotide, Nat. Commun. 7 (2016) 1–8.

[23] B. Yang, L. Hoober-Burkhardt, S. Krishnamoorthy, A. Murali, G.K.S. Prakash, S.R. Narayanan, High-Performance aqueous organic flow battery with quinone-based redox couples at both electrodes, J. Electrochem. Soc. 163 (2016) 1442–1449.

[24] M. Sun, L.-F. Zhai, W.-W. Li, H.-Q. Yu, Harvest and utilization of chemical energy in wastes by Microbial Fuel Cells, Chem. Soc. Rev. 45 (2016) 2847–2870.

[25] A. González del Campo, P. Cañizares, J. Lobato, M. Rodrigo, F.J. Fernandez Morales, Effects of external resistance on Microbial Fuel Cell's performance, in: E.J. and B.C. (eds. G. Lefebvre (Ed.), Environ. Energy Clim. Chang. II Energies from New Resour. Clim. Chang., Springer International Publishing (2014) 175–197.

[26] S. Jung, J.M. Regan, Influence of external resistance on electrogenesis, methanogenesis and anode prokaryotic communities in Microbial Fuel Cells, Appl. Environ. Microbiol. 77 (2011) 564–571.

[27] D. Ucar, Y. Zhang, I. Angelidaki, An overview of electron acceptors in Microbial Fuel Cells, Front. Microbiol. 8 (2017) 1–14.

[28] K. Rabaey, S.T. Read, P. Clauwaert, S. Freguia, P.L. Bond, L.L. Blackall, J. Keller, Cathodic oxygen reduction catalyzed by bacteria in Microbial Fuel Cells, ISME J. 21 (2008) 519–527.

[29] X.I.N. Wang, S. Cheng, Use of carbon mesh anodes and the effect of different pretreatment methods on power production in Microbial Fuel Cells, 43 (2009) 6870–6874.

[30] S. Oh, B. Min, Cathode performance as a factor in electricity generation in Microbial Fuel

Cells, 38 (2004) 4900–4904.

[31] D.H. Park, J.G. Zeikus, Improved Fuel Cell and electrode designs for producing electricity from microbial degradation, Biotechnol. Bioeng. 81 (2003) 348–355.

[32] C.H. Wu, C.Y. Lai, C.W. Lin, M.H. Kao, Generation of power by Microbial Fuel Cell with ferricyanide in biodegradation of benzene, Clean - Soil, Air, Water. 41 (2013) 390–395.

[33] J. Li, Q. Fu, Q. Liao, X. Zhu, D. ding Ye, X. Tian, Persulfate: A self-activated cathodic electron acceptor for Microbial Fuel Cells, J. Power Sources. 194 (2009) 269–274.

[34] O. Lefebvre, A. Al-Mamun, H.Y. Ng, A Microbial Fuel Cell equipped with a biocathode for organic removal and denitrification, Water Sci. Technol. 58 (2008) 881–885.

[35] S. You, Q. Zhao, J. Zhang, J. Jiang, S. Zhao, A Microbial Fuel Cell using permanganate as the cathodic electron acceptor, J. Power Sources. 162 (2006) 1409–1415.

[36] A. Rhoads, H. Beyenal, Z. Lewandowski, Microbial Fuel Cell using anaerobic respiration as an anodic reaction and biomineralized manganese as a cathodic reactant, Environ. Sci. Technol. 39 (2005) 4666–4671.

[37] D. Ucar, Y. Zhang, I. Angelidaki, An overview of electron acceptors in Microbial Fuel Cells, Front. Microbiol. 8 (2017) 1–14.

[38] Z. Wang, B. Lim, C. Choi, Removal of Hg^{2+} as an electron acceptor coupled with power generation using a Microbial Fuel Cell, Bioresour. Technol. 102 (2011) 6304–6307.

[39] A. ter Heijne, H.V.M. Hamelers, V. De Wilde, R.A. Rozendal, C.J.N. Buisman, A bipolar membrane combined with ferric iron reduction as an efficient cathode system Microbial Fuel Cells, Environ. Sci. Technol. 40 (2006) 5200–5205.

[40] A. ter Heijne, F. Liu, R. Van Der Weijden, J. Wenjma, C.J.N. Buisman, H.V.M. Hamelers, Copper recovery combined with electricity production in a Microbial Fuel Cell, Environ. Sci. Technol. 44 (2010) 4376–4381.

[41] G. Wang, L. Huang, Y. Zhang, Cathodic reduction of hexavalent chromium [Cr(VI)] coupled with electricity generation in Microbial Fuel Cells, Biotechnol. Lett. 30 (2008) 1959–1966.

[42] X. Cao, X. Huang, P. Liang, N. Boon, M. Fan, L. Zhang, X. Zhang, A completely anoxic Microbial Fuel Cell using a photo-biocathode for cathodic carbon dioxide reduction, Energy Environ. Sci. 2 (2009) 498–501.

[43] B. Zhang, H. Zhao, C. Shi, S. Zhou, J. Ni, Simultaneous removal of sulfide and organics

with vanadium (V) reduction in Microbial Fuel Cells, J. Chem. Technol. Biotechnol. 84 (2009) 1780–1786.

[44] B. Zhang, C. Tian, Y. Liu, L. Hao, Y. Liu, C. Feng, Y. Liu, Z. Wang, Simultaneous microbial and electrochemical reductions of vanadium (V) with bioelectricity generation in Microbial Fuel Cells, Bioresour. Technol. 179 (2015) 91–97.

[45] D. Cecconet, A. Callegari, A.G. Capodaglio, Bio-Electrochemical Systems for removal of selected metals and perchlorate from groundwater: A review, Energies. 11 (2018) 1–21.

[46] J.S. Deutzmann, A.M. Spormann, Enhanced microbial electrosynthesis by using defined co-cultures, ISME J. 11 (2017) 704–714.

[47] X. Xie, M. Ye, P.-C. Hsu, N. Liu, C.S. Criddle, Y. Cui, Microbial Battery for efficient energy recovery, Proc. Natl. Acad. Sci. 110 (2013) 15925–15930.

[48] S.D. Molenaar, A.R. Mol, T.H.J.A. Sleutels, A. ter Heijne, C.J.N. Buisman, A. Heijne, Microbial Rechargeable Battery: energy storage and recovery through acetate, Environ. Sci. Technol. Lett. 3 (2016) 144–149.

[49] K. Wedege, J. Azevedo, A. Khataee, A. Bentien, A. Mendes, Direct solar charging of an organic-inorganic, stable, and aqueous alkaline Redox Flow Battery with a hematite photoanode, Angew. Chemie Int. Ed. 55 (2016) 7142–7147.

[50] J. Azevedo, T. Seipp, J. Burfeind, C. Sousa, A. Bentien, J.P. Araújo, A. Mendes, Unbiased solar energy storage: Photoelectrochemical Redox Flow Battery, Nano Energy. 22 (2016) 396–405.

[51] G.L. Soloveichik, Flow Batteries: current status and trends, Chem. Rev. 115 (2015) 11533–11558.

[52] G. Yu, S. Peng, C. Zhang, Y. Zhao, Y. Ding, X. Guo, G. He, L. Zhang, Progress and prospects of next-generation Redox Flow Batteries, Energy Storage Mater. 15 (2018) 324–350.

[53] X. Huang, M.-Z. Fan, C. Wang, P. Liang, X.-X. Cao, Composition and distribution of internal resistance in three types of Microbial Fuel Cells, Appl. Microbiol. Biotechnol. 77 (2007) 551–558.

[54] J.M. Bruce, Light-induced reactions of quinones, Q. Rev. Chem. Soc. 21 (1967) 405–428.

[55] P. Aelterman, S. Freguia, J. Keller, W. Verstraete, K. Rabaey, The anode potential regulates bacterial activity in Microbial Fuel Cells, Appl. Microbiol. Biotechnol. 78 (2008) 409–

418.

[56] A. Cadena, A.–C. Texier, I. González, F.J. Cervantes, J. Gómez, Qualitative and quantitative determination of a humic model compound in microbial cultures by cyclic voltammetry, Environ. Technol. 28 (2007) 1035–1044.

[57] C. Liu, J.M. Zachara, N.S. Foster, J. Strickland, Kinetics of reductive dissolution of hematite by bioreduced anthraquinone-2,6-disulfonate, Environ. Sci. Technol. 41 (2007) 7730–7735.

[58] L. Peixoto, A.L. Rodrigues, G. Martins, A. Nicolau, A.G. Brito, M.M. Silva, P. Parpot, R. Nogueira, A flat Microbial Fuel Cell for decentralized wastewater valorization: process performance and optimization potential, Environ. Technol. 34 (2013) 1947–1956.

[59] C. Batchelor-mcauley, Q. Li, S.M. Dapin, R.G. Compton, Voltammetric characterization of DNA Iintercalators across the full pH range : anthraquinone-2,6-disulfonate and anthraquinone-2-sulfonate, J. Phys. Chem. B. 114 (2010) 4094–4100.

[60] I.C. Clark, H.K. Carlson, A.T. Iavarone, J.D. Coates, Bioelectrical redox cycling of anthraquinone-2,6-disulfonate coupled to perchlorate reduction, Energy Environ. Sci. 5 (2012) 7970–7978.

[61] C.P. de León, A. Frías-Ferrer, J. González-García, D.A. Szánto, F.C. Walsh, Redox Flow Cells for energy conversion, J. Power Sources. 160 (2006) 716–732.

[62] K. Rabaey, R.A. Rozendal, Microbial Electrosynthesis - revisiting the electrical route for microbial production., Nat. Rev. Microbiol. 8 (2010) 706–716.

[63] S. Orsetti, C. Laskov, S.B. Haderlein, Electron transfer between iron minerals and quinones estimating the reduction potential of the Fe(II)-goethite surface from AQDS Speciation, Environ. Sci. Technol. 47 (2013) 1–6.

[64] S.T. Read, P. Dutta, P.L. Bond, J. Keller, K. Rabaey, Initial development and structure of biofilms on Microbial Fuel Cell anodes., BMC Microbiol. 10 (2010) 1–10.

[65] P. Aelterman, S. Freguia, J. Keller, The anode potential regulates bacterial activity in Microbial Fuel Cells, Appl Microbiol Biotechno. 78 (2008) 409–418.

[66] J. Wei, P. Liang, X. Cao, X.I.A. Huang, A new insight into potential regulation on growth and power generation of *Geobacter sulfurreducens* in Microbial Fuel Cells based on energy viewpoint, Environ. Sci. Technol. 44 (2010) 3187–3191.

[67] D.R. Bond, D.R. Lovley, Electricity Production *by Geobacter sulfurreducens* attached to

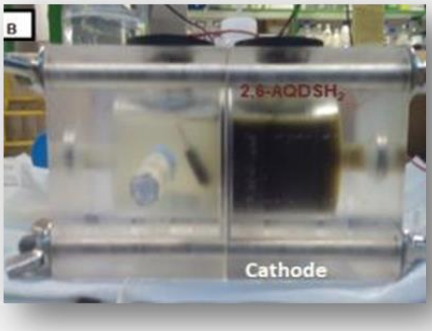
electrodes, Appl. Environ. Microbiol. 69 (2003) 1548–1555.

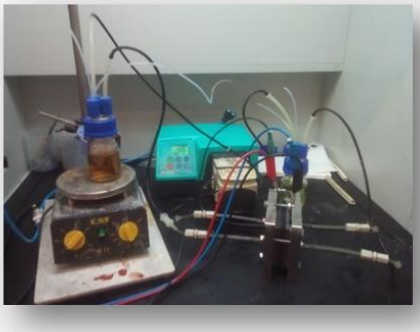
[68] K. Scott, E.H. Yu, Microbial Electrochemical and Fuel Cells: Fundamentals and applications, Elsevier, 2016.

[69] A.W. Bott, Characterization of chemical reactions coupled to electron transfer reactions using cyclic voltammetry, Curr. Sep. 18 (1999) 9–16.

[70] R.S. Kim, T.D. Chung, The electrochemical reaction mechanism and applications of quinones, Bull. Korean Chem. Soc. 35 (2014) 3143–3155.

[71] K. Lin, Q. Chen, M.R. Gerhardt, L. Tong, S.B. Kim, L. Eisenach, A.W. Valle, D. Hardee, R.G. Gordon, M.J. Aziz, M.P. Marshak, Alkaline Quinone Flow Battery, Science (80) 349 (2015) 1529–1532.





Chapter 3

Microbial electrochemical fuel

for energy storage in a Redox Flow Cell

Abstract[1]

A Bioelectrochemical System (BES) is used for charging an electrochemical fuel to be used in a Redox Flow Cell (RFC), demonstrating the first proof of concept of a microbial electrochemical fuel. *Geobacter sulfurreducens*, electroactive bacteria, was used to charge anthraquinone-2,6-disulfonate (2,6-AQDS) producing current densities of *ca.* 0.02-0.05 mA cm^{-2} and maximum power densities of *ca.* 0.03 mW cm^{-2}. The microbial electrochemical fuel and ferricyanide ($[Fe(CN)_6]^{3-}$) were introduced in a RFC producing a potential difference of 0.620 V, with a *ca.* 80 % energy conversion efficiency. The use of a BES for charging the posilyte of a RFC is now envisioned. The bio-conversion of waste biomass energy into electrochemical fuels (microbial electrochemical fuel for negalyte and posilyte) for later use in a RFC to produce electricity is a promising approach of converting biomass into storable and easy to use energy.

.

[1]The work presented in this chapter corresponds to the following scientific article: **M.S.S. Santos**, L. Peixoto, J. Azevedo, R.A.R. Monteiro, C. Dias-Ferreira, M.M. Alves, A. Mendes, Microbially-charged electrochemical fuel for energy storage in a Redox Flow Cell, J. Power Sources. 445 (2020) 1–10.

Chapter 3

3.1. Introduction

For making renewable energy, such as solar electricity, dispatchable, it is necessary to use energy storage systems [1]. Despite the advantage of conventional batteries and supercapacitors to store and making available energy with a very high round-trip-efficiency, their energy density is still quite low when compared with the high-energy density displayed by fuels. Redox Flow Cells (RFCs) are an electrochemical storage technology where energy is stored in soluble redox pairs [1, 2]. The soluble redox pairs introduced in external tanks and pumped into the cell, where the redox reactions take place, is the feature that allows setting power and energy capacity independently; power is determined by the stack size and energy by the volume of the electrolytes. Also, the design of RFC offers fast diffusion of both redox pairs and charge carriers in the electrolyte [3].

The best known RFCs technologies use aqueous solutions of vanadium and sulfuric acid and are used for stationary applications competing favorably with lithium based batteries [4, 5]. Ion metals such as vanadium [6, 7], chromium [8], iron [9], zinc [10] and other simple inorganic compounds and metal complexes [10, 11] have been studied for RFC; recently introduced organic redox species are a step forward for use in RFC since they can be produced from renewable sources, are stable and show reversible redox reaction [12], good redox potential windows, high flexibility, tunability and solubilities [13]. Among the different choices for organic RFCs redox couples, quinones have recently been proposed as promising for their low cost [12–15]. These compounds exhibit reversible redox reactions: quinones are reduced to the respective hydroquinones forms [16], and these redox reactions are explored to charge and discharge RFCs [11], with inorganic compounds such as bromide [17] or ferricyanide ($[Fe(CN)_6]^{3-}$) [18] as redox couples. Also, the non-aqueous solvents are more expensive than water and may raise safety and environmental issues [3].

Energy efficiencies of 90 % were reported for vanadium RFCs [19,20], lithium RFCs [21,22] or organic RFCs [23–25]. In the all-vanadium RFCs, power density of *ca*. 9.0×10^3 mW cm^{-2} was reported [26] while for quinone-based RFCs this value is *ca.* 1.0×10^2 mW cm^{-2} [25, 27] (Figure 3.1).

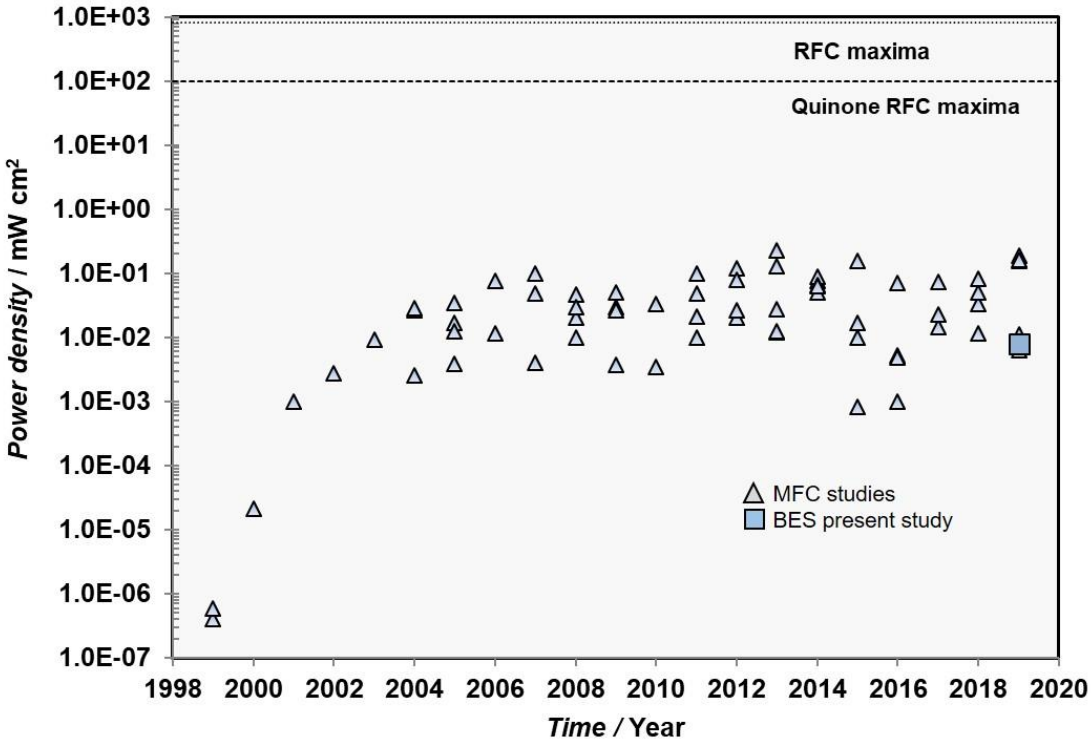


Figure 3.1. Power densities reported for BES (normalized to electrode-projected surface areas) and power density of MFC for the conversion of microbially-charged electrochemical fuel (BES of the present study) (adapted from [69]).

The use of quinones in organic RFCs is safer than the use of metals, like vanadium, that exhibit some toxicity [28, 29]. Some studies reported the use of anthraquinones in RFCs [30]; the first organic–inorganic aqueous flow cell used anthraquinone-2,7-disulfonate and bromine (Br_2/HBr) as redox pairs [24]. This quinone was also used in the development of a solar Redox Flow Cell [31, 32]; this device converts the solar energy in storable electrochemical energy, easily converted in electrical energy. Anthraquinone-2,6-disulfonate (2,6-AQDS) and benzoquinone-1,3-disulfonate were studied as redox species in RFC with bromine [25, 33]; 2,6-AQDS coupled with $[Fe(CN)_6]^{3-}$ a fast redox couple can be used to operate a RFC.

Bioelectrochemical systems (BESs) are systems capable of converting chemical energy into electricity or hydrogen/chemical products [34, 35]. A basic configuration of a BES is the Microbial Fuel Cell (MFC) that generates electrons through the conversion of organic biodegradable compounds by electroactive bacteria [36]. When these electrons migrate from the anode to the cathode in a MFC, there is a direct production of electricity [37, 38]. In a broader sense, BES include many more configurations and have been demonstrated in several applications and configurations, such as in energy production coupled to wastewater treatment

[39, 40], synthesis of hydrogen in Microbial Electrolysis Cells [41, 42], synthesis of methane [43, 44] or other biochemical products (*e.g.* 1,3-propanediol) in Microbial Electrosynthesis Cell [45] or water treatment such as in Microbial Desalination Cells [46]. BES are expected to play an important role in small and onsite applications such as biosensors and automatisms [47, 48], in situ bioremediation [49] and wastewater treatment [50, 51]. BES are also promising as the core technology in bioeletrorefineries including biofuels production [52].

One of the critical limitations of BESs is their low cell potential output, which is not suitable for practical applications [53]. During the initial development of BES, there was an exponential increase in power densities. This trend ended around 2007 when power densities tended to stabilize around $1.0x10^{-2}$ mW cm^{-2} [54-67] (Figure 3.1.). This tendency was due to the initial focus on the optimization of configurations and electrode materials, which, when optimized, led to the search for new applications for this technology to the detriment of improvements in the generated power. Nowadays, BESs has been coupled with others electrochemical devices, such as photo-driven coupling systems [68], or energy-harvesting circuits and BESs coupled-power management systems [53] to improve cell potential without reversal.

BES can also be used for charging redox pairs, which can be fed in a RFC for efficiently converting the stored electrochemical energy (microbial electrochemical fuel) into electricity. Several redox pairs suitable for working in alkaline or in acid media and exhibiting quasi continuous redox potentials and potential differences are available [52]. This allows choosing the best suited redox pair and operating conditions for a given microorganism that permits the electrochemical conversion of these redox pairs in BES and their use in RFC without bias potential applied. This flexibility is not observed in Microbial Electrolysis Cells, where the electrode potentials and potential difference are set from the beginning [54]. The bioelectrochemical conversion of redox pairs in BES for electrical energy storage purposes has not been explored, so far.

In this work 2,6-AQDS was converted in a BES forming a microbial electrochemical fuel which, together with electrochemically charged posilyte $[Fe(CN)_6]^{3-}$ were supplied to a RFC for producing electricity. This work also demonstrates the feasibility of coupling a BES with a RFC for making a Microbial Redox Flow Cell (Figure 3.2). This new approach is a proof of concept of bioelectrochemical energy storage for easily producing electricity in a RFC.

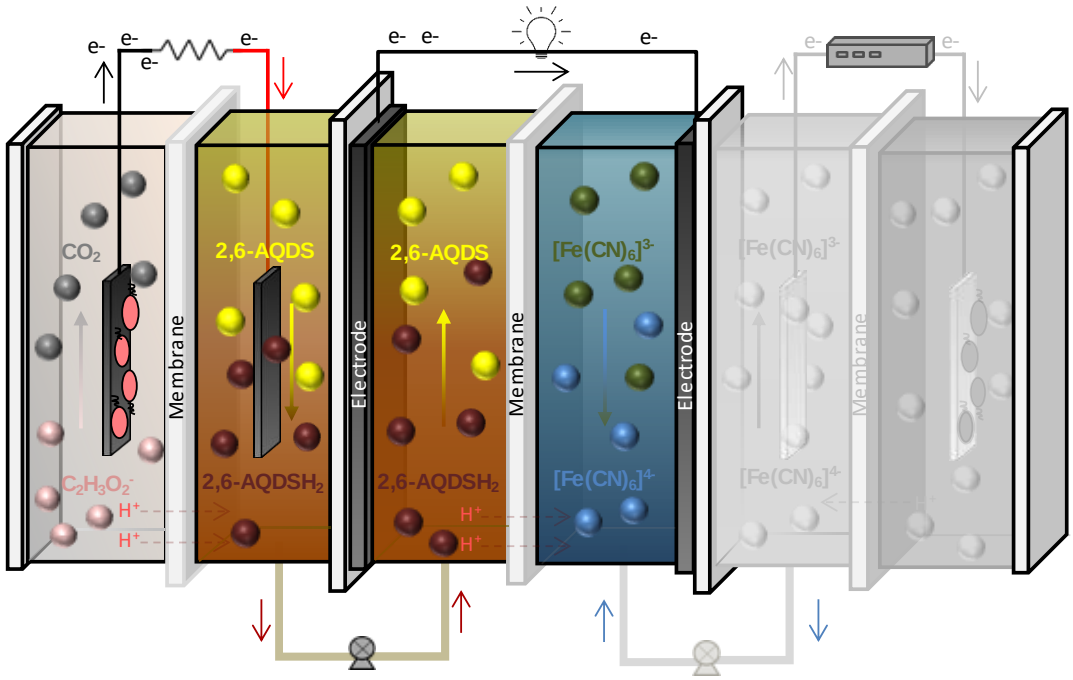


Figure 3.2. Diagram of the proposed Microbial Redox Flow Cell: BES (at the left) for the direct charge of the negalyte (2,6-AQDS→2,6-AQDSH$_2$), coupled with a RFC (2,6-AQDS||[Fe(CN)$_6$]$^{4-}$). On the right side, a second BES (in grey, not reported) is set for charging the posilyte of the RFC.

3.2. Material and methods

Chemicals and materials

The chemicals used in this study were of analytical grade from Sigma Aldrich; the water used was purified using a Milli-Q® Integral Water Purification system. The anthraquinone-2,6-disulfonate (2,6-AQDS; $C_{14}H_6Na_2O_8S_2$) was used as purchased. The Nafion™NM 117 Proton Exchange Membrane (PEM) and carbon felt electrodes were acquired from Quintech. For the RFC carbon felt GFD4.6 EA from SGL was purchased.

Bacteria's strains and culture conditions

Geobacter sulfurreducens (DSM 12127) was cultivated at 30 °C and 150 rpm until exponential growth phase in the Geobacter medium 826 (adapted from DSMZ). This medium was prepared with 1.50 g L^{-1} NH_4Cl, 0.60 g L^{-1} Na_2HPO_4, 0.10 g L^{-1} KCl, 10 mL L^{-1} of the trace element solution and 1 mL L^{-1} selenite-tungstate solution. The trace element and the selenite-tungstate solutions were from stock solutions prepared and reserved in sterile glass bottles at 4 °C. The

trace element solution contains: 1.50 g L^{-1} nitrilotriacetic acid, 3.00 g L^{-1} $MgSO_4 \cdot 7H_2O$, 0.50 g L^{-1} $MnSO_4 \cdot 7H_2O$, 1.00 g L^{-1} NaCl, 0.10 g L^{-1} $FeSO_4 \cdot 7H_2O$, 0.18 g L^{-1} $CoSO_4 \cdot 7H_2O$, 0.10 g L^{-1} $CaCl \cdot 2H_2O$, 0.18 g L^{-1} $ZnSO_4 \cdot 7H_2O$, 0.01 g L^{-1} $CuSO_4 \cdot 5H_2O$, 0.02 g L^{-1} $KAl(SO_4)_2 \cdot 12H_2O$, 0.01 g L^{-1} H_3BO_3, 0.01 g L^{-1} $Na_2MoO_4 \cdot 2H_2O$, 0.03 g L^{-1} $NiCl_2 \cdot 6H_2O$, 0.0003 g L^{-1} $Na_2SeO_3 \cdot 5H_2O$. The selenite-tungstate solution was prepared with 0.50 g L^{-1} NaOH, 0.003 g L^{-1} $Na_2SeO_3 \cdot 5H_2O$ and 0.004 g L^{-1} $Na_2WO_4 \cdot 2H_2O$. The medium was boiled and cooled down with ice until room temperature while deaerated with a stream of N_2:CO_2 (80 %:20 %). After cooling down, 2.50 g L^{-1} of $NaHCO_3$ was dissolved in the medium, with the gas mixture flowing, for buffering it at pH = 6.8.

Then the medium was divided in culture bottles (50 mL each) and covered with rubber caps and aluminum caps. Afterwards, the headspace of the culture bottles was flushed with N_2:CO_2 (80 %:20 %) gas mixture for removing the headspace air; the pressure was controlled using a manifold system connected to a vacuum and compressor systems. Finally, the medium was autoclaved (121 °C, 21 min).

Before inoculation with 10 % of *G. sulfurreducens*, 5 mL L^{-1} of the trace vitamin solution was added to the culture bottles. The vitamin solution was prepared and stored as the other stock solutions and contains 4.00 mg L^{-1} biotin, 4.00 mg L^{-1} folic acid, 20.00 mg L^{-1} pyridoxine-HCl, 10.00 mg L^{-1} thiamine-$HCl \cdot H_2O$, 10.00 mg L^{-1} riboflavin, 10.00 mg L^{-1} nicotinic acid, 10.00 mg L^{-1} D-Ca-pantothenate, 0.20 mg L^{-1} vitamin B12, 10.00 mg L^{-1} p-aminobenzoic acid, 10.00 mg L^{-1} lipoic acid. *G. sulfurreducens* is capable to oxidize different organic compounds like acetate, fumarate, or other carbon sources [57, 59, 70]. Na-acetate and Na_2-fumarate were also added. Na-acetate served as carbon source and electron donor and Na_2-fumarate served as electron receptor [60, 61]. The Na-acetate and Na_2-fumarate were previously prepared, filtered with a sterilized filter (0.22 µm) and stored at 4 °C in sterile conditions and were used as final concentration of 1.64 g L^{-1} and 8.00 g L^{-1} in the culture bottles, respectively.

BESs setup and experimental conditions

BESs made of transparent acrylic were used, as represented in Figure 3.2. The anode and cathode chambers were built with a volume of 50 cm^3 each. Between the chambers, a Nafion™ NM 117 PEM was tightened. The membrane was previously regenerated with 10 % H_2SO_4, during 3 h at 40 °C and rinsed several times with Milli-Q® water. Two carbon felt electrodes (0.1 x 4 cm^2) were electrically connected to two electrical wires held using carbon cement (Leit-C, Sigma Aldrich). They were connected using a resistor (500 Ω).

Anode and cathode containers were washed with chloramine and rinsed several times with Milli-Q® water to remove sources of microbial contamination, and the BESs were assembled in a laminar flux chamber. Geobacter medium and bacteria *G. sulfurreducens* (10 %) were introduced in the anode chamber using sterile syringes. Cathode chamber was filled with 20 mM 2,6-AQDS prepared in buffer solution (0.10 M sodium phosphate buffer solution, pH = 7). The BESs in the end was flushed with a gas mixture of N_2:CO_2 (80 %:20 %) using sterile filters to guarantee anaerobic conditions.

Two BESs experiments were run. In both cases the anode chamber was stirred using a stirring plate and the BES were kept at room temperature. In the first experiment (BES A), the 2,6-AQDS reduction was identified by visual color change, as seen in previous report [71]. The BES operated in three consecutive time series stages (series I, II, III) to assess the biofilm's capacity for bioelectricity production while observing the color change of the redox conversion (reduction of 2,6-AQDS). The 2,6-AQDS solution was refreshed when the color red was persistent for more than 24 h and the current density decreased. In BES A experiment, acetate (20 mM) was added at the time zero and every 3 days to minimize carbon source limitations, so that the maximum current densities (j, mA cm^{-2}) during time (t, h) could be reached.

In the second experiment (BES B), two BESs (BES B1 and BES B2) were operated in parallel as duplicates in order to estimate Coulombic Efficiency (CE) of BES operation and to quantify the 2,6-$AQDSH_2$ concentrations in the end of the experiment.

UV-Vis Spectrophotometry analyses were performed as follows: samples were taken from the anode chamber to evaluate the microbial growth by Optical Density (OD) at 600 nm (OD_{600}) at the initial and at final time of the experiment and read in a spectrophotometer DR 2800 (Hach Lange, Düsseldorf, Germany). Acetate consumption over time was measured to calculate CE of

the system. The concentration of acetate present in the anode chamber of BESs was analyzed by High-Performance Liquid Chromatography (Jasco, Japan) using a UV detector (210 nm) and a Chrompack column (6.5 x 30 mm^2) at 60 °C, where sulphuric acid (0.50 mol L^{-1}) as mobile phase was used at a flow rate of 0.60 mL min^{-1}.

The electrochemical fuel (microbial electrochemical fuel) reduced in the cathode chamber was collected at the end of the trials, and immediately introduced in a serum vial previously washed with N_2 (100 %) and moved to an anaerobic chamber for UV-Vis spectrophotometry analyses, as described in the UV-Vis spectrophotometry section. All experiments were performed sheltered to minimize light induced redox reactions. In the end of all assays, the polarization and power curves were performed.

BESs electrochemical characterization

The open circuit potential (OCP) of the BESs was measured using a multimeter (HP Hewlett Packard 34401A multimeter). It should be emphasized that no bias potential was applied during this experiment. The potential difference between the anode and cathode (*E*, mV) was recorded using an Ecograph T data logger (RSG 30 Endress+Hauser B.V., Naarden). The polarization and power curves were performed using a series of resistances ranging between 31 kΩ to 10 Ω [47]. The maximum power density (*P*, mW cm^{-2}) is calculated as indicated in literature [37].

The CE (η_{cb}, %) is the recovery of electrons, defined as the fraction of electrons recovered as current versus the organic matter depletion; the oxidation of the substrate occurs with the removal of electrons, with the moles defined of each substrate based on writing out a half reaction [65]. The CE is described in 3.1:

$$\eta_{cb} = \frac{M\int_0^t Idt}{FzV_{an}\Delta C} \qquad \textbf{3.1.}$$

where the integral of the current (*I*) over time (*dt*) is determined; *M* is the molecular mass of the substrate (g mol^{-1}) (acetate), *F* is the Faraday's constant (A mol^{-1}), V_{An} is the volume of liquid in

the anode compartment (L), *z* is the number of electrons exchanged per mol of substrate and Δ*C* is the change of substrate concentration (g L^{-1}) over the batch cycle.

Cyclic Voltammetry

Cyclic Voltammetry (CV) of culture medium of *G. sulfurreducens* was performed using BES as electrochemical cell. A three-electrode configuration was settled, with Ag/AgCl (3M) as reference electrode, carbon felt electrode as working electrode, and 0.10 M KCl in the opposite chamber with an electrode of carbon felt as counter electrode. A Nafion™ NM 117 PEM was used and a scan rate of 20 mV s^{-1} was executed.

The 2,6-AQDS (1.0 mM in 0.10 M sodium phosphate buffer solution, pH = 7) and the $[Fe(CN)_6]^{3-}$ (1.0 mM in 0.10 M sodium phosphate buffer solution, pH = 7) were also studied by CV using an electrochemical cell in a three electrode configuration with Ag/AgCl (3 M) as reference electrode, glassy carbon (working electrode) and platinum/titanium (counter-electrode). All electrochemical experiments were made with a potentiostat (Ec-Lab Potentiostat, BioLogic Scientific Instruments) and all solutions were deaerated with N_2 (100 %), prior to experiments. All results were converted to Normal Hydrogen Electrode (NHE).

UV-Vis spectrophotometry

UV-Vis spectrophotometry was used to estimate the concentration of 2,6-AQDS (oxidized form) present in the cathode chamber of BESs. The 2,6-AQDS concentration is normally quantified within 250-350 nm wavelength [66,72,73]; in this work it was quantified at 330 nm. A standard curve was obtained by measuring the absorbance of reference solutions with concentrations ranging between 0.10 mM and 0.75 mM (obtained by dilution of a stock solution of 1.0 mM 2,6-AQDS). All the samples were analyzed inside an anaerobic chamber using a GENESYS™ 20 Visible Spectrophotometer using a 10 mm quartz cell. The concentration of 2,6-AQDS was quantified at the end of the experiments with BESs and the concentration of the microbial electrochemical fuel was estimated. The dilutions required for the quantification were performed inside an anaerobic chamber.

RFC experimental setup and operation

A RFC with 16 cm^2 active membrane area was assembled in a flow-through configuration. Nafion™ NM 117 PEM was used for separating the anode from the cathode. The Carbon felt GFD4.6 EA from SGL was thermal treated at 400 °C for 6 h based on previous literature [74, 75]. The bipolar plates were made of graphite (RCGBPP01) from RoyCarbon, China. Contacts to the current collectors were made with nickel-coated copper plates. Charging/discharging studies were carried out using a ZENNIUM (Zahner Elektrik, Germany) electrochemical workstation in a two-electrode galvanostatic configuration. On the anode side, the microbial electrochemical fuel (2,6-AQDSH_2) was placed in a hotplate stirrer that was used at 50 °C with 1100 rpm; on the cathode side, no temperature or agitation was applied. The supporting electrolyte was 0.10 M sodium phosphate buffer solution, pH = 7. Watson Marlow 323 pump was used to maintain an electrolyte flow rate of 20 mL min^{-1} during the cycling measurements. Both reservoirs were argon purged before and during test to minimize oxidation of species. Cycling measurements were conducted at default current densities of 3.75 mA cm^{-2}. The Coulombic Efficiency (CE), Potential Efficiency (PE) and Energy Efficiency (EE) of the RFC were determined as described in the literature [76].

3.3. Results and discussion

Electric current generation during quinone reduction – first experiment in BES A

The BESs were assembled to study the bioelectrochemical conversion of 2,6-AQDS (20 mM 2,6-AQDS) to the reduced form (2,6-AQDSH_2) using *G. sulfurreducens* as Electrochemically Active Bacteria (EAB). Figure 3.3. shows the BES assembled and the color change from yellow (2,6-AQDS) at the beginning to dark red (microbial electrochemical fuel, 2,6-AQDSH_2) at the end.

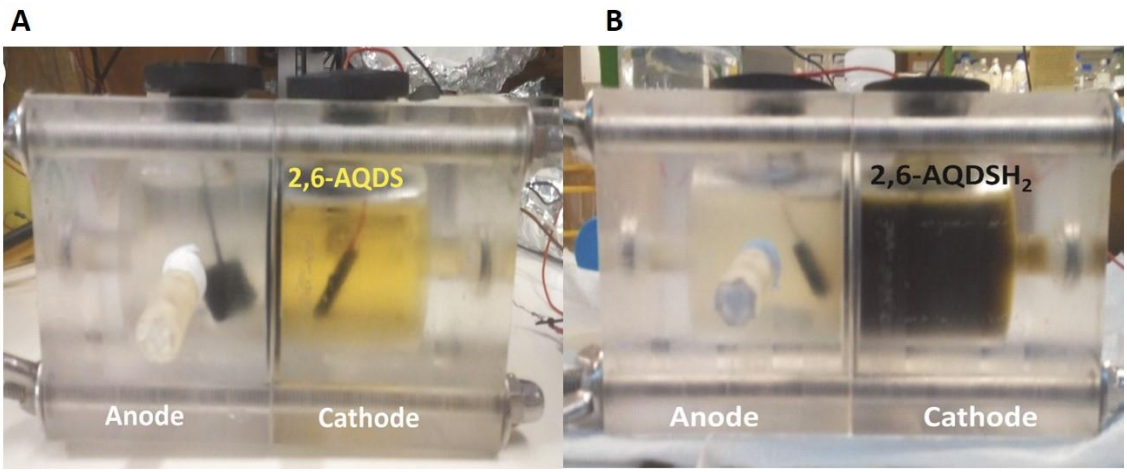


Figure 3.3. BES with *G. sulfurreducens* (anode) and 2,6-AQDS (cathode) at instant zero (A) and at the end of the assay (B).

The current density over time of the first BES A experiment (external resistance load of 500 Ω) is plotted in Figure 3.4.; after 2,6-AQDS being reduced, the solution was removed from the BES using a syringe and a fresh solution of 2,6-AQDS reintroduced for running the next series.

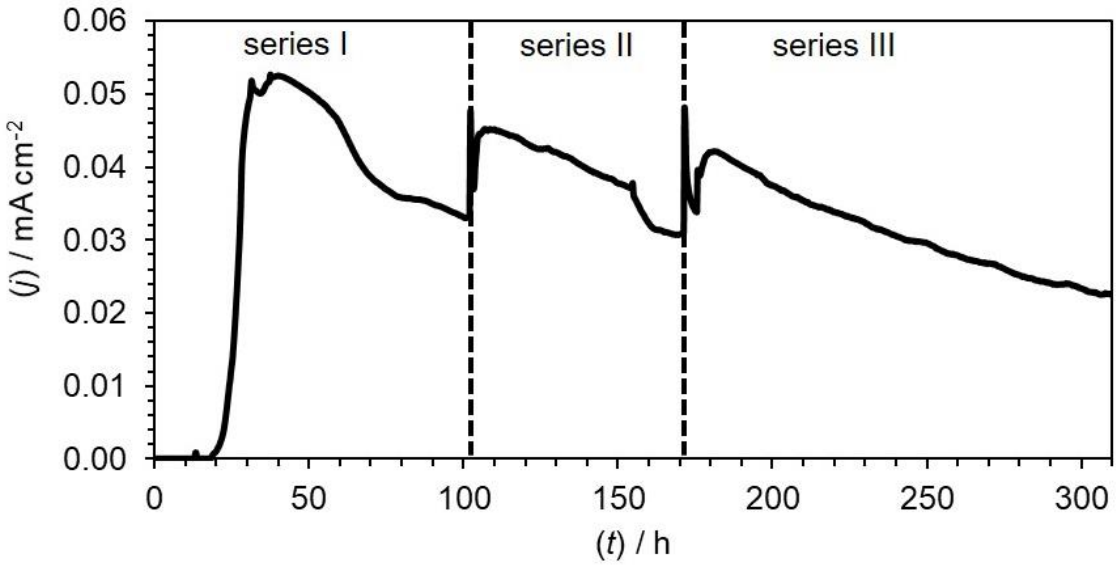


Figure 3.4. Current density over time for the bioelectrochemical reduction of 2,6-AQDS in BES A operated in series; (------) corresponds to the removal of the exhausted 2,6-AQDS.

The redox reactions and conditional potentials (an acetate oxidizing anode (acetate and bicarbonate concentration of 5 mM and 20 mM AQDS in basal medium at 25 ºC and at pH = 7, achieved with the Nernst Equation) [44,77]:

$C_2H_4O_2 + 2H_2O \rightarrow 2CO_2 + 8H^+ + 8e^-$ E^0_{oxd} = 0.289 V *vs.* NHE **3.2.**

$C_{14}H_6Na_2O_8S_2 + 2e^- + 2H^+ \rightarrow C_{14}H_8Na_2O_8S_2$ E^0_{red} = - 0.184 V *vs.* NHE **3.3.**

Acetate was added during the electrochemical conversion of the quinone in order to avoid carbon source limitations and promote the maximum current densities. Fresh 2,6-AQDS was added at the beginning of each time series in order to take advantage of the anodic biofilm established at the surface of the electrode and to promote a low activation potential needed for the bioelectrochemical conversion of the fuel.

In the first day (series I), the observed lag phase (the adaptation phase necessary for the *G. sulfurreducens* to grow as anode biofilm, [78]) was followed by an increase of the current density up to 0.52 mA cm^{-2}, obtained in the second day of operation (38 h). For series II and III, the respective maximum current densities were 0.45 mA cm^{-2} and 0.41 mA cm^{-2}.

The current density decreased after reaching the maximum as a result of the acetate consumption and quinone reduction. The BES current density decreased slowly over time (from series I to III) due to the increase of BES internal resistance, which is normal in long operations due to membrane fouling and to changes in anode medium mineral composition [78].

To analyze the BES A performance, polarization and power curves were determined at the end of each series (Figure 3.5).

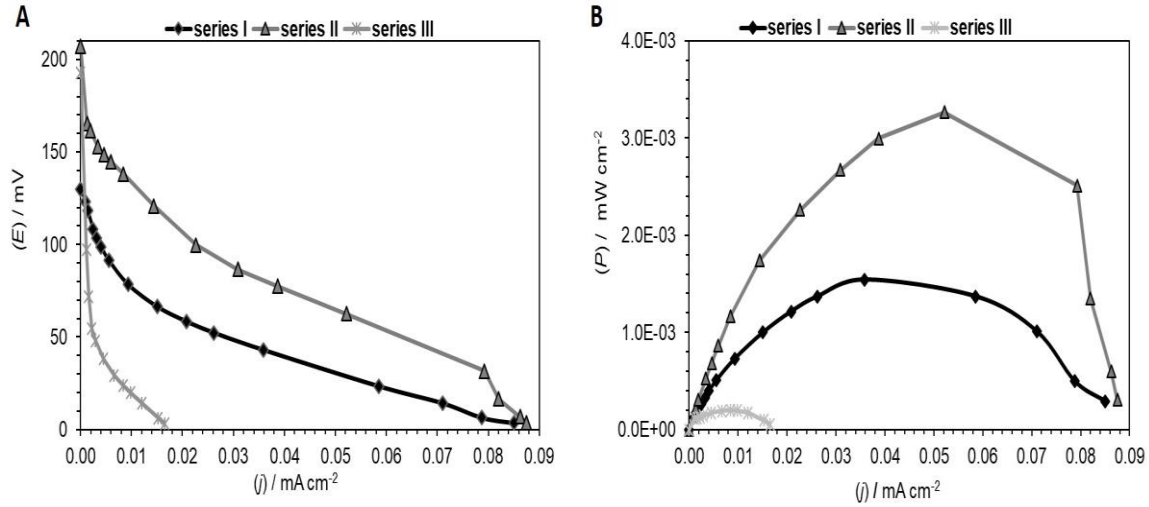


Figure 3.5. Polarization (A) and power curves (B) obtained for BES A operated in series. The lines were added for readability.

The OCP was determined at the stable phase of power generation for series I (129 mV), series II (207 mV) and series III (193 mV). The power curves show that, for series I, the highest power density achieved was $1.5x10^{-3}$ mW cm^{-2} with a current density of 0.03 mA cm^{-2}; for series II the maximum power density of $3.3x10^{-3}$ mW cm^{-2} was achieved, with a current density of 0.05 mA cm^{-2}; and for series III the maximum power density was $0.1x10^{-3}$ mW cm^{-2} with a current density of 0.01 mA cm^{-2}.

The polarization curves show an initial phase where activation losses predominate, followed by a region dominated by ohmic losses; the internal resistances were estimated from the slope of the curve in this region [37]. Internal resistance of 219 Ω for series I, 325 Ω for series II and 648 Ω for series III were estimated, showing an ohmic resistance increase. From Figure 3.5 it can be concluded that the power efficiency was higher for series II.

Electric current generation during quinone reduction – second experiment in BESs B1 and B2

The current density over time for an external resistance load of 500 Ω in the BESs B1 and B2 are shown in Figure 3.6. The maximum current density was reached at *ca*. 90 h (0.28 mA cm^{-2}) for BES B1 and at 27 h (0.42 mA cm^{-2}) for BES B2. The characteristic color change suggesting the reduction of 2,6-AQDS (from a yellow to a dark red color) was observed in both devices. The current generation achieved during the conversion of organic molecules (acetate, glucose, etc.) in batch or fed-batch BESs systems is typically low [51], as a consequence of the bacterial growth and other competitive processes [37].

Here, the current density produced in BES B2 was faster than in BES B1, and the highest current density was observed in the initial hours. As the current generation is directly proportional to the anode biofilm growth [59], the result obtained was expected as the measured OD_{600} in BES B1 increased from 0.09 to 0.28 whereas in BES B2 the initial cell concentration was higher and OD_{600} increased from 0.36 to 0.42. Notwithstanding the slower start-up of BES B1, both cells evolved to reach similar current densities, evidencing that a lower inoculum concentration do not impair the establishment of a proper electroactive biofilm.

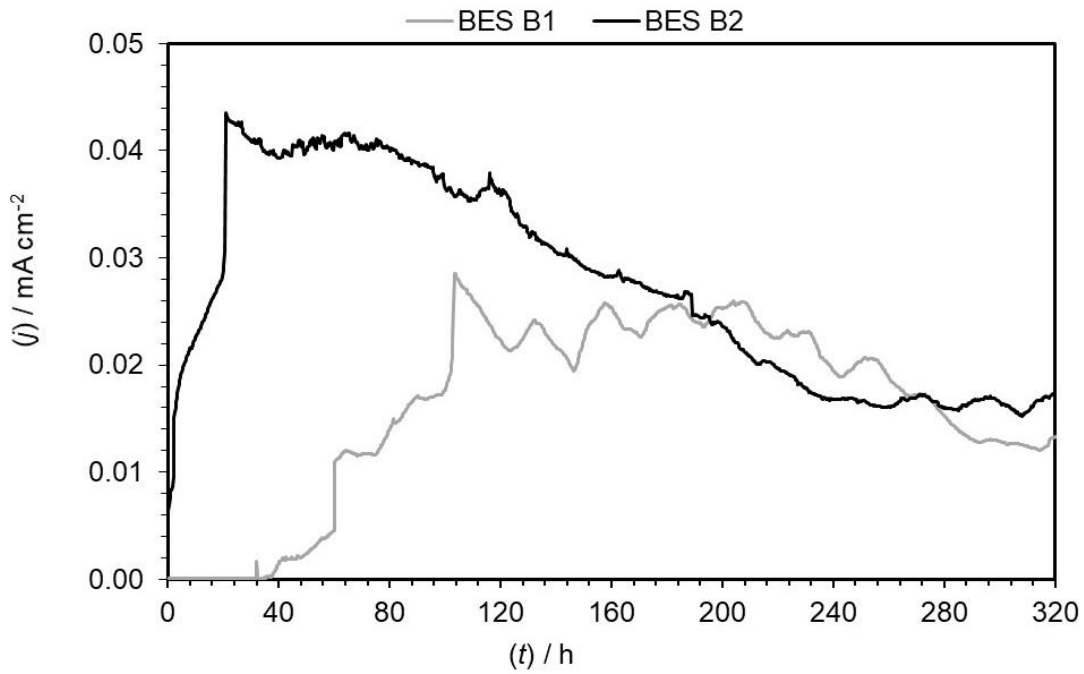


Figure 3.6. Current density over time for the bioelectrochemical reduction of 2,6-AQDS in BESs (BES B1 and BES B2).

The polarization and the power curves were determined at the end of the BES B1 and BES B2 (Figure 3.7).

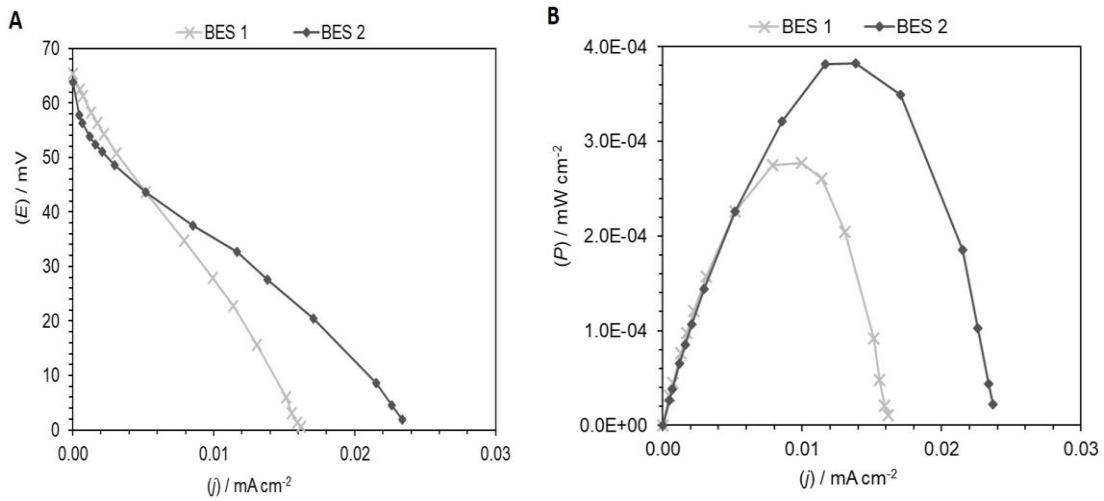


Figure 3.7. The polarization curve (A) and power curve (B) for BESs (BES B1 and BES B2).

The OCP of 65 mV was recorded at the stable phase of the power generation; internal resistances as low as 3.8 MΩ and 2.3 MΩ were estimated for BES B1 and BES B2, respectively, from the slope of the polarization curve (Figure 3.7). These values were smaller than the ones observed in the experiment with BES A operated in series. The highest power

density obtained for BES B1 was $2.9x10^{-4}$ mW m^{-2} (0.01 mA cm^{-2}) and for BES B2 was $4.0x10^{-4}$ mW cm^{-2} (0.01 mA cm^{-2}) (Figure 3.7).

The CE was estimated in BES B1 and BES B2, resulting in *ca.* 20 %, for the 320 h, respectively. The CE obtained was smaller than the one obtained in a previous work with *G. sulfurreducens* and acetate as carbon source [62]. The lower value of CE in the current work could be related to the smaller fraction of electrons from the reaction that were transferred to the anode [62, 79]. The smaller area of the electrodes and volume of the reactor may have influenced this result. An improvement in the CE could be reached with optimization procedures [80, 81]. But for the proof-of-concept the model organism, *G. sulfurreducens* was seen as the best EAB [82], and acetate as a simple carbon source.

BESs have been largely used to generate and store energy in the form of hydrogen with the consumption of organic compounds, however the application of potential is required [83]. One of the biggest achievements in the BES under assessment in the present work (in both experiments) is that no bias potential was applied. This proves that EAB in a BES are able to promote the conversion of the redox pair 2,6-AQDS/2,6-$AQDSH_2$, as a microbial electrochemical fuel. Optimization procedures, new materials or physical designs reactors could help to reduce the period of time for these redox reactions in BESs [32, 80, 81].

After 320 h the microbial electrochemical fuel was removed for analysis. The final 2,6-$AQDSH_2$ concentration was estimated as the difference between the initial (20 mM) and the final concentrations of 2,6-AQDS (oxidized form) (15.6 mM at BES B1 and 16.7 mM at BES B2). The reduction of 2,6-AQDS to 2,6-$AQDSH_2$ was also confirmed by the visual color change [71] from yellow to dark red, as seen in Figure 3.3. for BES A. A CV of the culture medium, present in the Figure 3.8., indicates the absence of any redox elements. There is actually no other species promoting the reduction of the 2,6-AQDS.

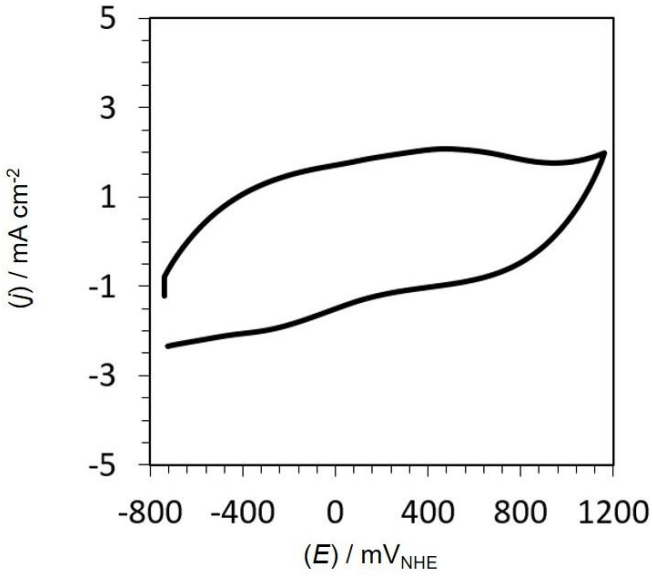


Figure 3.8. Cyclic voltammograms at 20 mV s^{-1} of the culture medium of *Geobacter sulfurreducens.*

RFCs results

Cyclic Voltammetry (CV) of 1 mM 2,6-AQDS (electrochemically reduced) and 1 mM $[Fe(CN)_6]^{3-}$ at 20 mV s^{-1} were performed to confirm the RFC potential using the selected redox pair. It was confirmed that the redox pairs are electrochemically reversible and the redox potentials are as expected from previous reports [84, 85] (Figure 3.9).

The microbial electrochemical fuel (2,6-$AQDSH_2$) from BES B2 and BES A operated in series (series II) was used in a RFC as negalyte, with $[Fe(CN)_6]^{3-}$ as posilyte.

The discharging redox reactions (E^0 [V, 25 °C, pH = 7]) are [87]:

$C_{14}H_8Na_2O_8S_2 \rightleftharpoons C_{14}H_6Na_2O_8S_2 + 2H^+ + 2e^-$ E^0_{oxd} = 0.184 V *vs.* NHE **3.4.**

$[Fe(CN)_6]^{3-} + e^- \rightleftharpoons [Fe(CN)_6]^{4-}$ E^0_{red} = 0.436 V *vs.* NHE **3.5.**

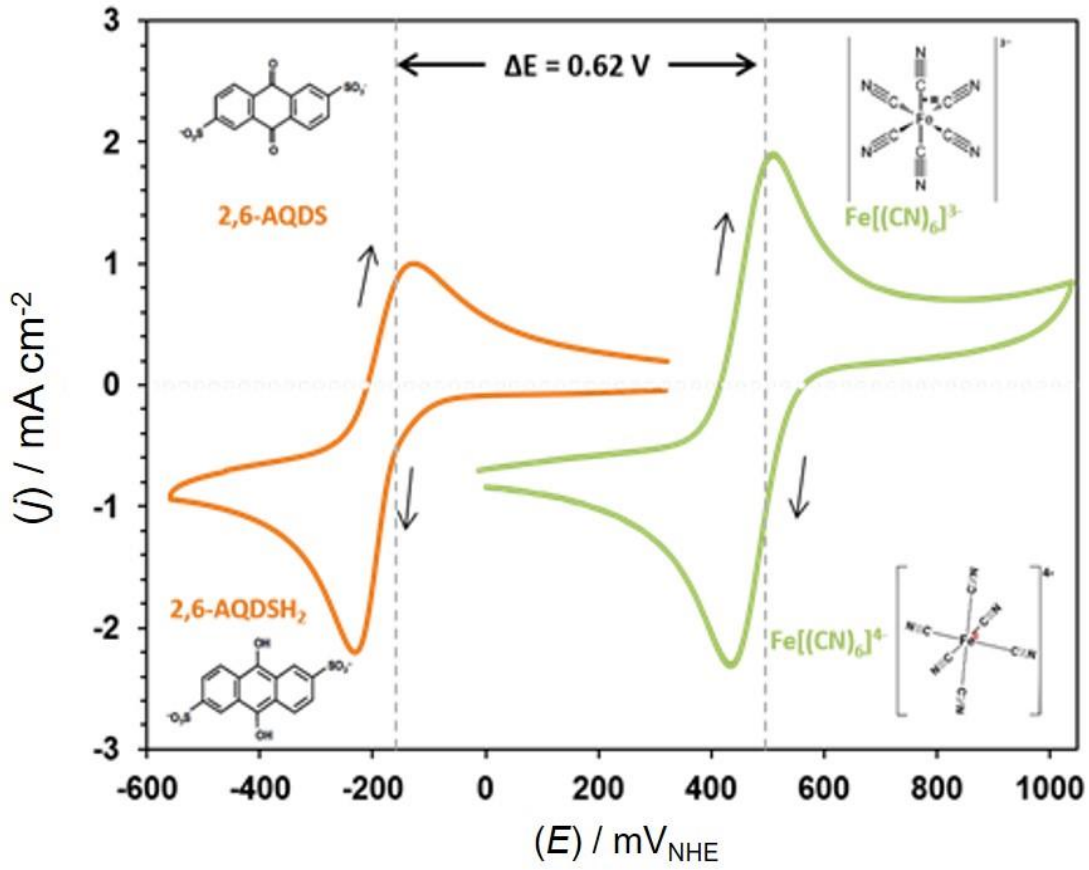


Figure 3.9. Cyclic voltammograms at 20 mV s^{-1} for 1.0 mM 2,6-AQDS (orange color, left) and 1.0 mM $[Fe(CN)_6]^{3-}$ (green color, right), at pH = 7.

The charging/discharging studies are depicted in Figure 3.10A. The CE for the 10 cycles was *ca.* 100 % and the PE was *ca.* 85 %; the EE was *ca.* 85 % (Figure 3.10B). These results were achieved by starting at the discharged mode, with a microbial electrochemical fuel from BES B2. The same discharge test with the RFC for the microbial electrochemical fuel obtained in the BES A series II was performed, however problems with assembling the cell (*e.g.* precipitation of the quinone in negalyte electrode) were observed.

The results from Figure 3.10 that used 2,6-AQDSH_2 as negalytes from a BES operated in batch cycles (Figure 3.6) suggested that a complete batch cycle to convert the microbial electrochemical fuel is more efficient for the reduction of the quinone, and this is implicit in the results of the cell discharge curves. These charge-discharge curves show that microbial electrochemical fuel detain the redox potential and the chemical properties of a redox pair of a RFC, achieving high CE and EE. The CE and EE achieved in Figure 3.10B, are in the same range of RFC efficiencies with 2,6-AQDS used as negalyte [25]. In this proof-of-concept, the

RFCs were operated with a current density of 3.75 mA cm^{-2}, whereas high-performance RFCs reach 100-500 mA cm^{-2} @ 80 % of round-trip-efficiency [86].

Even though the RFC did not reach the cell potentials seen in some Aqueous Organic RFC, it was still possible to reach EE superior to *ca.* 80 %, even using a lower concentration of quinone (20 mM) than the one usually reported in literature (a maximum solubility of 0.5 M and cycling performance at 0.2 M concentration of 2,6 AQDS [29]). The concentration of 20 mM 2,6-AQDS was selected for the MRFC, since its solubility at room temperature in water is H_2O<3.0 % (10.00 mg mL^{-1} H_2O). The use of new redox pairs, displaying higher energy density, such as anthraquinone-2,7-disulfonate [87] and polyoxometalate (POM) [88], should now be initiated; this last system allows energy densities up to 150 Wh L^{-1}.

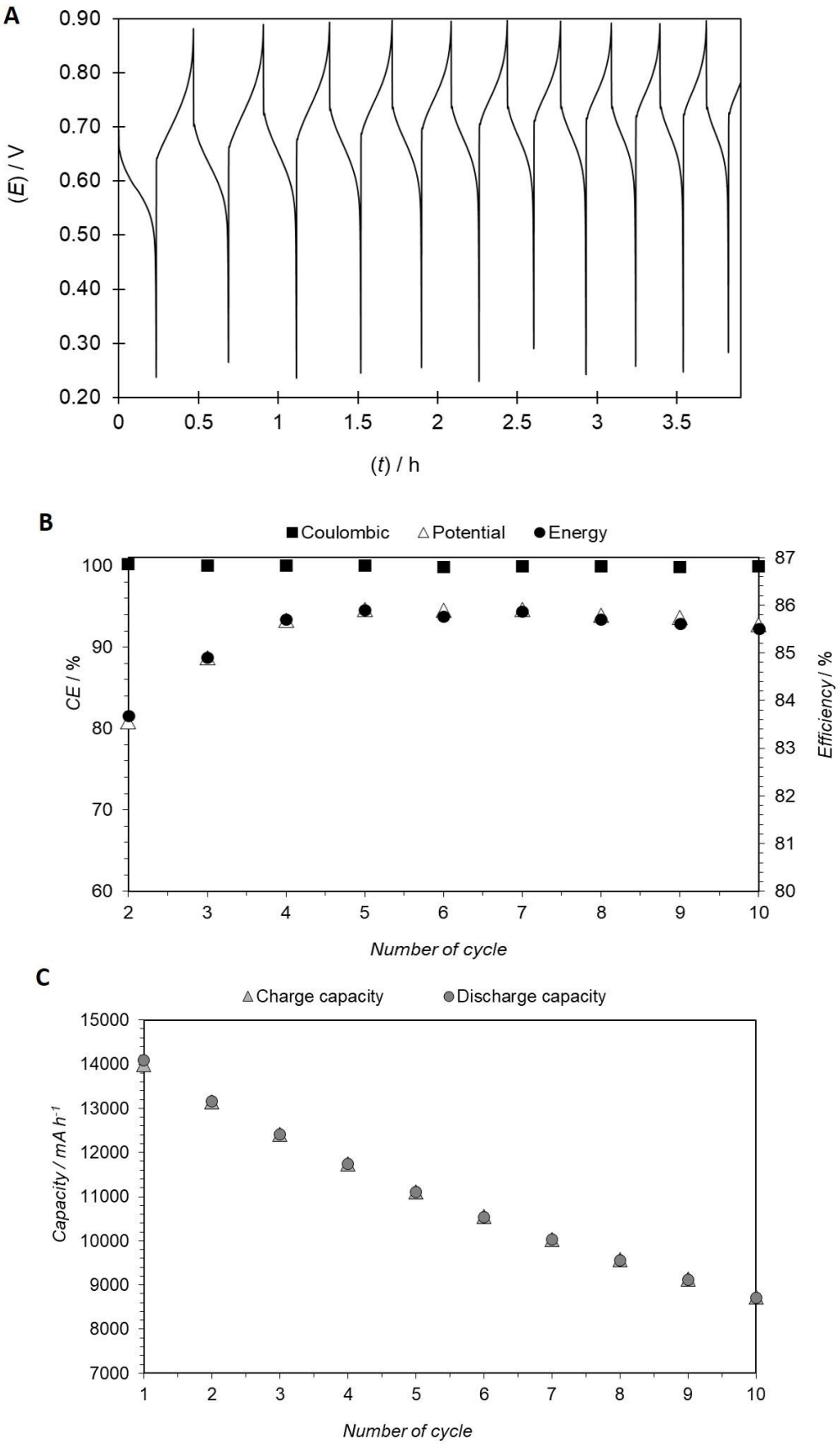


Figure 3.10. Charge–discharge curves versus time (A), Coulombic (black square), Potential (black triangle) and Energy efficiencies (black circle) versus the cycle number (B) in the RFC at current density of 3.75 mA cm^{-2} and (C) capacity for 10 cycles for RFC with 2,6-$AQDSH_2$ from the BES B2.

3.4. Conclusion

BESs were used to reduce 2,6-AQDS to 2,6-AQDSH_2 to be used as a microbial electrochemical fuel in a RFC. The reduction of 2,6-AQDS was confirmed by UV-Vis spectrophotometry and CV, obtaining a maximum of *ca*. 5 mM of microbial electrochemical fuel. The 2,6-AQDS was bio-reduced to 2,6-AQDSH_2 with a maximum current density in the range of 0.04-0.05 mA cm^{-2} and a maximum power density of 0.03 mW cm^{-2} in MFC operated in series.

It was demonstrated that the microbial electrochemical fuel developed in the BESs can be used as negative redox pair of the 2,6-AQDS||$[Fe(CN)_6]^{4-}$ in a RFC, promoting EE *ca.* 80 %. The research team is now developing the bio-charging of the positive redox pair, $[Fe(CN)_6]^{4-}$, aiming at the development of a feasible technology for converting bio-energy into storable electrochemical energy - that we designated Microbial Redox Flow Cell. Microbial electrochemical fuels using EAB are advantageous compared with converting bio-energy into hydrogen; actually, a Microbially Redox Flow Cell can be charged unbiased while microbially water splitting is a biased process [89].

3.5. Acknowledgements

M.S.S. Santos is grateful to Portuguese Foundation for Science and Technology (FCT) for her PhD grant (reference: SFRH/BD/104087/2014). J. Azevedo is grateful to the FCT for is Postdoctoral Grant (Reference: SFRH/BPD/116648/2016) and for funding (CEECIND/03937/2017). Ricardo Monteiro was also grateful for their Postdoctoral Grant by FCT (Reference: SFRH / BPD / 112900 / 2015). C. Dias-Ferreira has been funded through FCT by POCH – Programa Operacional Capital Humano within ESF – European Social Fund and by national funds from MCTES (SFRH/BPD/100717/2014). The authors would like to acknowledge to the FCT under the scope of the strategic funding of UID/BIO/04469 unit and COMPETE 2020 (POCI-01-0145-FEDER-006684) and BioTecNorte operation (NORTE-01-0145-FEDER-000004) funded by the European Regional Development Fund (ERDF), under the scope of Norte2020 - Programa Operacional Regional do Norte. The authors also acknowledge the Projects: i) POCI-01-0145-FEDER-006939 (LEPABE - Laboratory for Process Engineering, Environment, Biotechnology and Energy – UID/EQU/00511/2013), funded by the ERDF,

through COMPETE2020 – Programa Operacional Competitividade e Internacionalização (POCI) and by national funds through FCT, ii) by the Project SunStorage - Harvesting and storage of solar energy", with reference POCI-01-0145-FEDER-016387, funded by ERDF, through COMPETE 2020 --POCI), and by national funds, through FCT; (iii) Project PTDC/EQU-EQU/30510/2017 - POCI-01-0145-FEDER-030510 – Sunflow "Solar energy storage into redox flow batteries" funded by FEDER funds through COMPETE2020 - Programa Operacional Competitividade e Internacionalização (POCI) and by national funds (PIDDAC) through FCT/MCTES and iv) NORTE-01-0145-FEDER-000005 – LEPABE-2-ECO-INNOVATION, supported by North Portugal Regional Operational Programme (Norte 2020), under the Portugal 2020 Partnership Agreement, through the ERDF. The authors are indebted with all the colleagues who assisted in the laboratory work, in particular to Dr. Sónia Barbosa for help with microbial fuel cell operation.

3.6. References

[1] A.Z. Weber, M.M. Mench, J.P. Meyers, P.N. Ross, J.T. Gostick, Q. Liu, Redox flow batteries: a review, J. Appl. Electrochem. 41 (2011) 1137–1164.

[2] J. Noack, N. Roznyatovskaya, T. Herr, P. Fischer, The chemistry of Redox-Flow Batteries, Angew. Chemie - Int. Ed. 54 (2015) 9776–9809.

[3] Y. Zhu, F. Yang, Z. Niu, H. Wu, Y. He, H. Zhu, J. Ye, Y. Zhao, X. Zhang, Enhanced cyclability of organic redox flow batteries enabled by an artificial bipolar molecule in neutral aqueous electrolyte, J. Power Sources. 417 (2019) 83–89.

[4] Jason Deign, Study: flow batteries beat lithium ion - Energy Storage Report, (2017).

[5] O. Schmidt, A. Hawkes, A. Gambhir, I. Staffell, The future cost of electrical energy storage based on experience rates, Nat. Energy. 2 (2017) 1–8.

[6] L. Li, S. Kim, W. Wang, M. Vijayakumar, Z. Nie, B. Chen, J. Zhang, G. Xia, J. Hu, G. Graff, J. Liu, Z. Yang, A stable vanadium redox-flow battery with high energy density for large-scale energy storage, Adv. Energy Mater. 1 (2011) 394–400.

[7] C. Choi, S. Kim, R. Kim, Y. Choi, S. Kim, H. young Jung, J.H. Yang, H.T. Kim, A review of vanadium electrolytes for vanadium redox flow batteries, Renew. Sustain. Energy Rev. 69 (2017) 263–274.

[8] C. Bae, E.P.L. Roberts, M.H. Chakrabarti, M. Saleem, A008. All-Chromium Redox Flow Battery for renewable energy storage, Int. J. Green Energy. 8 (2011) 248–264.

[9] K. Gong, F. Xu, J.B. Grunewald, X. Ma, Y. Zhao, S. Gu, Y. Yan, All-soluble All-Iron Aqueous Redox-Flow Battery, ACS Energy Lett. 1 (2016) 89–93.

[10] B. Li, Z. Nie, M. Vijayakumar, G. Li, J. Liu, V. Sprenkle, W. Wang, Ambipolar zinc-polyiodide electrolyte for a high-energy density aqueous redox flow battery., Nat. Commun. 6 (2015) 1–8.

[11] F. Pan, Q. Wang, Redox species of redox flow batteries: a review, Molecules. 20 (2015) 20499–20517.

[12] W. Wang, V. Sprenkle, Energy storage: Redox flow batteries go organic, Nat. Chem. 8 (2016) 204–206.

[13] K. Wedege, E. Dražević, D. Konya, A. Bentien, Organic Redox Species in Aqueous Flow Batteries: redox potentials, chemical stability and solubility, Sci. Rep. 6 (2016) 1–13.

[14] E.J. Son, J.H. Kim, K. Kim, C.B. Park, Quinone and its derivatives for energy harvesting and storage materials, J. Mater. Chem. A. 4 (2016) 11179–11202. doi:10.1039/C6TA03123D.

[15] B. Li, J. Liu, Progress and directions in low-cost redox-flow batteries for large-scale energy storage, Natl. Sci. Rev. 4 (2017) 91–105.

[16] R.S. Kim, T.D. Chung, The electrochemical reaction mechanism and applications of quinones, Bull. Korean Chem. Soc. 35 (2014) 3143–3155.

[17] B. Huskinson, M.P. Marshak, M.R. Gerhardt, M.J. Aziz, Cycling of a Quinone-Bromide Flow Battery for large-Scale electrochemical energy storage, ECS Trans. 61 (2014) 27–30.

[18] K. Lin, Q. Chen, M.R. Gerhardt, L. Tong, S.B. Kim, L. Eisenach, A.W. Valle, D. Hardee, R.G. Gordon, M.J. Aziz, M.P. Marshak, Alkaline quinone flow battery, Science (80). 349 (2015) 1529–1532.

[19] X. Liang, S. Peng, Y. Lei, C. Gao, N. Wang, S. Liu, D. Fang, Effect of l-glutamic acid on the positive electrolyte for all-vanadium redox flow battery, Electrochim. Acta. 95 (2013) 80–86.

[20] Z. He, G. Jin, C. Gao, Y. Chen, H. Han, J. Liu, A new redox flow battery of high energy density with V/Mn hybrid redox couples, J. Renew. Sustain. Energy. 6 (2014) 1–10.

[21] Y. Lu, J.B. Goodenough, Rechargeable alkali-ion cathode-flow battery, J. Mater. Chem. 21 (2011) 10113–10117.

[22] Y. Zhao, Y. Ding, Y. Li, L. Peng, H.R. Byon, J.B. Goodenough, G. Yu, A chemistry and material perspective on lithium redox flow batteries towards high-density electrical energy storage., Chem. Soc. Rev. 44 (2015) 7968–7996.

[23] T. Liu, X. Wei, Z. Nie, V. Sprenkle, W. Wang, A total organic aqueous redox flow battery employing a low cost and sustainable methyl viologen anolyte and 4-HO-TEMPO catholyte, Adv. Energy Mater. 6 (2016) 1–8.

[24] B. Huskinson, M.P. Marshak, C. Suh, S. Er, M.R. Gerhardt, C.J. Galvin, X. Chen, A. Aspuru-Guzik, R.G. Gordon, M.J. Aziz, A metal-free organic-inorganic aqueous flow battery., Nature. 505 (2014) 195–198.

[25] B. Yang, L. Hoober-Burkhardt, S. Krishnamoorthy, A. Murali, G.K.S. Prakash, S.R. Narayanan, High-Performance aqueous organic flow battery with quinone-based redox couples at both electrodes, J. Electrochem. Soc. 163 (2016) 1442–1449.

[26] T. Davies, J. Tummino, High-Performance Vanadium Redox Flow Batteries with Graphite Felt Electrodes, J. Carbon Res. 4 (2018) 1–17.

[27] A. Orita, M.G. Verde, M. Sakai, Y.S. Meng, A biomimetic redox flow battery based on flavin mononucleotide, Nat. Commun. 7 (2016) 1–8.

[28] M. Skyllas-Kazacos, C. Menictas, T. Lim, Redox flow batteries for medium- to large-scale energy storage, in: Ziad Melhem (Ed.), Electr. Transm. Distrib. Storage Syst., Elsevier, (2013) 398–441.

[29] B. Yang, L. Hoober-Burkhardt, F. Wang, G.K. Surya Prakash, S.R. Narayanan, An inexpensive aqueous flow battery for large-scale electrical energy storage based on water-soluble organic redox couples, J. Electrochem. Soc. 161 (2014) A1371–A1380.

[30] M.R. Gerhardt, L. Tong, R. Gómez-Bombarelli, Q. Chen, M.P. Marshak, C.J. Galvin, A. Aspuru-Guzik, R.G. Gordon, M.J. Aziz, Anthraquinone derivatives in aqueous flow batteries, Adv. Energy Mater. 7 (2017) 1–9.

[31] J. Azevedo, T. Seipp, J. Burfeind, C. Sousa, A. Bentien, J.P. Araújo, A. Mendes, Unbiased solar energy storage: Photoelectrochemical redox flow battery, Nano Energy. 22 (2016) 396–405.

[32] K. Wedege, J. Azevedo, A. Khataee, A. Bentien, A. Mendes, Direct solar charging of an organic-inorganic, stable, and aqueous alkaline redox flow battery with a hematite photoanode, Angew. Chemie Int. Ed. 55 (2016) 7142–7147.

[33] X. Li, Modeling and simulation study of a metal free organic–inorganic aqueous flow battery with flow through electrode, Electrochim. Acta. 170 (2015) 98–109.

[34] B.E. Logan, Microbial fuel cells, Wiley-Interscience, Hoboken, NJ, USA, 2008.

[35] K. Scott, E.H. Yu, Microbial Electrochemical and Fuel Cells: Fundamentals and applications, Elsevier, 2016.

[36] D. Pant, A. Singh, G. Van Bogaert, S. Irving Olsen, P. Singh Nigam, L. Diels, K. Vanbroekhoven, Bioelectrochemical systems (BES) for sustainable energy production and product recovery from organic wastes and industrial wastewaters, RSC Adv. 2 (2012) 1248–1263.

[37] B.E. Logan, B. Hamelers, R. Rozendal, U. Schröder, J. Keller, S. Freguia, P. Aelterman, W. Verstraete, K. Rabaey, Microbial fuel cells: methodology and technology, Environ. Sci. Technol. 40 (2006) 5181–5192.

[38] M. Balat, Microbial fuel cells as an alternative energy option, Energy Sources Part A Recover. Util. Environ. Eff. 32 (2010) 26–35.

[39] S. Ishii, S. Suzuki, T. M.Norden-Krichmar, A. Wu, Y. Yamanaka, K.H. Nealson, O. Bretschger, Identifying the microbial communities and operational conditions for optimized wastewater treatment in microbial fuel cells, Water Res. 47 (2013) 7120–7130.

[40] E. Blásquez, D. Grabiel, J.A. Baeza, A. Guisasola, Treatment of high-strength sulfate wastewater using an autotrophic biocathode in view of elemental sulfur recovery, Water Res. 105 (2016) 395–405.

[41] B.E. Logan, D. Call, S. Cheng, H.V.M. Hamelers, T.H.J.A. Sleutels, A.W. Jeremiasse, R.A. Rozendal, Microbial Electrolysis Cells for high yield hydrogen gas production from organic matter, Environ. Sci. Technol. 42 (2008) 8630–8640.

[42] M. Kitching, R. Butler, E. Marsili, Microbial bioelectrosynthesis of hydrogen: current challenges and scale-up, Enzyme Microb. Technol. 96 (2017) 1–13.

[43] P.F. Beese-Vasbender, J.P. Grote, J. Garrelfs, M. Stratmann, K.J.J. Mayrhofer, Selective microbial electrosynthesis of methane by a pure culture of a marine lithoautotrophic archaeon, Bioelectrochemistry. 102 (2015) 50–55.

[44] K. Rabaey, R.A. Rozendal, Microbial electrosynthesis - revisiting the electrical route for microbial production., Nat. Rev. Microbiol. 8 (2010) 706–16.

[45] O. Choi, T. Kim, H.M. Woo, Y. Um, Electricity-driven metabolic shift through direct electron uptake by electroactive heterotroph *Clostridium pasteurianum*, Sci. Rep. 4 (2015) 1–10.

[46] Y. Kim, B.E. Logan, Microbial desalination cells for energy production and desalination, Desalination. 308 (2013) 122–130.

[47] L. Peixoto, A.L. Rodrigues, G. Martins, A. Nicolau, A.G. Brito, M.M. Silva, P. Parpot, R. Nogueira, A flat microbial fuel cell for decentralized wastewater valorization: process performance and optimization potential, Environ. Technol. 34 (2013) 1947–1956.

[48] E. Comission, Bioelectrochemical systems: Wastewater treatment, bioenergy and valuable chemicals delivered by bacteria, 2013.

[49] J.M. Morris, S. Jin, Feasibility of using microbial fuel cell technology for bioremediation of hydrocarbons in groundwater., J. Environ. Sci. Health. A. Tox. Hazard. Subst. Environ. Eng. 43 (2008) 18–23.

[50] Z. Ge, L. Wu, F. Zhang, Z. He, Energy extraction from a large-scale microbial fuel cell system treating municipal wastewater, J. Power Sources. 297 (2015) 260–264.

[51] C. Santoro, C. Arbizzani, B. Erable, I. Ieropoulos, Microbial fuel cells: from fundamentals to applications. A review, J. Power Sources. 356 (2017) 225–244.

[52] F. Harnisch, Bioelectrorefeneries: joining the forces of microbiology and electrochemistry for production of chemicals and fuels, in: ISMET 6, Lisbon (2017) 7.

[53] T. Kim, J. Yeo, Y. Yang, S. Kang, Y. Paek, J.K. Kwon, J.K. Jang, Boosting voltage without electrochemical degradation using energy-harvesting circuits and power management system-coupled multiple microbial fuel cells, J. Power Sources. 410–411 (2019) 171–178.

[54] T.C. Pannell, R.K. Goud, D.J. Schell, A.P. Borole, Effect of fed-batch *vs.* continuous mode of operation on microbial fuel cell performance treating biorefinery wastewater, Biochem. Eng. J. 116 (2016) 85–94.

[55] S.G. Barbosa, L. Peixoto, A. Ter Heijne, P. Kuntke, M.M. Alves, M.A. Pereira, Investigating bacterial community changes and organic substrate degradation in microbial fuel cells operating on real human urine, Environ. Sci. Water Res. Technol. 3 (2017) 897–904.

[56] S.G. Barbosa, L. Peixoto, O.S.G.P. Soares, M.F.R. Pereira, A. ter Heijne, P. Kuntke, M.M. Alves, M.A. Pereira, Influence of carbon anode properties on performance and microbiome of Microbial Electrolysis Cells operated on urine, Electrochim. Acta. 267 (2018) 122–132.

[57] L. Peixoto, R. Nogueira, A. Brito, C. Póvoa, P. Kroff, P. Parpot, Electroactivity of *Geobacter sulfurreducens* evaluated by cyclic voltammetry, in: II Int. Conf. Environ. Ind. Appl. Microbiol. (BioMicroWorld 2007), Ind. Appl. Microbiol. (BioMicroWorld 2007) (2007) 176.

[58] C. Koch, A. Kuchenbuch, J. Kretzschmar, H. Wedwitschka, J. Liebetrau, S. Müller, F. Harnisch, Coupling electric energy and biogas production in anaerobic digesters – impacts on the microbiome, RSC Adv. 5 (2015) 31329–31340.

[59] G. Reguera, K.P. Nevin, J.S. Nicoll, S.F. Covalla, T.L. Woodard, D.R. Lovley, Biofilm and nanowire production leads to increased current in *Geobacter sulfurreducens* fuel cells, Appl. Environ. Microbiol. 72 (2006) 7345–7348.

[60] K.P. Nevin, H. Richter, S.F. Covalla, J.P. Johnson, T.L. Woodard, A.L. Orloff, H. Jia, M. Zhang, D.R. Lovley, Power output and columbic efficiencies from biofilms of *Geobacter sulfurreducens* comparable to mixed community microbial fuel cells, Environ. Microbiol. 10 (2008) 2505–2514.

[61] M.S. Kim, Y.J. Lee, Optimization of culture conditions and electricity generation using *Geobacter sulfurreducens* in a dual-chambered microbial fuel-cell, Int. J. Hydrogen Energy. 35 (2010) 13028–13034.

[62] A.M. Speers, G. Reguera, Electron donors supporting growth and electroactivity of *Geobacter sulfurreducens* anode biofilms, Appl. Environ. Microbiol. 78 (2012) 437–444.

[63] M.-S. Kim, J. Cha, D.-H. Kim, Enhancing factors of electricity generation in a microbial fuel cell using *Geobacter sulfurreducens*., J. Microbiol. Biotechnol. 22 (2012) 1395–400.

[64] G. Martins, L. Peixoto, D.C. Ribeiro, P. Parpot, A.G. Brito, R. Nogueira, Towards implementation of a benthic microbial fuel cell in lake Furnas (Azores): Phylogenetic affiliation and electrochemical activity of sediment bacteria, Bioelectrochemistry. 78 (2010) 67–71.

[65] B.E. Logan, Microbial Fuel Cells, John Wiley & Sons, Inc., Hoboken, NJ, USA, 2007.

[66] G. Nöll, G. Hauska, P. Hegemann, K. Lanzl, T. Nçll, M. Von Sanden-flohe, B. Dick, C.W.V. Gmbh, C. Kgaa, T. Nöll, M. von Sanden-Flohe, B. Dick, Redox properties of LOV domains: chemical versus photochemical reduction, and influence on the photocycle, ChemBioChem. 8 (2007) 2256–2264.

[67] B.R. Ringeisen, E. Henderson, P.K. Wu, J. Pietron, R. Ray, B. Little, J.C. Biffinger, J.M. Jones-Meehan, High power density from a miniature microbial fuel cell using *Shewanella oneidensis* DSP10, Environ. Sci. Technol. 40 (2006) 2629–2634.

[68] L. Zeng, X. Li, S. Fan, M. Zhang, Z. Yin, M. Tadé, S. Liu, Photo-driven bioelectrochemical photocathode with polydopamine-coated TiO_2 nanotubes for self-sustaining MoS_2 synthesis to facilitate hydrogen evolution, J. Power Sources. 413 (2019) 310–317.

[69] M.S.S. Santos, L. Peixoto, C. Dias-Ferreira, A. Mendes, M.M. Alves, Microbially charged redox flow batteries for bioenergy storage, in: R.N. Krishnaraj, R.K. Sani (Eds.), Bioelectrochemical Interface Eng., Wiley, 14 (2019) 251–269.

[70] D. Sun, J. Chen, H. Huang, W. Liu, Y. Ye, S. Cheng, The effect of biofilm thickness on electrochemical activity of *Geobacter sulfurreducens*, Int. J. Hydrogen Energy 41 (2016) 2–7.

[71] A. Cadena, A.–C. Texier, I. González, F.J. Cervantes, J. Gómez, Qualitative and quantitative determination of a humic model compound in microbial cultures by cyclic voltammetry, Environ. Technol. 28 (2007) 1035–1044.

[72] C. Liu, J.M. Zachara, N.S. Foster, J. Strickland, Kinetics of reductive dissolution of hematite by bioreduced anthraquinone-2,6-disulfonate, Environ. Sci. Technol. 41 (2007) 7730–7735.

[73] C. yuan Wu, L. Zhuang, S. gui Zhou, Y. Yuan, T. Yuan, F. bai Li, Humic substance-mediated reduction of iron(III) oxides and degradation of 2,4-D by an alkaliphilic bacterium, *Corynebacterium humireducens* MFC-5, Microb. Biotechnol. 6 (2013) 141–149.

[74] R. Monteiro, J. Leirós, M. Boaventura, A. Mendes, Insights into all-vanadium redox flow battery: A case study on components and operational conditions, Electrochim. Acta. 267 (2018) 80–93.

[75] B.Sun, M. Skyllas-Kazacos, Modification of graphite electrode materials for vanadium redox flow battery application—I. Thermal treatment, Electrochim. Acta. 37 (1992) 1253–1260.

[76] C.P. de León, A. Frías-Ferrer, J. González-García, D.A. Szánto, F.C. Walsh, Redox flow cells for energy conversion, J. Power Sources. 160 (2006) 716–732.

[77] S. Orsetti, C. Laskov, S.B. Haderlein, Electron transfer between iron minerals and quinones estimating the reduction potential of the Fe(II)-goethite surface from AQDS Speciation, Environ. Sci. Technol. 47 (2013) 1–6.

[78] M.D. Rolfe, C.J. Rice, S. Lucchini, C. Pin, A. Thompson, A.D.S. Cameron, M. Alston, M.F. Stringer, R.P. Betts, J. Baranyi, M.W. Peck, J.C.D. Hinton, Lag phase is a distinct growth phase that prepares bacteria for exponential growth and involves transient metal accumulation, J. Bacteriol. 194 (2012) 686–701.

[79] N. Degrenne, F. Buret, B. Allard, P. Bevilacqua, Electrical energy generation from a large number of microbial fuel cells operating at maximum power point electrical load, J. Power Sources. 205 (2012) 188–193.

[80] P. Pandey, V.N. Shinde, R.L. Deopurkar, S.P. Kale, S.A. Patil, D. Pant, Recent advances in the use of different substrates in microbial fuel cells toward wastewater treatment and simultaneous energy recovery, Appl. Energy. 168 (2016) 706–723.

[81] S. Chen, S.A. Patil, R.K. Brown, U. Schröder, Strategies for optimizing the power output of microbial fuel cells: Transitioning from fundamental studies to practical implementation, Appl. Energy. 233–234 (2019) 15–28.

[82] D.R. Lovley, T. Ueki, T. Zhang, N.S. Malvankar, P.M. Shrestha, K.A. Flanagan, M. Aklujkar, J.E. Butler, L. Giloteaux, A.-E. Rotaru, D.E. Holmes, A.E. Franks, R. Orellana, C. Risso, K.P. Nevin, Geobacter: the microbe electric's physiology, ecology, and practical applications, in: Adv. Microb. Physiol. 59 (2011) 1–100.

[83] F. Fischer, S. Mermoud, G. Diouf, C. Bastian, Bio-inspired chemical hydrogen storage and discharge as a source of electrical energy, J. Appl. Electrochem. 42 (2012) 419–425.

[84] Y. Wu, F. Li, T. Liu, R. Han, X. Luo, pH dependence of quinone-mediated extracellular electron transfer in a bioelectrochemical system, Electrochim. Acta. 213 (2016) 408–415.

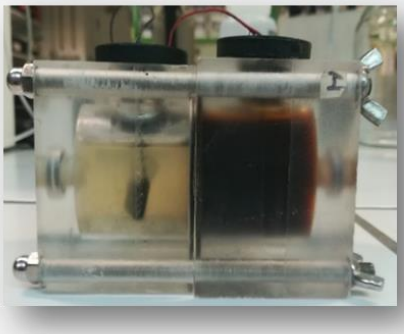
[85] M. Pandurangachar, B.E. Kumara Swamy, B.N. Chandrashekar, O. Gilbert, S. Reddy, B.S. Sherigara, Electrochemical investigations of potassium ferricyanide and dopamine by 1-butyl-4-methylpyridinium tetrafluoro borate modified carbon paste electrode: A cyclic voltammetric study, Int. J. Electrochem. Sci. 5 (2010) 1187–1202.

[86] P. Leung, X. Li, C.P. de León, L. Berlouis, C.T.J. Low, F.C. Walsh, H., Progress in redox flow batteries, remaining challenges and their applications in energy storage, RSC Adv. 2 (2012) 10125–10156.

[87] T.J. Carney, S.J. Collins, S.J. Moore, F.R. Brushett, Concentration-dependent dimerization of anthraquinone disulfonic acid and its impact on charge storage, Chem. Mater. 29 (2017) 4801–4810.

[88] J. Chen, M.D. Symes, L. Cronin, Higly reduced and protonated aqueous solutions of $[P_2W_{18}O_{62}]^{6-}$ for on-demand hydrogen generation and energy storage, Nat. Chem. 10 (2018) 1042–1047.

[89] J.P. Torella, C.J. Gagliardi, J.S. Chen, D.K. Bediako, B. Colón, J.C. Way, P.A. Silver, D.G. Nocera, Efficient solar-to-fuels production from a hybrid microbial – water-splitting catalyst system, Proc. Natl. Acad. Sci. 112 (2015) 2337–2342.





Chapter 4

Wastewater as a renewable energy source for a Microbial Redox Flow Cell

Abstract[1]

Bioelectrochemical Systems (BESs) can use wastewater for the direct conversion of chemical energy into electrical energy. However, in BES energy is not stored. In this work, the direct biotransformation of the chemical energy present in a real wastewater into electrochemical energy is reported. A Microbial Redox Flow Cell was gathered allowing for storable, and efficiently convertible electrochemical fuels into electricity. Aqueous solutions of anthraquinone-2,6-disulfonate (2,6-AQDS) at pH = 7, pH = 9 and pH = 12 were reduced in the BES cathode chamber, being thus converted into an electrochemical fuel suitable to be converted into electricity in a Redox Flow Cell (RFC). Current densities (*e.g.* 0.10 mA cm^{-2} for BES experiments at cathode pH = 7), power curves, polarization curves and Coulombic efficiencies (*e.g.* 51 % for BES experiments at cathode pH = 7) were determined. The microbial electrochemical fuels (anthrahydroquinone-2,6-disulfonate, 2,6-$AQDSH_2$) were examined by Cyclic Voltammetry and UV-Vis Spectrophotometry. Subsequently these microbial electrochemical fuels at pH = 7, pH = 9 and pH = 12 were tested in RFCs as negalyte with Ferricyanide ($[Fe(CN)_6]^{3-}$) as posilyte. The charge–discharge curves over time of RFCs were performed, and the coulombic, potential and energy efficiencies were computed. The results demonstrate that microbial electrochemical fuel in a RFC, in neutral conditions, can be assembled, in a Microbial Redox Flow Cell, for unbiased energy generation and storage from a real wastewater.

[1] The work presented in this chapter corresponds to the following scientific article: **M.S.S. Santos**, J. Azevedo, R.A. Monteiro, C. Dias-Ferreira, A. Mendes, M.M. Alves, L. Peixoto, Wastewater as a renewable energy source for a Microbial Redox Flow Cell (2020) (redrafted from Journal of Renewable Energy Journal (submitted)).

Chapter 4

4.1. Introduction

Municipal wastewater including domestic and industrial effluents contains resources that can be transformed into renewable energy (*e.g.* biogas [1]) or recovered (*e.g.* nutrients [2]).

In Bioelectrochemical Systems (BESs) this wastewater can be treated for water disposal [3] and nutrient recovery [4] while transformed electrochemically into electrical energy [5, 6]. Bacteria are capable to convert wastes, releasing electrons to an external circuit, that transports these electrons from the anode to the cathode chamber. The protons migrate through a proton exchange membrane positioned between two chambers [7].

Different works with wastewater in BESs reported power densities in the range of $5x10^{6}$ mW cm^{-2} [8] and Coulombic efficiencies (CEs) *ca.* 40 % [9], in some cases overcoming CEs reached with Electrochemically Active Bacteria (EAB) such as *Geobacter sulfurreducens* [10]. The power densities and cell potential outputs of BESs are inferior to the achieved for others electrochemical technologies, such as Redox Flow Cells (RFCs) [11]. Nevertheless, BESs are capable to promote unbiased energy production [12–14], without external potentials applied, for direct conversion of chemical energy into electrical energy.

Furthermore, BESs fed with wastewater as carbon source have been coupled with other devices, such as membrane bioreactors [15,16], Microbial Photoelectrochemical Cells [17,18], and hybrid up flow designs coupled with BES for simultaneous wastewater treatment and energy recovery [19,20].

The RFCs are electrochemical devices for energy conversion and storage, able to store energy in the form of electrochemical fuels, and transform them into electricity [21]. The electrochemical fuels are accessible in the form of redox chemical species and their redox reactions convert the chemical energy (fuel) into electrical energy. The redox pairs used in RFCs show, ideally, reversible kinetic reactions and a large window of redox potentials that allow to advance RFCs with high cell potentials [22–24].

RFCs use aqueous solutions of vanadium and sulfuric acid [4, 5], chromium [8], iron [9], zinc [10] and other simple inorganic compounds and metal complexes [10, 11]. Organic redox species are a step forward for use in RFCs, since they can be produced from renewable sources, are stable and show reversible redox reaction [12]. RFCs with organic redox species,

with high tunability and solubilities, achieve good redox potential windows [13] and Energy efficiencies (EEs) *ca.* 90 % [23–25].

Among the different choices for organic redox couples, quinones have been proposed due to their capacity to be reduced to the respective hydroquinone forms [16], redox potentials and chemical tunability, and are promising redox pairs due to their low cost [12–15]. In RFCs, quinones have been studied with inorganic compounds such as bromide [17] or ferricyanide ($[Fe(CN)_6]^{3-}$) [18] as redox couples to charge and discharge the RFCs [11].

The aim of this work is to assess the feasibility to transform bioelectrochemically the energy content of a real wastewater and store it, by reducing anthraquinone-2,6-disulfonate ($C_{14}H_6Na_2O_8S_2$; 2,6-AQDS) in the cathode chamber of a BES, and subsequently using this electrochemical fuel, as redox pair, in a RFC (designated as microbial electrochemical fuel). The design of a Microbial Redox Flow Cell (MRFC) is herein proposed (Figure 4.1). The 2,6-AQDS has been well studied in terms of stability, redox potential and solubility in RFCs [25–29].

The concept is an approach to generate (and store) renewable energy from carbonaceous contaminants present in municipal wastewater.

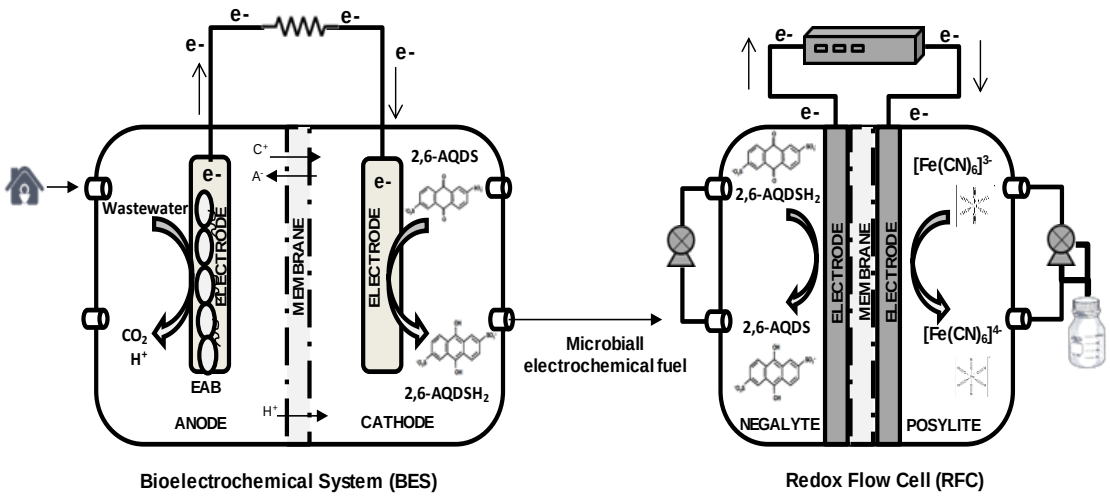


Figure 4.1. Scheme of the Microbial Redox Flow Cell (MRFC) with wastewater: Bioelectrochemical Systems (BES) for the direct charge of the negalyte (2,6-AQDS -> $2,6\text{-AQDSH}_2$) (at the left), coupled with a Redox Flow Cell (RFC) ($2,6\text{-AQDS}||[Fe(CN)_6]^{4-}$), set for charging the posilyte of the RFC on the right hand side.

4.2. Materials and methods

Chemicals and materials

The chemicals were of analytical grade from Sigma Aldrich; the water used was purified using a Milli-Q® Integral Water Purification System. The Nafion™ NM 117 Proton Exchange Membrane (PEM) and carbon felt were acquired from Quintech.

Wastewater collection

A pre-screened municipal wastewater (with an average Chemical Oxygen Demand (COD) concentration of 0.67 g L^{-1}, conductivity of 790.0 mS cm^{-1} and pH = 7) was collected at Frossos Wastewater Treatment Plant (Braga). After sampling, the wastewater was deoxygenated with nitrogen gas (100 %) and kept at 4 ºC until use.

BESs Configuration and operation

The BESs were composed by two cubic dual-chamber Microbial Fuel Cells with a Nafion™ NM 117 PEM between the chambers (50 cm^3 each) (Figure 4.1). The electrodes were manufactured with carbon felt (0.1 x 4 cm^2), previously prepared and connected to two electrical wires using carbon cement, as previously reported in [30].

Wastewater was introduced in the anode chambers and deoxygenated with nitrogen gas (100 %) to maintain anaerobic conditions. The pH of wastewater was always 7. For the cathode chamber, 20 mM of 2,6-AQDS was prepared in aqueous solutions at three pH conditions: pH = 7 (0.10 M phosphate buffer solution), pH = 9 (0.10 M bicarbonate buffer solution) and pH = 12 (0.10 M sodium hydroxide). The choice to operate with the three pH cathode conditions was based on the reported RFCs with quinones and $Fe(CN)_6]^{3-}$, at neutral [31] and alkaline conditions [32]. The high pH cathode conditions can increase the conductivity in the cathode chamber of BESs [33], and the greater pH difference between anodic and cathodic electrolytes in BESs is ideal for higher current densities and cell potentials [34].

The BESs with different pH cathode conditions, were studied with two duplicates (named BES 1 and BES 2); all were operated in batch conditions, at room temperature and anode side stirring

conditions. The electric circuits were closed, connected with external resistance load (1000 Ω), and linked to a register data system (unbiased conditions). The potential difference of the BES (mV) over time (*t*, h) was recorded every 15 min with the register data system (RSG 30 Endress+Hauser B.V., Naarden), and the current density was calculated. The wastewater was refreshed during the experimental time of BES, to avoid organic carbon limitations in the cell, when the current densities were too low and the reduction of 2,6-AQDS was not detected by further color change. The microbial electrochemical fuel was seen when a dark red almost brown color was observed (bio-charged 2,6-AQDSH_2), as pointed in previous literature [35].

BESs electrochemical characterization

The Open Circuit Potential (OCP) and was measured with a multimeter (HP Hewlett Packard 34401A multimeter). The current density (*j*, mA cm^{-2}) of the cells was calculated using the equation 4.1,

$$j = E\left(R \times A\right)^{-1} \qquad \textbf{4.1.}$$

being *E* (mV) the cell potential, *R* (Ω) the resistance and *A* (cm^2) the area of the electrode surface (0.1 x 4 cm^2).

After reduction of 2,6-AQDS in the cathode, a series of resistance loads between 31 kΩ to 10 Ω were applied to determine the polarization and power curves, as described in literature [36]. The internal resistance of BESs was estimated with the slope of the polarization curve where the maximum power density (*P*, mW cm^{-2}) was observed [36, 37].

The Coulombic Efficiency (CE), (η_{cb}, %) evaluates the fraction of electrons recovered (current) from the wastewater conversion for each BESs, integrating the current (*I*) over time (*dt*) [37], according to equation 4.2.

$$\eta_{cb} = \frac{M\int_0^t I dt}{FzV_{an}\Delta COD} \qquad \textbf{4.2.}$$

Where M is the molecular mass of oxygen (g mol^{-1}), F is the Faraday's constant (C mol^{-1}), V_{An} is the volume of wastewater in the anode compartment (L^{-1}), z is the number of electrons exchanged per mol and Δ_{COD} is the change in Chemical Oxygen Demand (COD) (mg L^{-1}). The wastewater COD was measured in the initial and final time of each cycle, using Hach-Lange cuvette tests (Hach Lange) and a spectrophotometer DR 2800 (Hach Lange).

Microbial electrochemical fuel analysis

After the reduction of 2,6-AQDS (bio-charged 2,6-$AQDH_2$) was completed for each BESs, when the dark red color was for more than 24 h seen [35], the BESs experiments were finished. Cyclic Voltammetry (CV) analysis of the bio-charged 2,6-$AQDSH_2$ was performed in the BESs for each pH condition. For the CV, the wastewater was replaced in the anode chamber by 0.10 M KCl, and the BESs were deoxygenated with nitrogen gas (100.0 %). The CVs were executed with a potentiostat (Ec-Lab Potentiostat, BioLogic Scientific Instruments) and data acquisition software (EC-Lab software). The working electrode was the electrode placed in the cathode chamber, the counter-electrode was the electrode in the anode chamber and an Ag/AgCl (3 M) reference electrode was positioned close to the working electrode. All results were presented with Normal Hydrogen Electrode (NHE).

The microbial electrochemical fuel concentration (concentration of bio-charged 2,6-$AQDSH_2$) was estimated using UV-Vis spectrophotometry (UV-Vis). Microbial electrochemical fuels of respective BESs were collected and introduced in serum vials, previously to the CVs analysis. The serum vials were moved to an anaerobic chamber after sampling. Inside the anaerobic chamber, the samples were analyzed with a GENESYS™ 20 Visible Spectrophotometer in a 10 mm quartz cell. The concentration of bio-charged 2,6-$AQDSH_2$ was estimated, through the difference between the concentration of 2,6-AQDS inserted in the cell and the concentration of 2,6-AQDS measured in the end of experiment. A calibration curve for the 2,6-AQDS at pH = 7, pH = 9 and pH = 12 was previously performed inside the anaerobic chamber and analyzed at the same conditions.

RFCs experimental setup and operation

RFC experiments with the bio-charged 2,6-AQDSH$_2$ (microbial electrochemical fuels), at pH = 7, pH = 9 and pH = 12 as negalyte and respective posilyte – $[Fe(CN)_6]^{3-}$ were performed. A 16 cm^2 RFC was assembled with a Nafion™ NM 117 PEM and carbon felt electrodes (Carbon felt GFD4.6 EA previously treated at 400 °C for 6 hours). The bipolar plates were made of graphite (RCGBPP01) from RoyCarbon, China. Contacts to the current collectors were made with nickel-coated copper plates.

The bio-charged 2,6-AQDSH$_2$, at each pH condition, was introduced in an external flask, and $[Fe(CN)_6]^{3-}$, prepared with 40 mM of $[Fe(CN)_6]^{3-}$ was introduced in the other external flask, at room temperature; each was settled according to the pH condition of the microbial electrochemical fuel: a) pH = 7 obtained using a 0.1 M phosphate buffer aqueous solution; b) pH = 9 obtained using a 0.1 M bicarbonate buffer solution and; c) pH = 12 using a 0.1 M NaOH. Both external flasks were purged with nitrogen (100 %) during the assay to minimize oxidation of species. A Watson-Marlow 323 pump was used to maintain the electrolytes flowing at 20 mL min^{-1}.

The charge-discharge curves studies were carried out using a ZENNIUM (Zahner Elektrik, Germany) electrochemical workstation in a two-electrode galvanostatic configuration. The electrolyte was discharged and charged using the electrochemical station at 3.75 mA cm^{-2}, between 0.20 V and 0.90 V [38]. The Coulombic (CE), Potential (PE) and Energy (EE) efficiencies of the RFCs were computed as described elsewhere [39].

4.3. Results and discussion

BESs electrochemical characterization and determinations

The current densities over time were followed, and the electrochemical conversion of the microbial electrochemical fuels were checked with the dark red color observation [35]. The results for the BESs current densities over time are presented in Figure 4.2.

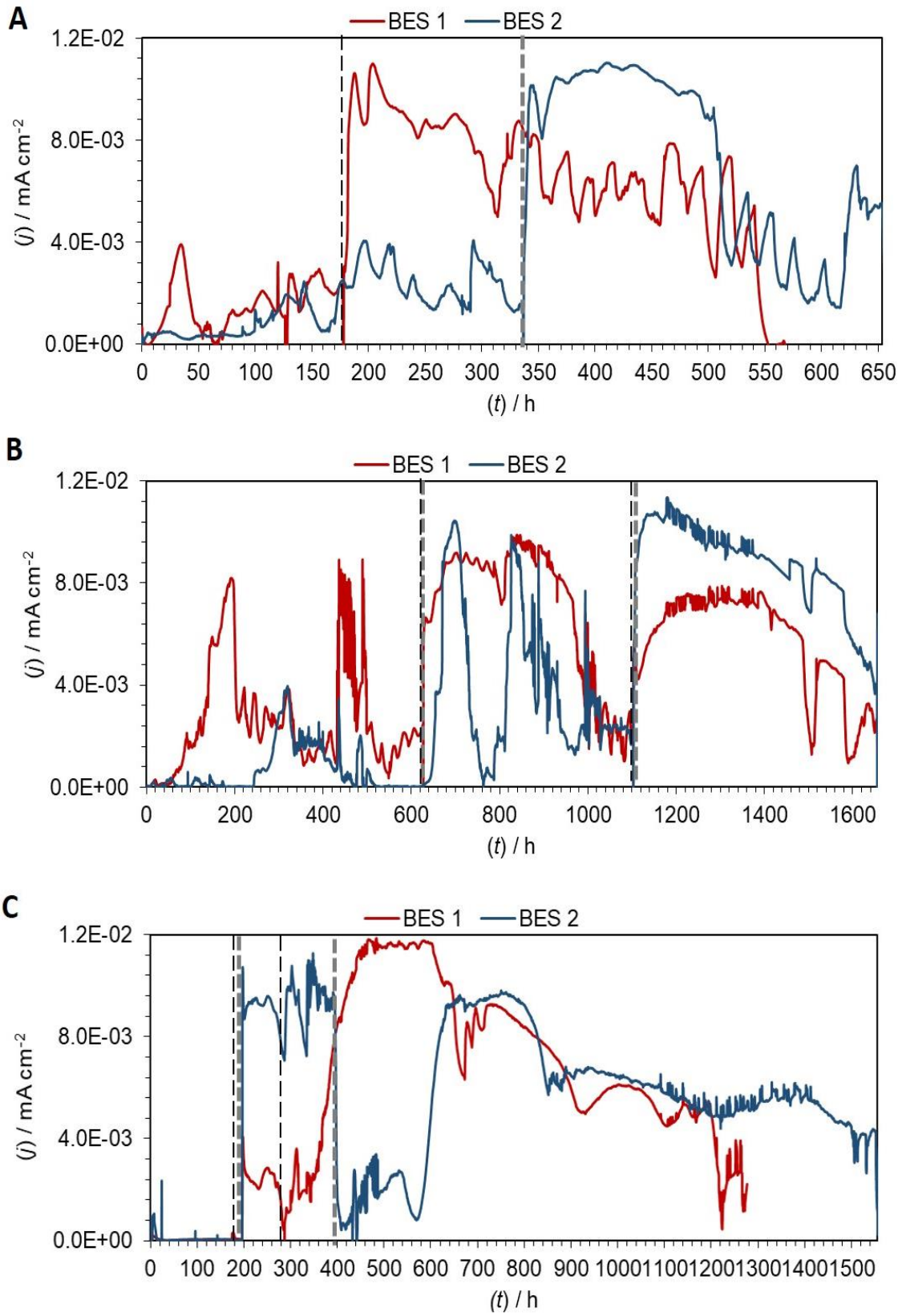


Figure 4.2. Current density over time for the BESs during bioelectrochemical reduction of 2,6-AQDS in cathode solution at A) pH = 7, B) pH = 9 and C) pH = 12 (BES 1 and BES 2 represent the duplicates). The black dash line represents the wastewater refresh for BES 1 and the grey dash line represents the wastewater refresh for BES 2.

In the first days, the current density was very low because the bacteria present in the wastewater (mixed community) need time to establish the biofilm in the anode surface, for all BES (Figure 4.2) [12].

The anode in BESs acts as electron acceptor, and its potential is determined by the potential of the microbially produced electron donor to the electrode and the rate of respiration [40]. During this adaptation period, the refreshment of wastewater was needed to decrease the limitations of carbon sources, detected when the current intensity decreased abruptly.

The wastewater was replaced at different periods of time for each BES, as identified with the black dash lines for BES 1 and the grey dash lines for BES 2, in each BESs assay (Figure 4.2). The wastewater was replaced in the anode chamber, as previously explained and also at this time the COD was analyzed (Table 4.1). After this adaptation period, the maximum current densities were reached. An average of $1.1x10^{-2}$ mA cm^{-2} for BES assembled with 2,6-AQDS at pH = 7 (Figure 4.2A), an average of $1.1x10^{-2}$ mA cm^{-2} for BES assembled with 2,6-AQDS at pH = 9 (Figure 4.2B) and an average of $1.2x10^{-2}$ mA cm^{-2} for BES assembled with 2,6-AQDS at pH = 12 (Figure 4.2C). The maximum current densities were thus similar for the diverse pH-cathode conditions studied.

Despite reports pointing out that the high pH cathode conditions can increase the conductivity in the cathode chamber of BESs [35], and highest pH difference between anodic and cathodic electrolytes in BES is ideal for higher current densities and cell potentials [36], such relation was not established in these BESs. The current densities of the BESs are related with the biofilm established in the anode surface [41], and were similar to reports with wastewater as anolyte and others chemical electrolytes as catholyte in BES [42, 43].

The OCP (mV), the CE per cycle and the concentrations of the microbial electrochemical fuels (mM) are depicted in Table 4.1 for BESs with the three cathode pH conditions studied. At steady state (OCP) low cell potentials in BESs were a result of the low potential difference established for the cells (Table 4.1), where several over potentials may occur, that were confirmed by the polarization curves results. The difference in potential between the cathode and anode varied according to the pH of the catholyte [36], from 361 mV to 805 mV for BES; In the case of OCP for BES pH = 7 the duplicates present an initial OCP (Table 4.1.) was very different in the reactors, as a result of different internal resistances, such as bioelectrochemical

adaptation to the anode culture medium and electrode. However, comparison of BESs established with 2,6-AQDS as catholyte is not direct with BES assembled with other different catholytes.

The highest CE corresponded to the cycles when the current densities reached the highest values. The highest CE were similar for the three studied conditions namely 50.8 % for BES assembled with 2,6-AQDS at pH = 7, 43.7 % BES assembled with 2,6-AQDS at pH = 9 and 46.4 % BES assembled with 2,6-AQDS at pH = 12. The values are also not very different from the reported CE (*ca.* 40 %) for BES with wastewater operated in batch conditions [44, 45].

Table 4.1. Results generated from BESs with the microbial electrochemical fuels at pH = 7, pH = 9 and pH = 12 (average values of BES 1 and BES 2).

Parameter	BES at pH = 7	BES at pH = 9	BES at pH = 12
OCP (mV)	326.5	40.9	41.3
COD (I cycle) (%)	70.2	43.1	12.6
COD (II cycle) (%)	30.5	22.1	44.9
COD (III cycle) (%)	-	62.9	31.6
CE (I cycle) (%)	4.6	12.5	1.0
CE (II cycle) (%)	50.8	43.7	7.8
CE (III cycle) (%)	-	22.6	46.4
[Microbial electrochemical fuel] (mM)	9.6	6.8	4.5

The change in COD is a measure of the concentration of organic compounds able to be oxidized in inorganic carbon [46]. A total average COD removal efficiency of 50.4 % was obtained for all cycles in the BES assembled with 2,6-AQDS at pH = 7, 42.7 % at BES assembled with 2,6-AQDS at pH = 9 and 29.7 % at BES assembled with 2,6-AQDS at pH = 12. These values are similar to previous reports with domestic wastewater as carbon source in BES operated in batch conditions [47, 48]; the COD removal in BES operated with 2,6-AQDS, has an additional advantage, that is to associate the production of an electrochemical fuel with the effluent treatment (or pre-treatment). It is thus possible to convert wastes into electrochemical energy, while treating the real wastewater.

In BES assembled with 2,6-AQDS at pH = 7 the highest COD removal efficiency was measured in cycle I, where the current densities were inferior to 1.0×10^{-2} mA cm^{-2} (Figure 4.2A); this was also the case in the BES assembled with 2,6-AQDS at pH = 12, where in cycle I the current densities were inferior to 1.2×10^{-2} mA cm^{-2}. This also confirms the relation between current

densities and the carbon oxidation by the anodic biofilm; maximum COD removal indicates a good biofilm established in the anode surface.

Polarization and power curves performed at the end of the bio-charge of 2,6-AQDSH_2 in BES 1 are represented in Figure 4.3.

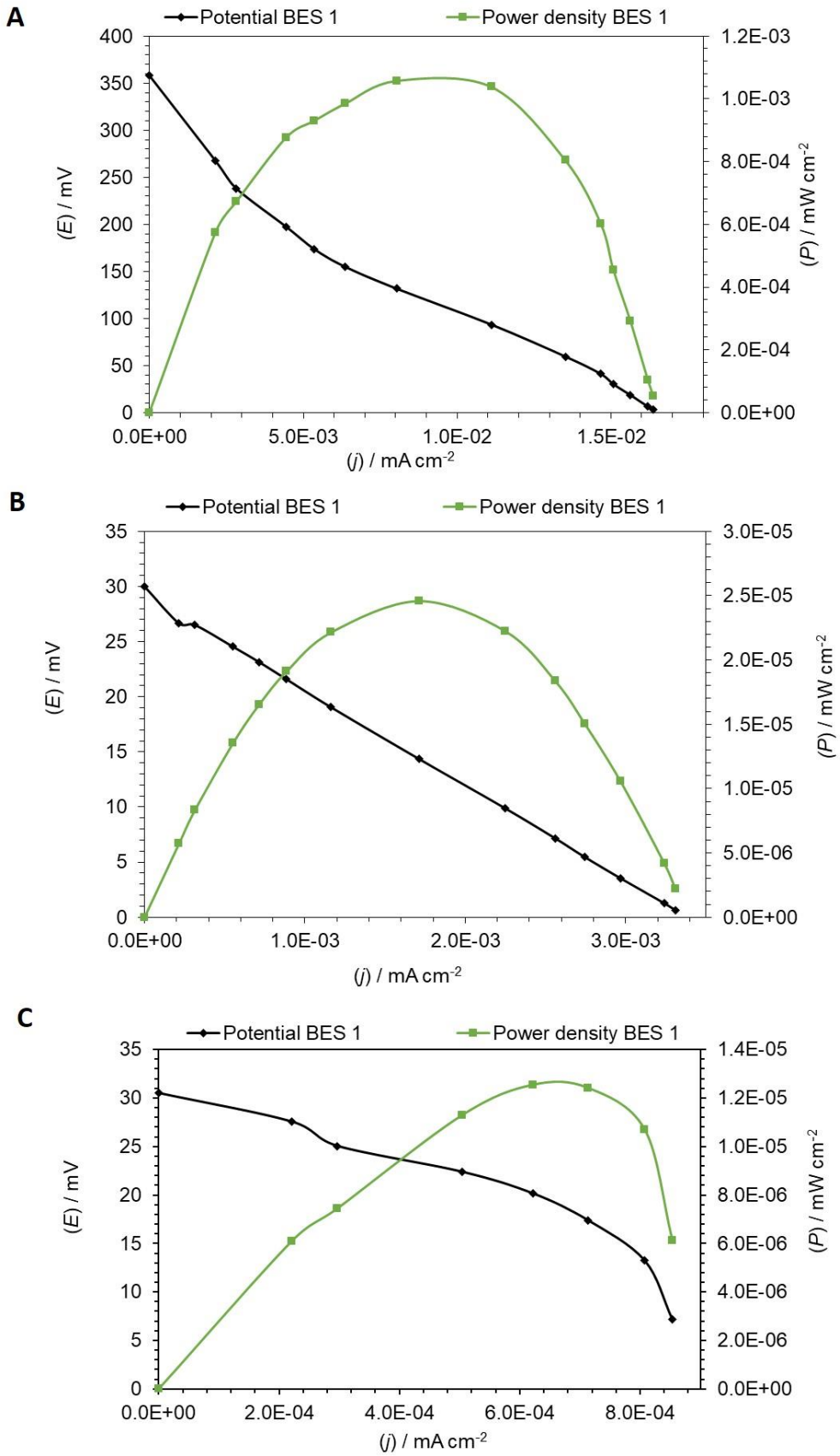


Figure 4.3. Polarization (black line) and power curves (green line) obtained at the end of BESs bio-charged 2,6-AQDSH$_2$: A) at pH = 7 (BES 1), B) at pH = 9 (BES 1) and C) at pH = 12 (BES 1). The lines were added for readability.

Maximum power densities were measured in the assay at pH = 7 (Figure 4.3A), that reached $1.1x10^{-2}$ mW cm^{-2} at $0.8x10^{-2}$ mA cm^{-2} for BES 1. Activation losses were observed to be predominant in the initial phase of the polarization curve. The second region was dominated by ohmic losses due to the influence of the internal membrane resistance, wastewater resistance and bacterial metabolism [30]; here the internal resistance was estimated in 3.6 KΩ. The mass transport affects the third region and was very accentuated due to the long-time operation and low COD in this phase.

A higher OCP was observed in the BES assembled with 2,6-AQDS at pH = 7 (326 mV). (Table 4.1; Figure 4.3A). At pH = 9 the assay recorded a low OCP of 40.9 mV (Table 4.1; Figure 4.3B), and an internal resistance of 2.1 KΩ was estimated. BES assembled with 2,6-AQDS at pH = 12 (Figure 4.3C) has also low OCP (41.3 mV) (Table 4.1) and an internal resistance of 5.5 KΩ was estimated.

The low OCP of the BES assembled with 2,6-AQDS at pH = 9 and pH = 12 can be the result of fouling of the membrane and long-time operation [49]. The nature of the microbial species/communities, with concurrent changes in the biofilm over time, the concentrations of electroactive metabolites and/or substrate may also be constantly changing with time and potential [50]. This is seen in the relation between current densities (Figure 4.1), carbon oxidation by the anodic biofilm settle at pH = 7, and the longest time for the bio-charging of BES at pH = 9 and pH = 12, with longest period of time for bacterial adaptation (current density growth); maximum COD removal indicates a good biofilm established in the anode surface at BES pH = 7. In Figure 4.3C, theirs a mass transfer resistance observed in the power density curve after usually caused by low bioanode performance or problems with the electrode assembled.

In Figure 4.4. the power and polarization curves for BES 2 are presented, showing the OCP and the researched power densities. For BES assembled with 2,6-AQDS at pH = 7 an internal resistance of 1.4 KΩ was estimated, for BES assembled with 2,6-AQDS at pH = 9 an internal resistance of 3.5 KΩ was estimated and for BES assembled with 2,6-AQDS at pH = 12 an internal resistance of 1.2 KΩ was estimated. The power and polarization curves of this duplicate were similar to the results from Figure 4.3.

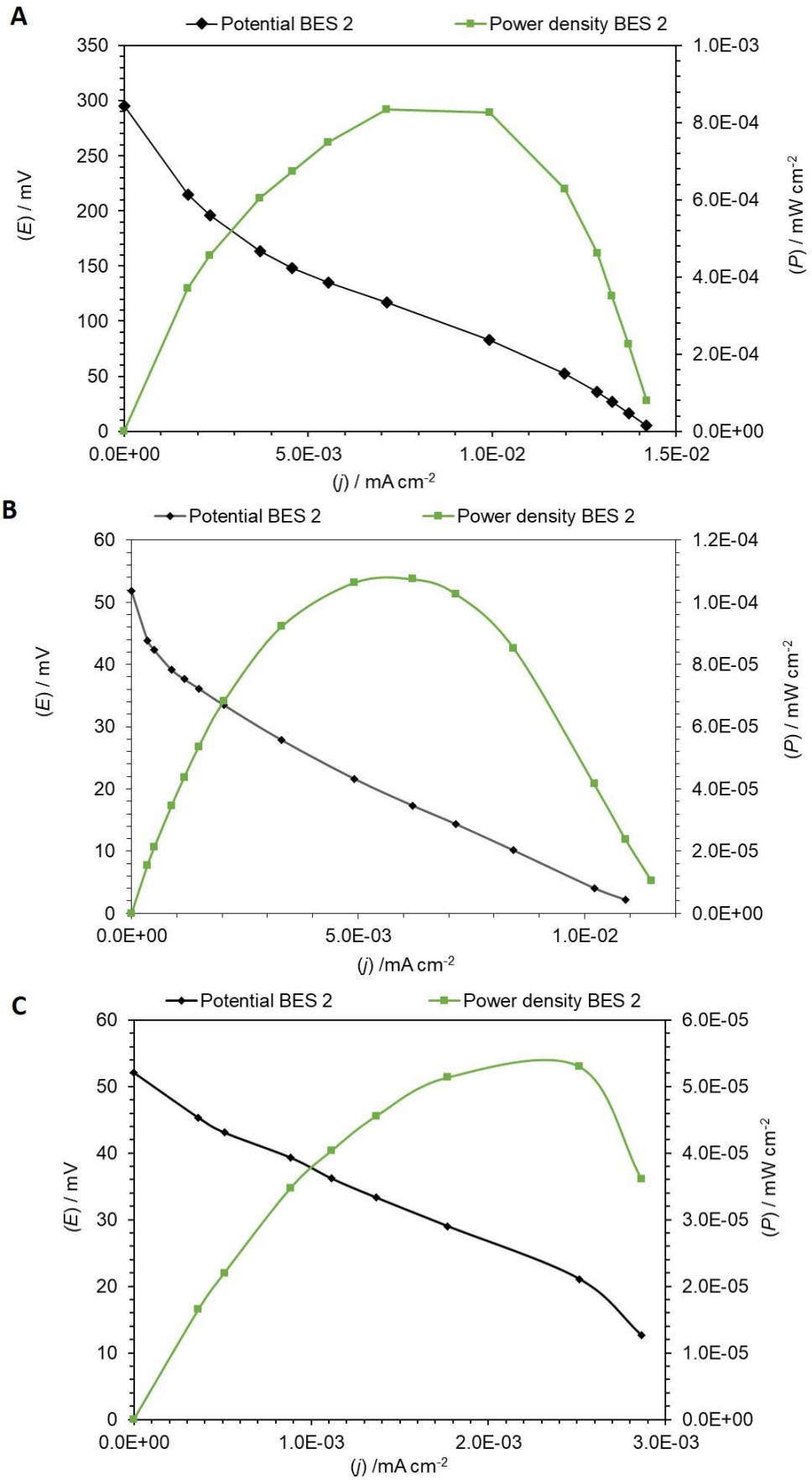


Figure 4.4. Polarization (black line) and power curves (green line) obtained at the end of BESs bio-charged 2,6-AQDSH$_2$: A) at pH = 7 (BES 2), B) at pH = 9 (BES 2) and C) at pH = 12 (BES 2). The lines were added for readability.

Microbial electrochemical fuels analysis

The concentrations of the microbial electrochemical fuels were estimated using UV-Vis Spectrophotometry, and the results are depicted in Table 4.1. The highest concentrations were reached in BES assembled with 2,6-AQDS at pH = 7 (9.6 mM), that corresponds to a 48.3 % of bio-charged 2,6-AQDSH_2.

The results are a consequence of the biofilm adaptation at the anode surface, and the high CE reached earlier in two cycles, being responsible for efficient electron and proton transfer to the cathode chamber and for the bioelectrochemical reduction (the reaction of 2,6-AQDS is a well-studied $2H^+$, $2e^-$ reaction over a full pH range of pH0-13 [27]).

At pH = 9 the concentration of the reduced quinone reached 6.8 mM and at pH = 12 the value was the lowest 4.5 mM (Table 4.1). This value was reached in a longer time of operation, as seen in the Figure 4.2. Long-time operation and lower estimated concentrations can be attributed to membrane biofouling that occurs at the membrane surface near the anode chamber [49]; this acts as physical barrier for proton transfer from the anode chamber to the cathode chamber, increasing the pH difference between chambers (pH splitting) [49], leading to deterioration of bacterial growth and reducing the performance of the BESs [51, 52].

The CV analysis of the bio-charged 2,6-AQDSH_2 for each pH conditions are represented in the Figure 4.5, for the BES used in the RFCs experiments (BES 1). The CVs in Figure 4.5 are similar to the results reported by Kim & Chung [53].

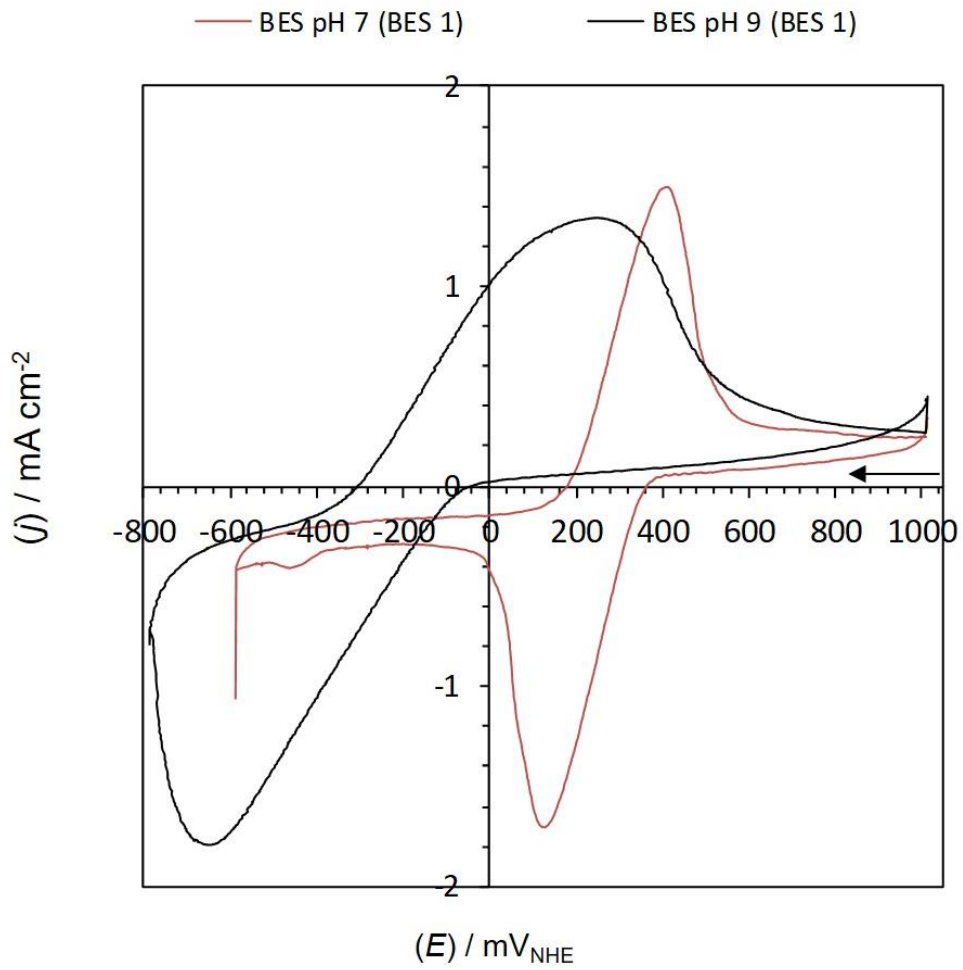


Figure 4.5. Cyclic voltammograms obtained at 1 mV s^{-1} for the bio-charged 2,6-AQDSH_2 at pH = 7 (red line) and for the bio-charged 2,6-AQDSH_2 at pH = 9 (black line) (black arrow indicates the start of scan).

The Formal Redox Potential ($E_{1/2}$) was estimated as indicated in the literature [54] and the results are presented in Table 4.2.

Table 4.2. Formal Redox Potential ($E_{1/2}$ / mV NHE) for the BESs with the three pH-cathode conditions obtained at 1 mV s^{-1}

	BES	$E_{1/2}$ / mV NHE
BES pH = 7	BES 1	281.010
BES pH = 9	BES 1	-201.290
BES pH = 12	BES 1	-32.550

The $E_{1/2}$ represents the average potential between the oxidation and reduction potentials [55]; $E_{1/2}$ is specific to the experimental conditions employed. The highest redox potential was observed with bio-charged 2,6-AQDSH_2 at pH = 7, where a quasi-reversible voltamogram was depicted (Table 4.2.). As for the $E_{1/2}$ for the bio-charged 2,6-AQDSH_2 at pH = 9, this is lower and

the effect of the pH in the redox peak is denoted as reported [27]. The $E_{1/2}$ of the bio-charged 2,6-AQDSH_2 at pH = 12 is reported, and the low value demonstrates a problem with BES, as seen in Figure 4.3.

In a general view, the BES assembled with wastewater (pH = 7) as anolyte and 2,6-AQDS at pH = 7 as catholyte, promoted the best conditions for the biofilm formation (seen in the current densities reached), that allows a higher conversion of 2,6-AQDS to 2,6-AQDSH_2. This is confirmed with the UV-Vis and the CV results. BES assembled with wastewater (pH = 7) as anolyte and 2,6-AQDS at pH = 9 and at pH = 12 as catholyte, respectively, promoted over potentials that influenced negatively the conversion to 2,6-AQDSH_2 (to be subsequently used as the negalyte in the RFCs).

RFCs results with Microbial electrochemical fuels

The RFC was loaded with the negalyte 2,6-AQDSH_2 bio-charged at pH = 7, 9 and 12, and with posilyte $[Fe(CN)_6]^{3-}$ charged using a power supply, for obtaining a potential *vs.* current discharge characteristic curves. The discharge redox reactions are the following (E^0 [V, 25 °C, pH=7], achieved with Nernst Equation) [56]:

$C_{14}H_8Na_2O_8S_2 \rightarrow C_{14}H_6Na_2O_8S_2 + 2H^+ + 2e^-$ E^0_{oxd} = 0.184 V *vs.* NHE **4.4.**

$[Fe(CN)_6]^{3-} + e^- \rightarrow [Fe(CN)_6]^{4-}$ E^0_{red} = 0.436 V *vs.* NHE **4.5.**

where $[Fe(CN)_6]^{3-}$ was selected as posilyte because of its fast reaction kinetics and because the reduction potential, which in combination with the 2,6-AQDSH_2 displays a nominal potential difference of 0.620 V.

Charge–discharge curves history is shown in Figure 4.6 for a current density of 3.75 mA cm^{-2}, between 0.200 V and 0.900 V, imposed by the electrochemical station. The concentration of the bio-charged 2,6-AQDSH_2 was 9.6 mM and the concentration of the posilyte was 20 mM. The potential history for the 9 cycles is represented in Figure 4.6A, while the battery efficiency and battery capacity are shown in Figure 4.6B and Figure 4.6C, respectively.

The efficiencies indicators of the RFC were stable over the performed number of cycles. It can be observed that the CE is *ca.* 100 %, the PE is *ca.* 55 % and the EE is *ca.* 54 %; a capacity loss of *ca.* 30 % was observed over the 9 cycles.

The same RFC operation conditions were set for the bio-charged negalytes at pH = 9 and at pH = 12, where the concentration of 2,6-AQDSH_2 was 6.8 mM and 4.5 mM, respectively. The concentration of the posilyte was 10 mM for both cases.

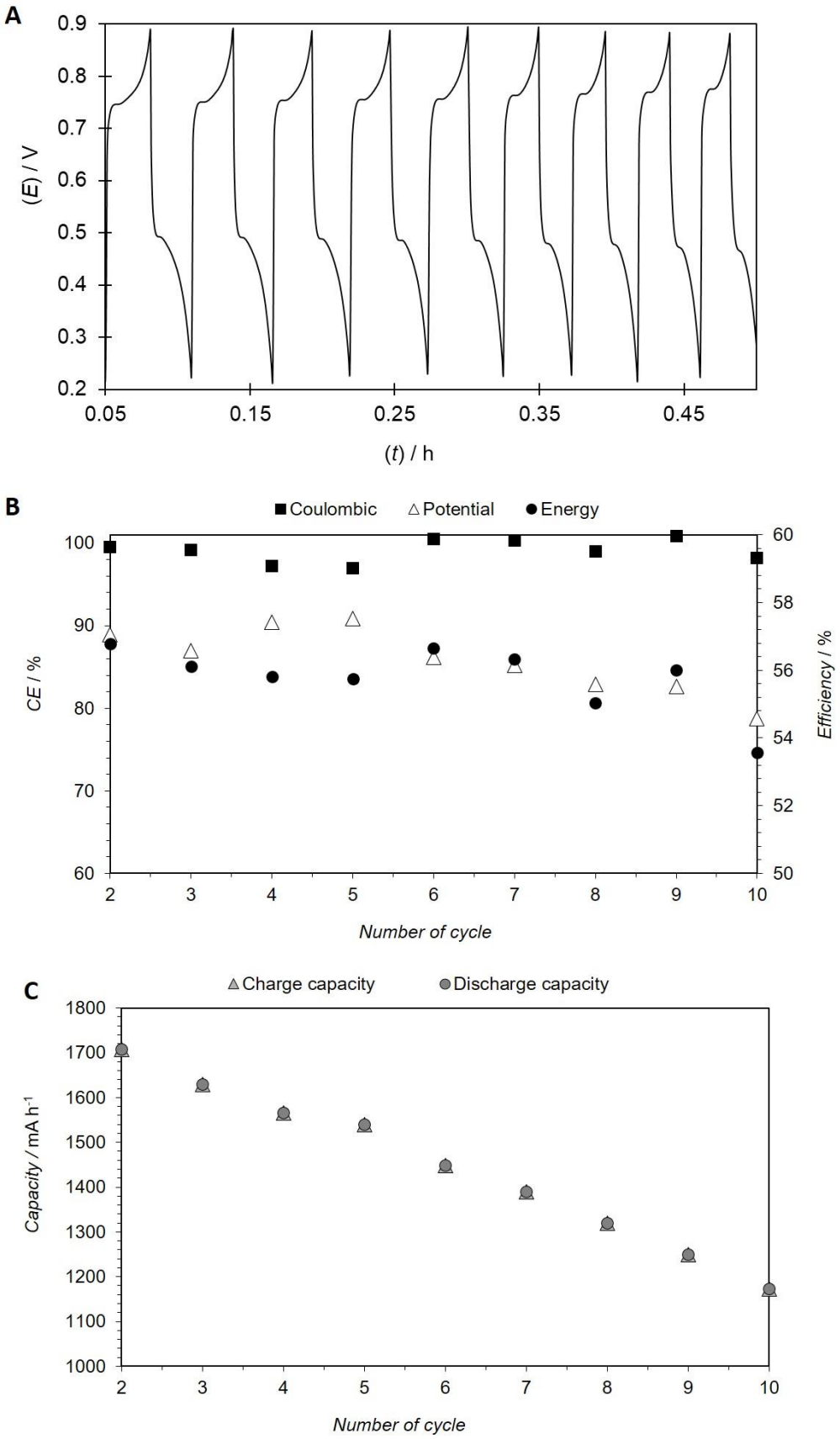


Figure 4.6. Charge–discharge curves history for 9 cycles (A), Coulombic (black square), Potential (white triangle) and Energy efficiencies (black circle) versus the cycle number (B) and capacity data (C) at a current density of 3.75 mA cm^{-2} for the RFC loaded with $[Fe(CN)_6]^{3-}$ – posilyte – with initially bioelectrochemically-charged 2,6-$AQDSH_2$ at pH = 7 – negalyte.

The potential history of RFCs with bio-charged negalyte at pH = 9 exhibited a CE of *ca.* 70 % (Figure 4.7), but a significant loss of capacity occurred, due to the high current density applied.

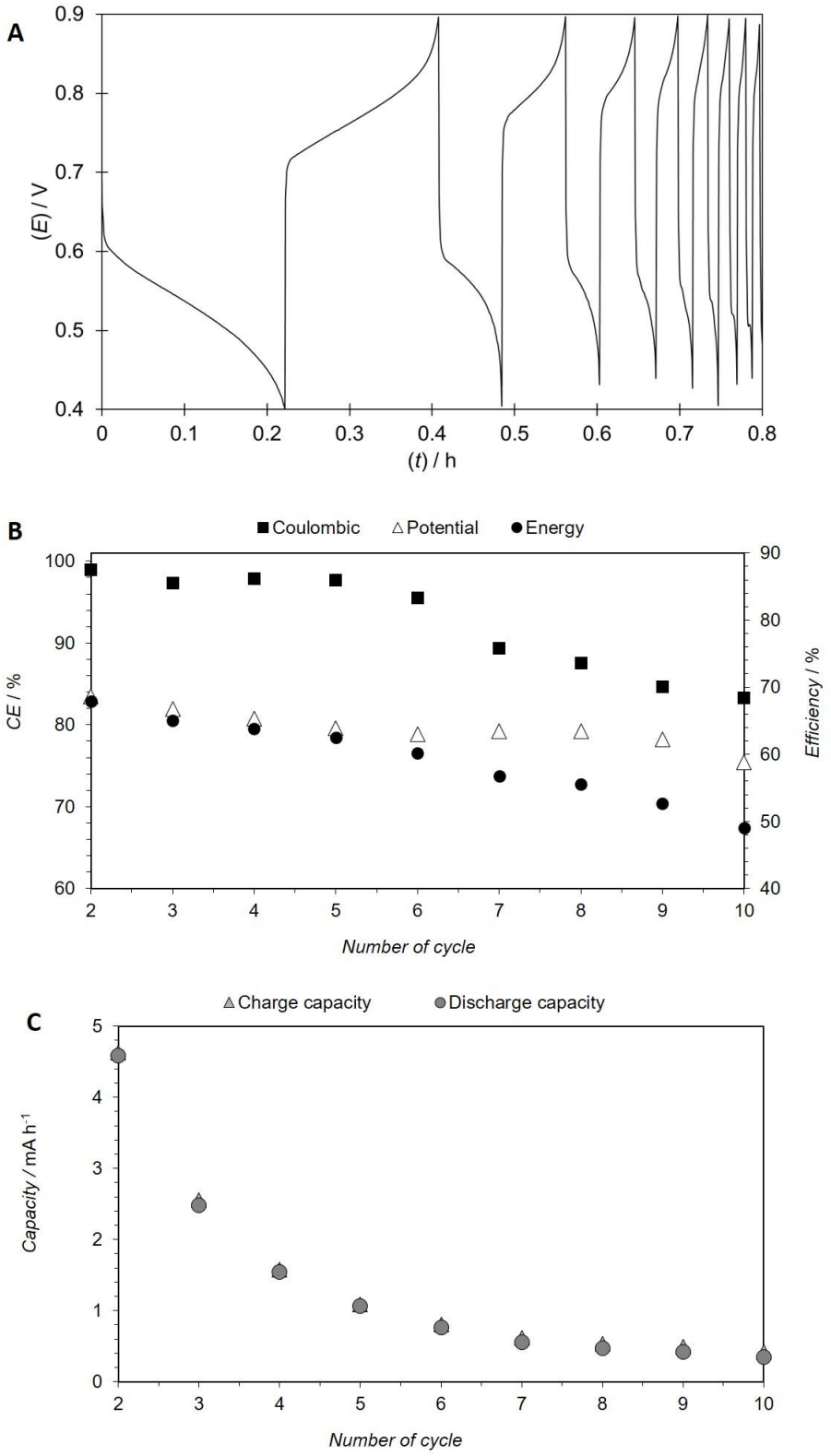


Figure 4.7. Charge–discharge curves history for 9 cycles (A), Coulombic (black square), Potential (white triangle) and Energy efficiencies (black circle) versus the cycle number (B) and capacity data (C) at a current density of 3.75 mA cm^{-2} for the RFC loaded with $[Fe(CN)_6]^{3-}$ – posilyte – with initially bioelectrochemically-charged 2,6-$AQDSH_2$ at pH = 9 – negalyte.

The CE bio-charged negalyte at pH = 12 (Figure 4.8) displays a much worse performance, with minimal charge-discharge energy.

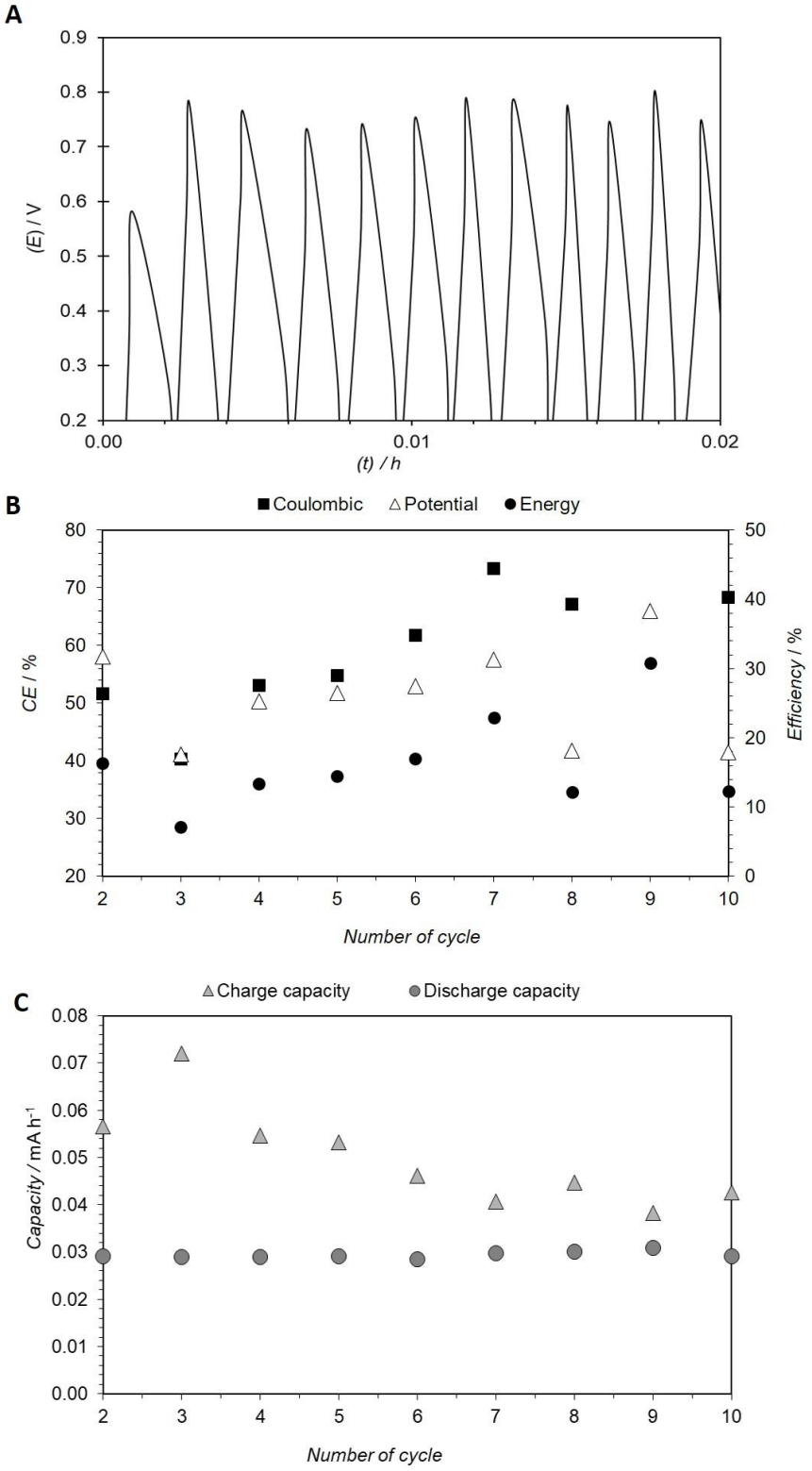


Figure 4.8. Charge–discharge curves history for 9 cycles (A), Coulombic (black square), Potential (white triangle) and Energy efficiencies (black circle) versus the cycle number (B) and capacity data (C) at a current density of 3.75 mA cm^{-2} for the RFC loaded with $[Fe(CN)_6]^{3-}$ – posilyte – with initially bioelectrochemically-charged 2,6-$AQDSH_2$ at pH = 12 – negalyte.

4.4. Conclusion

The coupling a BES with a RFC demonstrated a new way to convert wastewater biomass into electrochemical energy using microorganisms, in a device named Microbial Redox Flow Cell. The microbial electrochemical fuels are easily and efficiently discharged into electricity, making this electricity dispatchable. In the present work, only the negalyte, 2,6-AQDS, was bio-charged, while the posilyte $[Fe(CN)_6]^{4-}$ was charged using a power supply.

To charge the negalyte (2,6-AQDS) at pH = 7, a BES loaded with a mixed microbial community was used, which was able, after several days, to charge the electrolyte with CEs *ca.* 40 %. The bio-charged negalyte (2,6-$AQDSH_2$) was then used in a RFC with posilyte $[Fe(CN)_6]^{3-}$ and the 9 discharge-charge cycles performed at 3.75 mA cm^{-2}; after the first discharge cycle, the RFC was charged using the electrochemical station. The RFC displayed a CE close to 100 %, a PE of *ca.* 55 % and an EE of 54 %, when equipped with a Nafion™ NM 117 PEM. At pH = 9 and pH = 12 the obtained results were far worse.

The higher wastewater COD removal reached in BESs during the bio-charged of 2,6-$AQDSH_2$, set in the coupling process is a wastes valorization and a way to reach circular economy. A Microbial Redox Flow Cell with bio-charged redox pairs is advantageous and can be charged unbiased, while other processes such as microbially water splitting is a biased process [57].

4.5. Acknowledgements

M.S.S. Santos is grateful to Portuguese Foundation for Science and Technology (FCT) for her PhD Grant (reference: SFRH/BD/104087/2014). J. Azevedo would like to acknowledge the Portuguese Foundation for Science and Technology (FCT) for funding (CEECIND/03937/2017). The authors would like to acknowledge to the FCT under the scope of the strategic funding of UID/BIO/04469 unit and COMPETE 2020 (POCI-01-0145-FEDER-006684) and BioTecNorte operation (NORTE-01-0145-FEDER-000004) funded by the European Regional Development Fund (ERDF), under the scope of Norte2020 - Programa Operacional Regional do Norte. The authors also acknowledge the Projects: i) POCI-01-0145-FEDER-006939 (LEPABE - Laboratory for Process Engineering, Environment, Biotechnology and Energy – UID/EQU/00511/2013), funded by the ERDF, through COMPETE2020 – Programa Operacional

Competitividade e Internacionalização (POCI) and by nationals funds through FCT, ii) by the Project SunStorage - Harvesting and storage of solar energy", with reference POCI-01-0145-FEDER-016387, funded by ERDF, through COMPETE 2020 --POCI), and by national funds, through FCT, iii) NORTE-01-0145-FEDER-000005 – LEPABE-2-ECO-INNOVATION, supported by North Portugal Regional Operational Programme (Norte 2020), under the Portugal 2020 Partnership Agreement, through the ERDF and iv) Project PTDC/EQU-EQU/30510/2017 - POCI-01-0145-FEDER-030510 – Sunflow "Solar energy storage into redox flow batteries" funded by FEDER funds through COMPETE2020 - Programa Operacional Competitividade e Internacionalização (POCI) and by national funds (PIDDAC) through FCT/MCTES.. The authors are indebted with all the colleagues who assisted in the laboratory work, in particular to Dr. Sónia Barbosa for help with microbial fuel cell operation.

4.6. References

[1] Z. Guo, Y. Sun, S.-Y. Pan, P.-C. Chiang, Integration of green energy and advanced energy-efficient technologies for municipal wastewater treatment plants, Int. J. Environ. Res. Public Health. 16 (2019) 1–29.

[2] R. Kollmann, G. Neugebauer, F. Kretschmer, B. Truger, H. Kindermann, G. Stoeglehner, T. Ertl, M. Narodoslawsky, Renewable energy from wastewater - practical aspects of integrating a wastewater treatment plant into local energy supply concepts, J. Clean. Prod. 155 (2017) 119–129.

[3] M. Lu, S. Chen, S. Phadke, M. Salvacion, A. Mirhosseini, S. Chan, K. Carpenter, R. Cortese, O. Bretschger, Long-term performance of a 20-L continuous flow microbial fuel cell for treatment of brewery wastewater, J. Power Sources. 356 (2017) 274–287.

[4] K. Tota-Maharaj, P. Paul, Performance of pilot-scale microbial fuel cells treating wastewater with associated bioenergy production in the Caribbean context, Int. J. Energy Environ. Eng. 6 (2015) 213–220.

[5] F.J. Hernández-Fernández, A. Pérez De Los Ríos, M.J. Salar-García, V.M. Ortiz-Martínez, L.J. Lozano-Blanco, C. Godínez, F. Tomás-Alonso, J. Quesada-Medina, Recent progress and perspectives in microbial fuel cells for bioenergy generation and wastewater treatment, Fuel Process. Technol. 138 (2015) 284–297.

[6] D. Pant, G. Van Bogaert, L. Diels, K. Vanbroekhoven, A review of the substrates used in microbial fuel cells (MFCs) for sustainable energy production, Bioresour. Technol. 101 (2010) 1533–1543.

[7] K.J. Chae, M. Choi, F.F. Ajayi, W. Park, I.S. Chang, I.S. Kim, Mass transport through a Proton Exchange Membrane (Nafion) in Microbial Fuel Cells, Energy and Fuels. 22 (2008) 169–176.

[8] H. Wang, Z.J. Ren, Bioelectrochemical metal recovery from wastewater: A review, Water Res. 66 (2014) 219–232.

[9] O. Lefebvre, A. Uzabiaga, I.S. Chang, B.H. Kim, H.Y. Ng, Microbial fuel cells for energy self-sufficient domestic wastewater treatment-a review and discussion from energetic consideration, Appl. Microbiol. Biotechnol. 89 (2011) 259–270.

[10] K.P. Nevin, H. Richter, S.F. Covalla, J.P. Johnson, T.L. Woodard, A.L. Orloff, H. Jia, M. Zhang, D.R. Lovley, Power output and columbic efficiencies from biofilms of *Geobacter sulfurreducens* comparable to mixed community microbial fuel cells, Environ. Microbiol. 10 (2008) 2505–2514.

[11] M.S.S. Santos, L. Peixoto, C. Dias-Ferreira, A. Mendes, M.M. Alves, Microbially charged redox flow batteries for bioenergy storage, in: R.N. Krishnaraj, R.K. Sani (Eds.), Bioelectrochemical Interface Eng., Wiley, 14 (2019) 251–269.

[12] L. Peixoto, P. Parpot, G. Martins, Assessment of electron transfer mechanisms during a long-term sediment Microbial Fuel Cell operation, 12 (2019) 1–13.

[13] L. Peixoto, A.L. Rodrigues, G. Martins, A. Nicolau, A.G. Brito, M.M. Silva, P. Parpot, R. Nogueira, A flat microbial fuel cell for decentralized wastewater valorization: process performance and optimization potential, Environ. Technol. 34 (2013) 1947–1956.

[14] G. Martins, L. Peixoto, D.C. Ribeiro, P. Parpot, A.G. Brito, R. Nogueira, Towards implementation of a benthic microbial fuel cell in lake Furnas (Azores): Phylogenetic affiliation and electrochemical activity of sediment bacteria, Bioelectrochemistry. 78 (2010) 67–71.

[15] L. Ren, Y. Ahn, B.E. Logan, A two-stage Microbial Fuel Cell and Anaerobic Fluidized Bed Membrane Bioreactor (MFC-AFMBR) System for effective domestic wastewater Treatment, 48 (2014) 4199−4206.

[16] D.A. Jadhav, S. Ghosh Ray, M.M. Ghangrekar, Third generation in bio-electrochemical system research – a systematic review on mechanisms for recovery of valuable by-products from wastewater, Renew. Sustain. Energy Rev. 76 (2017) 1022–1031.

[17] Y. Zhang, M. Liu, M. Zhou, H. Yang, L. Liang, T. Gu, Microbial fuel cell hybrid systems for wastewater treatment and bioenergy production: synergistic effects, mechanisms and challenges, Renew. Sustain. Energy Rev. 103 (2019) 13–29.

[18] G. Lui, G. Jiang, M. Fowler, A. Yu, Z. Chen, A high performance wastewater-fed flow-photocatalytic fuel cell, J. Power Sources. 425 (2019) 69–75.

[19] Y.L. Oon, S.A. Ong, L.N. Ho, Y.S. Wong, Y.S. Oon, H.K. Lehl, W.E. Thung, Hybrid system up-flow constructed wetland integrated with microbial fuel cell for simultaneous wastewater treatment and electricity generation, Bioresour. Technol. 186 (2015) 270–275.

[20] K.P. Katuri, K. Scott, Electricity generation from the treatment of wastewater with a hybrid up-flow microbial fuel cell, Biotechnol. Bioeng. 107 (2010) 52–58.

[21] A.Z. Weber, M.M. Mench, J.P. Meyers, P.N. Ross, J.T. Gostick, Q. Liu, Redox flow batteries: a review, J. Appl. Electrochem. 41 (2011) 1137–1164.

[22] U. Er, C. Suh, M.P. Marshak, A. An Aspuru-Guzik, Computational design of molecules for an all-quinone redox flow battery, Chem. Sci. 6 (2015) 845–1592.

[23] Y. Moon, Y.-K. Han, Computational screening of organic molecules as redox active species in redox flow batteries, Curr. Appl. Phys. 16 (2016) 939–943.

[24] K. Arumugam, U. Becker, Computational redox potential predictions: applications to inorganic and organic aqueous complexes, and complexes adsorbed to mineral surfaces, Minerals. 4 (2014) 345–387.

[25] B. Yang, L. Hoober-Burkhardt, F. Wang, G.K. Surya Prakash, S.R. Narayanan, An inexpensive aqueous flow battery for large-scale electrical energy storage based on water-soluble organic redox couples, J. Electrochem. Soc. 161 (2014) A1371–A1380.

[26] Y. Wu, F. Li, T. Liu, R. Han, X. Luo, pH dependence of quinone-mediated extracellular electron transfer in a bioelectrochemical system, Electrochim. Acta. 213 (2016) 408–415.

[27] C. Batchelor-mcauley, Q. Li, S.M. Dapin, R.G. Compton, Voltammetric characterization of DNA Iintercalators across the full pH range : anthraquinone-2,6-disulfonate and anthraquinone-2-sulfonate, J. Phys. Chem. B. 114 (2010) 4094–4100.

[28] M.E. Rodrigues da Silva, P.I.M. Firmino, A.B. dos Santos, Impact of the redox mediator sodium anthraquinone-2,6-disulphonate (AQDS) on the reductive decolourisation of the azo dye Reactive Red2 (RR2) in one- and two-stage anaerobic systems, Bioresour. Technol. 121 (2012) 1–7.

[29] C. Feng, L. Ma, F. Li, H. Mai, X. Lang, S. Fan, A polypyrrole/anthraquinone-2,6-disulphonic disodium salt (PPy/AQDS)-modified anode to improve performance of microbial fuel cells, Biosens. Bioelectron. 25 (2010) 1516–1520.

[30] A. Faria, L. Gonçalves, J.M. Peixoto, L. Peixoto, A.G. Brito, G. Martins, Resources recovery in the dairy industry: bioelectricity production using a continuous microbial fuel cell, J. Clean. Prod. 140 (2017) 971–976.

[31] K. Wedege, E. Dražević, D. Konya, A. Bentien, Organic Redox Species in Aqueous Flow Batteries: redox potentials, chemical stability and solubility, Sci. Rep. 6 (2016) 1–13.

[32] D.G. Kwabi, K. Lin, Y. Ji, E.F. Kerr, M. Goulet, D. De Porcellinis, D.P. Tabor, D.A. Pollack, A. Aspuru-Guzik, R.G. Gordon, M.J. Aziz, Alkaline Quinone Flow Battery with long lifetime at pH 12, Joule. 2 (2018) 1894–1906.

[33] R. A. Rozendal, H.V.M. Hamelers, C.J.N. Buisman, Effects of membrane cation transport on pH and Microbial Fuel, Environ. Sci. Technol. 40 (2006) 5206–5211.

[34] G.S. Jadhav, M.M. Ghangrekar, Performance of microbial fuel cell subjected to variation in pH, temperature, external load and substrate concentration, Bioresour. Technol. 100 (2009) 717–723.

[35] A. Cadena, A.–C. Texier, I. González, F.J. Cervantes, J. Gómez, Qualitative and quantitative determination of a humic model compound in microbial cultures by cyclic voltammetry, Environ. Technol. 28 (2007) 1035–1044.

[36] B.E. Logan, B. Hamelers, R. Rozendal, U. Schröder, J. Keller, S. Freguia, P. Aelterman, W. Verstraete, K. Rabaey, Microbial fuel cells: methodology and technology, Environ. Sci. Technol. 40 (2006) 5181–5192.

[37] B.E. Logan, Microbial Fuel Cells, John Wiley & Sons, Inc., Hoboken, NJ, USA, 2007.

[38] J. Azevedo, T. Seipp, J. Burfeind, C. Sousa, A. Bentien, J.P. Araújo, A. Mendes, Unbiased solar energy storage: Photoelectrochemical redox flow battery, Nano Energy. 22 (2016) 396–405.

[39] R. Monteiro, J. Leirós, M. Boaventura, A. Mendes, Insights into all-vanadium redox flow battery: A case study on components and operational conditions, Electrochim. Acta. 267 (2018) 80–93.

[40] I. Torres, A.K. Marcus, B.E. Rittmann, Proton transport inside the biofilm limits electrical current generation by anode-respiring bacteria, Biotechnol. Bioeng. 100 (2008) 872–881.

[41] N.S. Malvankar, T.M. Tuominen, D.R. Lovley, Biofilm conductivity is a decisive variable for high-current-density *Geobacter sulfurreducens* microbial fuel cells, Energy Environ. Sci. 5 (2012) 5790–5797.

[42] S.B. Velasquez-Orta, I.M. Head, T.P. Curtis, K. Scott, Factors affecting current production in microbial fuel cells using different industrial wastewaters, Bioresour. Technol. 102 (2011) 5105–5112.

[43] S. Oh, B. Min, Cathode performance as a factor in electricity generation in Microbial Fuel Cells, Env. Sci Technol. 38 (2004) 4900–4904.

[44] T.C. Pannell, R.K. Goud, D.J. Schell, A.P. Borole, Effect of fed-batch *vs.* continuous mode of operation on microbial fuel cell performance treating biorefinery wastewater, Biochem. Eng. J. 116 (2016) 85–94.

[45] U. Karra, S.S. Manickam, J.R. McCutcheon, N. Patel, B. Li, Power generation and organics removal from wastewater using activated carbon nanofiber (ACNF) microbial fuel cells (MFCs), Int. J. Hydrogen Energy. 38 (2013) 1588–1597.

[46] B. Jiang, T. Muddemann, U. Kunz, H. Bormann, M. Niedermeiser, D. Haupt, O. Schläfer, M. Sievers, Evaluation of Microbial Fuel Cells with Graphite Plus MnO_2 and MoS_2 paints as oxygen reduction cathode catalyst, J. Electrochem. Soc. 164 (2017) H3083–H3090.

[47] I. Gajda, J. Greenman, C. Melhuish, I.A. Ieropoulos, Electricity and disinfectant production from wastewater: Microbial Fuel Cell as a self-powered electrolyser, Sci. Rep. 6 (2016) 1–9.

[48] M.H. Do, H.H. Ngo, W.S. Guo, Y. Liu, S.W. Chang, D.D. Nguyen, L.D. Nghiem, B.J. Ni, Challenges in the application of microbial fuel cells to wastewater treatment and energy production: A mini review, Sci. Total Environ. 639 (2018) 910–920.

[49] J.X. Leong, W.R.W. Daud, M. Ghasemi, K. Ben Liew, M. Ismail, Ion exchange membranes as separators in microbial fuel cells for bioenergy conversion: A comprehensive review, Renew. Sustain. Energy Rev. 28 (2013) 575–587.

[50] F. Zhao, R.C.T. Slade, J.R. Varcoe, Techniques for the study and development of microbial fuel cells : an electrochemical perspective, 7 (2009) 1–54.

[51] J. Xu, G.P. Sheng, H.W. Luo, W.W. Li, L.F. Wang, H.Q. Yu, Fouling of proton exchange membrane (PEM) deteriorates the performance of microbial fuel cell, Water Res. 46 (2012) 1817–1824.

[52] T.H. Choi, Y. Bin Won, J.W. Lee, D.W. Shin, Y.M. Lee, M. Kim, H.B. Park, Electrochemical performance of microbial fuel cells based on disulfonated poly(arylene ether sulfone) membranes, J. Power Sources. 220 (2012) 269–279.

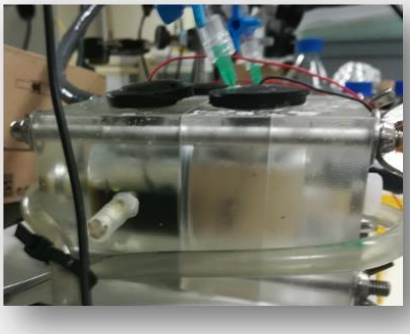
[53] R.S. Kim, T.D. Chung, The electrochemical reaction mechanism and applications of quinones, Bull. Korean Chem. Soc. 35 (2014) 3143–3155.

[54] M.F.C.G. Silva, Voltametria Cíclica — Aplicações ao estudo de mecanismos de reacções induzidas por transferência eletrónica, Técnicas Exp. 70 (1998) 20–26.

[55] N. Elgrishi, K.J. Rountree, B.D. McCarthy, E.S. Rountree, T.T. Eisenhart, J.L. Dempsey, A practical beginner's guide to Cyclic Voltammetry, J. Chem. Educ. 95 (2018) 197–206.

[56] K. Scott, E.H. Yu, Microbial Electrochemical and Fuel Cells: Fundamentals and applications, Elsevier, 2016.

[57] J.P. Torella, C.J. Gagliardi, J.S. Chen, D.K. Bediako, B. Colón, J.C. Way, P.A. Silver, D.G. Nocera, Efficient solar-to-fuels production from a hybrid microbial – water-splitting catalyst system, Proc. Natl. Acad. Sci. 112 (2015) 2337–2342.





Chapter 5

Bioelectrochemical energy storage in a Microbial Redox Flow Cell

Abstract[1]

Biomass is an efficient and a sustainable source of renewable energy with high potential to generate electricity. We report a Microbial Redox Flow Cell (MRFC) that demonstrates the integration of Bioelectrochemical Systems (BESs) with a Redox Flow Cell (RFC); it is an innovative approach to generate bioelectrochemical energy and store it in MRFC. The MRFC uses *Geobacter sulfurreducens* as Exoelectrogenic Bacteria for reduction of anthraquinone-2,6-disulfonate (2,6-AQDS) in anthrahydroquinone-2,6-disulfonate (2,6-$AQDSH_2$), and as electrotrophic bacteria for oxidation of the redox pair ferrocyanide, ($[Fe(CN)_6]^{4-}$). The bio-converted redox pairs, herein referred as microbial electrochemical fuels were integrated in a RFC as negalyte and posilyte. In the reduction of 2,6-AQDS, BES bioanodes generated the current density of 0.048 mA cm^{-2} with a conversion *ca.* 27 %. In the oxidation of $[Fe(CN)_6]^{4-}$, 66.7 % of $[Fe(CN)_6]^{4-}$ was oxidized to Ferricyanide ($[Fe(CN)_6]^{3-}$) in BES with biocathodes. The RFC with the microbial electrochemical fuels was operated with the Coulombic efficiency of *ca.* 90 %.

[1] The work presented in this chapter corresponds to the following scientific article: M.S.S. Santos, L. Peixoto, K. Mushtaq, C. Dias-Ferreira, A. Mendes, M.M. Alves, Bioelectrochemical energy storage in a Microbial Redox Flow Cell 2020 (redrafted from Nano Energy (submitted)).

Chapter 5

5.1. Introduction

Unbiased energy technologies should be used to generate dispatchable renewable energy [1]. Solar or wind are highly explored for different energy generation and storage devices [1, 2] and are attractive because they can operate at any place and in large systems [3, 4]. Nevertheless, these sources of renewable energy are intermittent, due to natural limitations, and demonstrate a high discrepancy between energy generation and consumption [5].

Biomass is a renewable energy source that can be transformed into solid, liquid, and gaseous fuels [6]. Electrochemically Active Bacteria (EAB) [7] use biomass to generate energy from oxidation of carbon sources which act as fuels in Microbial Fuel Cells (MFCs) [8]. In Microbial Electrolysis Cells, and in Microbial Electrosynthesis Cells, electrons are released from EAB and a biased potential is applied for the production of valuable compounds such as methane or hydrogen [9] or for the synthesis of organic acids [10]. The major advantages of the Bioelectrochemical Systems (BESs) include the low cost of reactor, type of fuels (widely available carbon sources) and environmentally friendly operating conditions [11]. BESs can be combined, integrated or coupled in hybrid electrochemical technologies [12], for example pretreatment/post treatment of wastewater with membrane bioreactor [13], forward osmosis [14], anaerobic digesters [15] and/or energy recovery [16].

Redox Flow Cells (RFCs) are electrochemical devices that can generate and store electrochemical energy including in large scale systems [17]. The chemical energy in RFCs is stored by redox electroactive species dissolved in aqueous solutions (redox pairs) [18]. The redox pairs are pumped from external tanks towards the power conversion unit, where redox reactions take place resulting in transformation of electrical energy into chemical energy and vice versa [18]. Aqueous organic RFCs are being investigated with several organic compounds, *e.g.* quinones [19] and flavins [20], to replace ion metals. Organic redox species are ideal due to abundancy, environment friendliness, their redox chemical window, solubility and low chemical cost (due to water based solvents) [21].

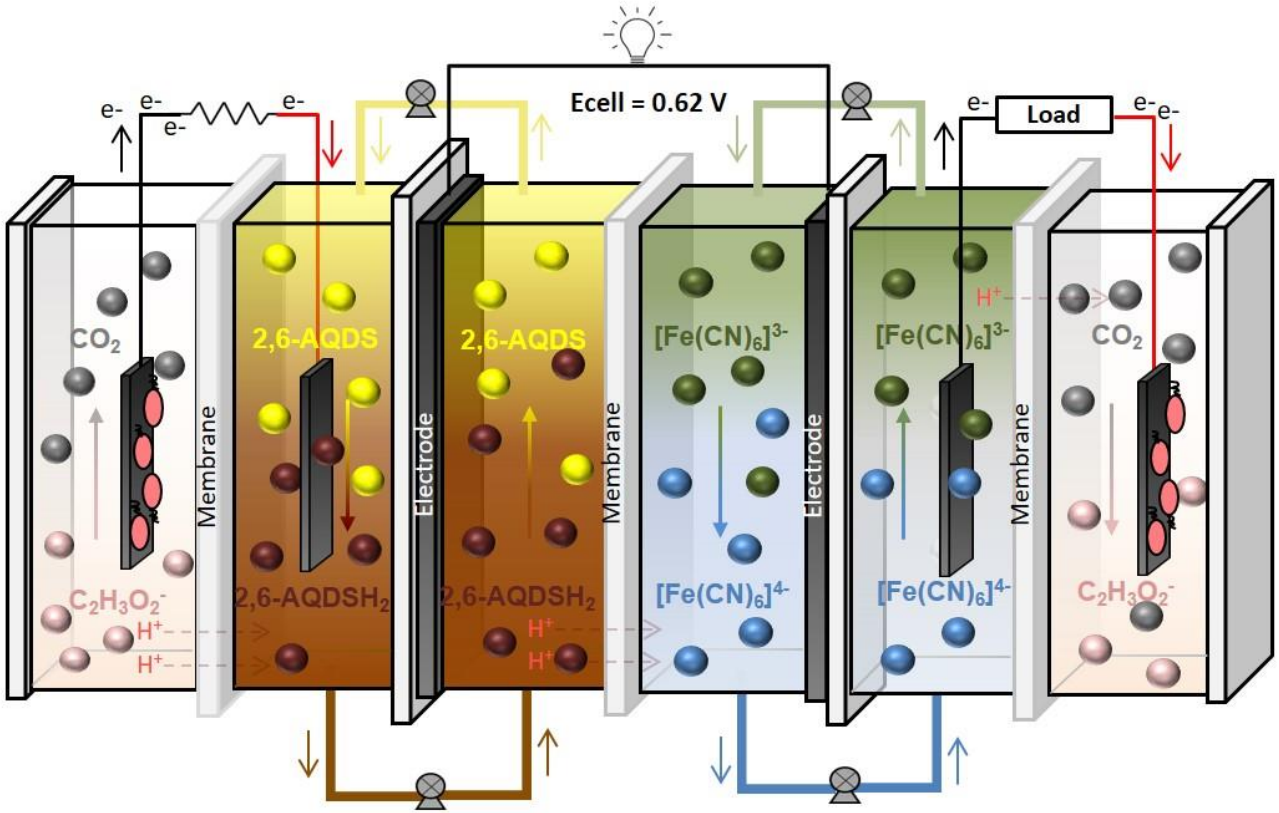
This study uses BESs to charge both negalyte and posilyte redox pairs (microbial electrochemical fuels) and feed them to a RFC for producing electricity. The whole system is herein named Microbial Redox Flow Cell (MRFC) and has the ability to transform the electrical energy generated by the EAB directly into storable energy, as illustrated in Figure 5.1.

Geobacter sulfurreducens was selected because it can operate as an exoelectrogenic and electrotrophic bacteria, presenting ideal characteristics to demonstrate the concept of the MRFC [22]. The MRFC loaded with *G. sulfurreducens* as exoelectrogenic bacteria (BES bioanode) was able to reduce the negalyte anthraquinone-2,6-disulfonate ($C_{14}H_6Na_2O_8S_2$, 2,6-AQDS) to anthrahydroquinone-2,6-disulfonate ($C_{14}H_8Na_2O_8S_2$, 2,6-AQDSH$_2$), with no external bias potential. As for the posilyte of the MRFC, the ferrocyanide ($[Fe(CN)_6]^{4-}$) was charged using *G. sulfurreducens* as electrotrophic bacteria to ferricyanide ($[Fe(CN)_6]^{3-}$), at the cathode side. The 2,6-AQDS and $[Fe(CN)_6]^{4-}$ were selected as redox pairs for their good electrochemical reaction kinetics, water solubility and redox potentials [23, 24].

5.2. Materials and methods

Bacteria cultivation

Geobacter sulfurreducens (DSM 12127) was used in both BES. Firstly, the culture medium was prepared with 1.50 g L^{-1} NH_4Cl, 0.60 g L^{-1} Na_2HPO_4, 0.10 g L^{-1} KCl, 10 mL L^{-1} trace element solution and 1 mL L^{-1} selenite-tungstate solution. The trace element solution contains: 1.50 g L^{-1} nitrilotriacetic acid, 3.00 g L^{-1} $MgSO_4.7H_2O$, 0.50 g L^{-1} $MnSO_4.7H_2O$, 1.00 g L^{-1} NaCl, 0.10 g L^{-1} $FeSO_4.7H_2O$, 0.18 g L^{-1} $CoSO_4.7H_2O$, 0.10 g L^{-1} $CaCl.2H_2O$, 0.18 g L^{-1} $ZnSO_4.7H_2O$, 0.01 g L^{-1} $CuSO_4.5H_2O$, 0.02 g L^{-1} $KAl(SO_4)_2.12H_2O$, 0.01 g L^{-1} H_3BO_3, 0.01 g L^{-1} $Na_2MoO_4.2H_2O$, 0.03 g L^{-1} $NiCl_2.6H_2O$, 0.0003 g L^{-1} $Na_2SeO_3.5H_2O$. The selenite-tungstate solution was prepared with 0.50 g L^{-1} NaOH, 0.003 g L^{-1} $Na_2SeO_3.5H_2O$ and 0.004 g L^{-1} $Na_2WO_4.2H_2O$. The trace element and the selenite-tungstate solutions were previously prepared and reserved in sterile glass bottles at 4 °C. Culture medium was boiled and cooled in ice bath until it reached room temperature, deoxygenated with a stream of N_2:CO_2 (80 %:20 %), whereas 2.50 g L^{-1} of $NaHCO_3$ was dissolved in the medium for buffering it at pH = 6.8. The medium was introduced in serum bottles, flushed and pressurized with N_2:CO_2 (80 %:20 %) gas mixture to retain anaerobic conditions and finally was autoclaved (121 °C, 21 min).



BES as bioanode

$C_2H_4O_2 + 2H_2O \rightarrow 2CO_2 + 8H^+ + 8e^-$ E^0_{oxd} = +0.289 V

2,6-AQDS + $2H^+ + 2e^- \rightarrow$ 2,6-AQDSH$_2$ E^0_{red} = -0.184 V

Redox Flow Cell

2,6-AQDSH$_2 \rightarrow$ 2,6-AQDS + $2H^+ + 2e^-$ E^0_{oxd} = +0.184 V

$[Fe(CN)_6]^{3-} + e^- \rightarrow [Fe(CN)_6]^{4-}$ E^0_{red} = +0.436 V

BES as biocathode

$[Fe(CN)_6]^{4-} \rightarrow [Fe(CN)_6]^{3-} + e^-$ E^0_{oxd} = -0.436 V

$2CO_2 + 8H^+ + 8e^- \rightarrow C_2H_4O_2 + 2H_2O$ E^0_{red} = -0.289 V

Figure 5.1. Illustration of Microbial Redox Flow Cell (MRFC). At the left side, first BES as bioanode for the charging of the negalyte (2,6-AQDS→2,6-AQDSH$_2$). At the center, the Redox Flow Cell (2,6-AQDS||$[Fe(CN)_6]^{4-}$) having negalyte from first BES and posilyte from second BES. On the right side, the second BES as biocathode established during the oxidation of $[Fe(CN)_6]^{4-}$ to $[Fe(CN)_6]^{3-}$.

The inoculation of *G. sulfurreducens* in the serum bottles used 10.0 % of mother culture, 5 mL L^{-1} of the trace vitamin solution, 1.64 g L^{-1} Na-acetate as electron donor, and 8.00 g L^{-1} Na_2-fumarate as electron acceptor [25, 26]. The vitamin solution was prepared and stored as the other stock solutions and contains 4.000 mg L^{-1} biotin, 4.0 mg L^{-1} folic acid, 20.0 mg L^{-1} pyridoxine-HCl, 10.0 mg L^{-1} thiamine-HCl.H_2O, 10.000 mg L^{-1} riboflavin, 10.0 mg L^{-1} nicotinic acid, 10.0 mg L^{-1} D-Ca-pantothenate, 0.20 mg L^{-1} vitamin B12, 10.0 mg L^{-1} p-aminobenzoic acid, 10.0 mg L^{-1} lipoic acid. The mentioned concentrations were added from stock solutions kept at 4 °C. The serum bottles were kept in an incubator at 30 °C and 100 rpm for several days.

Conversion of the negalyte redox pair 2,6-AQDS

Two BESs were run for the conversion of negalyte, in parallel as duplicates (identified as BES 1 and BES 2). The BES was assembled with two-chambers, with a volume of 50 cm^3. The electrodes of carbon felt were prepared linking carbon felt (QuinTech, 1 mm thick, 0.1 x 4 cm^2) to an electrical wire with electrically conductive cement (Leit-C, Sigma-Aldrich, Inc.); those were dried for 24 h before assembling. The chambers were separated by Nafion™ 117 PEM. The membranes were previously regenerated with 10 % H_2SO_4 at 40 °C for 3 h in a hot plate, and washed several times with Milli-Q® water (Milli-Q® Integral Water Purification System for Ultrapure Water, Millipore®, Merck KGaA).

The conversion of negalyte was performed with *G. sulfurreducens* introduced in the anode side and with 2,6-AQDS in the cathode side (BES with bioanode). The *G. sulfurreducens* was transferred from the serum bottle, previously cultivated and was fed with 20 mM of acetate, as carbon source and electron donor, for the biofilm formation in the electrode (primary electron receptor). The cathode side was complete with 20 mM of 2,6-AQDS prepared in 0.1 M phosphate buffer solution, at pH = 7. The cell was flushed with a gas mixture of N_2:CO_2 (80 %:20 %), to assure anaerobic conditions and keep at room temperature (approx. 22 °C).

The electric circuits of BESs were closed with an electrical resistance (500 Ω) and the potential difference (*E*, mV) was registered with an Ecograph T data logger (RSG 30 Endress+Hauser B.V., Naarden). The current density over time (*j*, mA cm^{-2}) was calculated by using Ohm law. It should be highlighted that no bias potential was applied. During this time, the Coulombic Efficiency (CE, %) was determined [27]. Open Circuit Potential (OCP) was measured using a

multimeter (HP Hewlett Packard 34401A multimeter). The polarization and power curves of cells were performed using a series of resistances ranging between 31 kΩ to 10 Ω [28].

The 2,6-AQDS, with a yellow color in aqueous solution, through redox conversion changes to a red dark color in aqueous solution, representative of the 2,6-AQDSH_2, as previously reported [29] and represented in the scheme plan (Figure 5.2A).

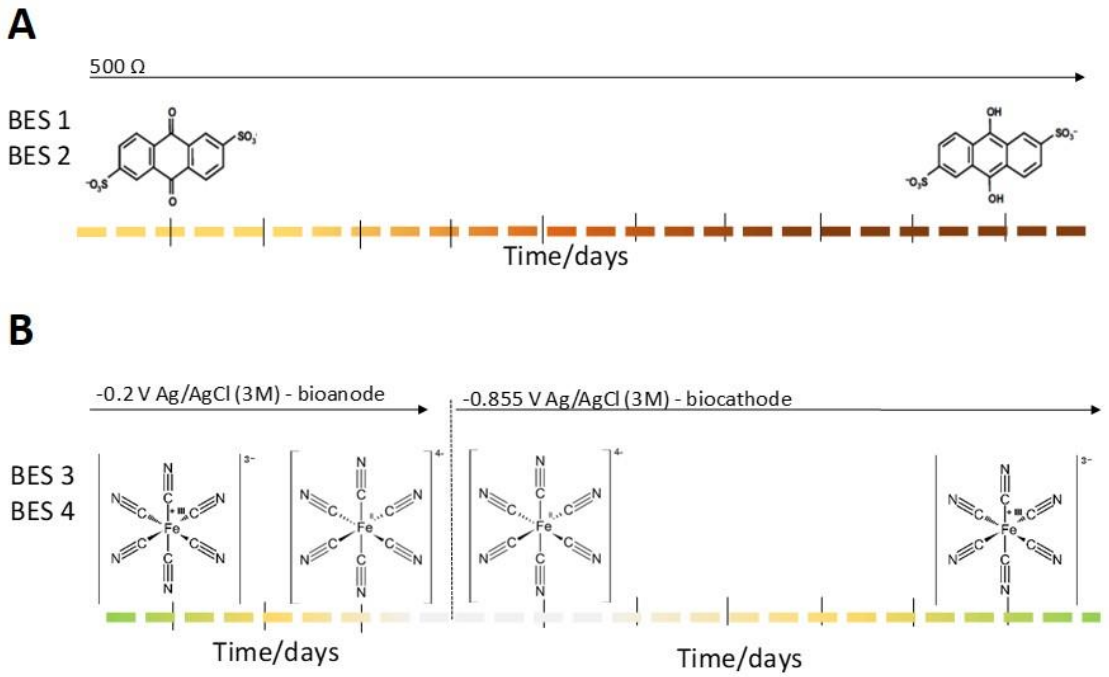


Figure 5.2. Scheme of the experimental plan: (A) BES 1 and BES 2 for charging of the negalyte (2,6-AQDS reduction to 2,6-AQDSH_2); (B) BES 3 and BES 4 operating firstly as bioanode for biofilm growth on the electrode surface and secondly as biocathode for the oxidation of $[Fe(CN)_6]^{4-}$ to $[Fe(CN)_6]^{3-}$.

When the microbial electrochemical fuel (negalyte) shown a red dark color for more than 24 h, the assays were ended. The negalyte was finally collected and introduced in serum bottles, previously deoxygenated with N_2 (100 %) [30]. This process was needed to avoid contact with oxygen which can oxidize the 2,6-AQDSH_2. The serum bottles were moved to an anaerobic chamber.

Conversion of the posilyte redox pair $[Fe(CN)_6]^{4-}$

The conversion of posilyte in a BES was performed with *G. sulfurreducens* in a two-steps process (Figure 5.2B). The posilyte conversion was operated in BESs in parallel as duplicates (named as BES 3 and BES 4). The BESs used were built equally to the ones used for the

negalyte conversion. Initially, BESs were operated to promote the growth of *G. sulfurreducens* in the electrode surface, operating it as a trivial acetate-oxidizing bioanodes. The anode side was filled with the *G. sulfurreducens*; in the cathode side $[Fe(CN)_6]^{3-}$ was introduced (40 mM of $[Fe(CN)_6]^{3-}$ prepared in 0.1 M phosphate buffer solution, at pH = 7). The anode potential was applied and controlled at -0.200 V *vs.* Ag/AgCl (3 M) with a potentiostat (Potentiostat / Galvanostat VSP, BioLogic Science Instruments, France) and respective data acquisition software (EC-Lab software), for biofilm formation at the electrode surface and to record the current density over time [31].

Posteriorly, the electrode potential was lowered from -0.200 V *vs.* Ag/AgCl (3 M) to -0.855 V *vs.* Ag/AgCl (3 M), the acetate-oxidizing bioanodes were converted to CO_2-reducing biocathodes [32], and the oxidation of $[Fe(CN)_6]^{4-}$ to $[Fe(CN)_6]^{3-}$ was conducted to achieve the posilyte (BES with biocathode) (Figure 5.2B). The respective data acquisition software was used to record the current density over time [31]. The OCP was measured using a multimeter, the power and polarization curves were performed [28], and the CE was determinates [33]. When the microbial electrochemical fuel (posilyte), characteristic of the $[Fe(CN)_6]^{3-}$ for more than 24 hours [34], the assays were ended (Figure 5.2B). The posilyte was collected and introduced in serum bottles.

The *G. sulfurreducens* at the end of assays were analyzed by Cyclic Voltammetry (CV). The CVs were performed with the biocathodes as the working electrode, an Ag/AgCl (3 M) reference electrode positioned at cathode side, and the counter electrode was at the anode side where the $[Fe(CN)_6]^{3-}$ was replaced with 0.1 M KCl. All electrodes were connected with a potentiostat and were recorded with respective software. A scan rate of 20 mV s^{-1} was run, between the potential -0.400 V *vs.* Ag/AgCl (3 M) and 1.000 V *vs.* Ag/AgCl (3M). All the results were changed to Normal Hydrogen Electrode (NHE).

Chemical analysis and measurements

The microbial growth of *G. sulfurreducens* during the negalyte conversion in BES 1 and BES 2 was measured in samples collected at time zero and at the end of the assays. Microbial growth of *G. sulfurreducens* as acetate-oxidizing bioanodes in BES 3 and BES 4 was measured in samples collected in the beginning and in the end of the applied potential (-0.200 V *vs.* Ag/AgCl (3 M)). All samples were evaluated by Optical Density (OD) at 620 nm (OD_{620}) [35] using a

spectrophotometer DR 2800 (Hach Lange, Düsseldorf, Germany). Acetate concentration in all BESs was assessed with volatile fatty acids (VFA) analysis method [36], in High-Performance Liquid Chromatography (HPLC) (Jasco, Tokyo, Japan) using a UV detector (210 nm), Agilent Hi-Plex H column (300 × 7.7 mm), at 60 °C, and sulphuric acid (0.5 mol L^{-1}) as mobile phase, at a flow rate of 0.600 mL min^{-1}.

UV-Vis Spectrophotometry analysis to estimate the concentration of 2,6-$AQDSH_2$ (negalyte) was executed inside an anaerobic chamber. A GENESYS™ 20 Visible Spectrophotometer and a 10 mm quartz cell was used. The 2,6-AQDS concentration present in the samples were quantified at 330 nm [23, 31, 37]. The concentration of the 2,6-$AQDSH_2$ was estimated, from the concentration difference between 2,6-AQDS in solution at time zero and the 2,6-AQDS present in the final solution. A standard curve was previously obtained by measuring the absorbance of 2,6-AQDS solutions with defined known concentrations. The UV-Vis Spectrophotometry was also used to determinate the concentration of $[Fe(CN)_6]^{4-}$ and $[Fe(CN)_6]^{3-}$ at 340 and 420 nm, respectively [38], in a 10 mm quartz cell and a Spectrophotometer DR 2800.

Microbial Redox Flow Cell characterization

Within the MRFC, the Redox Flow Cell was equipped with a Nafion™ 117 PEM and with 9 cm^2 active area electrodes. The cell was loaded with bio-charged electrolytes, with negalyte 2,6-$AQDSH_2$ and with posilyte $[Fe(CN)_6]^{3-}$. The membrane was pre-heated in 5 % H_2O_2 solution at 80 °C for 30 min, washed with deionized water and immersed in a solution of 10 % H_2SO_4 at 80 °C for 30 min. Then it was washed with deionized water for several times and left with deionized water overnight before assembly. The carbon felt electrodes (GFD 2.5 mm EA from SGL) were activated immersing in 1 M H_2SO_4 at 80 °C for 24 h followed by thermal treatment at 400 °C for 10 h in the presence of air. The graphite bipolar plates and current collectors of gold-coated copper plates were used. Teflon gaskets sealed the membrane and electrodes into the cell. Electrodes were compressed by 20 % resulting into the final thickness of 2 mm to ensure good contact between components. The negalyte and posilyte solutions were load in the respective external flasks. The same was operated at room temperature and at neutral pH conditions. Argon (100 %) was flushed continuously, to avoid oxidation during the test, to diminish oxidation

of species on both reservoirs. The ISMATEC peristaltic pump was used to maintain flowrate of 40 mL min^{-1} for both electrolytes at each side of RFC during the cycling measurements.

Electrochemical measurements were performed by Zahner Zennium (Zahner Elektrik, Germany) potentiostat that was used as electrochemical workstation in two-electrode galvanostatic configuration. Polarization curve at a scan rate of 50 mV s^{-1} was performed within the cutoff range of 0.200 V to 1.260 V. The charge-discharge cycling measurements were conducted at the current density of 3.75 mA cm^{-2}, having cutoff potentials from 0.100 V and 1.200 V [39]. The Coulombic Efficiency (CE), Potential Efficiency (EE) and Energy Efficiency (EE) were computed as described elsewhere [40]. The Polarization curve was performed after the charge discharge cycling. Electrochemical Impedance Spectroscopy (EIS) was used to measure the impedance of the cell [40]. The frequency range used for EIS was 250 kHz to 1 Hz and with the AC perturbation of 10 mV.

5.3. Results and discussion

Conversion of the negalyte redox pair 2,6-AQDS

G. sulfurreducens biofilms in BES 1 and BES 2 were responsible for the reduction of 2,6-AQDS to 2,6-$AQDSH_2$, visually observed by the color change. The change from yellow to red color observed in the cathode side of BES 1 and BES 2 was started in *ca.* 23 h, and both were completely dark red at *ca.* 259 h; experiments were ended in 260 h for both BESs. At this time, the bio-charged 2,6-$AQDSH_2$ was considered achieved in BES 1 and BES 2, as previously reported [39].

The BES 1 and BES 2 current density over time during the reduction of 2,6-AQDS are represented in Figure 5.3. The higher current densities observed at the microbial lag phase (startup stage) of the BESs are related to the biofilm formation at the electrodes surface; BES 1 and BES 2 displayed *ca.* 0.05 mA cm^{-2} after 24 hours of operation, decreasing afterwards. The decrease of the current density was attributed to the acetate consumption, membrane fouling and changes in anode medium mineral composition [41]. The measured OD_{620} in BES 1 increased from 0.20 at instant zero to 0.39 at the end of experiment, whereas in BES 2 OD_{620} increased from 0.10 to 0.53. The BES bioanode reactions are described in Figure 5.1.

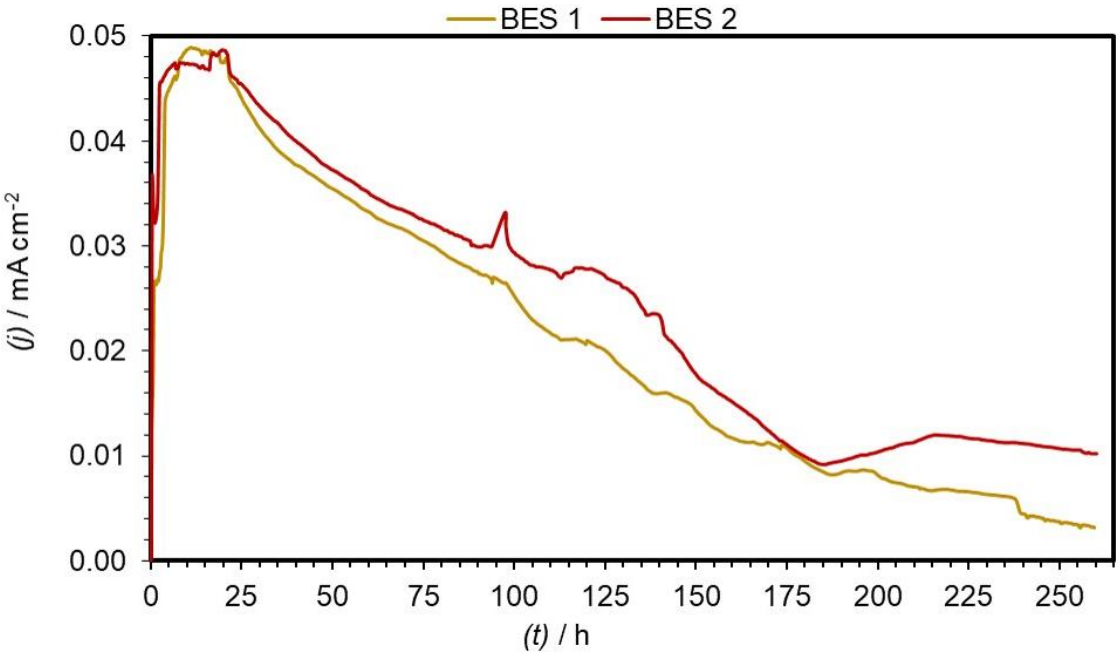


Figure 5.3. Current density history of BES 1 (yellow line) and BES 2 (red line), during the bioelectrochemical reduction of 2,6-AQDS (negalyte of MRFC).

The *G. sulfurreducens* in both BESs was responsible for the oxidation of acetate at the anode side and the release of electrons and protons for the cathode side. An average of 19 % CE was reached, in agreement to the literature [26, 42, 43]. The plot of the results from the polarization curves allow to estimate the internal resistance of BES 1 and BES 2, respectively 9.42 kΩ (3.08×10^{-5} mW cm^{-2}) and 1051 Ω (6.04×10^{-5} mW cm^{-2}). These high internal resistances result in small current densities and energy conversion efficiencies.

The concentration of the bio-charged 2,6-AQDSH_2 were estimated (Table 5.1), which corresponds to 21.8 % of reduced 2,6-AQDS to 2,6-AQDSH_2 in BES 1 and 32.7 % in BES 2.

Table 5.1. Coulombic Efficiency (CE) and the concentration of the bio-charged 2,6-AQDSH_2 (mM) at BES 1 and BES 2.

	CE (%)	[2,6-AQDSH_2], mM (negalyte)
BES 1	28.3	4.4
BES 2	11.5	6.5

Conversion of the posilyte redox pair $[Fe(CN)_6]^{4-}$

The current density history at BES 3 and BES 4 is shown in Figure 5.4. The *G. sulfurreducens* was responsible for the oxidation of acetate in the anode side (acetate-oxidizing bioanodes). An applied electrode potential of -0.200 V *vs.* Ag/AgCl (3 M) for promoting biofilm formation was performed during *ca*. 830 h for BES 3 and *ca*. 510 h for BES 4.

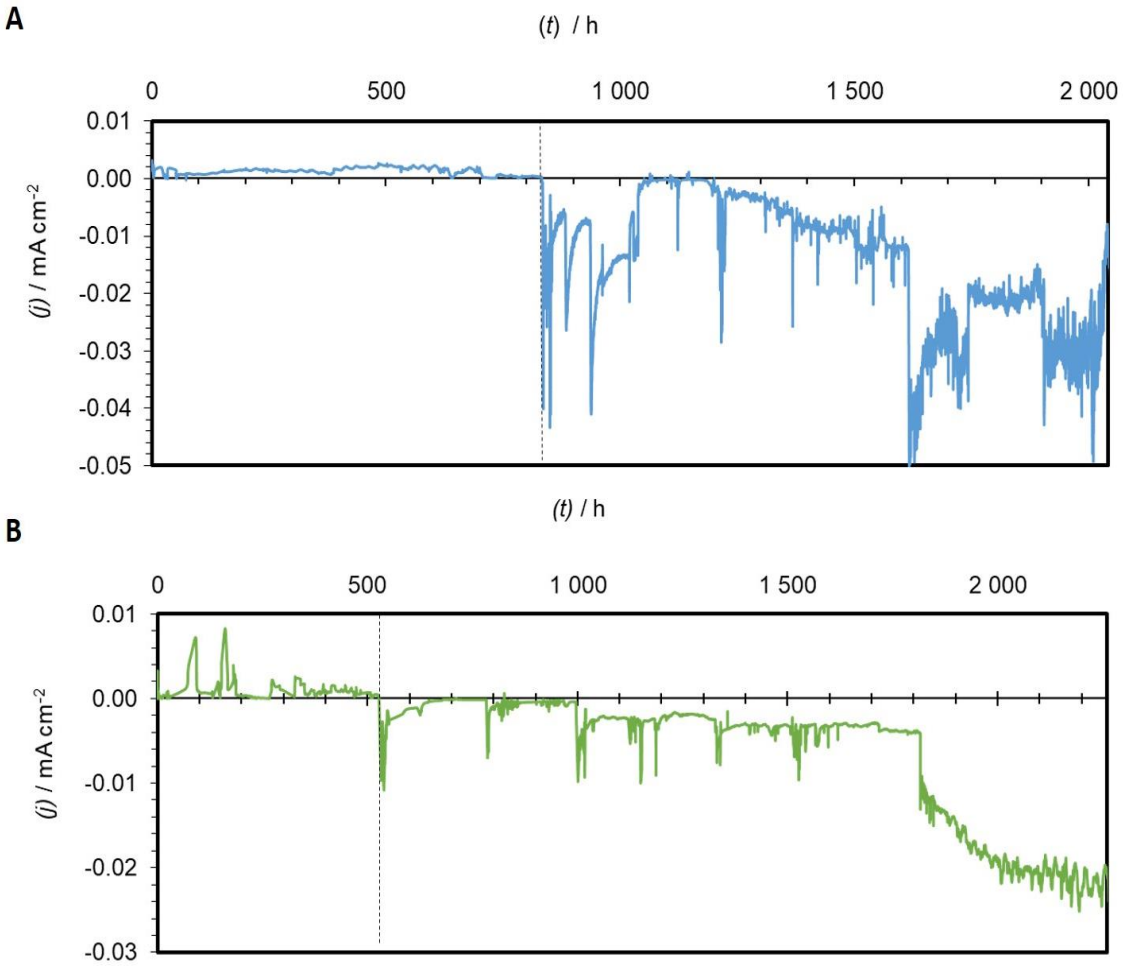


Figure 5.4. Current density over time generated in BES 3 and BES 4. Dashed lines indicated when the potential was lowered from -0.200 V *vs.* Ag/AgCl (3 M) to -0.855 V *vs.* Ag/AgCl (3 M) for BES 3 (blue line) and for BES 4 (green line).

At this moment, the potential of the bioanode was lowered to -0.855 V *vs.* Ag/AgCl (3 M), for transforming the bioanode into a biocathode (CO_2-reducing biocathodes) (indicated in the Figure 5.4 with the dashed line). As previously reported by Geelhoed and Stams [44], *G. sulfurreducens* can change from electron donating to electron uptake after reversing the applied

potential, where bacteria uses electrodes directly or via mediated extracellular electron transfer processes [45].

After the biofilm being formed in BES 3 and BES 4, the CE were estimated (3 % for BES 3 and 35 % for BES 4). The OD_{620} in BES 3 increased from 0.16 at 0 h (with acetate concentration measured at 32.9 mM) to 0.93 at 830 h (with acetate concentration measured at 18.2 mM). The low current density reached in BES 3, during this period of time was associated with the low CE caused by substrate consumption, high internal resistance estimated (5 KΩ) [42], possible membrane fouling and changes in anode medium mineral composition [45].

The results suggested that *G. sulfurreducens* grew more in the medium than in the electrode surface (biofilm). Whereas OD_{620} in BES 4 at 0 h was 0.18 (with acetate concentration measured at 26.7 mM) and increased to 0.55 at 510 h (with acetate concentration measured at 18.7 mM). The higher current density and CE during the biofilm being formed in BES 4 proposed a higher growth of bacteria in the electrode surface over the bacteria growth in medium. The BESs CE values were different for BES 1 and BES 2, but are in line with the literature [46,47]. The biofilm formation experiment was ended when the catholyte of the BES 3 and BES 4 was decolorized (green $[Fe(CN)_6]^{3-}$ to colorless $[Fe(CN)_6]^{4-}$) [34, 48], and also, the $[Fe(CN)_6]^{4-}$ concentration were estimated for the catholyte of BES 3 (0.3 mM) and BES 4 (0.3 mM).

Then, the BES biocathode was established during the oxidation of $[Fe(CN)_6]^{4-}$ to $[Fe(CN)_6]^{3-}$ (CO_2-reducing biocathodes) with -0.855 V *vs.* Ag/AgCl (3M), as the reactions in the Figure 5.1. In BES 3 the current density was. -0.01 mA cm^{-2} at 830 h and in BES 4 was -0.01 mA cm^{-2} at 510 h. The experiment was ended when the posilyte of the BES 3 and BES 4 was green, characteristic color of $[Fe(CN)_6]^{3-}$, for more than 24 h [31, 45]. The concentration of the bio-charged $[Fe(CN)_6]^{3-}$ (posilyte) was estimated to be 26.7 mM for BES 3 (66.7 % of $[Fe(CN)_6]^{4-}$) and 22.5 mM (61.5 % of $[Fe(CN)_6]^{4-}$) for BES 4.

In BES 3, during the posilyte conversion, the OD_{620} changed from 0.93 at 830 h (with acetate concentration measured at 18.2 mM), to 2.39 at the end of experiment (with acetate concentration at 1.1 mM). The results indicated, that during the posilyte conversion in BES 3, a consumption of acetate by the *G. sulfurreducens* was observed, due to reduction of acetate concentration *ca.* 17 mM, attributed to the bacteria growth in culture medium [49]. It was also

detected during HPLC analysis of samples collected the presence of others VFAs beside acetate, *e.g.* butyrate (at 830 h was measured 0.9 g L^{-1} and at the end of experiment was 0.03 g L^{-1}). In BES 4, during the posilyte conversion, the OD_{620} changed from 0.54 at 510 h (with acetate concentration measured at 18.7 mM), to 0.66 at the end of experiment (with acetate concentration measured at 3.7 mM). The consumption of acetate by the *G. sulfurreducens*, resulting in a reduction of 15 mM, was inferior to the BES 3 results [49], suggesting an adapted biofilm establish in electrode. The HPLC analysis of the samples collected for BES 4 detected also butyrate (at 510 h at the end of experiment was measured 0.06 g L^{-1}).

The polarization and power curves of BESs were obtained and the series resistances of the BESs were estimated at the end of the experiments. The series resistance and maximum power density of BES 3 were 9.4 kΩ and 7.7x10^{-3} mW m^{-2}, and of BES 4 were 1.1 kΩ and 9.3x10^{-4} mW m^{-2}.

The cyclic voltammograms of BES 3 and BES 4 were obtained before changing the potential (performed at 830 h for BES 3 and at 510 h for BES 4) and at the end of the experiments (performed at end of the experiments BES 3 and BES 4). The voltammograms are plotted in Figure 5.5.

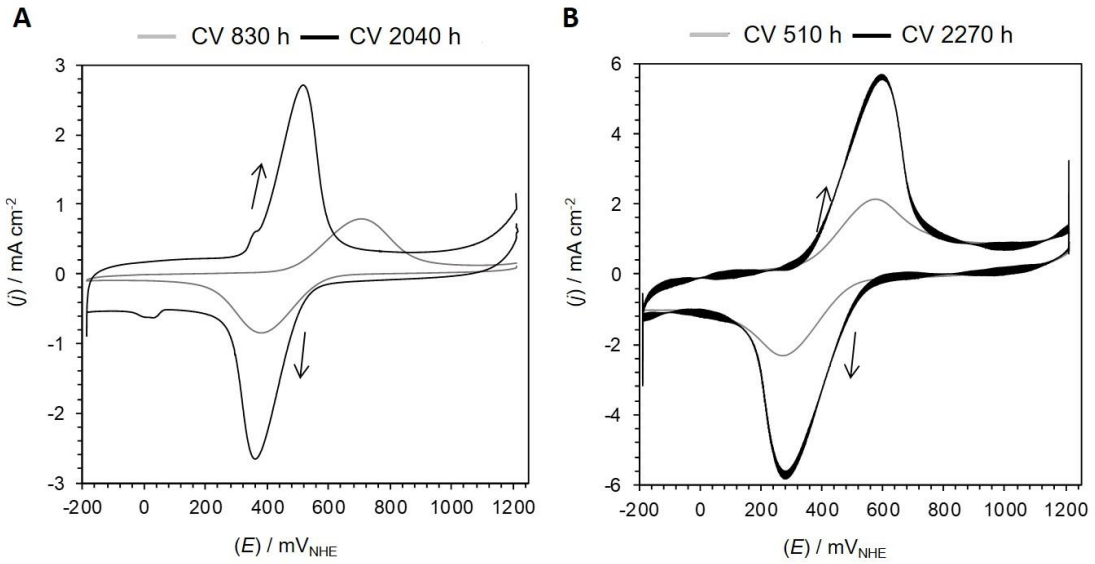


Figure 5.5. Voltammograms of bioelectrodes of the BES 3 (A) and BES 4 (B), achieved at 20 mV s^{-1}, before switching the potential from -0.200 V *vs.* Ag/AgCl (3 M) to -0.855 V *vs.* Ag/AgCl (3 M) (grey line), and when assays ended (black line).

The voltammograms of *G. sulfurreducens* obtained at the end of the assays indicate an adaptation of the bioelectrode as autotrophic biofilm [50, 51]. BES 3, at 830 h, shows a reduction peak with. -0.82 mA cm^{-2} at 327 mV; at the end of experiment the reduction peak was recorded at 364 mV and shows a current density of -2.63 mA cm^{-2} (Figure 5.5A). The increase of the absolute value of the current density at the reduction peak in BES 3 was attributed to the electro-autotrophic behavior of bacteria formed in the biocathode [52]. It is observed a shift of *ca.* 750 mV in the oxidation peak of the CV plot, at 830 h in BES 3; the shift was attributed to the redox potentials of cytochromes of bacteria that change in the biofilm environment [53]. In the CV of BES 4 (Figure 5.5B), the reduction peak with -2.29 mA cm^{-2} at 284 mV, at 510 h increased to - 5.80 mA cm^{-2} at 291 mV, at the end of experiment, exhibiting the electro-autotrophic behavior of biocathode. The CVs of *G. sulfurreducens* biocathodes are similar to the reported in literature [32, 54–56].

Microbial Redox Flow Cell characterization

The MRFC was tested with the bio-charged redox pairs loaded in the Redox Flow Cell, as sketched in the Figure 5.1. After discharging, the electrolytes were cyclically charged-discharged as illustrated in Figure 5.6A using a power supply. Therefore, electrochemical energy stored at BESs was converted into electrical energy at the RFC of the integrated MRFC device.

Figure 5.6B shows that the potential and energy efficiencies are similar and mostly constant over the 30 charge-discharge cycles and equal to *ca.* 50 %. And an CE of *ca.* 99 %. The Figure 5.6C shows a capacity loss over the time because of the high imposed current density.

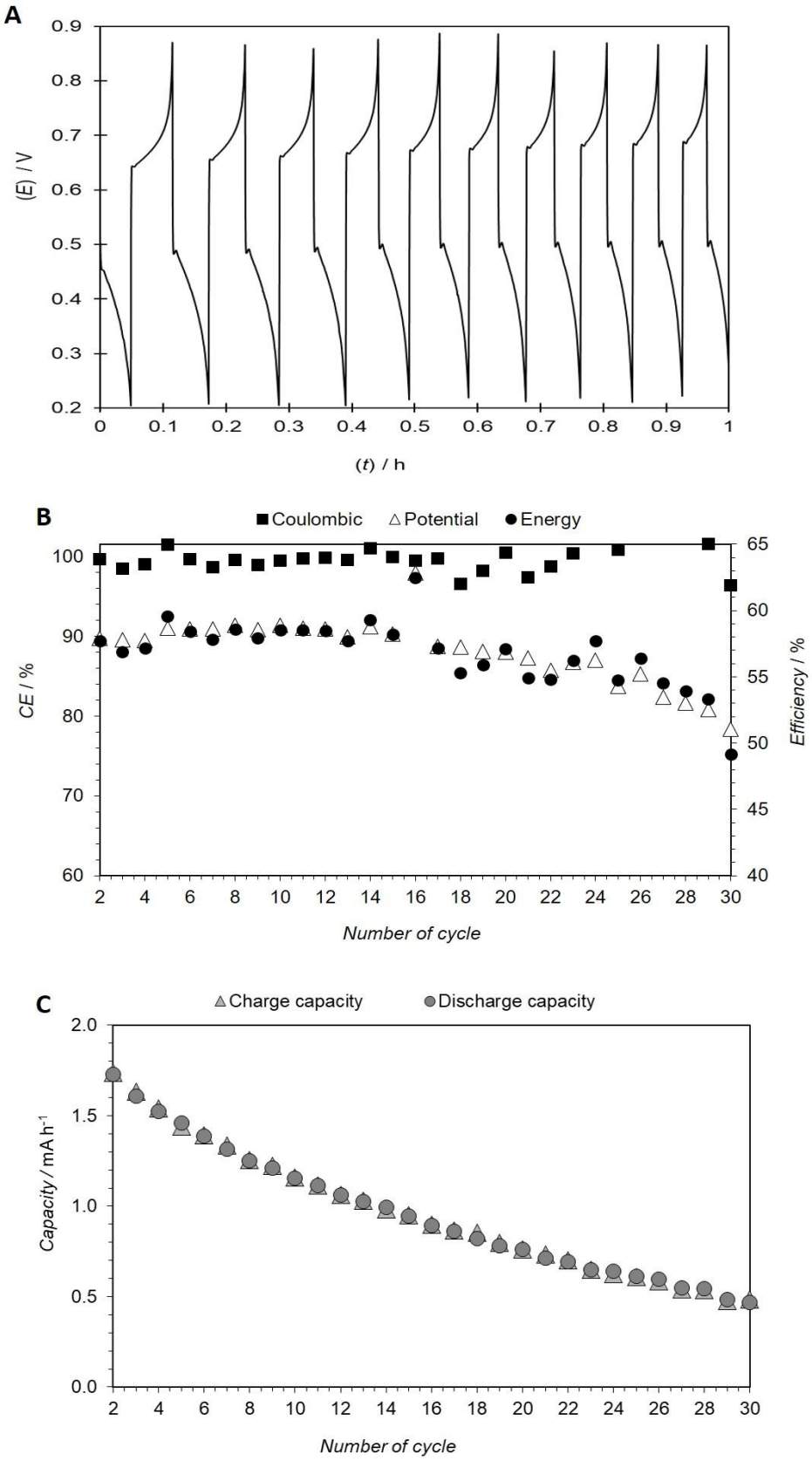


Figure 5.6. Redox Flow Cell assembled with negalyte 2,6-AQDSH$_2$ and with posilyte $[Fe(CN)_6]^{3-,}$ both charged bioelectrochemically: (A) potential *vs.* time response at current density of 3.75 mA cm^{-2}; (B) Coulombic Efficiency (CE), Potential Efficiency (PE) and Energy efficiency (EE) over the charge-discharge cycle number and (C) the loss in capacity.

The RFC characterization is performed using EIS measurements shown in Figure 5.7 and polarization measurements shown in Figure 5.8. The EIS measurements were plotted on a Nyquist plot which highlights the real and imaginary contribution for impedance of the cell. The high-frequency intercept highlights the series resistances. Individual contribution of the resistance by each component can be isolated using equivalent circuit fitting of this impedance curve. The inset of Figure 5.7. shows the magnified electrochemical fitting of first semi-circle using Randles Circuit. A Randles Circuit is the simplest equivalent electrical circuit consisting of an ohmic resistance (R_Ω) in series with the parallel combination of the Double-Layer Capacitance and a Charge Transfer Resistance.

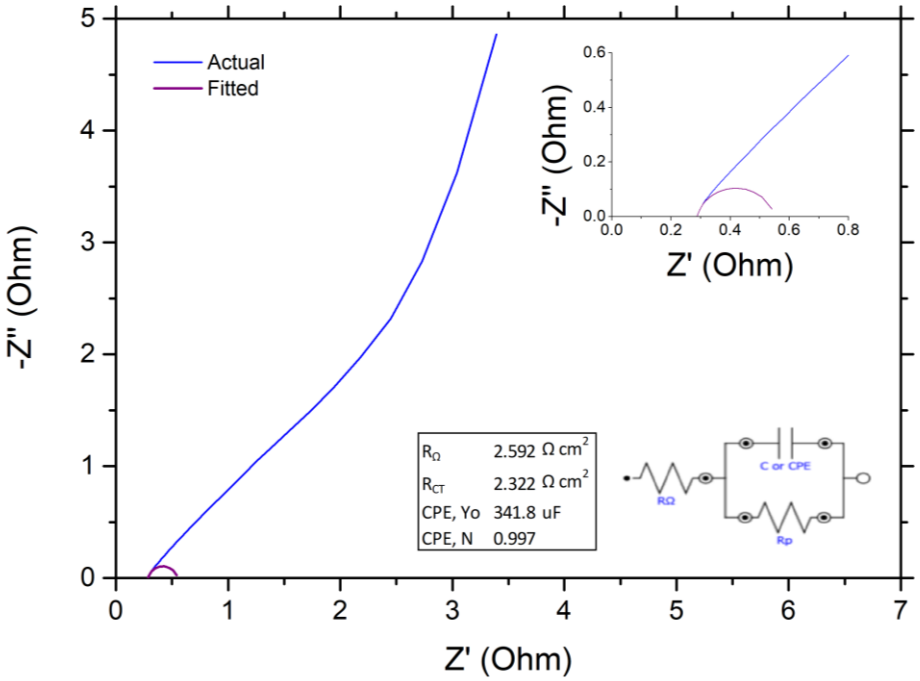


Figure 5.7. Impedance curve (Nyquist plot) obtained through EIS performed within range of 250 kHz to 1 Hz having AC perturbation of 10 mV. The inset shows the magnified for electrochemical fitting of first semi-circle using Randles Circuit.

The series resistance is mostly related to the cell membrane. In this study a membrane of Nafion™ NM 117 PEM was used to minimize the crossover, which allowed to obtain a quite high Coulombic efficiency, *ca.* 98 %. The polarization curve shown in Figure 5.8 shows a limiting current density of 18.73 mA cm^{-2}.

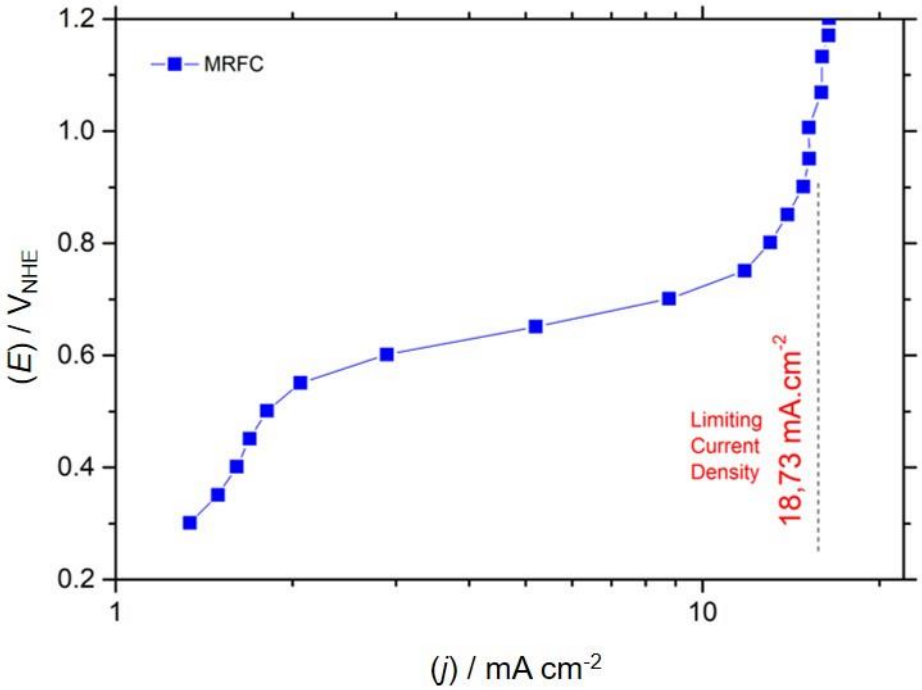


Figure 5.8. Polarization Curve at a scan rate of 50 mV s^{-1} performed within the potential range of 0.2 V to 1.2 V highlighting the limiting current density of the cell. The curve is starting from the open circuit potential of 0.280 V.

This work illustrates the concept of transforming waste biomass energy into electrochemical energy, easily transformable into dispatchable electricity, using microorganisms, in a so called Microbial Redox Flow Cell. However, an unbiased BES anode and a biased BES cathode were used. The authors are now investigating the development of a fully unbiased bioelectrochemical system for fully demonstrate the MRFC concept.

5.4. Conclusions

This study combines electrochemical conversions in Bioelectrochemical systems (BES) coupled with a Redox Flow Cell (RFC) for bioenergy storage, in an innovative system designated Microbial Redox Flow Cell (MRFC). The energy released by the EAB is directly converted into storable energy (microbial electrochemical fuels) easily and efficiently convertible into electricity, making this electricity dispatchable. The concept herein demonstrated used *G. sulfurreducens* for the oxidation of acetate and CO_2 reduction to reduce and oxidize the redox pairs 2,6-AQDS and $[Fe(CN)_6]^{4-}$, used as electrochemical fuels in the Redox Flow Cell. The concept explored the capacity of *G. sulfurreducens* to operate as electrogenic and electrotrophic bacteria.

The innovative system allows an average reduction of 24.6 % for 2,6-AQDS at BES bioanode and an average 35.7 % oxidation of $[Fe(CN)_6]^{4-}$ at the BES biocathode. The MRFC assembled with the microbial electrochemical fuels reached a *ca.* 98 % Coulombic efficiency.

Although the oxidation of $[Fe(CN)_6]^{4-}$ was biased, assisted with a power supply, MRFCs have the potential to display the highest energy conversion efficiency of any biological electrochemical system, due to the flexibility on setting the electrical potential of oxidation and reduction of the redox pairs, making them to match the electrical potential of the bacteria.

5.5. Acknowledgements

M.S.S. Santos is grateful to Portuguese Foundation for Science and Technology (FCT) for her PhD Grant (reference: SFRH/BD/104087/2014). The authors would like to acknowledge to the (FCT) under the scope of the strategic funding of UID/BIO/04469 unit and COMPETE 2020 (POCI-01-0145-FEDER-006684) and BioTecNorte operation (NORTE-01-0145-FEDER-000004) funded by the European Regional Development Fund under the scope of Norte2020 - Programa Operacional Regional do Norte. The authors also acknowledge the Projects: i) financially supported by project UID/EQU/00511/2019 - Laboratory for Process Engineering, Environment, Biotechnology and Energy – LEPABE funded by national funds through FCT/MCTES (PIDDAC)., ii) by the Project SunStorage - Harvesting and storage of solar energy", with reference POCI-01-0145-FEDER-016387, funded by European Regional Development Fund (ERDF), through COMPETE 2020 - Operational Programme for Competitiveness and Internationalisation (OPCI), and by national funds, through FCT - Fundação para a Ciência e a Tecnologia I.P and iii) NORTE-01-0145-FEDER-000005 – LEPABE-2-ECO-INNOVATION, supported by North Portugal Regional Operational Programme (Norte 2020), under the Portugal 2020 Partnership Agreement, through the European Regional Development Fund (ERDF). The authors are indebted with all the colleagues who assisted in the laboratory work, in particular to Dr kashif Mushtaq for help with RFC operation.

5.6. References

[1] H.L. Tuller, Solar to fuels conversion technologies: a perspective, Mater. Renew. Sustain. Energy. 6 (2017) 1–16.

[2] T.M. Gür, Review of electrical energy storage technologies, materials and systems: challenges and prospects for large-scale grid storage, Energy Environ. Sci. 11 (2018) 2696–2767.

[3] P.K. Leung, T. Martin, A.A. Shah, M.R. Mohamed, M.A. Anderson, J. Palma, Membrane-less hybrid flow battery based on low-cost elements, J. Power Sources. 341 (2017) 36–45.

[4] P. Leung, T. Martin, M. Liras, A.M. Berenguer, R. Marcilla, A. Shah, L. An, M.A. Anderson, J. Palma, Cyclohexanedione as the negative electrode reaction for aqueous organic redox flow batteries, Appl. Energy. 197 (2017) 318–326.

[5] W. Wang, V. Sprenkle, Energy storage: redox flow batteries go organic, Nat. Chem. 8 (2016) 204–206.

[6] R. Saidur, E.A. Abdelaziz, A. Demirbas, M.S. Hossain, S. Mekhilef, A review on biomass as a fuel for boilers, Renew. Sustain. Energy Rev. 15 (2011) 2262–2289.

[7] D.R. Lovley, Microbial energizers: Fuel cells that keep on going, Microbe. 1 (2006) 323–329.

[8] N.S. Malvankar, M.T. Tuominen, D.R. Lovley, Biofilm conductivity is a decisive variable for high-current-density *Geobacter sulfurreducens* microbial fuel cells, Energy Environ. Sci. 5 (2012) 5790–5797.

[9] C. Santoro, C. Arbizzani, B. Erable, I. Ieropoulos, Microbial fuel cells: From fundamentals to applications. A review, J. Power Sources. 356 (2017) 225–244.

[10] H. Liu, T. Song, K. Fei, H. Wang, J. Xie, Microbial electrosynthesis of organic chemicals from CO_2 by *Clostridium scatologenes* ATCC 25775T, Bioresour. Bioprocess. 5 (2018) 1-10.

[11] I. Ieropoulos, J. Greenman, C. Melhuish, Microbial fuel cells based on carbon veil electrodes: stack configuration and scalability, Int. J. Energy Res. 32 (2008) 1228–1240.

[12] A. El Mekawy, H.M. Hegab, G. Mohanakrishna, D. Pant, H. Wang, Integrated Bioelectrochemical Platforms, in: Microb. Electrochem. Technol., Elsevier, 2019: pp. 1037–1058.

[13] B. Gao, F. Yang, J. Liu, J. Crittenden, L. Liu, N. Ren, Integration of microbial fuel cell with independent membrane cathode bioreactor for power generation, membrane fouling mitigation

and wastewater treatment, Int. J. Hydrogen Energy. 39 (2014) 17865–17872.

[14] Y. Lu, M. Qin, H. Yuan, I.M. Abu-Reesh, Z. He, When bioelectrochemical systems meet forward osmosis: accomplishing wastewater treatment and reuse through synergy, Water (Switzerland). 7 (2015) 38–50.

[15] A.E. Inglesby, A.C. Fisher, Enhanced methane yields from anaerobic digestion of *Arthrospira maxima* biomass in an advanced flow-through reactor with an integrated recirculation loop microbial fuel cell, Energy Environ. Sci. 5 (2012) 7996–8006.

[16] Y. Kim, B.E. Logan, Microbial Reverse Electrodialysis Cells for synergistically enhanced power production, Environ. Sci. Technol. 45 (2011) 5834–5839.

[17] S.H. Shin, S.H. Yun, S.H. Moon, A review of current developments in non-aqueous redox flow batteries: Characterization of their membranes for design perspective, RSC Adv. 3 (2013) 9095–9116.

[18] A.Z. Weber, M.M. Mench, J.P. Meyers, P.N. Ross, J.T. Gostick, Q. Liu, Redox flow batteries: a review, J. Appl. Electrochem. 41 (2011) 1137–1164.

[19] K. Lin, Q. Chen, M.R. Gerhardt, L. Tong, S.B. Kim, L. Eisenach, A.W. Valle, D. Hardee, R.G. Gordon, M.J. Aziz, M.P. Marshak, Alkaline quinone flow battery, Science (80) 349 (2015) 1529–1532.

[20] A. Orita, M.G. Verde, M. Sakai, Y.S. Meng, A biomimetic redox flow battery based on flavin mononucleotide, Nat. Commun. 7 (2016) 1–8.

[21] R.M. Darling, K.G. Gallagher, J.A. Kowalski, S. Ha, F.R. Brushett, Pathways to low-cost electrochemical energy storage: a comparison of aqueous and nonaqueous flow batteries, Energy Environ. Sci. 7 (2014) 3459–3477.

[22] K. Scott, E.H. Yu, Microbial Electrochemical and Fuel Cells: Fundamentals and applications, Elsevier, 2016.

[23] C. Liu, J.M. Zachara, N.S. Foster, J. Strickland, Kinetics of reductive dissolution of hematite by bioreduced anthraquinone-2,6-disulfonate, Environ. Sci. Technol. 41 (2007) 7730–7735.

[24] M.T. McDermott, K. Kneten, R.L. McCreery, Anthraquinonedisulfonate adsorption, Electron-transfer kinetics, and capacitance on ordered graphite-electrodes - the important role of surface-defects, J. Phys. Chem. 96 (1992) 3124–3130.

[25] K.P. Nevin, H. Richter, S.F. Covalla, J.P. Johnson, T.L. Woodard, A.L. Orloff, H. Jia, M.

Zhang, D.R. Lovley, Power output and columbic efficiencies from biofilms of *Geobacter sulfurreducens* comparable to mixed community microbial fuel cells, Environ. Microbiol. 10 (2008) 2505–2514.

[26] M.S. Kim, Y.J. Lee, Optimization of culture conditions and electricity generation using *Geobacter sulfurreducens* in a dual-chambered microbial fuel-cell, Int. J. Hydrogen Energy. 35 (2010) 13028–13034.

[27] B.E. Logan, Microbial Fuel Cells, John Wiley & Sons, Inc., Hoboken, NJ, USA, 2007.

[28] L. Peixoto, A.L. Rodrigues, G. Martins, A. Nicolau, A.G. Brito, M.M. Silva, P. Parpot, R. Nogueira, A flat microbial fuel cell for decentralized wastewater valorization: process performance and optimization potential, Environ. Technol. 34 (2013) 1947–1956.

[29] A. Cadena, A. –C. Texier, I. González, F.J. Cervantes, J. Gómez, Qualitative and quantitative determination of a humic model compound in microbial cultures by cyclic voltammetry, Environ. Technol. 28 (2007) 1035–1044.

[30] I.C. Clark, H.K. Carlson, A.T. Iavarone, J.D. Coates, Bioelectrical redox cycling of anthraquinone-2,6-disulfonate coupled to perchlorate reduction, Energy Environ. Sci. 5 (2012) 7970–7978.

[31] C. yuan Wu, L. Zhuang, S. gui Zhou, Y. Yuan, T. Yuan, F. bai Li, Humic substance-mediated reduction of iron (III) oxides and degradation of 2,4-D by an alkaliphilic bacterium, *Corynebacterium humireducens* MFC-5, Microb. Biotechnol. 6 (2013) 141–149.

[32] S. Saheb-Alam, A. Singh, M. Hermansson, F. Persson, A. Schnürer, B.-M.M. Wilén, O. Modin, M. Hermansson, A. Singh, F. Persson, O. Modin, S. Saheb-Alam, B.-M.M. Wilén, Effect of start-Up strategies and electrode materials on carbon dioxide reduction on biocathodes, Appl. Environ. Microbiol. 84 (2017) 1–14.

[33] B.E. Logan, B. Hamelers, R. Rozendal, U. Schröder, J. Keller, S. Freguia, P. Aelterman, W. Verstraete, K. Rabaey, Microbial Fuel Cells: methodology and technology, Environ. Sci. Technol. 40 (2006) 5181–5192.

[34] B. Lai, S. Yu, P. V. Bernhardt, K. Rabaey, B. Virdis, J.O. Krömer, Anoxic metabolism and biochemical production in *Pseudomonas putida* F1 driven by a bioelectrochemical system, Biotechnol. Biofuels. 9 (2016) 1–13.

[35] C. Dumas, A. Bergel, DSA to grow electrochemically active biofilms of *Geobacter*

sulfurreducens, Electrochim. Acta. 53 (2008) 3200–3209.

[36] M.S. Duarte, S.A. Silva, A.F. Salvador, A.J. Cavaleiro, A.J.M. Stams, M.M. Alves, M.A. Pereira, Insight into the role of facultative bacteria stimulated by microaeration in continuous bioreactors converting LCFA to methane, Environ. Sci. Technol. 52 (2018) 6497–6507.

[37] G. Nöll, G. Hauska, P. Hegemann, K. Lanzl, T. Nçll, M. Von Sanden-flohe, B. Dick, C.W.V. Gmbh, C. Kgaa, T. Nöll, M. von Sanden-Flohe, B. Dick, Redox properties of LOV domains: chemical versus photochemical reduction, and influence on the photocycle, ChemBioChem 2007,. 8 (2007) 2256–2264.

[38] N. Frenzel, J. Hartley, G. Frisch, Voltammetric and spectroscopic study of ferrocene and hexacyanoferrate and the suitability of their redox couples as internal standards in ionic liquids, Phys. Chem. Chem. Phys. 19 (2017) 28841–28852.

[39] M.S.S. Santos, L. Peixoto, J. Azevedo, R.A.R. Monteiro, C. Dias-Ferreira, M.M. Alves, A. Mendes, Microbially-charged electrochemical fuel for energy storage in a redox flow cell, J. Power Sources. 445 (2020) 1–10.

[40] C.P. de León, A. Frías-Ferrer, J. González-García, D.A. Szánto, F.C. Walsh, Redox flow cells for energy conversion, J. Power Sources. 160 (2006) 716–732.

[41] M.D. Rolfe, C.J. Rice, S. Lucchini, C. Pin, A. Thompson, A.D.S. Cameron, M. Alston, M.F. Stringer, R.P. Betts, J. Baranyi, M.W. Peck, J.C.D. Hinton, Lag phase is a distinct growth phase that prepares bacteria for exponential growth and involves transient metal accumulation, J. Bacteriol. 194 (2012) 686–701.

[42] S. Ishii, K. Watanabe, S. Yabuki, B.E. Logan, Y. Sekiguchi, Comparison of electrode reduction activities of *Geobacter sulfurreducens* and an enriched consortium in an air-cathode microbial fuel cell, Appl. Environ. Microbiol. 74 (2008) 7348–7355.

[43] M.-S. Kim, J. Cha, D.-H. Kim, Enhancing factors of electricity generation in a microbial fuel cell using *Geobacter sulfurreducens*., J. Microbiol. Biotechnol. 22 (2012) 1395–400.

[44] J.S. Geelhoed, A.J.M. Stams, Electricity-assisted biological hydrogen production from acetate by *Geobacter sulfurreducens*, Environ. Sci. Technol. 45 (2011) 815–820.

[45] U. Schröder, F. Harnisch, L.T. Angenent, Microbial electrochemistry and technology: terminology and classification, Energy Environ. Sci. 8 (2015) 513–519.

[46] G.C. Premier, J.R. Kim, I. Michie, R.M. Dinsdale, A.J. Guwy, Automatic control of load

increases power and efficiency in a microbial fuel cell, J. Power Sources. 196 (2011) 2013–2019.

[47] G. Buitrón, I. López-Prieto, I.T. Zúñiga, A. Vargas, Reduction of start-up time in a microbial fuel cell through the variation of external resistance, Energy Procedia. 142 (2017) 694–699.

[48] P. Aelterman, S. Freguia, J. Keller, W. Verstraete, K. Rabaey, The anode potential regulates bacterial activity in microbial fuel cells, Appl. Microbiol. Biotechnol. 78 (2008) 409–418.

[49] P. Batlle-Vilanova, S. Puig, R. Gonzalez-Olmos, M.D. Balaguer, J. Colprim, Continuous acetate production through microbial electrosynthesis from CO_2 with microbial mixed culture, J. Chem. Technol. Biotechnol. 91 (2016) 921–927.

[50] S.M. Strycharz-Glaven, R.M. Snider, A. Guiseppi-Elie, L.M. Tender, On the electrical conductivity of microbial nanowires and biofilms, Energy Environ. Sci. 4 (2011) 4366–4379.

[51] L. Soussan, J. Riess, B. Erable, M.L. Delia, A. Bergel, Electrochemical reduction of CO_2 catalysed by *Geobacter sulfurreducens* grown on polarized stainless steel cathodes, Electrochem. Commun. 28 (2013) 27–30.

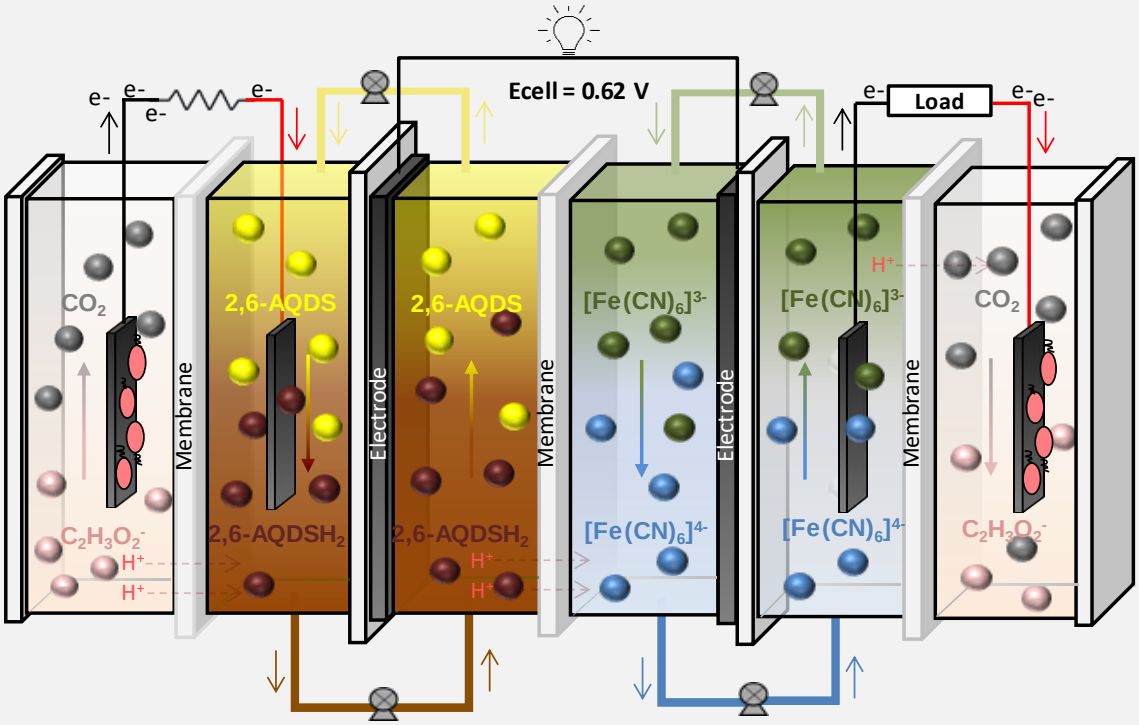
[52] D.F. Call, R.C. Wagner, B.E. Logan, Hydrogen production by geobacter species and a mixed consortium in a microbial electrolysis cell., Appl. Environ. Microbiol. 75 (2009) 7579–87.

[53] K.P. Katuri, P. Kavanagh, S. Rengaraj, D. Leech, *Geobacter sulfurreducens* biofilms developed under different growth conditions on glassy carbon electrodes: Insights using cyclic voltammetry, Chem. Commun. 46 (2010) 4758–4760.

[54] E. Marsili, J.B. Rollefson, D.B. Baron, R.M. Hozalski, D.R. Bond, Microbial biofilm voltammetry: Direct electrochemical characterization of catalytic electrode-attached biofilms, Appl. Environ. Microbiol. 74 (2008) 7329–7337.

[55] H. Richter, K.P. Nevin, H. Jia, D.A. Lowy, D.R. Lovley, L.M. Tender, Cyclic voltammetry of biofilms of wild type and mutant *Geobacter sulfurreducens* on fuel cell anodes indicates possible roles of OmcB, OmcZ, type IV pili, and protons in extracellular electron transfer, Energy Environ. Sci. 2 (2009) 506–516.

[56] S.S. Lim, E.H. Yu, W.R.W. Daud, B.H. Kim, K. Scott, Bioanode as a limiting factor to biocathode performance in microbial electrolysis cells, Bioresour. Technol. 238 (2017) 313–324.



Chapter 6

General conclusions and future perspectives

Different renewable energy sources such as solar, wind and biomass are being highly researched to make the energy dispatchable, using energy storage systems. Systems such Bioelectrochemical Systems (BESs) engender bioenergy from different carbon sources (*e.g.* wastewater) that are oxidized as fuels to convert electrochemical energy into electricity. Microbial Fuel Cells (MFCs) use inexpensive catalysts such as Electrochemically Active Bacteria (EAB), simple operating conditions (*e.g.* ambient temperature) and different carbon sources to generate electricity. In Microbial Electrolysis Cells (MECs) and Microbial Electrosynthesis Cells (MESs) the oxidation of fuels and microbial reduction are applied to generate renewable hydrogen or the synthesis of chemicals, respectively. BESs was coupled, combined and integrated with different technologies envisioning energy recovery and storage, *e.g.* the Microbial Rechargeable System. Energy storage systems well researched are the Redox Flow Cells (RFCs), electrochemical storage technologies where electrochemical energy is kept in soluble redox pairs and recirculated in a power unit to generate electrical energy. RFCs are also being coupled with other devices for energy generation and storage, such as the conversion of sunlight into electrochemical energy with a Solar Redox Flow Cell.

The results accomplished in this thesis demonstrate for the first time the coupling between BESs and RFCs, in a Microbial Redox Flow Cell (MRFC), an innovative bioelectrochemical conversion technology able to generate and store bioenergy. For the proof-of-concept of the MRFC, the conversion of anthraquinone-2,6-disulfonate (2,6-AQDS) to anthrahydroquinone-2,6-disulfonate (2,6-$AQDSH_2$) without bias potential applied was primarily studied and evidenced **(chapter 2)**. BESs were controlled with a bias anode potential at -0.200 V *vs.* Ag/AgCl (3 M) or with an electrical resistance load (500 Ω). The *Geobacter sulfurreducens* was the EAB and acetate was the carbon source. As seen in the literature, the electrolyte color changes from yellow (2,6-AQDS) to a dark red (2,6-$AQDSH_2$) as it gets charged. Current densities in BESs with a bias anode potential at -0.200 V *vs.* Ag/AgCl (3 M) reached. 0.21 mA cm^{-2}; BESs closed with an external resistance load of 500 Ω reached 0.05 mA cm^{-2}. The capacity of *G. sulfurreducens* as an electron donor (biocatalyst) for the electrochemical conversion of 2,6-AQDS was demonstrated. Notwithstanding that BESs with bias potential applied reached the highest current densities with the bio-charged 2,6-AQDS, the BESs with an external resistance load was responsible for the bio-charging 2,6-AQDS with no external energy applied.

Continuing this study, the work performed with BESs demonstrate the concept of microbial electrochemical fuels (bio-charged 2,6-$AQDSH_2$) to be used in a RFC as negalyte and the design of the MRFC **(chapter 3)**. Here is presented the envisaged bio-charging of the positive redox pair $[Fe(CN)_6]^{4-}$ directing the development of a feasible technology for converting bio-energy into storable electrochemical energy. The bioelectrochemical conversions of 2,6-AQDS without a bias potential applied (in series) produced current densities of 0.05 mA cm^{-2} and maximum power densities of 0.03 mW $cm^{-2,}$ in BESs. The results demonstrated an anodic biofilm established at the surface of the electrode, and also indicate that in the conditions established was indorsed a low activation potential needed for the bioelectrochemical conversion. The bio-conversion of 2,6-AQDS took a large period of time, perceived in the current density *vs.* time, but it is expected that optimization procedures improve the current density and decrease the time needed for the bio-conversions. The Coulombic efficiency (CE) of the BESs was *ca.* 20 %, similar to reported values with acetate oxidation in BESs. The concentration of 2,6-$AQDSH_2$ was estimated at *ca*. 5 mM. The microbial electrochemical fuel (bio-charged 2,6-$AQDSH_2$) and Ferricyanide ($[Fe(CN)_6]^{3-}$), were introduced in a 16 cm^2 RFC, producing a nominal potential difference of 0.620 V, with a *ca.* 80 % energy conversion efficiency.

The bioelectrochemical conversion of real wastewater into microbial electrochemical fuels following the proposed MRFC design was researched **(chapter 4)**. Redox pairs 2,6-AQDS and $[Fe(CN)_6]^{4-}$, were chosen again, since they are suitable for the RFC, namely in terms of pH and redox potentials. Additionally, to the use of wastewater over *G. sulfurreducens*, the redox pair 2,6-AQDS at pH = 7, pH = 9, pH = 12 were analysed in BESs during the conversion of microbial electrochemical fuels. These pH conditions were deliberate because it is stated that in BESs high pH cathode conditions can increase the conductivity of electrolytes in cathode chamber, and high pH differences between anodic and cathodic electrolytes is ideal for higher current densities and BESs cell potentials. Nonetheless, BESs results with the wastewater conversion shown no larger differences in the values of the current densities achieved with the selected pHs. The CEs reached in the different BESs were very similar (*ca.* 50 %), and no significant changes for the reduction of 2,6-AQDS were observed (*e.g.* color change). A total average in COD removal efficiency of 50.4 % was obtained in BES assembled with 2,6-AQDS at pH = 7,

was 42.7 % at BES assembled with 2,6-AQDS at pH = 9 and was 29.7 % at BES assembled with 2,6-AQDS at pH = 12. The COD removal efficiency demonstrates the conversion of microbial electrochemical fuels with the treatment of an effluent (or pre-treatment). It was established the opportunity to convert wastes into electrochemical energy, while treating real wastewater, an advantage for the MRFC. The highest concentration of 2,6-$AQDSH_2$ bioelectrochemically reduced was reached in pH = 7 (9.6 mM). The 16 cm^2 RFC was loaded with negalyte 2,6-$AQDSH_2$, charged bioelectrochemically at pH=7, and with the posilyte $[Fe(CN)_6]^{3-}$, charged using a power supply; the RFC displays a CE *ca.* 100 %, a PE *ca.* 56 % and a EE *ca.* 54 %; a capacity loss of *ca.* 30 % was observed during the 9 cycles.

The MRFC research with two microbial electrochemical fuels and the proof-of-concept of this unique system was settled **(chapter 5)**. The MRFC used *Geobacter sulfurreducens* as EAB to attain the 2,6-$AQDSH_2$ without bias potential applied in BESs (negalyte); and the *G. sulfurreducens* as EAB to oxidize $[Fe(CN)_6]^{4-}$ to $[Fe(CN)_6]^{3-}$, in BESs lowering the potential applied (posilyte). The conversion of 2,6-AQDS into 2,6-$AQDSH_2$ in BESs (BES 1 and BES 2) with an external resistance load was achieved with an average current density of 0.05 mA cm^{-2}, an average CE of 19 % and a concentration of the bio-charged 2,6-$AQDSH_2$ estimated at an average of *ca.* 5 mM. BESs operated with $[Fe(CN)_6]^{3-}$, with an external potential applied (-0.855 V *vs.* Ag/AgCl (3 M)) resulted in an average current density of -0.01 mA cm^{-2}; a concentration of the bio-charged $[Fe(CN)_6]^{3-}$ was estimated at an average of 24.6 mM. The novelty in this work was the bio-charged posilyte achieved in BES, $[Fe(CN)_6]^{3-}$, a microbial electrochemical fuel. *G. sulfurreducens* was capable to change from electron donating to electron uptake after lowering the bias potential applied, where the bacteria use electrodes directly or via Mediated Extracellular Electron Transfer (EET) processes. The RFC was assembled with negalyte 2,6-$AQDSH_2$, charged bioelectrochemically, and with posilyte $[Fe(CN)_6]^{3-}$, charged bioelectrochemically, for obtaining a potential *vs.* current discharge characteristic curve. RFC was operating in discharge mode and the results display for 30 cycles a CE *ca.* 98 %, a PE *ca.* 50 % and a EE *ca*. 50 %.

In a retrospective of the work developed in the scope of this thesis, the coupling process between BES and RFCs describes a process intensification, where the energy released by the EAB is directly converted into storable energy (microbial electrochemical fuels) easily and

efficiently convertible into electricity, making this electricity dispatchable. This makes the BES energy more attractive and cost effective. The work to develop a MRFC needs more research in order to fulfil its potential, reach new insights and advantages and overcome different problematics. BESs conversion of microbial electrochemical fuels could be researched with more electrode materials, *e.g.* carbon nanotubes as catalysts to improve the bio-conversion of the redox pairs, such as the case of 2,6-AQDS. It is expected that with other electrode materials to decrease the period of time of the catholyte conversions. The area of electrode and volume of the cell may be adjusted. Other carbon sources, like glucose or other wastes feed stocks could be used for the redox reactions to increase CE of the MRFC, to reach higher power densities and higher current densities during the bio-electrochemical conversions of redox pairs. Microbial electrochemical fuels could be knowledgeable with other organic redox chemical species, that were assembled in aqueous organic Redox Flow Cells. The 2,2,6,6-Tetramethylpiperidin-1-yl)oxyl (TEMPO) or aza-aromatic compounds could be established.

The MRFC, in a future perspective, could be explored for the coupling with Electro-fermentation of several chemical products with other EAB. A premise of research is the electrotrophic bacteria *Clostridium pasteurianum,* researched in MESs as biocathodes for the generation of chemicals. This alternative could be an interesting opportunity for MRFC applications - the saved energy could be used for chemical synthesis and by-products. Different working conditions, such as the BES operated in fed-batch systems can be researched. Other types of BESs, such as Microbial Electrosynthesis Cells, and RFCs coupling principles could be examined, linking other types of renewable energy sources, such as solar energy, that may be interesting to pursuit.